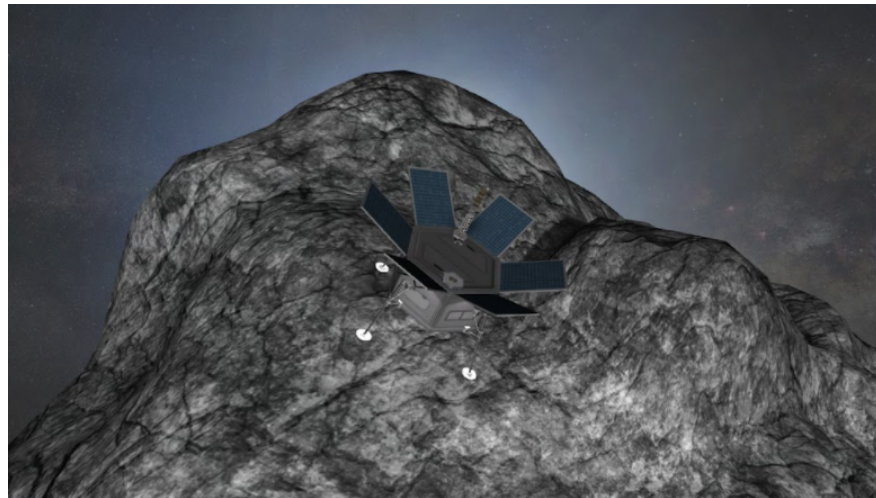


Hercules Comet Lander Probe

Final Design Review

MANE 4250 - Space Vehicle Design
Section 2 Design Team #7



Prepared By:
Keith Beadle
Kevin Morrison
Joseph Scaglione
Spencer Taub
Christopher Walter
Kenny Zheng

Report Submission Date: December 7th, 2021

EXECUTIVE SUMMARY

The following report summarizes the design and analysis of the Hercules Comet Lander Probe (CLP). This mission involves landing on the comet 46P/Wirtanen and carrying out scientific experiments that seek to measure the elemental, molecular, and mineralogical composition of the comet's surface and subsurface, and analyze its lower atmosphere. These scientific objectives will be achieved by an onboard tool suite that includes an imaging system, spectrometer, gas analyzer, radio sounder system, and magnetic sensor. The CLP will be delivered to the comet by a primary vehicle (PV), upon which it will separate and insert itself into a circular parking orbit. Once a suitable landing site has been determined, the CLP will then perform two additional burns to begin its descent and then approach the surface without a tangential velocity component. A harpoon will then fire upon touch down in order to ensure the CLP remains attached to the surface of the comet.

The design of the CLP is split up into nine primary subsystems: structures, mechanism and deployables, spaceflight mechanics, propulsion, attitude determination and control, thermal management, power management, command and data, and telecommunications. For each of these subsystems, existing products and technologies were selected, and quantitative analysis was performed to create a suitable design. The initial background, objectives, and design for each CLP subsystem was outlined in the Preliminary Design Review - as presented in Appendix Q. The design of the CLP, both in the PDR and in this report, were based on several key considerations that included: mass, power usage, cost, safety, performance, and reliability. Risk management was another key point of focus, with the goal of identifying significant hazards to the mission and mitigating their likelihoods and effects. Beyond the technical requirements of the mission, special considerations were also made for public health and safety, global, cultural, social, environmental, economic, and professional ethics circumstances surrounding this mission.

The CLP is expected to require a maximum power of approximately 160W during the landing phase of the mission. The initial design comes in with an estimated total mass of 230 kg and a volume of 0.96 m³. Furthermore, the overall cost for the mission is estimated to be around 300 million USD.

TABLE OF CONTENTS

1 INTRODUCTION	1
2 PROJECT SCOPE	2
2.1 CUSTOMER NEEDS	2
2.2 OBJECTIVES	2
2.3 CONSTRAINTS	3
2.4 REQUIREMENTS	4
2.5 ASSUMPTIONS	4
3 MISSION OVERVIEW	5
3.1 MISSION SELECTIONS	5
3.2 SENSOR SUITE SELECTION	6
3.3 RISK ANALYSIS AND MITIGATION	6
3.4 NON-TECHNICAL CONSIDERATIONS	6
4 DESIGN APPROACH	7
4.1 STRUCTURES	7
4.1.1 SUBSYSTEM DEFINITION	7
4.1.2 PRELIMINARY DESIGN OVERVIEW	7
4.1.3 PRODUCT SELECTION	7
4.1.4 STRUCTURAL LOAD DESIGN AND ANALYSIS	8
4.1.5 STRUCTURAL VIBRATIONS DESIGN AND ANALYSIS	13
4.1.6 RISK ANALYSIS AND MITIGATION	15
4.1.7 NON-TECHNICAL CONSIDERATIONS	15
4.1.8 PLAN OF PROCESSION	15
4.2 MECHANISMS AND DEPLOYABLES	16
4.2.1 SUBSYSTEM DEFINITION	16
4.2.2 PRELIMINARY DESIGN OVERVIEW	16
4.2.3 PRODUCT SELECTION	17
4.2.3.1 Shock Dampening Crushable Material	18
4.2.3.2 Pyrotechnic Release: Separation Nuts	18
4.2.3.3 Surface Penetrating Tethering Harpoon	19
4.2.3.4 Deployable Landing Leg Base	20
4.2.3.5 Telecommunications Radio Stem Boom	21
4.2.3.6 Manipulable Robotic Arm	22
4.2.4 FINAL ANALYSIS: SOLAR PANEL DEPLOYMENT	25
4.2.5 RISK ANALYSIS AND MITIGATION	32
4.2.6 NON-TECHNICAL CONSIDERATIONS	33

4.2.7 PLAN OF PROCESSION	33
4.3 SPACEFLIGHT MECHANICS	33
4.3.1 SUBSYSTEM DEFINITION	33
4.3.2 PRELIMINARY DESIGN OVERVIEW	33
4.3.3 COMET PARAMETERS	34
4.3.4 LAUNCH WINDOW DESIGN AND ANALYSIS	35
4.3.5 ORBITAL TRAJECTORY DESIGN AND ANALYSIS	37
4.3.6 RISK ANALYSIS AND MITIGATION	41
4.3.7 NON-TECHNICAL CONSIDERATIONS	41
4.3.8 PLAN OF PROCESSION	41
4.4 PROPULSION	42
4.4.1 SUBSYSTEM DEFINITION	42
4.4.2 PRELIMINARY DESIGN OVERVIEW	42
4.4.3 PRODUCT SELECTION	43
4.4.4 PROPELLANT TANK DESIGN AND ANALYSIS	44
4.4.5 RISK ANALYSIS AND MITIGATION	46
4.4.6 NON-TECHNICAL CONSIDERATIONS	46
4.4.7 PLAN OF PROCESSION	46
4.5 ATTITUDE DETERMINATION AND CONTROL	46
4.5.1 SUBSYSTEM DEFINITION	46
4.5.2 PRELIMINARY DESIGN OVERVIEW	47
4.5.3 PRODUCT SELECTION	47
4.5.4 CONTROL LAW DESIGN AND ANALYSIS	49
4.5.5 RISK ANALYSIS AND MITIGATION	56
4.5.6 NON-TECHNICAL CONSIDERATIONS	57
4.5.7 PLAN OF PROCESSION	57
4.6 THERMAL MANAGEMENT	57
4.6.1 SUBSYSTEM DEFINITION	57
4.6.2 PRELIMINARY DESIGN OVERVIEW	58
4.6.3 PRODUCT SELECTION	58
4.6.4 THERMAL DESIGN AND ANALYSIS	59
4.6.5 RISK ANALYSIS AND MITIGATION	62
4.6.6 NON-TECHNICAL CONSIDERATIONS	62
4.6.7 PLAN OF PROCESSION	62
4.7 POWER MANAGEMENT	62
4.7.1 SUBSYSTEM DEFINITION	62
4.7.2 PRELIMINARY DESIGN OVERVIEW	63
4.7.3 PRODUCT SELECTION	63

4.7.4 POWER GENERATION DESIGN AND ANALYSIS	63
4.7.5 POWER STORAGE DESIGN AND ANALYSIS	66
4.7.6 RISK ANALYSIS AND MITIGATION	67
4.7.7 NON-TECHNICAL CONSIDERATIONS	67
4.7.8 PLAN OF PROCESSION	67
4.8 COMMAND AND DATA	68
4.8.1 SUBSYSTEM DEFINITION	68
4.8.2 PRELIMINARY DESIGN OVERVIEW	68
4.8.3 PRODUCT SELECTION	68
4.8.4 COMPUTER ARCHITECTURE DESIGN AND ANALYSIS	69
4.8.5 OPERATING REGIME PROTOCOL DESIGN AND ANALYSIS	71
4.8.6 RISK ANALYSIS AND MITIGATION	73
4.8.7 NON-TECHNICAL CONSIDERATIONS	73
4.8.8 PLAN OF PROCESSION	73
4.9 TELECOMMUNICATION	73
4.9.1 SUBSYSTEM DEFINITION	73
4.9.2 PRELIMINARY DESIGN OVERVIEW	73
4.9.3 PRODUCT SELECTION	74
4.9.4 TELECOMMUNICATIONS DESIGN AND ANALYSIS	75
4.9.5 RISK ANALYSIS AND MITIGATION	76
4.9.6 NON-TECHNICAL CONSIDERATIONS	76
4.9.7 PLAN OF PROCESSION	77
5 DESIGN BUDGETS	77
5.1 MASS BUDGET	77
5.2 VOLUME BUDGET	79
5.3 COST BUDGET	79
5.4 PROPELLANT BUDGET	81
5.5 POWER BUDGET	82
6 CONCLUSION	84
REFERENCES	85
APPENDICES	94
APPENDIX A: DEFINITION AND ASSESSMENT OF RISK	94
APPENDIX B: RISK TABLES	96
APPENDIX C: NON-TECHNICAL CONSIDERATION TABLES	104
APPENDIX D: GANTT CHART	111
APPENDIX E: ORGANIZATIONAL CHART	112

APPENDIX F: TEAM MEMBER RESPONSIBILITIES	113
APPENDIX G: STRUCTURES	114
APPENDIX H: MECHANISMS AND DEPLOYABLES	116
APPENDIX I: SPACEFLIGHT MECHANICS	124
APPENDIX J: PROPULSION	131
APPENDIX K: ATTITUDE DETERMINATION AND CONTROL	136
APPENDIX L: THERMAL MANAGEMENT	147
APPENDIX M: POWER MANAGEMENT	149
APPENDIX N: COMMAND AND DATA	154
APPENDIX O: TELECOMMUNICATION	159
APPENDIX P: SENSOR SUITE	164
APPENDIX Q: PRELIMINARY DESIGN REPORT	166

LIST OF FIGURES

- Figure 4.1.1: Top Down View
 Figure 4.1.2: Horizontal View
 Figure 4.1.3: Close Up of Cross Section
 Figure 4.1.4: FEA Model of Frame
 Figure 4.1.5: Stresses Caused by 6G Loading
 Figure 4.1.6: Stress Concentrations
 Figure 4.1.7: Strain Caused by 6G Loading
 Figure 4.1.8: Stress Caused by 7.15Hz Natural Frequency
 Figure 4.1.8: Stress Caused by 4.02Hz Natural Frequency
 Figure 4.2.1: Plascore’s CrushLite™ Material, with Option of Pre-Crushing
 Figure 4.2.2: RemoveDEBRIS Project’s Experimental Space Harpoon
 Figure 4.2.3: Schematic of Physical Model of Landing Legs
 Figure 4.2.4: Schematic of 90°Spaced Leg Deployment Angle
 Figure 4.2.5: NASA’s STEM Boom Design Options [10]
 Figure 4.2.6: Example of Deployable STEM Boom’s Cross Section
 Figure 4.2.7: Example of Deployable STEM Boom’s Compactness
 Figure 4.2.8: Perseverance Rover’s Robotic Arm and “Turret”
 Figure 4.2.9: SHERLOC and WATSON Sensors, Aboard Perseverance
 Figure 4.2.10: PIXL Sensor, Aboard Perseverance
 Figure 4.2.11: Conceptual Stowed Configuration of Solar Panel Arrays
 Figure 4.2.12: Conceptual Deployed Configuration of Solar Panel Arrays
 Figure 4.2.13: SMA-R&R Latch Mechanism Detailing Stowed Configuration
 Figure 4.2.14: SMA-R&R Latch Mechanism Detailing Deployed Configuration
 Figure 4.2.15: SMA-R&R Latch Mechanism with Removed Panel for Clarity
 Figure 4.2.16: Ansys CAD Model of Solar Panel Hinging Mechanism

- Figure 4.2.17: Ansys Static Structural Model, Detailing Loads and Supports
Figure 4.2.18: Equivalent Elastic Strain
Figure 4.2.19: Total Deformation
Figure 4.2.20: Maximum Principal Stress
Figure 4.3.1: JPL Small-Body Lookup Orbit Viewer
Figure 4.3.2: Proposed Orbital Trajectories of PV and CLP
Figure 4.3.3: CLP Engine Cutoff Analysis
Figure 4.3.4: Effect of Inclination Plane Change on Total Required Delta-V
Figure 4.5.1: Tetrahedral Configuration of Reaction Wheels
Figure 4.5.2: Three-Tiered Sensor Suite
Figure 4.5.3: System Level Orientation Control Block Diagram
Figure 4.5.4: Orientation PID Controller Block Diagram
Figure 4.5.5: Angular Velocity vs. Time ($\omega_0 = 6.5 \text{ rad/s}$)
Figure 4.5.6: Orientation vs. Time ($\omega_0 = 6.5 \text{ rad/s}$)
Figure 4.5.7: Control Moments vs. Time ($\omega_0 = 6.5 \text{ rad/s}$)
Figure 4.5.8: Angular Velocity vs. Time ($\omega_0 = 3 \text{ rad/s}$)
Figure 4.5.9: Orientation vs. Time ($\omega_0 = 3 \text{ rad/s}$)
Figure 4.5.10: Control Moments vs. Time ($\omega_0 = 3 \text{ rad/s}$)
Figure 4.5.11: Angular Velocity vs. Time ($\omega_0 = 1 \text{ rad/s}$)
Figure 4.5.12: Orientation vs. Time ($\omega_0 = 1 \text{ rad/s}$)
Figure 4.5.13: Control Moments vs. Time ($\omega_0 = 1 \text{ rad/s}$)
Figure 4.6.1: Structural Mesh with Loads for Thermal Analysis
Figure 4.6.2: Temperature Distribution From Thermal Analysis
Figure 4.7.1: Power Requirements by Mission Phase
Figure 4.7.2: Power Generation Throughout Mission
Figure 4.8.1: Command and Data Computer Architecture
Figure D1: Gantt Chart
Figure E1: Organizational Chart
Figure G1: HexTow HM54 Carbon Fiber Product Datasheet
Figure G2: Metco Aluminum 1100Gr Datasheet
Figure H1: Plascore CrushLite™ Honeycomb Crushable Material Datasheet
Figure H2: Pacific Scientific Energy Materials Company Separation Nut Datasheet
Figure H3: Schematic of Physical Model of a Single Proposed Dampened Landing Leg
Figure H4: Perseverance's Robotic Arm Imaging Equipment Datasheet
Figure H5: Perseverance's SHERLOC and WATSON Specification Sheet
Figure H6: Perseverance's Robotic Arm Collection Equipment Datasheet
Figure H7: SMA-R&R Conceptual Schematic
Figure J1: AST GmbH Cold Gas Thruster Datasheet
Figure J2: AST GmbH Electronic Pressure Regulator Datasheet
Figure K1: Honeywell IMU Spec Sheet

Figure K2: Redwire Coarse Sun Sensor Pyramid
Figure K3: Sinclair Interplanetary ST-16RT2
Figure K4: Suitable Star Trackers for Small Spacecraft
Figure L1: Looped Heat Pipe Specifications
Figure L2: Estimated Temperature Operation Ranges
Figure M1: Saft Lithium-Ion Battery Selections
Figure M2: Eagle Picher Lithium-Ion Batteries
Figure M3: Spectrolab UTJ Description
Figure M4: Spectrolab UTJ Characteristics
Figure N1: BAE Systems RAD750 6U Extended Datasheet
Figure N2: BAE Systems RAD5545 Space VPX Datasheet
Figure O1: HCT 400 or 437 MHz Heritage QHA Datasheet
Figure O2: ISIS-QMS-TPL-0045 S-Band Patch Antenna Datasheet
Figure O3: STC-MS03 S-Band TT&C Transceiver Datasheet
Figure P1: Rosetta's CIVA Sensor Unit Datasheet
Figure P2: Rosetta's APXS Sensor Unit Datasheet
Figure P3: Rosetta's COSAC Sensor Unit Datasheet
Figure P4: Rosetta's CONSERT Sensor Unit Datasheet
Figure P5: Rosetta's ROMAP Sensor Unit Datasheet

LIST OF TABLES

Table 2.3.1: Project Constraints
Table 2.4.1: Project Requirements
Table 3.2.1: Product Selection Table Based on Philae
Table 3.2.1: Product Selection Table Based on Philae
Table 4.1.1: Structures Product Selection
Table 4.1.2: Resonance Frequencies
Table 4.2.1: Mechanisms and Deployables Product Selection
Table 4.2.2: Calculated Properties of Solar Panels
Table 4.2.3: Tabulated Physical Properties of Aluminum Alloy from Ansys Materials Library
Table 4.2.4: Tabulated Data from Ansys Static Structural FEA Analysis
Table 4.3.1: 46P/Wirtanen Orbital and Physical Properties
Table 4.3.2: Spaceflight Mechanics Final Design Parameters
Table 4.3.3: Estimated Delta-V and Time Requirements by CLP Mission Segment
Table 4.4.1: Propulsion Product Selection
Table 4.4.2: Propulsion Tank Specifications
Table 4.5.1: Attitude Determination and Control Product Selection
Table 4.6.1 Thermal Management Product Selection
Table 4.7.1: Power Management Product Selection
Table 4.7.2: Solar Generation Inefficiencies

- Table 4.8.1: Command and Data Product Selection
Table 4.9.1: Telecommunications Product Selection
Table 5.1.1: Mass Budget
Table 5.2.1: Volume Budget
Table 5.3.1: Cost Budget
Table 5.4.1: Nitrogen Propellant Budget
Table 5.5.1: Power Budget
Table A1: Severity/Probability Risk Assessment Matrix
Table A2: Risk Acceptance and Approval Level
Table A3: Severity Definitions
Table A4: Probability Definitions
Table B1: Mission Risk Analysis and Mitigation
Table B2: Structures Risk Analysis and Mitigation
Table B3: Mechanisms and Deployables Risk Analysis and Mitigation
Table B4: Spaceflight Mechanics Risk Analysis and Mitigation
Table B5: Propulsion Risk Analysis and Mitigation
Table B6: Attitude Determination and Control Risk Analysis and Mitigation
Table B7: Thermal Management Risk Analysis and Mitigation
Table B8: Power Management Risk Analysis and Mitigation
Table B9: Command and Data Risk Analysis and Mitigation
Table B10: Telecommunication Risk Analysis and Mitigation
Table C1: Mission Non-Technical Considerations
Table C2: Structures Non-Technical Considerations
Table C3: Mechanisms and Deployables Non-Technical Considerations
Table C4: Spaceflight Mechanics Non-Technical Considerations
Table C5: Propulsion Non-Technical Considerations
Table C6: Attitude Determination and Control Non-Technical Considerations
Table C7: Thermal Management Non-Technical Considerations
Table C8: Power Management Non-Technical Considerations
Table C9: Command and Data Non-Technical Considerations
Table C10: Telecommunication Non-Technical Considerations
Table F1: Primary and Secondary Leads by Mission Component
Table F2: Report Sections by Team Member
Table G1: Carbon Fiber Coating Decision Matrix
Table H1: NASA Dampened Landing Leg Axial Strength Datasheet
Table H2: NASA Dampened Landing Leg Inclination and Velocity Datasheet
Table H3: NASA STEM Boom Thin-Ply Material and Form Factor Datasheet
Table H4: SMA-R&R Specification Sheet
Table H5: Pyrotechnic Separation Method Decision Matrix
Table H6: Telecommunications Radio System Decision Matrix

Table H7: Robotic Arm Decision Matrix
Table J1: Cold Gas Thruster Decision Matrix
Table J2: Propulsion Tank Material Selection Matrix
Table K1: IMU Decision Matrix
Table L1: MLI Material Decision Matrix
Table L2: Radiator Spec Sheet
Table N1: Command and Control Decision Matrix
Table N2: BAE Systems RAD750 Model Decision Matrix
Table O1: Secondary Patch Antenna Decision Matrix
Figure P1: Rosetta's CIVA Sensor Unit Datasheet
Figure P2: Rosetta's APXS Sensor Unit Datasheet
Figure P3: Rosetta's COSAC Sensor Unit Datasheet
Figure P4: Rosetta's CONSERT Sensor Unit Datasheet
Figure P5: Rosetta's ROMAP Sensor Unit Datasheet

LIST OF ACRONYMS

- ADCS - Attitude Determination and Control System
- AST - Advanced Space Technologies
- AU - Astronomical Unit
- BMR - Body Mounted Radiator
- CAD - Computer-Aided Design
- CGT - Cold Gas Thruster
- CLP - Comet Lander Probe
- EPR - Electronic Pressure Regulator
- ESA - European Space Agency
- FDR - Final Design Review
- FEA - Finite Element Analysis
- IMU - Inertial Measurement Unit
- JPL - Jet Propulsion Lab
- MPC - Model Predictive Controller
- PDR - Preliminary Design Report
- PHP - Powered Heating Pipe
- PI - Parallel Interface
- PV - Primary Vehicle
- R&R - Retention and Release
- RHU - Radioactive Heater Unit
- SMA - Shape-Memory Alloy
- SNR - Signal to Noise Ratio
- UHF - Ultra High Frequency

1 INTRODUCTION

Comets are the remains of the complex processes that formed the solar system billions of years ago. Scientifically, their compositions provide critical information regarding the formation of the early solar system and provide insight as to how carbon-based molecules were first brought to Earth [121]. Although numerous missions have been conducted to investigate the composition of comets, a majority of these missions have not landed on the comets to conduct experiments on their surface. Missions such as Stardust [70] only collected samples from the coma of the comet, Deep Impact only conducted impact testing and imaging [73], and the first mission to make a soft landing on a comet, Rosetta, failed to land properly and could not complete its scientific mission on the surface [71]. A more successful mission by JAXA, Hayabusa 2 successfully landed and conducted research on the asteroid Ryugu along with collecting a return sample [78]. The landing and experimentation on the surface of a comet provides superior scientific data as compared to orbiters, as a result of the diverse array of scientific experiments that can be conducted. Consequently, analyzing the physical properties and composition of both the surface and subsurface of a comet are the primary objectives for the Hercules CLP mission.

The Hercules Comet Lander Probe mission aims to conduct research on the short-period comet 46P/Wirtanen, the comet originally chosen for the Rosetta/Philae mission that was discovered in 1948 by Carl A. Wirtanen [2]. With its short orbital period and close proximity to Earth, it has been a notable scientific target for multiple space missions, but has yet to be investigated with a lander or other form of spacecraft. A notable characteristic of 46P/Wirtanen is the fact that it is a "hyperactive" comet - a comet that ejects more water than it should given the size of its nucleus, making this an even more attractive target [113]. Furthermore, an upcoming approach to Earth will allow for sufficient time to develop, launch, and reach this comet in August of 2029 [72].

The Hercules CLP mission intends to study the surface and composition of 46P/Wirtanen during its approach, landing, and subsequent ground studies while anchored to the comet. This report is focused on the final design of the CLP component of the mission and expands upon design decisions that were discussed in the Hercules Lander Probe Mission Preliminary Design Report. This includes a quantitative analysis of the decisions made, along with expectations for the performance of designs throughout the mission, and a discussion of work that still needs to be completed.

2 PROJECT SCOPE

2.1 CUSTOMER NEEDS

The needs of the customer pertaining to this mission are understood by both the team and the customer, and were agreed upon before this analysis began. These needs are listed below.

- CLP must be able to autonomously soft land on the target comet at the landing site identified by the PV and mission control
- CLP must be able to execute sustained exploration/data collection on the comet's surface, in order to maximize mission possibilities and findings
- CLP contains relevant sensor and analysis suite to collect scientific data, and must have the capacity to store this data temporarily until it is uplinked to the PV
- CLP must have two-way communication capabilities with the PV
- Proposed CLP design must properly account for public health and safety, global, cultural, social, environmental, economic, and professional ethics considerations
- Proposed CLP design must properly account for risk and seek appropriate means to mitigate such risks
- CLP must meet all proposed budgets agreed upon by the design team, customer, and launch vehicle vendor

2.2 OBJECTIVES

Mission objectives are considered to be either scientific goals or technical achievements that the mission hopes to accomplish. For scientific goals, this mission is designed to achieve the following:

- Categorization of the type of comet based on physical properties, such as size and mass
- Measure the elemental, molecular, and mineralogical composition of 46P/Wirtanen's surface and subsurface
- Drill into the subsurface in order to collect samples for microscopic inspection
- Analyze the lower atmosphere of 46P/Wirtanen
- Determine the age of the comet and its origin

In order to achieve these scientific goals, the following technical goals will also need to be accomplished:

- Safely land the CLP on the surface of 46P/Wirtanen in a desirable target location
- Deploy solar panels to create power needed for the scientific instruments and subsystems
- Keep all systems within operational limits of temperature, stress, and pressure

- Communicate regularly with the PV to relay both telemetry data and scientific data for eventual downlink to the DSN

Secondary objectives are not necessary for the success of the mission but can increase the yield of the mission once the primary objectives are met. These objectives are as follows:

- Relocate the CLP through a series of maneuvers to sample another area on the comet
- Dislodge a portion of 46P/Wirtanen's surface for detailed imaging and analysis by the orbiting PV

2.3 CONSTRAINTS

There is an abundance of constraints, both technical and non-technical, that increase the complexity of this project. The key constraints that have directly impacted the proposed design of this mission have been summarized below in Table 2.3.1.

Table 2.3.1: Project Constraints

Technical Constraints	<ul style="list-style-type: none"> • Delayed communication forces autonomous operation of the CLP • PV represents a singular point of failure for communications due to intermediate nature in communications chain • Relatively little information known about the environmental/geographical conditions of 46P/Wirtanen • Technical issues posed by individual subsystems (described in detail in subsequent sections) • Total payload (PV+CLP) mass is limited to launch capabilities of current launch vehicles
Time Constraints	<ul style="list-style-type: none"> • Limited launch window to reach 46P/Wirtanen at target location before waiting an additional 5 years • Abundance of deadlines agreed upon by the CLP design team and customer (outlined in Gantt chart) that must be met
Environmental Constraints	<ul style="list-style-type: none"> • Mission should not excessively pollute or disrupt the environment of 46P/Wirtanen or Earth • Technologies must be selected that properly consider impact to Earth's environment rather than purely for technical merit (RTGs were not selected for this reason)
Political Constraints	<ul style="list-style-type: none"> • Mission must ensure high probability of success due to the influence this mission will have on the general sentiment of the public towards space exploration • Funding for this mission is influenced by political opinions and current political parties holding office
Cost Constraints	<ul style="list-style-type: none"> • Mission must ensure a high probability of success due to the support from taxpayer dollars • Cost of mission is limited to financial capacity of the customer and funding from governmental agencies

2.4 REQUIREMENTS

Table 2.4.1 below summarizes the overall mission requirements and the subsystem level requirements that have been set forth and agreed upon by the customer and CLP design team.

Table 2.4.1: Project Requirements

Mission Level Requirements	
M1	CLP must be able to autonomously land on 46P/Wirtanen at a target site identified by the PV and mission control
M2	CLP must contain relevant sensor suite to conduct sustained exploration/data collection of the surface-ice, dust, and atmosphere of 46P/Wirtanen
System Level Requirements	
S1	CLP structure must be sufficiently strong enough to support the impact forces and vibrations from a pyrotechnic release, while being light enough to minimize the relative mass budget
S2	CLP must successfully deploy landing legs, a telecommunication antenna, solar panels, a harpoon, and a robotic arm for sample retrieval
S3	CLP design must use propellant efficiently and safely to avoid contamination of 46P/Wirtanen while landing on its surface
S4	CLP must be able to determine and control its orientation in normal and extreme circumstances
S5	CLP must be able to measure and control the temperatures required by different subsystems
S6	CLP must be able to generate and store enough power in order to follow a reasonable operating schedule that allows for efficient use of resources and time after landing on 46P/Wirtanen
S7	CLP must be able to autonomously monitor subsystems/payload, and carry out corrective or mitigative actions, in addition to the capability to process data and interpret external commands
S8	CLP must be able to effectively send and receive data to/from the PV

2.5 ASSUMPTIONS

The final design outlined in this report is reliant upon several key assumptions that influence nearly every aspect of this mission. These general mission assumptions are summarized below. Some individual subsystems have been designed with additional assumptions in the absence of more detailed information.

- All analysis and design selections were conducted in the metric system and follow standard engineering practices followed in the United States
- This mission has a preliminary launch window in November of 2028, and assumes that there will be sufficient time to complete all of the remaining development requirements necessary for a mission of this nature and complexity

- All design selections are assumed to be compatible with the PV and launch vehicle even though a PV and launch vehicle have not been selected for this mission
- The PV is assumed to depart from the CLP within the SOI of 46P/Wirtanen, such that two-body equations of motion are a valid model for the trajectory determination of the CLP and PV
- The PV is assumed to have a sensor suite that is capable of determining a viable landing site for the CLP
- It is assumed that the CLP design team has sufficient personnel, resources, expertise, and testing facilities to carry out the remaining portions of the design outlined in the plan of procession sections of individual subsystems
- In the absence of more detailed constraints communicated by the customer, similar previous missions and intuition have been used to develop appropriate mission budgets

3 MISSION OVERVIEW

3.1 MISSION SELECTIONS

After the consideration of many mission-critical criteria, such as the feasibility of the mission, the scientific significance of the research, the degree of coordination of the CLP design timeline with the approach window of the comet, and known physical properties like the gravitational attraction and terrain, the CLP team selected to land on 46P/Wirtanen. This comet shows superior potential scientific significance, time feasibility with the design schedule, and an optimal orbital period. Additionally, the ESA's prior selection of this comet provides a degree of validation to the CLP team's comet selection. While a fair amount of information is known about 46P/Wirtanen, there are still many unknown factors regarding the geography and physical properties of the comet. Consequently, reasonable expectations and crude analysis have been used when appropriate to safely design for these unknown conditions. Furthermore, some design selections, such as the target landing site, will be determined once additional information is gathered by the PV during the actual mission.

The proposed launch period of the PV and CLP is set to be in late November of 2028 in order to arrive on the surface of 46P/Wirtanen around August of 2029 at the desirable point in its orbit. However, if this timeline is deemed too aggressive for the expected design schedule, a new launch date can be accommodated for its next close approach in January of 2035 (which would require a launch around April of 2034). The scientific mission length is proposed to be approximately 18 months in length, starting from the CLP's touchdown landing with the comet. From there, it will deploy its self-sustaining mechanisms and conduct scientific experimentation that seeks to characterize the elemental, molecular, and mineralogical compositions of the ice and dust, as well as analyze the lower atmosphere of the comet. Once all the main objectives of the mission are met, a secondary mission that may be pursued is the relocation of the CLP to

another nearby location of interest. This would require the release of the tethering harpoon mechanism and the launch of the CLP from the surface of the comet in order to relocate itself.

3.2 SENSOR SUITE SELECTION

In order for the CLP to complete its scientific objectives, an array of scientific instruments are included in the CLP's sensor suite. The primary focus of these instruments is to collect scientific data such as images, molecular spectroscopy, gas compositions, nucleus radio and sound wave behaviors, and magnetic and plasma monitor behaviors in order to determine important attributes about 46P/Wirtanen and its role in the formation of the solar system and life on Earth. In Table 3.2.1, the scientific instruments that will be used onboard the Hercules lander are summarized by their role in scientific collection. This instrument suite is derived from the Philae probe used in the Rosetta mission, and is chosen for its high-level scientific capabilities and superior flight heritage [31].

Table 3.2.1: Product Selection Table Based on Philae [30, 31]

Component	Manufacturer	Model
Imaging System	ESA	CIVA (Comet Nucleus Infrared and Visible Analyzer), ROLIS (Rosetta Lander Imaging System)
Spectrometer		APXS (Alpha Proton X-Ray Spectrometer)
Gas Analyzer		COSAC (Cometary Sampling and Composition Experiment)
Radio Sounder System		CONSERT (Comet Nucleus Sounding Experiment by Radiowave Transmission)
Magnetic Sensor		ROMAP (Rosetta Lander Magnetometer and Plasma Monitor)

3.3 RISK ANALYSIS AND MITIGATION

The risk analysis and mitigation for the overall mission can be found in [Appendix B](#) Table B1.

3.4 NON-TECHNICAL CONSIDERATIONS

The non-technical considerations for the overall mission can be found in [Appendix C](#) Table C1.

4 DESIGN APPROACH

4.1 STRUCTURES

4.1.1 SUBSYSTEM DEFINITION

The structures subsystem outlines the design and analysis of the primary structure for the CLP. More specifically, the structures subsystem ensures that all necessary subsystems, devices, and mechanisms can be supported while being able to withstand any expected stresses with a factor of safety to ensure a successful mission. Furthermore, the structure of the CLP is a mass intensive subsystem that must be intelligently designed to limit the overall mass. Finally, in addition to being strong and light, the structure must be made with a material that is able to withstand the adverse climate of 46P/Wirtanen and deep space.

4.1.2 PRELIMINARY DESIGN OVERVIEW

The preliminary design of the structure described in the PDR specified a hexagonal shape that is made out of carbon fiber coated with a material that is able to enhance the thermal properties of the structure. The primary reasons for these selections were the great volume and rigidity that a hexagonal layout provided. For the material selection, carbon fiber's high strength to weight ratio makes it an attractive option for space applications, even with its known poor thermal properties.

This design must be able to provide ample internal volume for other subsystems and components, while also providing mounting points for external structures, such as solar panels, antennas, and so forth. The hexagonal structure accomplishes these requirements, while also providing a naturally rigid shape that is able to distribute loads that are placed on it. In the preliminary design of this subsystem, the landing of the CLP was identified as a critical phase of the mission for the structures subsystem. When the CLP touches down onto 46P/Wirtanen, it will experience a shock caused by its deceleration, and these forces, if not properly accounted for, can lead to the failure of the structure and potentially the mission. Consequently, there will be a design focus for conditions that exceed the potential forces the CLP will experience during landing. This will be accomplished by conducting a transient finite element analysis of the CLP under extreme loads that can be possible during landing.

4.1.3 PRODUCT SELECTION

This section seeks to define the products that will be used in the design of the structure moving forward. As decided in the PDR, carbon fiber is the desired material for the structure, and after thorough research, Hexcel has been selected as the supplier. Their HexTow® model of carbon fiber can be found in products such as the Airbus A350 and military V22 Osprey [48].

Additionally, the coating that has been previously discussed to assist with the poor thermal properties of carbon fiber has been decided to be aluminum as seen in Table G1. This

decision was made primarily due to its lightweight and favorable thermal properties under the application process that will be used.

Table 4.1.1: Structures Product Selection

Component	Manufacturer	Model
Carbon Fiber Frame	Hexcel	HexTow® HM54
Aluminum Coating	Metco	Aluminum 1100Gr

4.1.4 STRUCTURAL LOAD DESIGN AND ANALYSIS

The structure of the CLP must provide adequate protection of all internal components while allowing all components to be mounted to it. As specified in the PDR, a hexagonal structure was chosen to provide ample internal volume and external surface area.

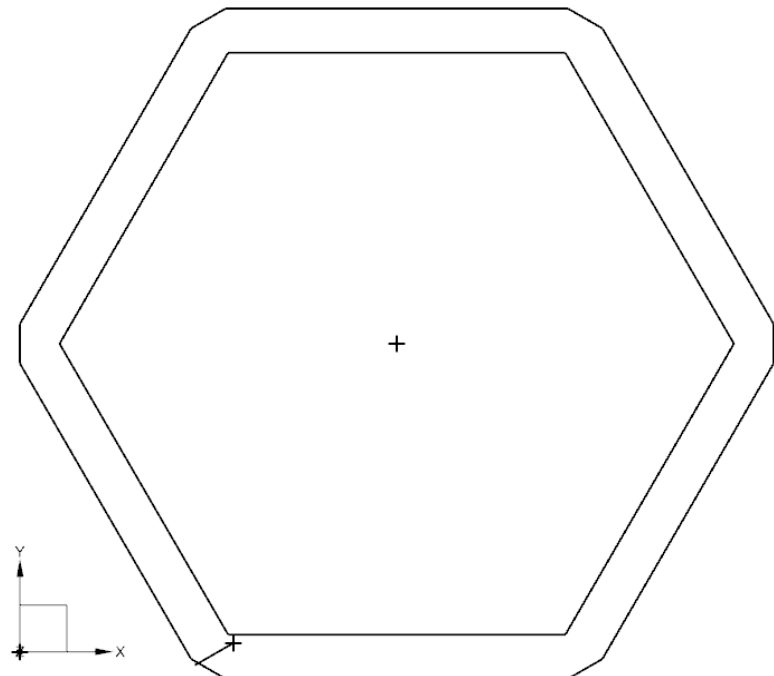


Figure 4.1.1: Top Down View

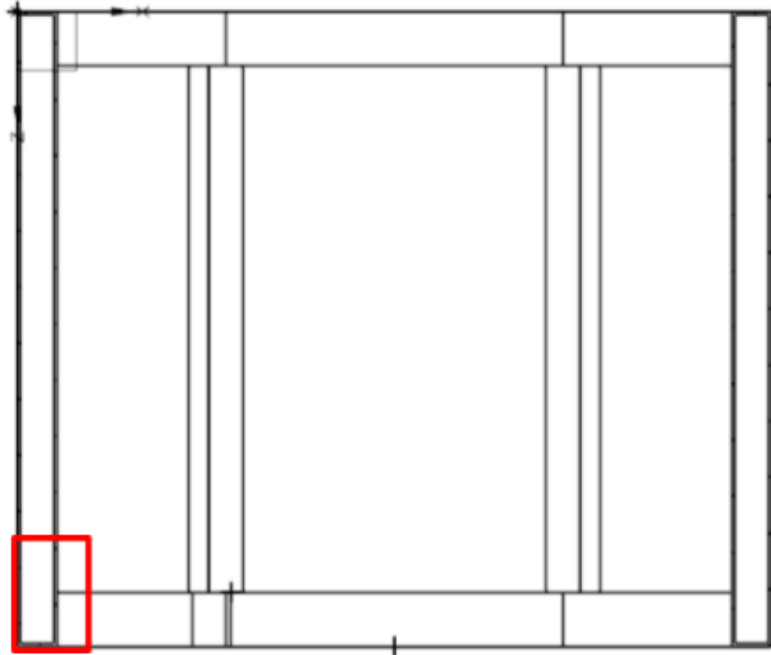


Figure 4.1.2: Horizontal View

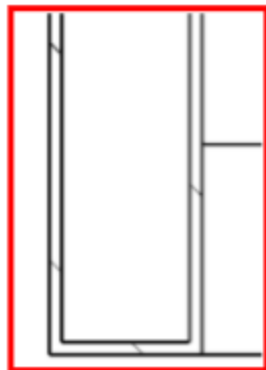


Figure 4.1.3: Close Up of Cross Section

In order to reduce the overall mass of the system, carbon fiber tubing was selected over solid beams. Due to its high tensile strength of 4,826 MPa [49], the design implemented thin walls that minimized mass while mitigating the risk of damage to internal components during the mission. Aluminum 7075 panels will also be included as face sheets on all six sides of the spacecraft for increased protection of internal systems, and greater rigidity and strength. However, it should be noted that the following analysis and model do not include these face sheets in order to limit the complexity of the design. Implementation of these panels will be outlined in section 4.1.7.

With the structural architecture decided upon, a model was created within NX to be able to perform FEA analysis and determine the integrity of the structure. Although the aluminum

face sheets will provide additional support, effectively altering the result of this model, this first pass serves as a proof of concept of the initially specified design parameters.

In the model shown below, two major forces were considered. The first of these was the 6G load that acts on the entire frame during liftoff. The solar panel mounts were also added to the frame to provide force at the 6G loading. This was done by creating a node at their assumed center of mass and connecting that node to nodes on the frame using RBE2 elements. As additional components and systems become more defined and their exact mass and manner of mounting become known, this model will be expanded to account for the appropriate additional loads.

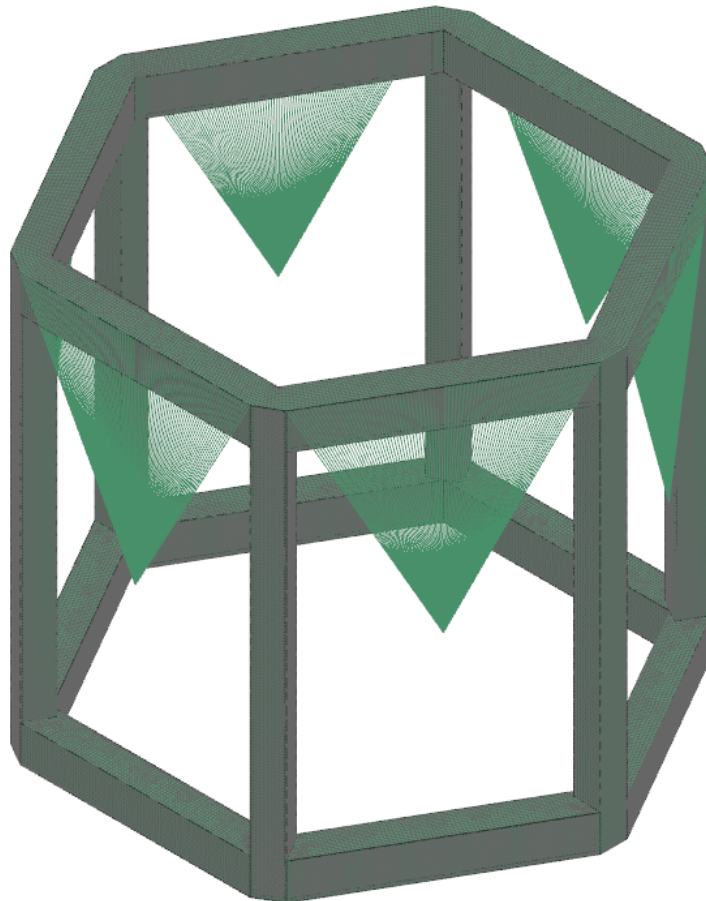


Figure 4.1.4: FEA Model of Frame

Once the model was run, the stress values were plotted on the model, as shown in Figure 4.1.4. The gradient on the left was set to have units of MPa and an upper limit stress value of the tensile strength of the material (4,826 MPa). As seen in the model, the maximum stress that occurred appeared at the joints of the tubes, but never exceeded 365 MPa, indicating that the structure is more than capable of handling this load. As more masses were connected to the model and the magnitude of the force exerted on it increased, this stress is clearly expected to

rise. However, this is not of great concern, as the aluminum panels will take much of this load off of the carbon fiber frame.

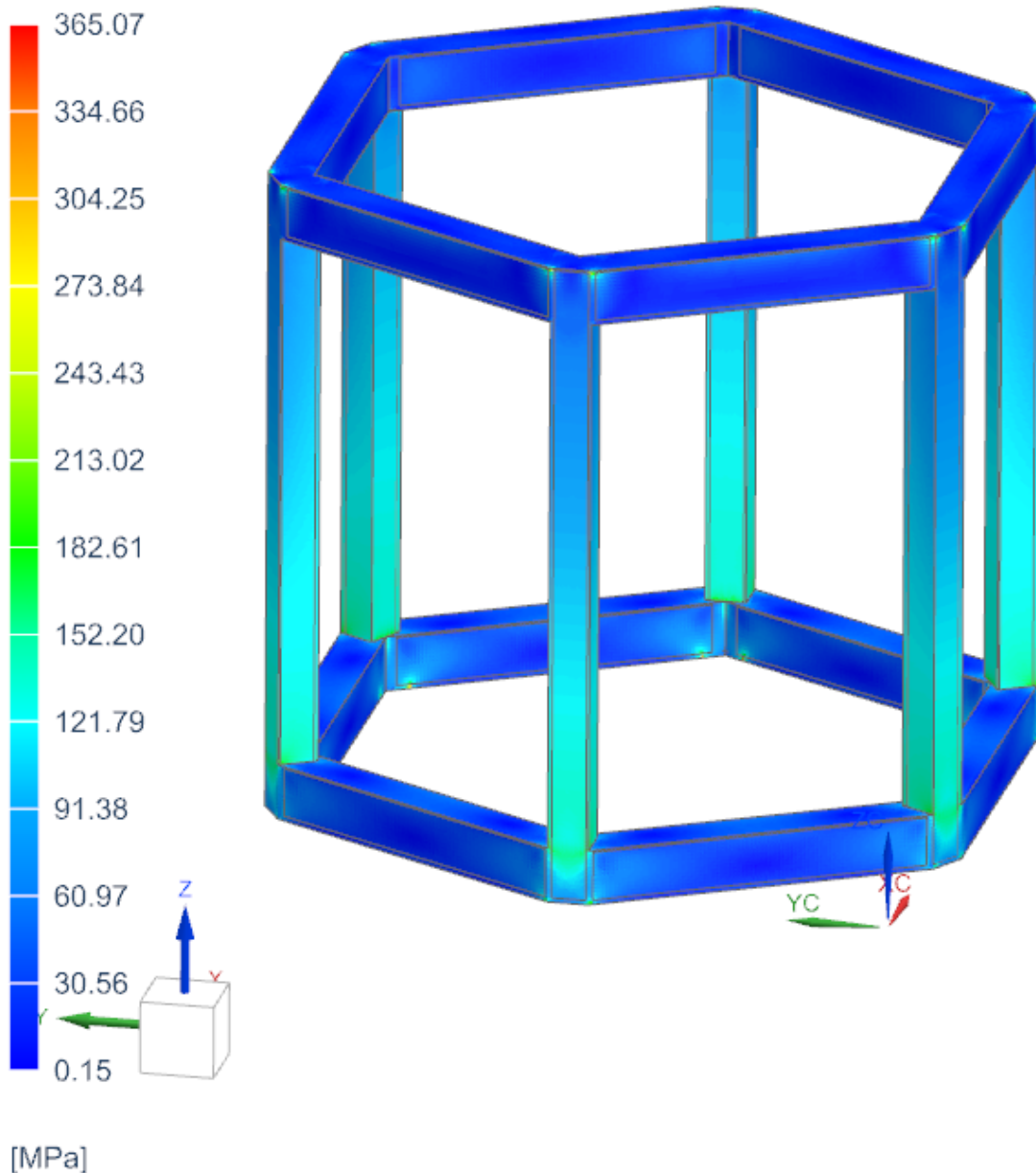


Figure 4.1.5: Stresses Caused by 6G Loading

It should be noted that the stress concentrations found on the base of the frame occur at the corners, as shown in Figure 4.1.5. This is due to the boundary conditions set there, which limit the motion in all directions. This was intended to be a rudimentary way of modeling the coupling points to the PV without having an idea of the precise functionality yet. As a result, the actual stresses experienced by the structure will likely be even lower.

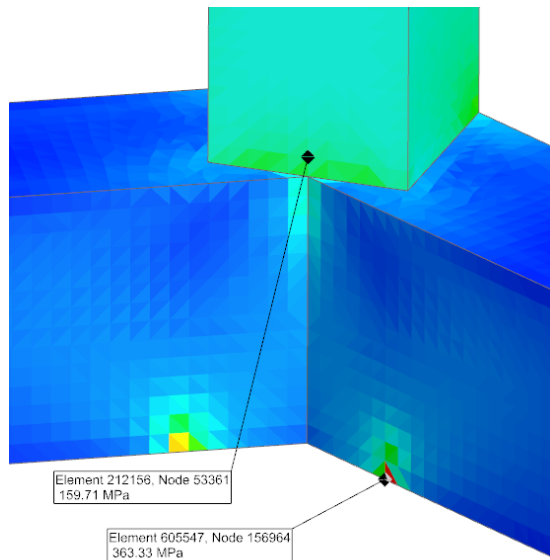


Figure 4.1.6: Stress Concentrations

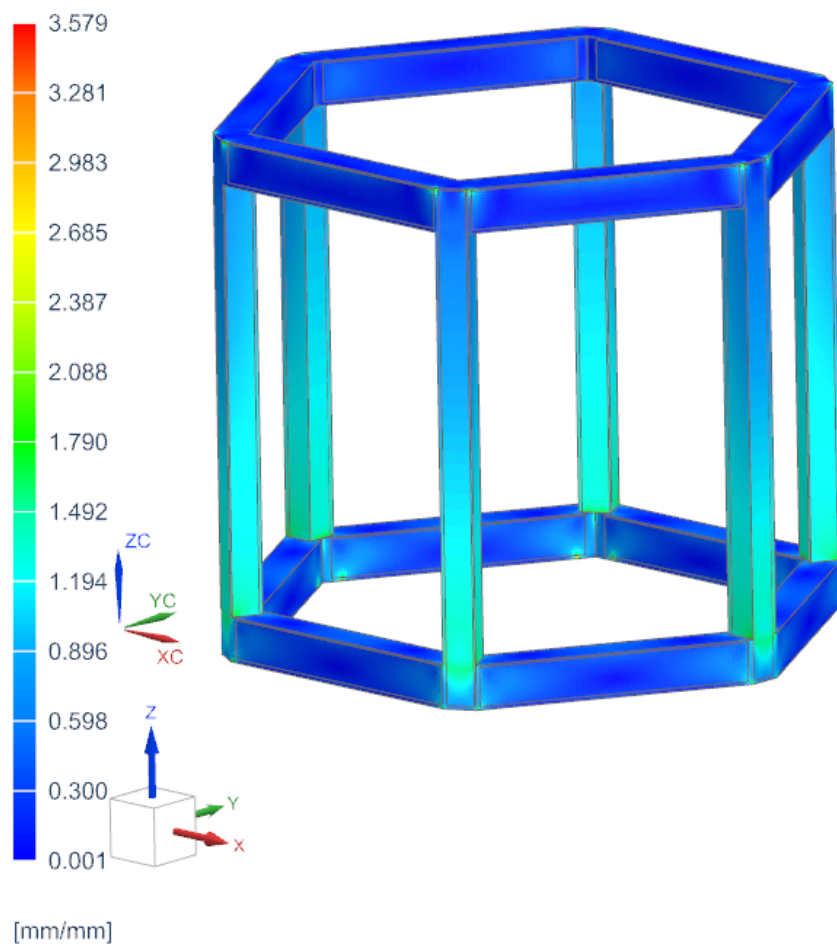


Figure 4.1.7: Strain Caused by 6G Loading

In the case of the strain in particular, a peak percent strain of 3.58% was reached, but the carbon fiber is said to fail at 1.3% strain based on the supplier's specifications. As previously discussed, however, the aluminum panels are expected to limit these strain values, although a refined model with the panels will be needed to verify this.

4.1.5 STRUCTURAL VIBRATIONS DESIGN AND ANALYSIS

The second major structural analysis that was conducted was a modal simulation that utilized the same FEA model as the previous results. Shown below are two stress plots caused by two different modes, or resonant frequencies, out of the ten found in this simulation. For all of the ten modes, the resonant frequencies and their corresponding peak stresses can be found in Table 4.1.2.

The first of these plots was from the mode 7 frequency and is shown due to the high relative stress and its distribution of stress throughout the structure. The additional stress found in this simulation suggests that further analysis must be conducted to investigate whether the carbon fiber tubing must be strengthened with additional material. The majority of resonant frequencies found in this analysis occurred at low frequencies due to the relatively low stiffness of the structure. This may be problematic due to the low resonant frequencies that are expected to occur on the launch vehicle. However, it is expected that once the aluminum panels are added to the structure, the natural frequencies found at these various modes will increase significantly, mitigating these concerns.

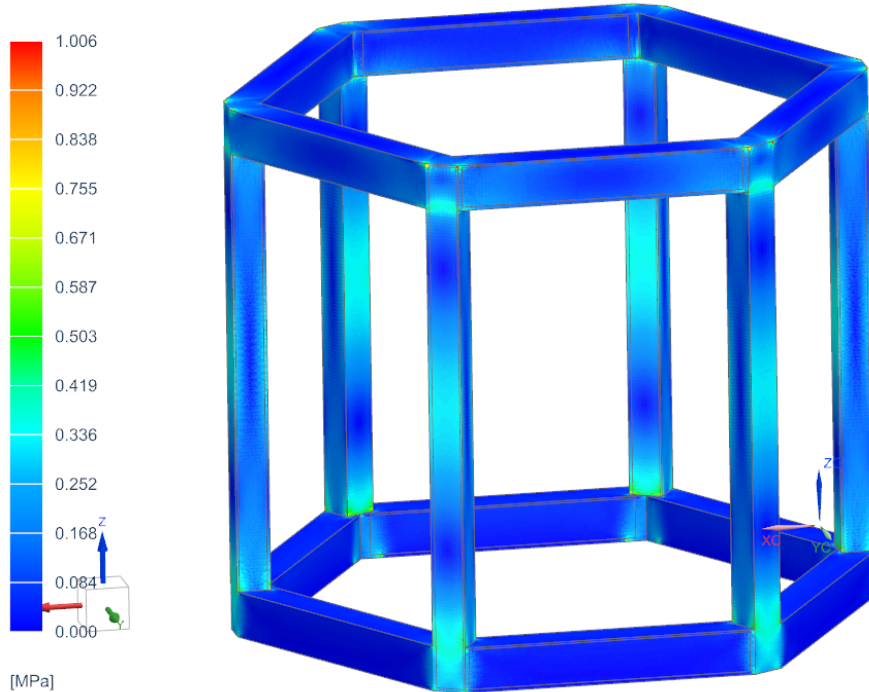


Figure 4.1.8: Stress Caused by 7.15 Hz Natural Frequency

In addition to the notable results from the mode 7 frequency, the mode 4 frequency (which occurred at 4.017 Hz) produced the highest relative stress (1.924 MPa) on the frame out of all of the simulated modes. These stresses, unlike the previously shown modal simulation result, were focused almost exclusively on the top corners of the frame at the connection points of multiple carbon fiber tubes, as shown in Figure 4.1.9.

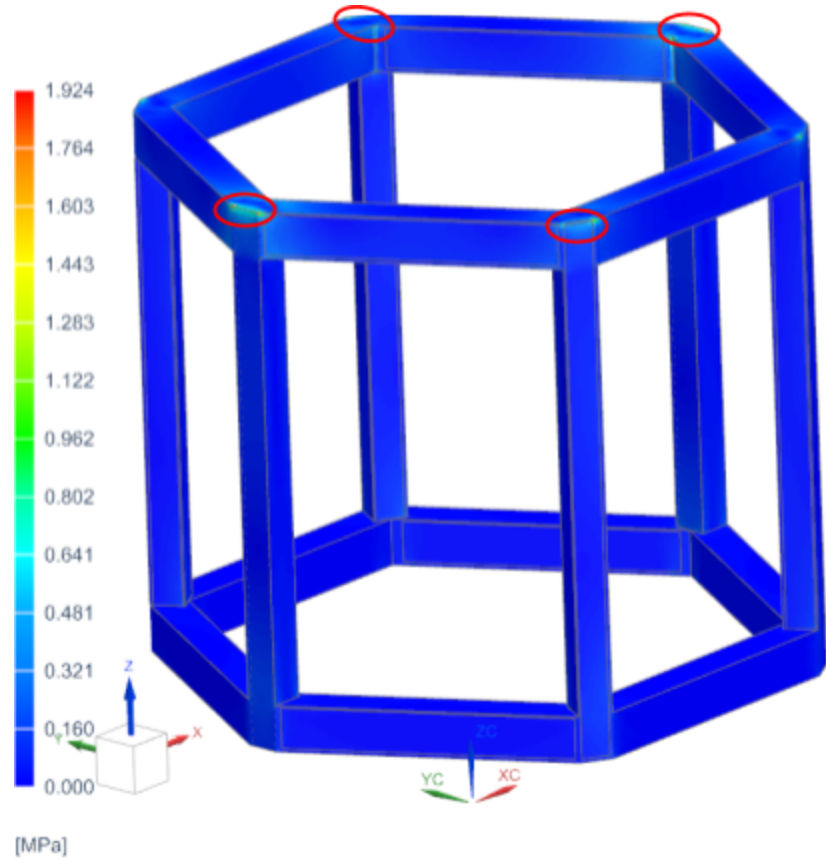


Figure 4.1.9: Stress Caused by 4.017 Hz Natural Frequency

Table 4.1.2: Resonance Frequencies

Mode	Frequency (Hz)	Peak Stress (MPa)
1	1.1770	0.169
2	1.1774	0.167
3	1.3867	0.138
4	4.0177	1.924
5	4.0202	1.871
6	6.1826	1.427
7	7.1525	1.006
8	7.5615	1.252
9	7.5625	1.252
10	7.8983	1.257

4.1.6 RISK ANALYSIS AND MITIGATION

The risk analysis and mitigation for the structures subsystem can be found in [Appendix B](#) Table B2.

4.1.7 NON-TECHNICAL CONSIDERATIONS

The non-technical considerations for the structures subsystem can be found in [Appendix C](#) Table C2.

4.1.8 PLAN OF PROCESSION

With the initial FEA analysis performed, there are still several necessary steps to increase the model's accuracy to the final product. The first of these is the addition of load cases that model the shock that will occur during landing on 46P/Wirtanen, and that will occur during separation from the primary vehicle. The honeycomb material will also need to be added into the model in order to assess its efficacy in the dampening of these shocks. Furthermore, the aluminum face sheets will need to be added to get a more accurate representation of the actual stresses experienced by the structure. Similarly, as exact models of individual components are brought into the model, mounting points will be finalized so that the space of all components is optimized and the mesh boundary condition can be refined. Finally, the decoupling mechanism will also be incorporated into the model to investigate how it will interact with the completed model.

4.2 MECHANISMS AND DEPLOYABLES

4.2.1 SUBSYSTEM DEFINITION

The mechanisms and deployables subsystem details the mechanical processes that must occur post-landing. Specifically, this subsystem will discuss the necessary machinery that will activate and deploy in order to complete the original scientific mission objectives. The main mechanisms that will be deployed are as follows: landing legs, solar panel arrays, a telecommunications antenna, and robotic arm for sample collection. This section will not only describe the mechanisms themselves, but also describe the decision-making process that was used in the selection of specific products, as well as a thorough numerical analysis of the mechanical interactions and mechanical dynamics at play.

4.2.2 PRELIMINARY DESIGN OVERVIEW

Based on the decisions made in the PDR, several general conceptual mechanisms were selected to be used in the final iteration of the CLP. These selections involved crude analysis and a rigorous down-selection process in order to decide upon the final design. The first selection that was made in the PDR involved the detachment of the CLP from the PV. It is the CLP design team's recommendation to the PV team that the CLP will detach from within the PV using explosive charges called pyrotechnics. The specific type of pyrotechnic device used will be separation nuts. The ability to control these charges, coupled with their ability to spontaneously activate with high accuracy, makes this detachment method an ideal choice.

The final stage of the spaceflight mechanics portion of this mission will involve the CLP approaching the target landing site from directly above it. Prior to impact, the CLP will deploy its landing base, consisting of four legs that fold outwards from beneath the chassis. These legs have independent rotational and extension abilities, allowing the CLP to balance on uneven surfaces. Once a successful landing is achieved, the legs may be actuated independently at any point to maintain a level standing relative to the surface of the comet. While not explicitly considered a deployable mechanism, an aluminum honeycomb crushable material will also be used to dampen the shock of landing.

As the CLP touches down on the surface of 46P/Wirtanen, it will also launch a high-velocity harpoon with a spiked point to penetrate the surface in order to achieve a physical tether and mitigate the risk of bouncing or relocation. In addition, once the harpoon has penetrated the surface, it will deploy anti-disengagement fins from within its spear pointed head in order to prevent unlatching from below the surface at the point of penetration.

Once landing has occurred, the post-landing mechanisms within the CLP may be deployed. Six solar panel arrays attached to the hexagonal body of the CLP will be deployed from a stowed position, in which each panel is initially parallel to one face of the CLP's main chassis. Successful deployment consists of rotating and folding the panels radially outwards and upwards. In addition, the panels will also have the capability of rotating on a perpendicular axis

relative to the original deployment axis of rotation, in order to face its photovoltaic cells towards incoming incident solar rays for maximum power generation.

Next, a telecommunications radio will be deployed. The telecommunications radio that is selected will be mounted atop a vertically telescoping mechanism. The mechanism will solely deploy the transmitter vertically upwards, due to the omnidirectional capabilities of the radio. The telescoping mechanism itself will allow for variable-height deployment, so that the telecommunications antenna may be deployed to an adjustable, desirable height depending on a number of factors.

Finally, upon completing these technical requirements and beginning the scientific experiments outlined in the mission objectives section, the CLP will deploy its mission-critical robotic arm. The robotic arm will have access to full mobility capabilities using advanced motors, and will be used to retrieve surface-ice and debris samples for further analysis by the interior tool suite. These items will be picked up efficiently and reliably using a three-roller system that requires little accuracy to draw the desired samples inwards.

4.2.3 PRODUCT SELECTION

In order to deliver the probe payload to Wirtanen's surface and complete the desired scientific objectives, specific concepts, designs, and products must be selected from real-world sources based on criteria that will operate in the conditions of deep space. Therefore, in the accompanying Table 4.2.1, products have been researched and have been selected for their superior properties and proven flight heritage. The manufacturer and model have been specified as well. The decision-making and justifications for the selection of each product, based on its ability to perform the assigned task, is explained further in their specific subsections. Furthermore, product datasheets will be provided in Appendix H, where applicable.

Table 4.2.1: Mechanisms and Deployables Product Selection

Component	Manufacturer	Model
Crushable Material	Plascore	CrushLite™
Pyrotechnic Release	Pacific Scientific Energetic Materials Company	2-502640 (Sep-Nuts)
Tethering Harpoon	Surrey Space Centre	RemoveDEBRIS
Deployable Legs	NASA	Custom
Telescopic Mast		Custom (STEM Boom)
Scientific Robotic Arm		Perseverance
Solar Array Deployer		Shape Memory Alloy - Retention & Release (SMA-R&R)

4.2.3.1 Shock Dampening Crushable Material

Previously, it was determined that a crushable material would be implemented in the structures to maintain CLP stability while it is within the PV. In addition to this task, crushable materials will also be implemented in the shock absorption in the landing legs upon touchdown. The CLP team has opted to move forward with the CrushLite™ material produced by Plascore, rated for its multitude of applications in industrial safety, transportation, and aerospace [92]. Plascore's crushable material has a wide range of properties that can be manufactured to the required specifications, including a wide range of densities, cell shapes, cell sizes, thicknesses, as well as corrosion and temperature ratings. In addition, Plascore offers the advantage of pre-crushed materials that will allow high predictability of energy absorption, especially in the activation of high-energy loads, such as in the pyrotechnics.

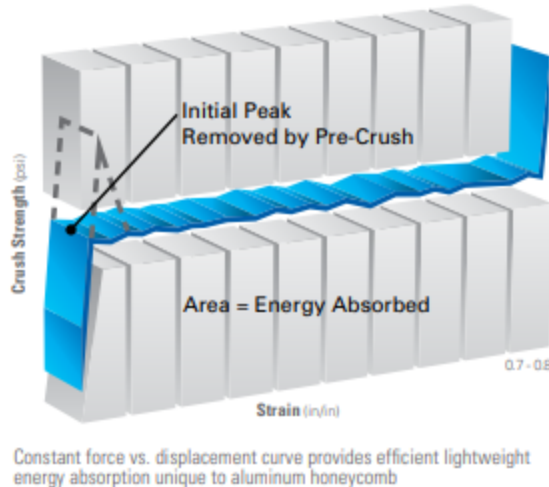


Figure 4.2.1: Plascore's CrushLite™ Material, with Option of Pre-Crushing [92]

Pre-crushing will be desired as it removes the unpredictability of sudden loading in the initially lower-density portion on the surface of the crushable material. As such, Plascore's crushable material product will be selected for its high customizability for the intended purpose, as well as providing an advantage via pre-crushing, while adhering to NASA's recommendation towards an aluminum honeycomb pattern for ideal and uniform energy dispersion [56, 40].

4.2.3.2 Pyrotechnic Release: Separation Nuts

The CLP team has also opted to use a pyrotechnically-actuated release mechanism, as previously determined. This will use separation nuts manufactured by the Pacific Scientific Energetic Materials Company, which were chosen for their flight heritage and implementation on the successful launch and landing of NASA's Apollo mission. They are also used in a wide variety of applications, such as rocket launches, CubeSat deployment systems, antennas, scientific instruments, solar arrays, booms, masts, satellites, spacecrafts, and payloads [89].

Separation nuts provide both initial restraint, as well as release when desired, upon receiving an electrical signal. Their high fastening strength and on-demand nature of actuation are highly desirable in a timing-critical space mission. From the specifications provided, the separation nut can fire upon demand on the order of several milliseconds, as opposed the several full seconds a mechanically-based actuation would require. In addition, these separation nuts will operate in a large range of temperatures of -53°C to over 100°C, rendering them ideal for conditions in deep space. Lastly, their load capacity can accommodate over 13,000 kg axially, which is well over the mass envelope determined for the overall CLP [89]. Considering these criteria, the separation nuts produced by the Pacific Scientific Energetic Materials Company will be an optimal choice.

4.2.3.3 Surface Penetrating Tethering Harpoon

Next, upon landing on 46P/Wirtanen's surface, the CLP will explore a relatively new solution devised by the RemoveDEBRIS project, in partnership between the European Commission and the Surrey Space Centre [4]. The RemoveDEBRIS project consists of a mission in which a payload, in the form of a satellite platform, is launched and propelled to the International Space Station via SpaceX's Falcon 9 rocket. Once orbit is successfully achieved, scientific experiments will occur to analyze effective methods to complete the payload's mission: retrieval of space debris. The project aims to use a high-speed harpoon to deploy and strike pieces of space debris and metal [4].

Due to the high-speed and high-energy nature of the deployment of the harpoon, penetration is achieved, allowing for the satellite to reel the debris back to the station base. The RemoveDEBRIS team has already prototyped a product for this purpose, designating it a "space harpoon" [23]. An initial experiment has even been successfully conducted, allowing for a launch speed of 20 m/s [112].



Figure 4.2.2: RemoveDEBRIS Project's Experimental Space Harpoon [23]

The CLP team acknowledges the conceptual and experimental nature of this product. As such, for the successful deployment of such a system, further engineering analysis must occur. In the absence of a finished product to select, the CLP team recognizes the need for the following analysis to occur: mass envelope of the harpoon assembly in order to achieve high momentum in relation to the CLP's overall mass budget, material selection, and bending rigidity for protection against sudden shock from striking the comet's surface, design of the tip geometry, hardness determination, construction for successful penetration, and physical properties of the attached tether for successful reeling. While constrained by the timeline of this project, the CLP team believes that a working version of this product would be extremely feasible if the aforementioned analysis was conducted.

4.2.3.4 Deployable Landing Leg Base

Next, the CLP team has selected a style of the landing base from the design choice made previously in the PDR. The deployable legs in this landing base system are based on a design and model developed by NASA. This will consist of a main beam element using a pinned connection to the underside of the probe, supported by an off-angle beam, also using a pinned connection to the underside. The leg will also have a hinged, flat plate upon which it will rest on for stability on the comet surface. Four legs will be implemented, separated by 90° between each.

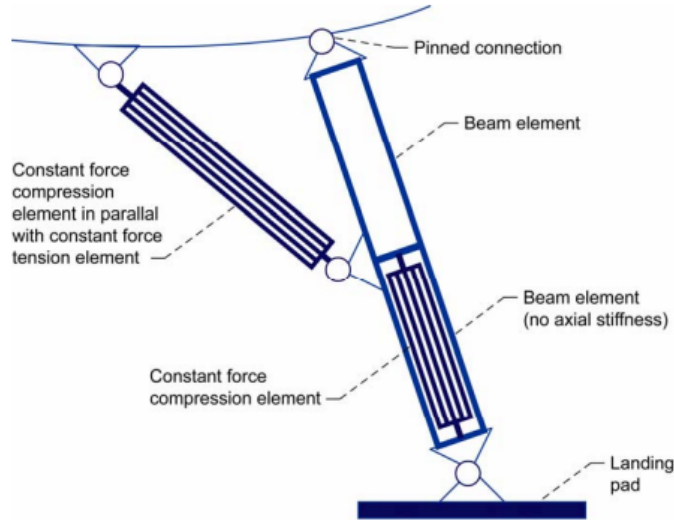


Figure 4.2.3: Schematic of Physical Model of Landing Legs [61]

In addition, a combination of pistons within the leg strut and compressible, crushable material will be implemented for energy absorption. The crushable material will again be the crushable product from Plascore in a honeycomb pattern for maximum energy dispersion, primarily from the energy of surface touchdown. A secondary objective of these

compression-loaded struts aims to absorb energy from uneven loading on a leg due to the uneven surface of the comet.

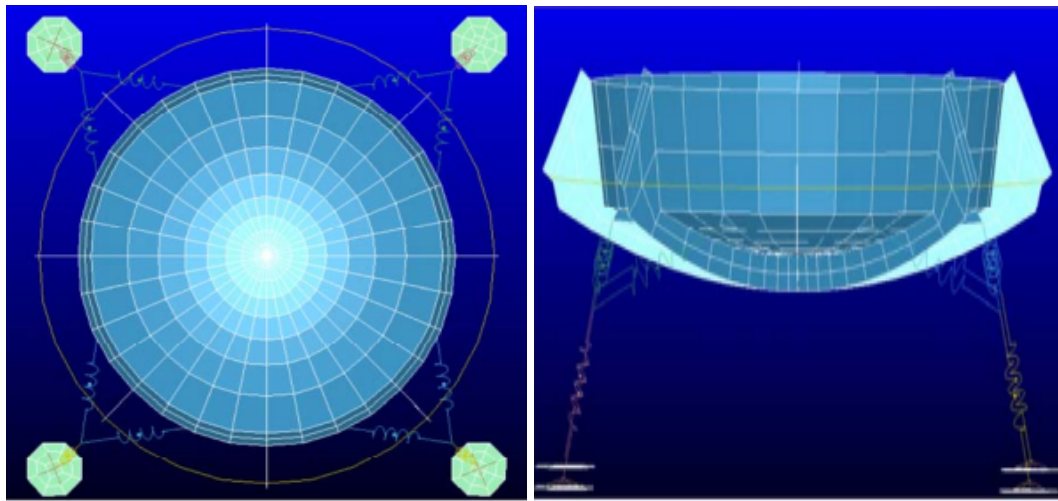


Figure 4.2.4: Schematic of 90° Spaced Leg Deployment Angle [61]

4.2.3.5 Telecommunications Radio Stem Boom

After achieving a successful landing, the CLP will also need to deploy its telecommunications antenna for successful wireless transmission of information back to the PV. Due to the selection of a telecommunications device with omnidirectional transmission capabilities, rotational orientation will not be considered a priority. Instead, height will be the primary focus, where the optimal height will be when line-of-sight can be ideally achieved between the transmitter and receiver. In this case, a telescoping mast will be utilized [38]. Once again proposed and designed by NASA, this telescopic arm will use NASA's STEM (Storable Extendible Tubular Member) boom technology.

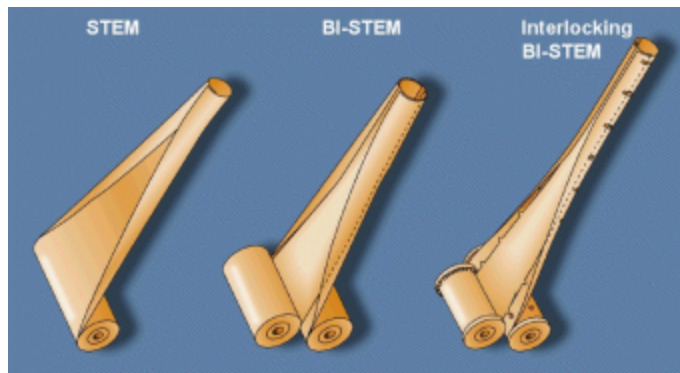


Figure 4.2.5: NASA's STEM Boom Design Options [38]

Two long, flat members are adhered to one another, leaving a gap between the fastened outer edges. These combined members are flexible enough to be rolled upon themselves, similar

to that of a roll of a tape, with a high rigidity when deployed, in which the gapped portion mechanically expands [38]. When stowed, this mechanism is extremely compact, primarily due to its ability to collapse flatly and roll up on itself.

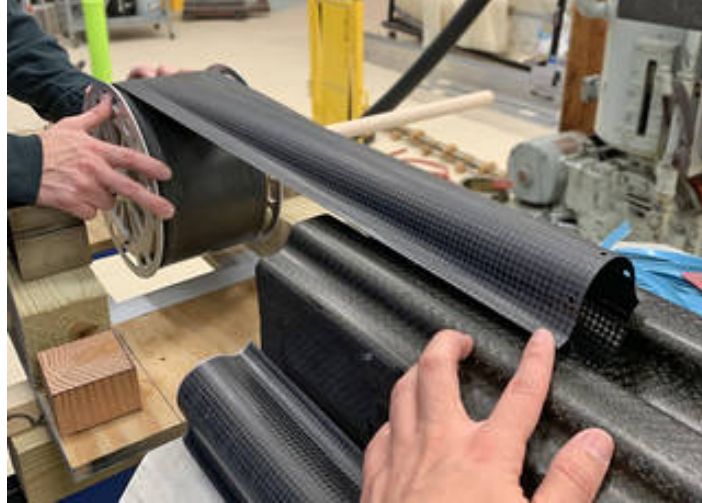


Figure 4.2.6: Example of Deployable STEM Boom's Cross Section [116]

Considering the collapsibility of this mechanism even when using a high-rigidity, high-strength material, low volume-mass profile, along with its superior flight heritage stemming from the 1960s, this telescopic mast implementing a STEM boom is highly desirable [38, 116].

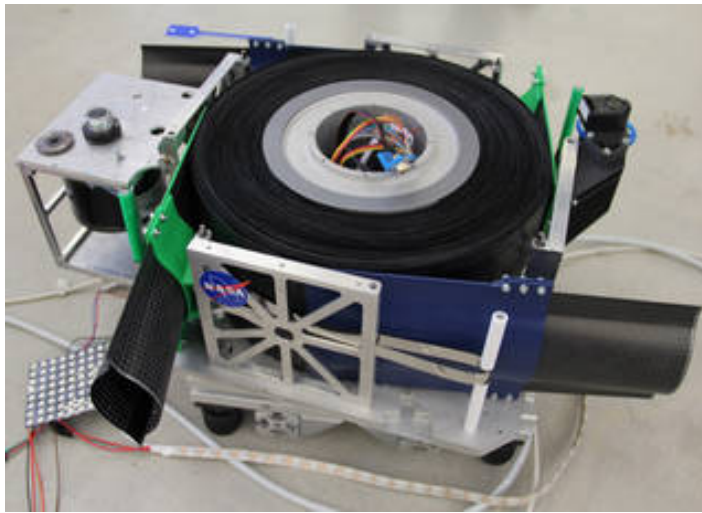


Figure 4.2.7: Example of Deployable STEM Boom's Compactness [116]

4.2.3.6 Manipulable Robotic Arm

Once the CLP has made a successful landing on 46P/Wirtanen's surface and deployed its essential mechanisms for self-sustaining operations, the CLP will be ready to execute its scientific objectives. In order to execute its scientific mission, the CLP will operate a robotic arm

to work with the samples of interest on the comet surface. A robotic arm modeled after the one aboard the Perseverance Rover in the 2020 Mars Space mission has been selected for this endeavor [81].

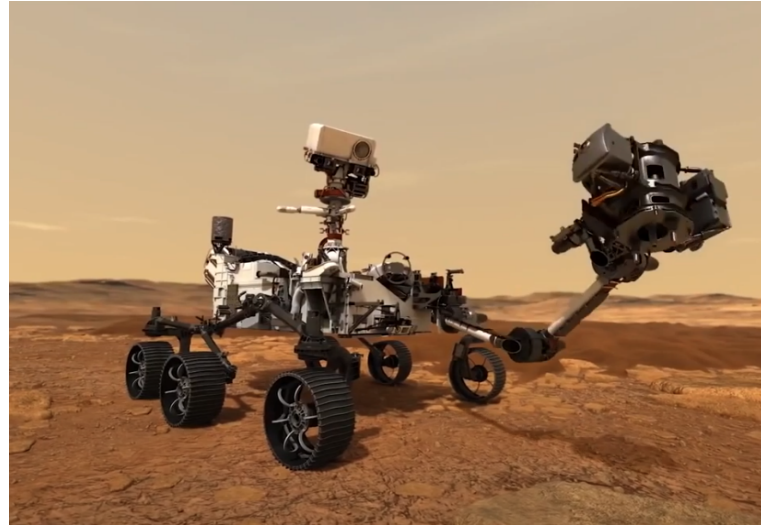


Figure 4.2.8: Perseverance Rover’s Robotic Arm and “Turret” [39]

This robotic arm has several desirable features that will aid in the successful completion of the proposed scientific mission. The robotic arm has a total extended length of 2.1 meters (7 feet), paired with five rotational degrees of freedom, providing superior maneuverability and reach within its work envelope. In addition, its end effector consists of a “turret” mechanism, housing several specialized tools, including high-strength drill bits, scientific mineral and chemical-analyzing sensors, and cameras [81].

The cylindrical drill bit set aboard the robotic arm will be able to cut and remove 1-inch core samples from the surface for collection and on-board analysis. In addition, a specialized drill bit will allow for collection of loose rocky material from the surface, known as “regolith”. In order to collect these samples, a final specialized bit known as an “abrader” will be used to scrape and induce wear on a desired surface in order to expose a fresh, unweathered surface for analysis [39, 52, 81].

The “turret” will also feature several sampling instruments. A paired sensor suite, known as SHERLOC (Scanning Habitable Environments with Raman & Luminescence for Organics and Chemicals) and WATSON (Wide Angle Topographic Sensor for Operations and eNgineering), will work in conjunction to study mineral samples in close proximity with the arm. SHERLOC will utilize spectrometers, lasers, and a camera for potential signs of organic matter, minerals, and water that may indicate signs of past microbial life. The WATSON camera aids SHERLOC by magnifying the image texture and quality from SHERLOC. Lastly, the PIXL (Planetary Instrument for X-ray Lithochemistry) instrument is used to image surfaces, seeking changes in texture and chemical make-up, allowing for the identification of ancient microbial life and the selection of the most scientifically interesting targets [79, 80, 81, 82].

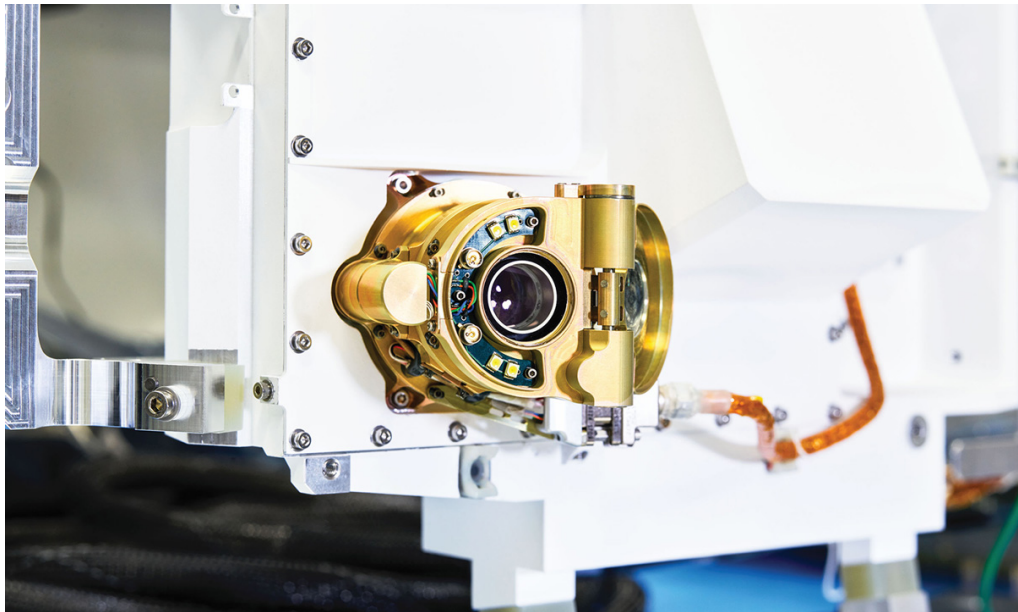


Figure 4.2.9: SHERLOC and WATSON Sensors, Aboard Perseverance [82, 79]

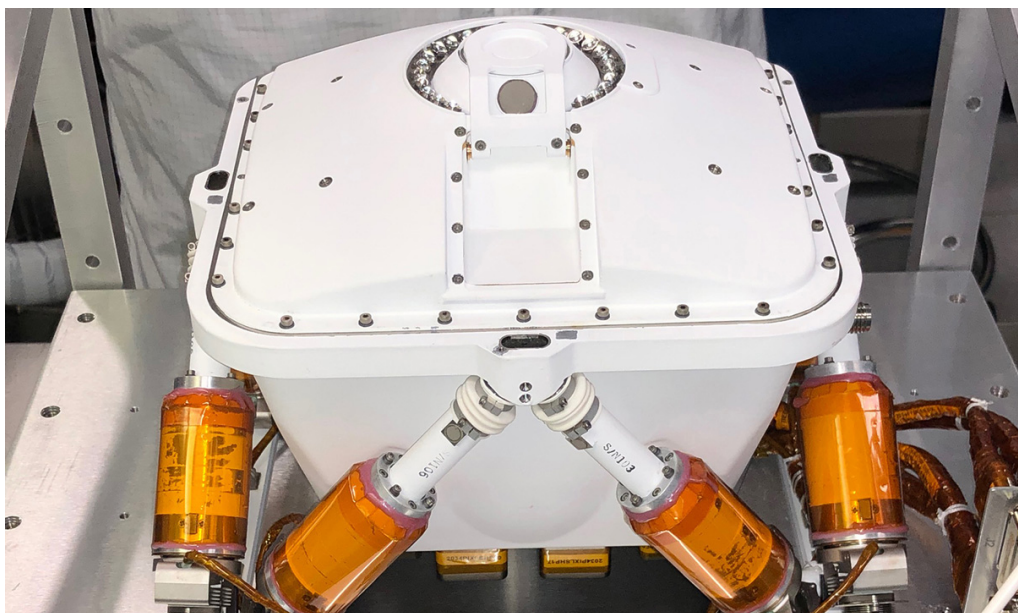


Figure 4.2.10: PIXL Sensor, Aboard Perseverance [80]

Using a robotic arm developed based on the Perseverance rover provides the CLP team with greater confidence in the lander's ability to collect and analyze surface-ice, dust, debris, and mineral samples. However, the CLP team acknowledges that, given the necessary time frame, further engineering analysis would be performed to ensure that this product is appropriate for all aspects of this mission. A completely original design may also be proposed if this was deemed desirable.

4.2.4 FINAL ANALYSIS: SOLAR PANEL DEPLOYMENT

Because the solar panel array is imperative to the success of the overall mission, the CLP team has opted to conduct in-depth engineering analysis on this subsystem. Based on the overall power requirements of the various subsystems, a preliminary power schedule was developed by the power management team, and the required surface area and mass of space-grade solar cells was specified. Using these specifications, an FEA model was generated to analyze the critical solar panel deployment mechanism.

In order to deploy the selected solar panel array, the CLP team decided to use a derivative mechanism based on a NASA model called the SMA-R&R (Shape-Memory Alloy Retention and Release) system. SMAs are metallic alloys that may be deformed as desired in a cold state, but will return to their previous “remembered” state when heat is applied. In this application, an SMA will be used as a retention standoff, in which its heated state will cause it to extend, releasing a retention latch system [45]. Similar to pyrotechnic devices such as pin-pullers or separation nuts, heat is applied when an electrical signal is provided via a wiring harness. Initially, in their stowed configuration, the solar panels will remain parallel to the body of the CLP. One solar panel will correspond to each of the six faces of the hexagonal probe structure. A hinging system will also be used at the top edge of each face, allowing the panels to radially fold outward when deployment is required.

Figures 4.2.11 and 4.2.12 show the conceptual stowed and deployed configurations of the solar panels along the CLP’s faces. Their primary purpose is to show the actuating hinges that will allow for the panels to deploy, rather than actual configuration angles and orientation. The panels in the CLP design will instead face outwards when stowed, and are actuated by hinges near the top edge of the body when deployed. In addition to the solar panels facing outwards as opposed to inwards when stowed, the solar panels will deploy to a maximum angle of 90 degrees from the body, rather than the near-180 degree deployment angle depicted.

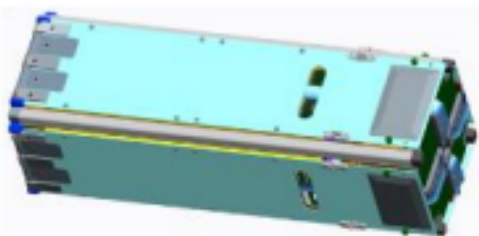


Figure 4.2.11: Conceptual Stowed Configuration of Solar Panel Arrays [45]

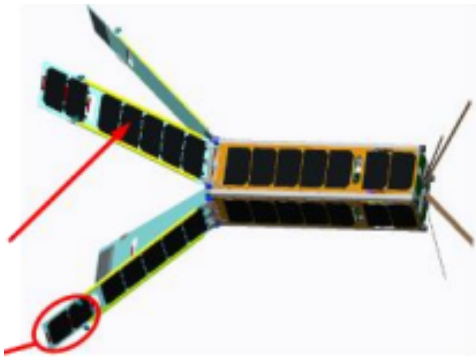


Figure 4.2.12: Conceptual Deployed Configuration of Solar Panel Arrays [45]

Figures 4.2.13 and 4.2.14 show the mechanical actuation associated with the SMA-R&R system. Initially, a single solar array is stowed in a parallel state to the body. Retention hooks, built into the solar array, are latched onto the central SMA-R&R system, composed primarily of two base plates compressed by a standoff-spring system. The base plates are held close together via a pinned connection between the plates. A single pin slides into the hole, disabling movement, while keeping the springs compressed and primed. However, once heat is applied to a circuit board between the plates via an electrical signal, a connected SMA-based pin puller will attempt to return to its original state, in which the pin is retracted. This will remove the retaining pin from the pinned connection, allowing the board to quickly separate due to the release of potential energy in the compressed springs returning to an equilibrium state. The extension causes the retention latches to fall out of alignment, releasing the solar panels from their rigid holding against the CLP body.

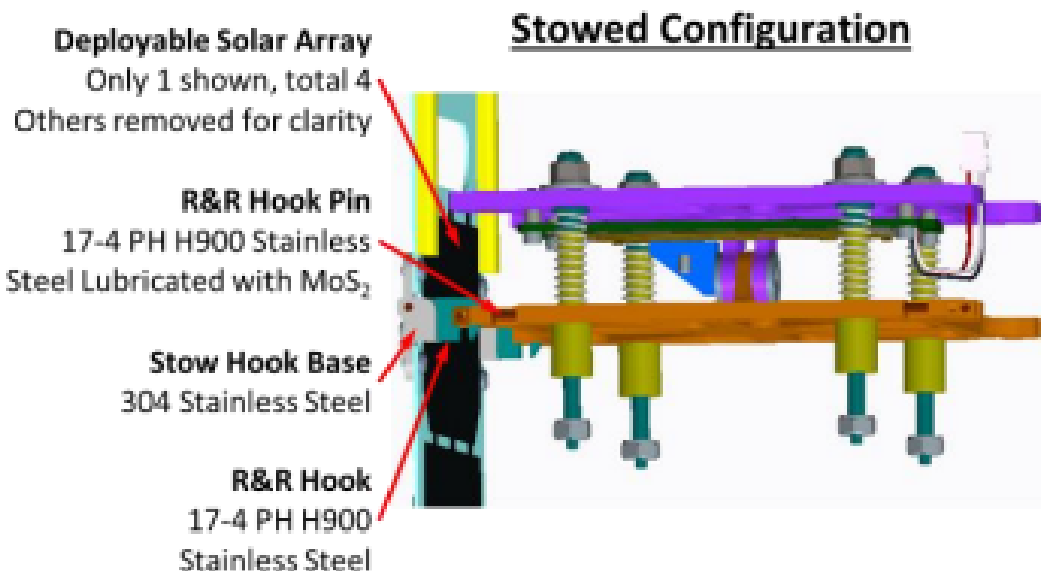


Figure 4.2.13: SMA-R&R Latch Mechanism Detailing Stowed Configuration [45]

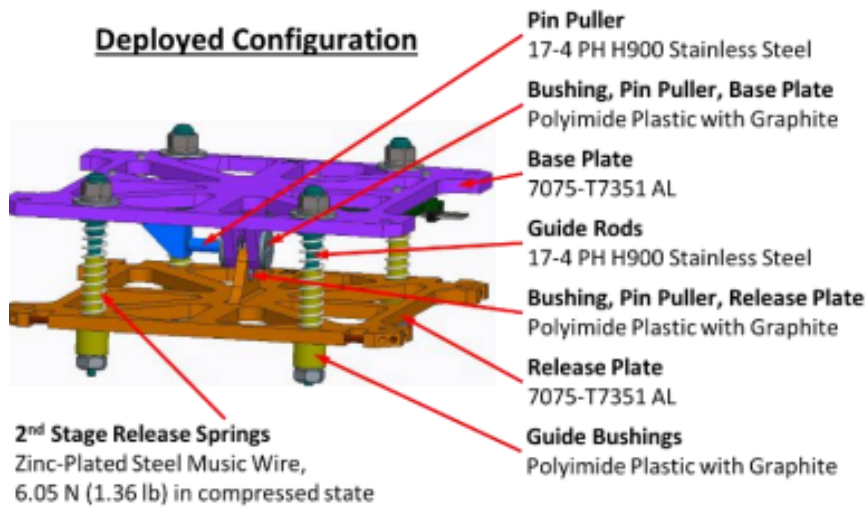


Figure 4.2.14: SMA-R&R Latch Mechanism Detailing Deployed Configuration [45]

Figure 4.2.15 shows the pin puller mechanism in greater clarity, with the bottom base plate removed. With the securing pin disengaged, the plates are free to move away from each other, giving the retention pins clearance to unlatch.

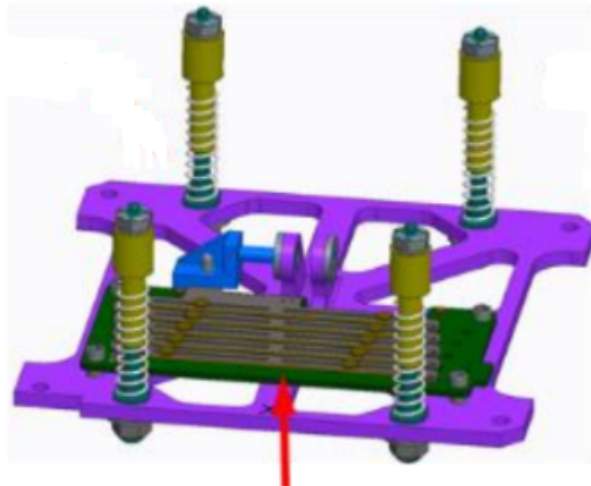


Figure 4.2.15: SMA-R&R Latch Mechanism with Removed Panel for Clarity [45]

Due to the relative simplicity of the SMA-R&R system and the low predicted chance of failure, analysis is chosen to be conducted on the mechanical deployment of the solar arrays. Specifically, given a solar panel configuration based on bounding dimensions and mass, a bending moment analysis was conducted to ensure a successful radial rotation without permanent deformation or failure to the hinge mechanism, which is the interface between the actuator and solar panel. The following Table 4.2.2 describes the CLP team's analysis of the peak

power requirement obtained from the preliminary power schedule, as well as the necessary dimensions and mass of the solar panel to achieve these power requirements. Each of the six solar arrays present on the vehicle will require a rectangular area of 0.372 m^2 , resulting from a length and width value of 0.87 m by 0.42 m, respectively. Based on the density of the selected solar panel and the necessary surface area, the mass of each solar panel was estimated to be about 4 kg. Furthermore, due to each individual solar panel having a rectangular profile, the resultant force from the weight of the panel can be resolved to occur at half the length of the solar panel, starting from the hinging point with the CLP. It should also be noted that the weight properties calculated in the following analysis are based on the gravitational acceleration on 46P/Wirtanen due to the lower gravitational parameter.

Table 4.2.2: Calculated Properties of Solar Panels

Parameter	Value
Mass of Single Solar Panel	4 kg
Total Mass of all (6) Solar Panels	24 kg
Weight of Single Solar Panel	39.24 N
Length of Single Solar Panel	0.87 m
Width of Single Solar Panel	0.42 m
Surface Area of Single Solar Panel	0.37 m^2
Total Surface Area of all (6) Solar Panels	2.23 m^2
Location of Resultant Force Along Length	0.44 m
Resulting Bending Moment of Single Solar Panel	17.07 N·m

The remainder of this section will describe the engineering analysis of an individual solar panel and the stress that it places on a hinge. Figure 4.2.16 shows a 3D CAD model of the hinging mechanism that will allow the solar panel to rotate within the finite element analysis software, Ansys. Its four-pronged design allows for multiple fastening points with the solar panel, which will be advantageous for distributing the loads placed on the solar panel. Furthermore, an aluminum alloy has been selected as the material for this mechanism due to its high strength-to-density ratio, which is shown in Table 4.2.3.

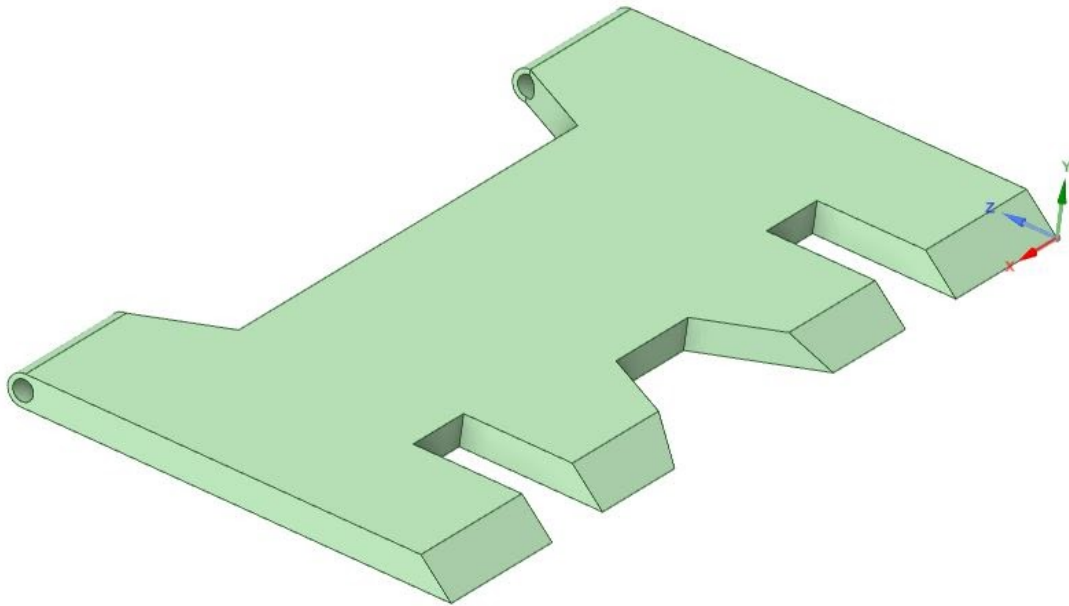


Figure 4.2.16: Ansys CAD Model of Solar Panel Hinging Mechanism

Table 4.2.3: Tabulated Physical Properties of Aluminum Alloy from Ansys Materials Library

Mechanical Property	Value
Density	$2770 \frac{\text{kg}}{\text{m}^3}$
Coefficient of Thermal Expansion	$2.3 \cdot 10^{-5} \text{ } ^\circ\text{C}^{-1}$
Young's Modulus of Elasticity	$7.1 \cdot 10^{10} \text{ Pa}$
Poisson's Ratio	0.33
Bulk Modulus	$6.96 \cdot 10^{10} \text{ Pa}$
Shear Modulus	$2.67 \cdot 10^{10} \text{ Pa}$
Tensile Yield Strength	$2.8 \cdot 10^8 \text{ Pa}$
Compressive Yield Strength	$2.8 \cdot 10^8 \text{ Pa}$
Tensile Ultimate Strength	$3.1 \cdot 10^8 \text{ Pa}$

In the following analysis, a hinged support is placed at the cylindrical holes in the plate. As a result, only axial rotation will occur. The previously calculated bending moment is applied at the tabbed ends in order to simulate the load the solar panel will apply on the hinge plate in Figure 4.2.17. Then, finite elements of 0.005 m size are generated to mesh the object.

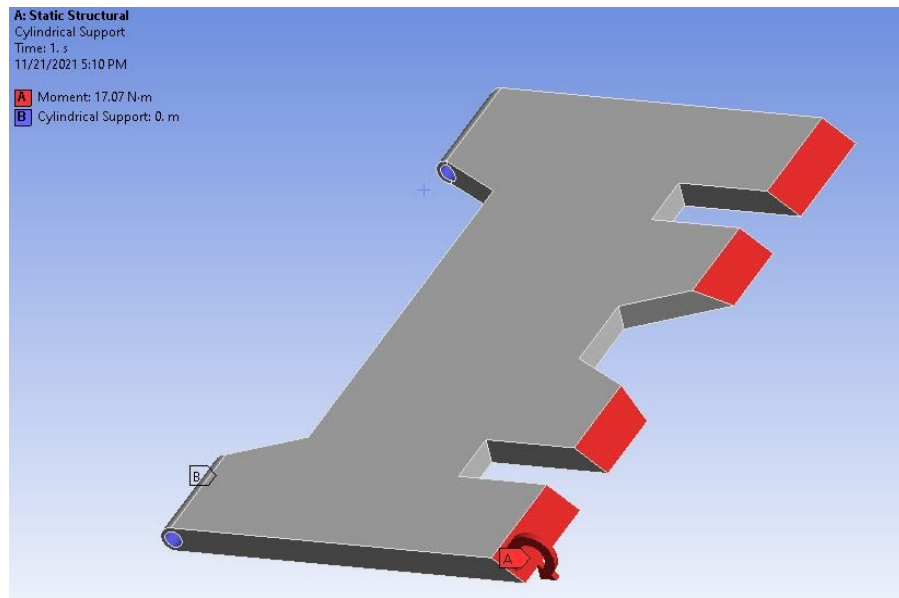


Figure 4.2.17: Ansys Static Structural Model, Detailing Loads and Supports

After the mesh was generated and the static supports and load were added, Ansys was used to find solutions of interest, including the elastic strain, total deformation, and maximum principal stresses experienced. The generated results are shown in Figure 4.2.18, Figure 4.2.19, and Figure 4.2.20, respectively, and tabulated in Table 4.2.4.

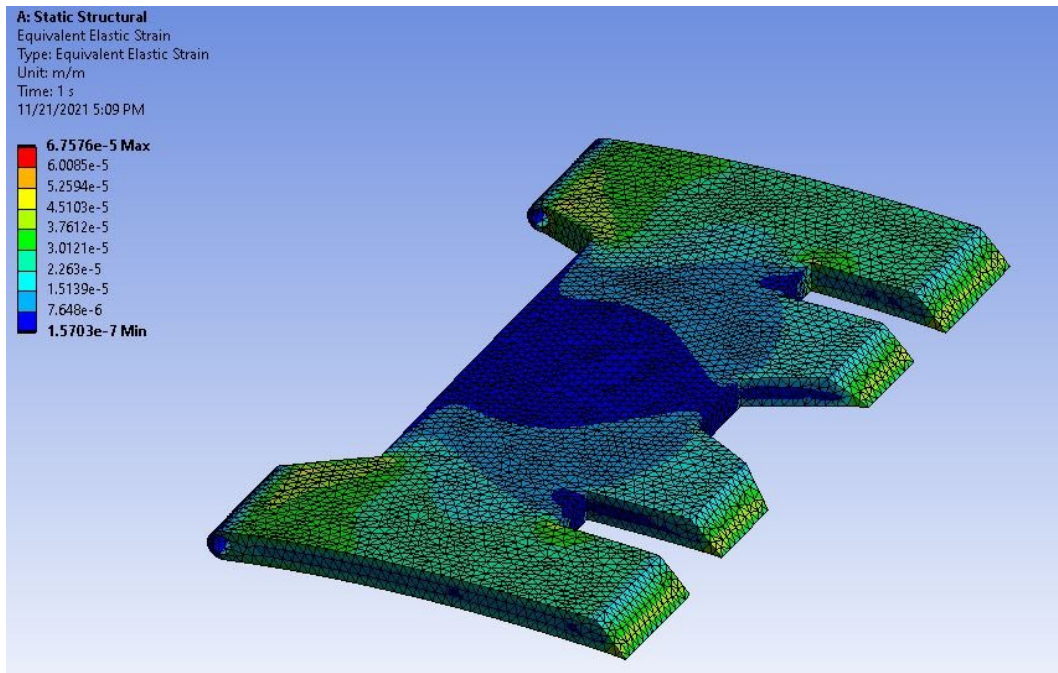


Figure 4.2.18: Equivalent Elastic Strain

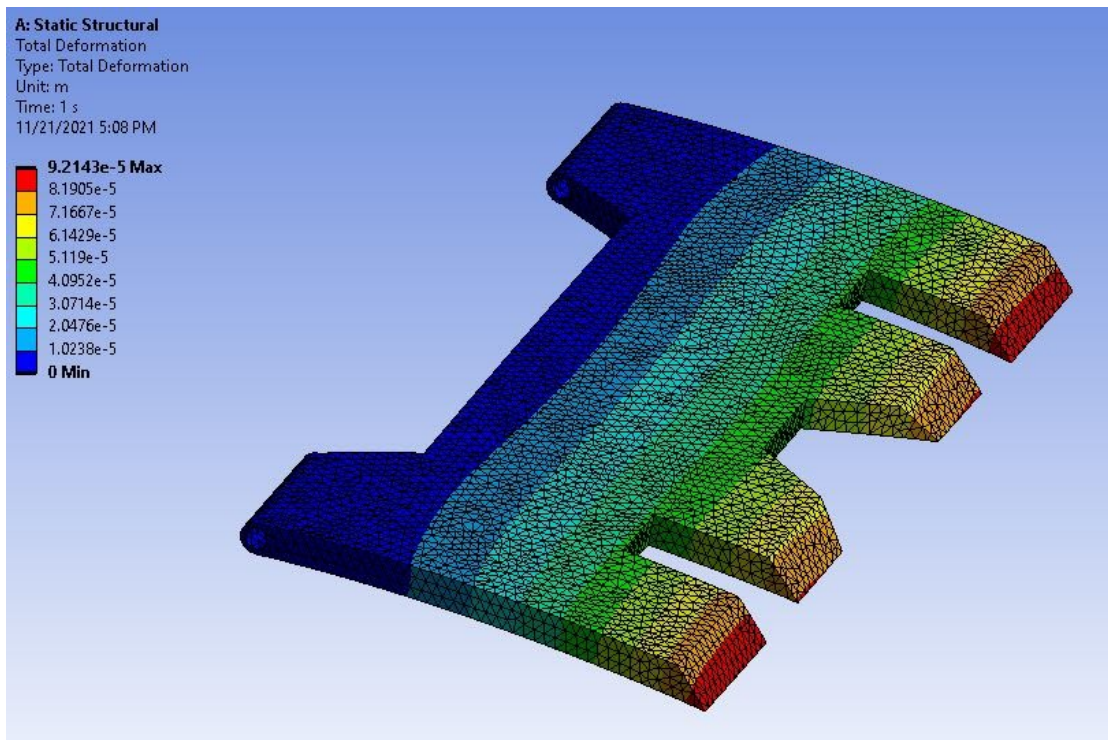


Figure 4.2.19: Total Deformation

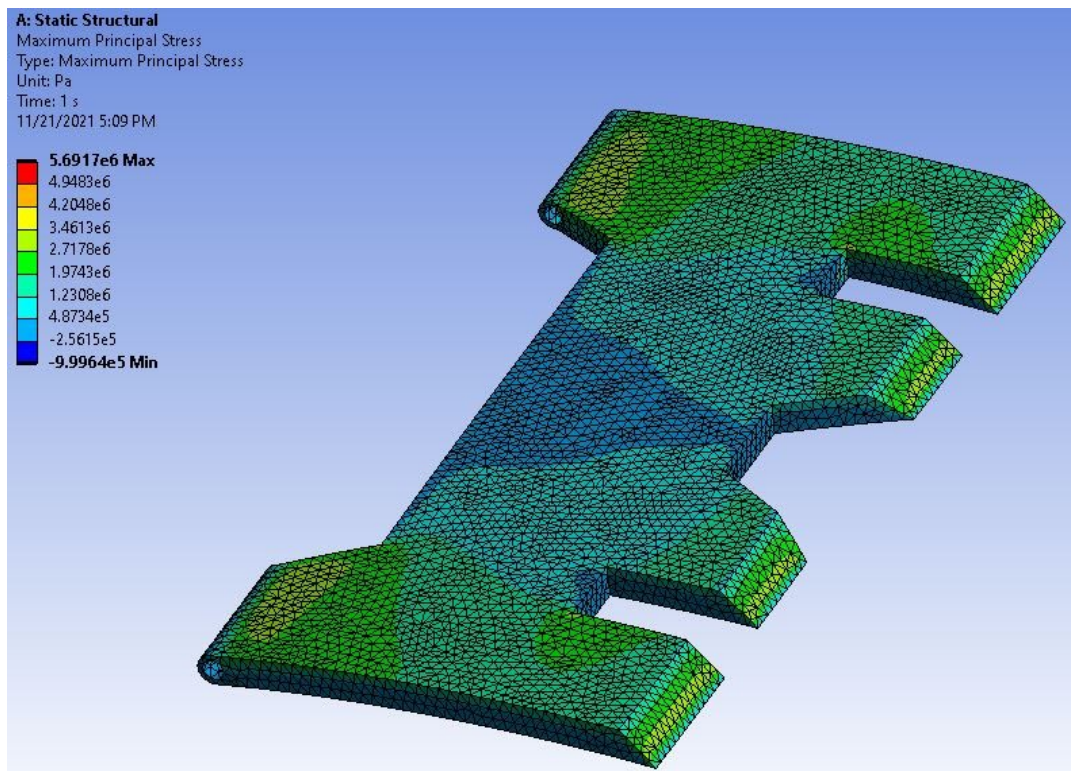


Figure 4.2.20: Maximum Principal Stress

Table 4.2.4: Tabulated Data from Ansys Static Structural FEA Analysis

Parameter	Value
Resulting Bending Moment of Single Solar Panel	$17.07 \text{ N} \cdot \text{m}$
Finite Element Size	5 mm
Maximum Equivalent Elastic Strain	$6.76 \cdot 10^{-5} \text{ m/m}$
Maximum Total Deformation	0.0921 mm
Maximum Principal Stress	5.69 MPa

From the finite element analysis conducted, it can be concluded that this hinge-based mechanism will be able to successfully deploy the solar panels. At its maximum value the elastic strain is shown to be a minuscule percentage ($6.76 \times 10^{-7} \%$), indicating that no significant deflection will occur. It should also be noted that the greatest elastic strain occurs primarily in the center region of the hinge plate, where failure is less likely to occur.

The total deformation due to the bending deflection is predicted to be under a tenth of a millimeter (0.092143 mm) at its peak loading condition, representing a minuscule predicted deflection. Finally, the bending stress is predicted to be relatively low for the overall plate. Most areas will experience less than half the maximum bending stress (5.6917 MPa), which only occurs at locations of high stress concentration, such as small radii and corners. Furthermore, with additional mesh refinement at these concentration points, the bending stress values would likely become smaller. Once again, these solutions have been generated using local gravitational conditions present on Earth. It is expected that these values will be several orders of magnitude lower during the mission, due to the significantly smaller gravitational acceleration on 46P/Wirtanen. Consequently, it is expected that the calculations performed here provides assurance, similar to a factor of safety, that the design will be successful when deployed on 46P/Wirtanen.

Although the previous analysis suggests that the design of this mechanism will be successful, the CLP team would like to acknowledge that unforeseen and potential sources of risk and failure are possible. Therefore, along with the conducted FEA analysis, a thorough risk analysis and mitigation plan has been developed and is presented in section 4.2.5. Finally, the plan of procession will also outline additional measures that will be taken to ensure a successful design of this hinge plate and the general mechanisms and deployables subsystem as a whole.

4.2.5 RISK ANALYSIS AND MITIGATION

The risk analysis and mitigation for the mechanisms and deployables subsystem can be found in [Appendix B](#) Table B3.

4.2.6 NON-TECHNICAL CONSIDERATIONS

The non-technical considerations for the mechanisms and deployables subsystem can be found in [Appendix C](#) Table C3.

4.2.7 PLAN OF PROCESSION

Given the semester-long time frame of this space vehicle design endeavor, it is impossible to develop a fully original, complete design of each mechanism aboard the CLP. Therefore, proven designs used in previous missions have been reviewed and submitted. However, with additional time a greater emphasis would be placed on analyzing and developing custom systems and solutions that are tailored to the needs of this mission. Additionally, a large portion of the development of this subsystem would involve modeling the mechanisms or subsystems under the control of this respective design team. Additionally, similar FEA analysis would be conducted and expanded upon for other mechanisms covered in this section, and more detailed electrical and thermal analysis would also take place. Finally, all designs developed for this subsystem would undergo an intensive and iterative process, being reviewed and verified by multiple professional engineers.

4.3 SPACEFLIGHT MECHANICS

4.3.1 SUBSYSTEM DEFINITION

The spaceflight mechanics subsystem involves the planning and modeling of maneuvers to ensure the CLP lands at the desired target location on the surface of 46P/Wirtanen in a safe and efficient manner. Specifically, it is responsible for evaluating and determining the parking orbit that the CLP will enter, including the locations and magnitudes of the propulsive maneuvers necessary to achieve the parking orbit, desired descent path, and landing phase. The design of these trajectories must also properly consider the amount of propellant and time needed to achieve the planned paths, in order to ensure that they do not conflict with defined mission constraints.

4.3.2 PRELIMINARY DESIGN OVERVIEW

In the preliminary design of the spaceflight mechanics portion of the CLP's mission from the PDR, the spaceflight mechanics analysis was divided into four major sections: departure from the PV, inclination change and orbit capture, descent towards the surface, and landing. Although ultimately a decision for the PV design team, it was determined that a pyrotechnic mechanism in the form of separation nuts will be the most ideal method for detaching from the PV. The main reasons for this design selection were the superior reliability and accuracy of a pyrotechnic device.

Upon detaching from the PV, it was determined that the CLP will perform a propulsive maneuver to enter a circular parking orbit and change inclination planes if deemed necessary. A

circular parking orbit was selected to allow the CLP to determine a viable landing site, perform preliminary hardware checks, and communicate with the PV in consistent time windows. Once the landing site is determined and the CLP is cleared for descent, the CLP will then perform another retroburn slightly prior to periapsis with the selected landing site in order to begin the descent phase. Although a Hohmann type transfer would be more energy efficient than this descent method, it would also take significantly longer due to the low gravitational parameter of 46P/Wirtanen. Thus, in order to address this time concern, a more aggressive descent path was deemed to be favorable.

The CLP will then perform a retroburn slightly above the surface of 46P/Wirtanen in order to eliminate any excess velocity and mitigate the risk of bouncing or impacting the surface with a significant velocity. It is important to consider that the altitude of this burn cannot be excessively close to the surface of the comet or there will be a risk of contaminating the target landing site and jeopardizing the scientific objectives of this mission.

Finally, in the PDR it was determined that the CLP will free-fall to the surface of the comet from an undetermined height and rely on attitude control methods to orient itself properly for landing (although based on analysis conducted later in this section, it was determined that the CLP would maintain its radial velocity instead of free falling to the surface). It should also be noted that nitrogen cold-gas propellant will be used for all propulsive maneuvers due to its high storage density, limited necessary infrastructure, and superior reliability.

4.3.3 COMET PARAMETERS

Before moving on to a more detailed analysis of the CLP's orbital capture and descent, it was necessary to define some critical properties of 46P/Wirtanen. Since 46P/Wirtanen was originally the target of the Rosetta and Philae mission, a fair amount of information is available to the public. This information, which includes orbital parameters such as the eccentricity, period and semi-major axis, as well as physical features, like the comet's mean diameter, are summarized in Table 4.3.1. However, because there has not been a previous mission to this comet, some critical information, such as the gravitational parameter, is still unknown. This parameter is critical to the spaceflight mechanics analysis, as it governs the equations of motion for the CLP, so an analysis was performed to determine an approximate gravitational parameter. This analysis relies on the assumptions that 46P/Wirtanen and 67P/Churyumov-Gerasimenko (for which the mass and diameter are known) are spherical and have the same density. This analysis was conducted in MATLAB and is presented in the Engine_Cutoff_Analysis.m script shown in Appendix I. The surface gravity was also estimated using Newton's law of gravitation once this estimated gravitational parameter was found.

Table 4.3.1: 46P/Wirtanen Orbital and Physical Properties [72]

* Gravitational Parameter*	$1.554 \times 10^{-8} \frac{\text{km}^3}{\text{s}^2}$
Surface Gravity	$4.316 \times 10^{-5} \frac{\text{m}}{\text{s}^2}$
Diameter	1.2 km
Eccentricity	0.6588
Semi-Major Axis	3.093 au
Orbital Period	5.44 years
Earth Minimum Orbit Intersection Distance	0.0713 au
Perihelion Distance	1.055 au
Aphelion Distance	5.131 au

Estimated from the analysis described above

4.3.4 LAUNCH WINDOW DESIGN AND ANALYSIS

As 46P/Wirtanen approaches its perihelion point, its SOI will decrease due to the greater gravitational attraction posed by the Sun. The preliminary spaceflight mechanics analysis conducted in the PDR relied on the assumption that the lander would begin its descent when 46P/Wirtanen was approximately 228×10^6 km (semimajor axis of Mars' orbit) from the Sun [24]. At this distance from the Sun, the SOI of 46P/Wirtanen was determined to be about 5.5 km (this analysis is conducted in the Engine_Cutoff_Analysis.m script shown in Appendix I), which should allow the PV to drop off the CLP at a reasonable distance from the surface of the comet and enter a parking orbit of its own. As a result, the mission timeline must account for the PV's trajectory to 46P/Wirtanen at a distance of the semimajor axis of Mars' orbit, and the time it takes for the CLP to descend after detaching from the PV.

Although the launch window design is a more primary focus for the PV design team, an approximate launch date was desirable for the creation of a preliminary design schedule, so a crude analysis of the expected launch window will be summarized below. Provided with more constraints from the PV team, ideally this analysis would be conducted with a porkchop plot to determine an ideal launch window that considers propellant use and suitable launch dates. In order to determine an appropriate launch date for the crude analysis conducted below, however, JPL's small-body database, which includes future trajectories and timelines of small-bodies such as 46P/Wirtanen, was used to determine approaches of 46P/Wirtanen that aligned with the expected design schedule of this mission. As is shown in Figure 4.3.1 below, the next reasonable time window when 46P/Wirtanen will approach this distance will be in August of 2029 [72].

However, if this timeline is deemed too aggressive with the design schedule, there is another similar approach in January of 2035 [72].

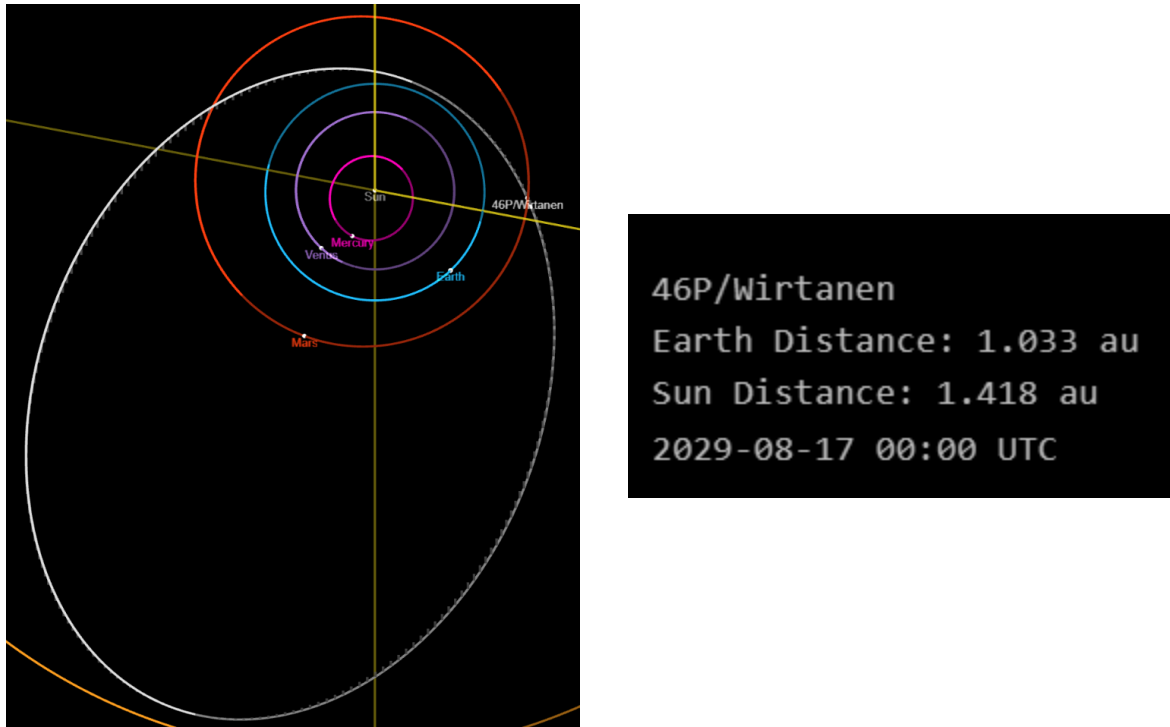


Figure 4.3.1: JPL Small-Body Lookup Orbit Viewer [72]

Next, the approximate launch date was determined by working backwards from expectations of the PV transfer and CLP descent timelines. The preliminary analysis of the CLP orbital capture and descent (which will be explained in greater detail in subsequent sections) suggested this portion of the mission would take about 7 days. The PV's transfer to the comet will take significantly longer and will have a larger degree of uncertainty based on the gravitational assists or insertion methods that are selected by the PV spaceflight mechanics team. For a rough estimate of this transfer time, however, a Hohmann transfer was assumed from Earth to 46P/Wirtanen at this target date. Based on this analysis (which can be found in Appendix I) the PV transfer will take approximately 259 days.

Although the PV spaceflight mechanics team will likely reduce this figure considerably by utilizing gravitational assists, this preliminary analysis should be sufficiently precise for planning the remainder of this mission and the design schedule. Based on these figures and 46P/Wirtanen's future approaches, this mission will aim to launch in late November of 2028. Alternatively, if this window is missed, 46P/Wirtanen can be reached on its next approach by launching around the middle of April in 2034.

4.3.5 ORBITAL TRAJECTORY DESIGN AND ANALYSIS

For the final spaceflight mechanics design analysis, a MATLAB script was developed to propagate the position and velocity of the CLP and PV around 46P/Wirtanen by numerically integrating the two-body equations of motion for a given initial position and velocity in the comet-centric frame. By developing a script to perform these calculations, a variety of parameters could quickly be experimented with to determine their effect on the necessary change in velocity and time of trajectory. Based on the previous analysis of 46P/Wirtanen's SOI, and an abundance of trial and error, the following parameters were determined to be the most favorable for the objectives of this subsystem.

Table 4.3.2: Spaceflight Mechanics Final Design Parameters

PV Periapsis Altitude	4.4 km
PV Apoapsis Altitude	6.4 km
PV Parking Orbit Period	8.57 Earth days
PV Parking Orbit Escape Velocity (Minimum)	$6.66 \times 10^{-2} \frac{m}{s}$
CLP Parking Orbit Altitude	4.4 km
CLP Parking Orbit Period	6.52 Earth days
CLP Parking Orbit Escape Velocity	$7.88 \times 10^{-2} \frac{m}{s}$

One concern that arose from this analysis was the extremely small escape velocities that both the PV and CLP will be subject to in their parking orbits. As a result of solar radiation pressure, micro-collisions, gravitational perturbations from additional celestial bodies, and the effects of the comet's inhomogeneous densities, and non-spherical geometry, the velocities of these spacecrafts will likely deviate from this two-body analysis significantly enough to warrant these concerns. To address these concerns, frequent propulsive corrections will need to be made in order to prevent the spacecraft from reaching an escape velocity. Although there is insufficient time to properly model these minor effects, the telemetry sensors and propulsion systems must be sufficiently accurate to perform the necessary burns required to maintain these parking orbits.

Although an elliptical parking orbit for the PV was ultimately modeled in the following design and analysis, further research after the PDR indicated that the PV may also choose to trail 46P/Wirtanen instead of entering a parking orbit, which would limit the need for these constant corrections, and mitigate concerns of reaching an escape velocity. Although this approach may be deemed more favorable by the PV design team, there was insufficient information about the method that would be chosen at the time of this analysis. If the trailing method were to be chosen, the communication windows with the PV would need to be further analyzed to ensure that they occur frequently enough, and the initial detachment location and orientation of the detachment procedure would likely change.

After propagating the initially proposed design parameters, the positions of these spacecrafts with respect to 46P/Wirtanen were plotted, as shown in Figure 4.3.2 below. The MATLAB script used to produce this plot can be found under “CLP_Flight_Mechanics.m” in Appendix I. It should be noted that input parameters were defined for the location of the descent initiation burn and percent reduction of the velocity, which allowed many types of trajectories to be quickly iterated in order to find both a suitable location and reduction in velocity. Ultimately, it was decided that the descent initiation would occur at 306 degrees counterclockwise from the line of apsis with a 70% reduction in velocity.

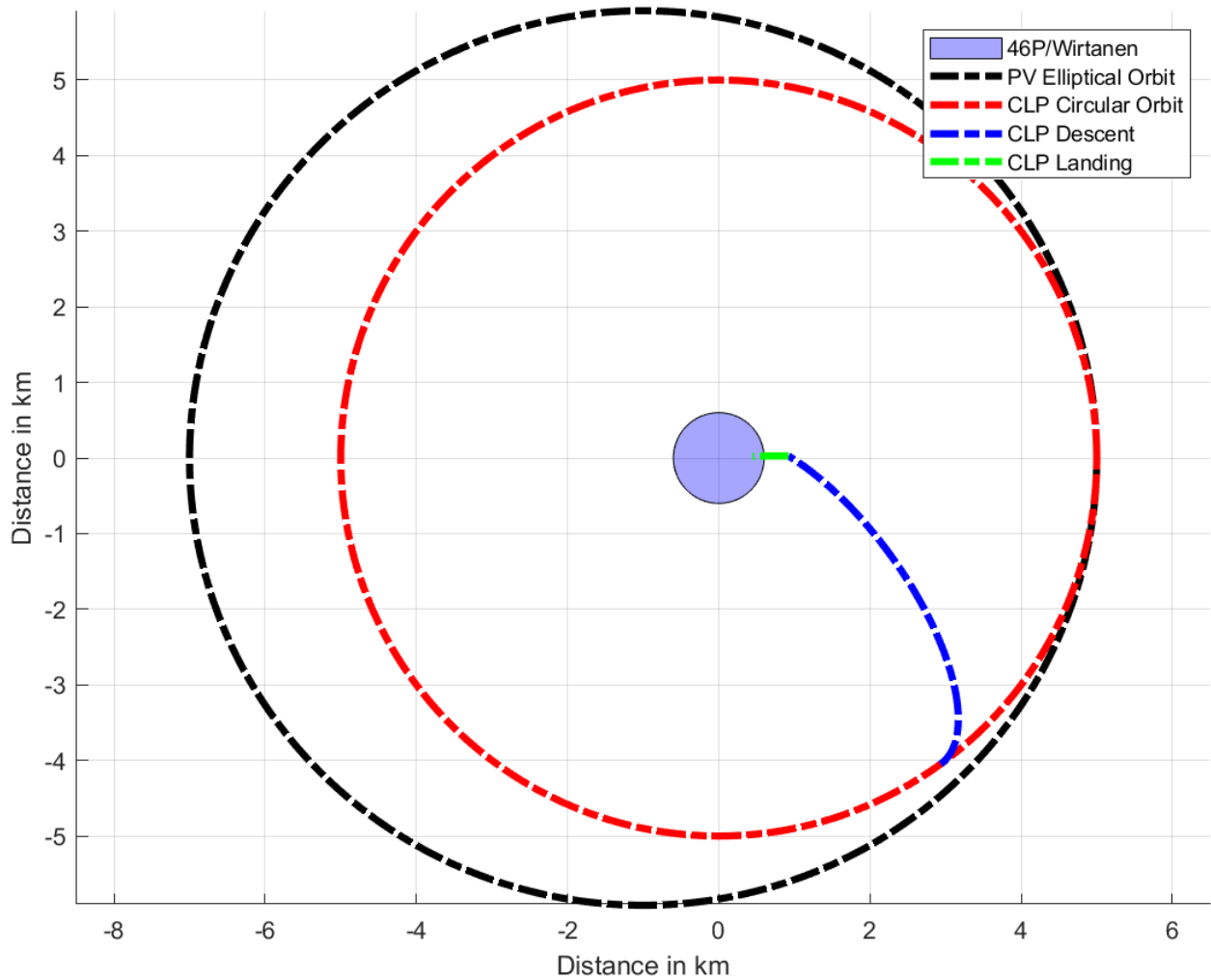


Figure 4.3.2: Proposed Orbital Trajectories of PV and CLP

In the preliminary analysis of this subsystem, it was suggested that the CLP would perform a final landing burn to eliminate all excess velocity and free fall the rest of the way to the surface of 46P/Wirtanen. However, when this process was modeled in MATLAB, the small gravitational attraction of the comet yielded final landing procedures that would take weeks to complete. The MATLAB script used to model this landing procedure is shown in Appendix I

under the “Engine_Cutoff_Analysis.m” script, and the results are summarized in the plot below. Evidently, the impact velocities are on the order of micrometers per second, indicating that a “free fall” is unreasonable for the final approach.

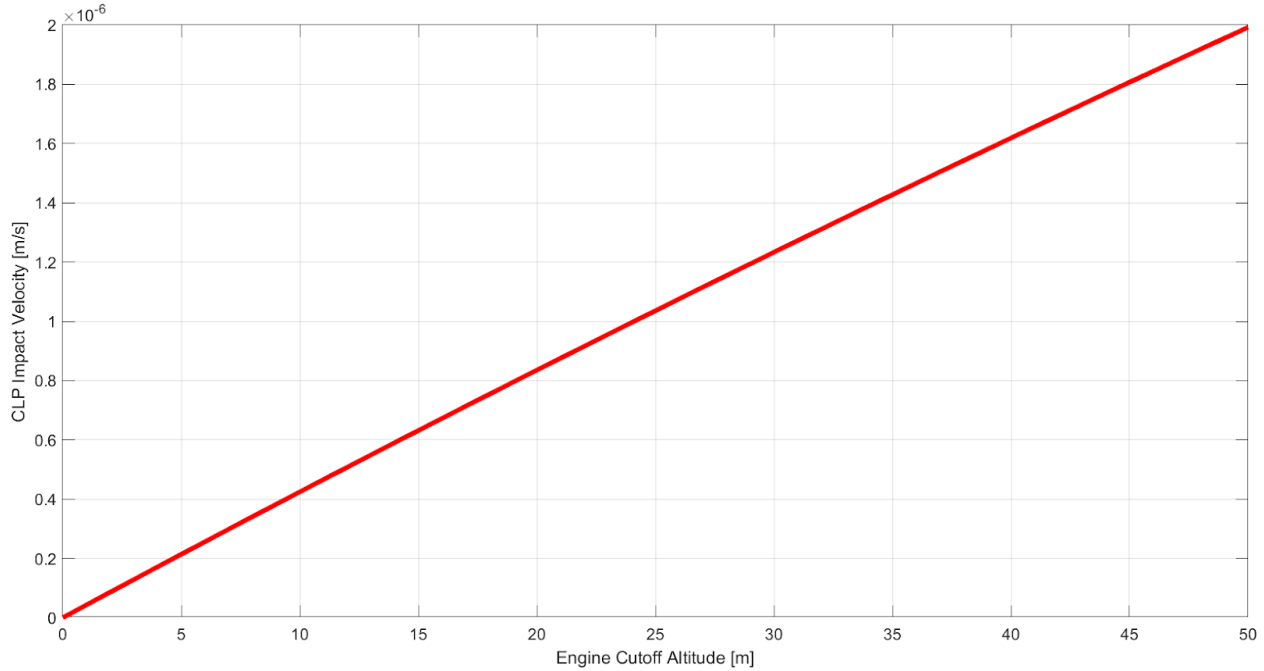


Figure 4.3.3: CLP Engine Cutoff Analysis

Instead of this full retroburn, a new landing procedure was deemed necessary to deliver the CLP to the surface of the comet in a reasonable time frame. Ultimately, it was decided that a burn would be used to eliminate any tangential velocity to 46P/Wirtanen’s surface, while keeping the radial component of the velocity from the descent phase. This type of maneuver will allow the CLP to approach the surface of the comet from above rather than at an angle, which will decrease the complexity of the ADCS maneuvers and landing procedure. Additionally, it was found that the CLP will impact the surface of 46P/Wirtanen at about 0.35 meters per second using this approach, which should be a sufficiently slow speed for the design of the landing legs and supporting structure.

The next portion of this analysis dealt with quantifying the delta-V and time that would be required for the CLP to achieve the modeled trajectories. In order to quantify the time necessary to complete this trajectory, it was assumed that the CLP would initiate its descent without completing an entire parking orbit due to the significant period of this parking orbit. This would drastically increase the trajectory time if the first opportunity was missed. Furthermore, the times were estimated for the descent and landing portions of this trajectory by manipulating the length of these mission segment simulations on the trajectory plot until they agreed with the desired trajectory. Although this method introduces a fair degree of uncertainty into these parameters, it was deemed sufficiently accurate until higher order models are implemented for

this design. The quantification of the necessary changes in velocity should be significantly more accurate, however, due to the use of the patched conics method and low integration tolerances used to numerically integrate the initial parameters. However, as previously mentioned, this model did not account for the frequent correction burns that would need to be performed in order to keep the CLP in its desired parking orbit.

There is also a secondary objective of this mission to relocate the CLP to a nearby landing site by taking off from 46P/Wirtanen's surface. Although there is insufficient time to model this procedure, a large safety factor will be applied to the required delta-V in order to ensure that there is sufficient propellant on board the CLP for the aforementioned discrepancies and objectives. The results of this portion of the analysis are summarized in Table 4.3.3 below.

Table 4.3.3: Estimated Delta-V and Time Requirements by CLP Mission Segment

Phase	Delta-V (m/s)	Time (hours)
Parking Orbit	4.47E-3	133.1
Descent	3.90E-2	28.3
Landing	2.42E-2	0.74
Total	6.77E-2	162.1

Although the previous analysis has provided valuable insight into the general geometry, required time, and necessary velocity changes of the proposed trajectory, the analysis thus far has neglected to consider a change in inclination planes. Changes in the inclination plane of an orbit require extensive changes in velocity, making these maneuvers expensive to perform. While inclination plane changes should be avoided to the largest extent possible, it is very likely that a desirable target landing site will fall outside of the original inclination plane. As a result, an additional study was performed to analyze the necessary total change in velocity that would be required for a plane change of varying magnitudes ("CLP_Flight_Mechanics.m" in Appendix I). As is shown in Figure 4.3.4 below, the total required delta-V can differ significantly with a change in the inclination plane.

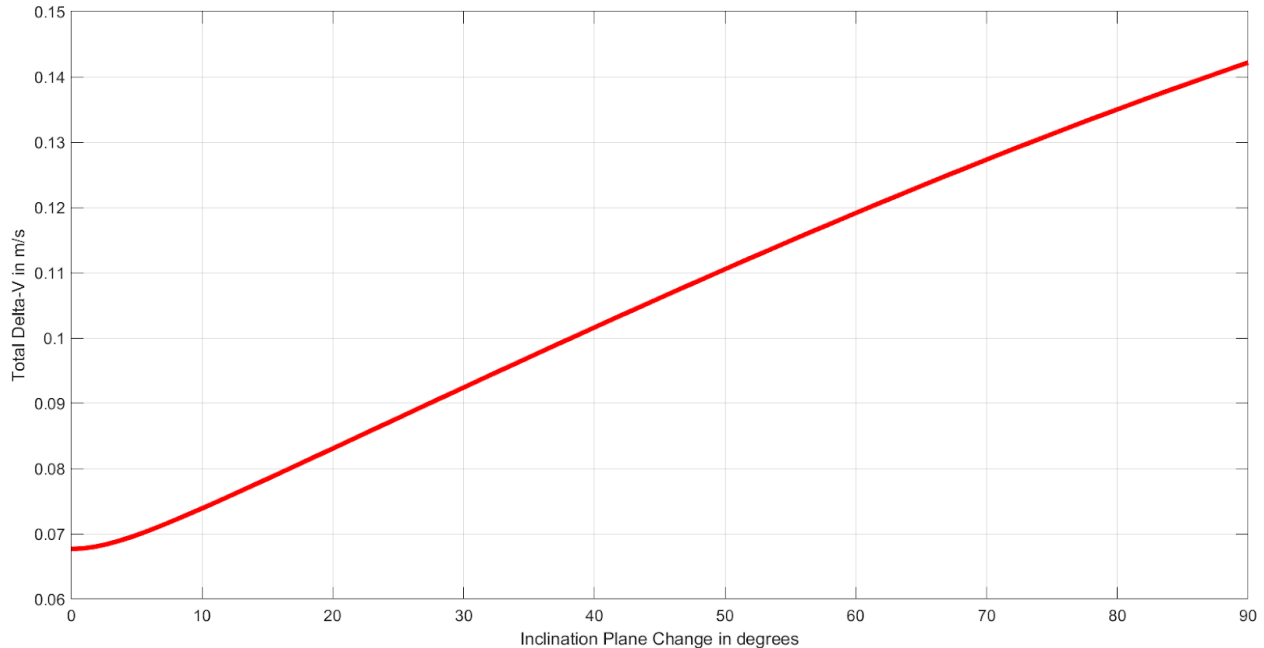


Figure 4.3.4: Effect of Inclination Plane Change on Total Required Delta-V

Based on the previous analysis, it is evident that the required delta-V determined by these basic models will be relatively low due to the small gravitational parameter of 46P/Wirtanen. However, there will be additional propulsive maneuvers that must be accounted for in order to keep the CLP in its parking orbit and allow the CLP to relocate from its original landing site to achieve its secondary objectives. Based on these models and some rough projections of these additional considerations, 1 m/s of total delta-V should be sufficient to move forward with the design of other CLP subsystems.

4.3.6 RISK ANALYSIS AND MITIGATION

The risk analysis and mitigation for the spaceflight mechanics subsystem can be found in [Appendix B](#) Table B4.

4.3.7 NON-TECHNICAL CONSIDERATIONS

The non-technical considerations for the spaceflight mechanics subsystem can be found in [Appendix C](#) Table C4.

4.3.8 PLAN OF PROCESSION

Moving forward with the development of the spaceflight mechanics subsystem would require a number of refined models that use higher order techniques and greater precision. Instead of modeling the equations of motion with a two-body assumption, it would be more accurate to expand this model to three or four bodies to account for the gravitational perturbations introduced by the Sun, Earth, and Mars. Techniques such as double precision

variables and more powerful computers should also be used to verify these preliminary models with more accurate results. Additionally, it would likely be beneficial to verify this preliminary model on industry software packages, such as STK, in order to mitigate human error.

Furthermore, while the parameters chosen for this analysis were found through trial and error, it would be beneficial to create a program to optimize these parameters, especially since the PV orbital parameters will likely change based on the constraints and objectives of this spacecraft. The effects of 46P/Wirtanen's non-spherical geometry and rotation should also try to be quantified through telescopic images or other optical techniques. Similarly, the effects of solar radiation pressure and micro-collisions should be estimated and incorporated into these spaceflight mechanics models. Although analysis was not conducted for the relocation of the CLP to a nearby landing site (a secondary mission objective), the necessary delta-V to take off from 46P/Wirtanen's surface must also be quantified and modeled to ensure feasibility.

Preliminary models should also be developed for alternative comets, in order to identify potential backup options that fit within the propellant design budgets in the event of a significant design delay. Finally, once these models are uploaded to the command and data subsystems, there should be extensive simulation testing in order to validate the command and control board's ability to maintain the modeled trajectory.

4.4 PROPULSION

4.4.1 SUBSYSTEM DEFINITION

The propulsion subsystem is responsible for applying the force to the CLP needed to execute all maneuvers. This includes orbital adjustments, guided descent, execution of evasive maneuvers, and a final descent burn prior to touchdown to eliminate the tangential velocity of the CLP. These maneuvers are defined by the spaceflight mechanics team in section 4.4 and must be executed in an accurate and timely manner.

4.4.2 PRELIMINARY DESIGN OVERVIEW

The preliminary design of the spacecraft proposed the type of propulsion system to be used, as well as its corresponding propellant. The propulsion system must execute four primary maneuvers. Entrance into a circular parking orbit, change of inclination plane (coupled with circular parking orbit burn if necessary), a retro-burn to put the CLP onto a desired descent trajectory, and a final retroburn to eliminate the CLP's tangential velocity so that it will approach the target landing site vertically.

For the propulsion system, a cold gas system was selected. The cold gas system has very low mass and infrastructure requirements - which were prime performance metrics for the parameters of this design. Additionally, cold gas propellants are comparatively stable and have moderate throttling capacity. While cold gas generally has a very low specific impulse, this was of low priority for the purposes of this mission due to the low total delta-V requirement. Nitrogen was ultimately selected as the propellant type. Nitrogen has contamination free

characteristics, is very stable, and is stored in a gaseous phase - eliminating the problems associated with propellant sloshing. Additionally, it has low mass requirements - as it does not require any additional infrastructure - and has a suitable specific impulse.

4.4.3 PRODUCT SELECTION

It was determined in the PDR that a nitrogen based cold gas thruster would be used for propulsive maneuvers. An overview of the product selection for the propulsion subsystem can be found below in Table 4.4.1, which is followed by a description of the down selection process. A pressure regulator was also selected at this stage. Furthermore, it was found that a commercial tank that meets the mission requirement was not available, and one would have to be independently designed.

Table 4.4.1: Propulsion Product Selection

Component	Manufacturer	Model
Cold Gas Thruster	Advanced Space Technologies GmbH (AST)	AST Cold Gas Thruster (CGT)
Pressure Regulator	Advanced Space Technologies GmbH (AST)	AST Electronic Pressure Regulator (EPR)

A variety of commercial cold gas thrusters were compared in Table J1 of Appendix J. The Advanced Space Technologies GmbH (AST) Cold Gas Thruster (CGT) was ultimately selected. The specifications for this thruster can be found in Appendix J Figure J1. One of the unique challenges of the propulsion system for the CLP is the need to make corrections for small orbital deviations, as laid out in section 4.3.5. This is in addition to the small escape velocity of the comet and the low delta-V of maneuvers. If the thrust is too high, the CLP may propel itself outside the escape velocity of the comet, yet lower thrusts limit the capacity for evasive maneuvers. As a result of these considerations the accuracy of the cold gas thruster was given prime importance. The AST CGT excelled in this category with a minimum capable impulse of $110 \mu\text{Ns}$ [12]. The reliability, which was judged on a combination of flight heritage and available testing information, was the next most important metric. The AST CGT performed moderately in this category with a single previous mission on FORMOSAT 5 and extensive available testing data [12]. The AST CGT also had very low mass, though this was judged to be of lower importance since all of the thrusters had comparatively low masses. The AST CGT fell on the lower spectrum for thrust, but the strengths in other categories and long orbital period resulted in its ultimate selection.

A pressure regulator must also be selected. For cold gas propulsion systems, the thrust of the system is proportional to the pressure feed of the propellant. As a result, the pressure regulator not only ensures that the feed pressure does not exceed the operating pressure of the thruster, but is also used to adjust the magnitude of thrust. The AST Electronic Pressure

Regulator (EPR) was ultimately selected. The specifications for this component can be found in Appendix J Figure J2. Using the AST EPR ensures compatibility and ease of use with the AST CGT. The component has an exceptionally low mass and volume, corresponding with the general mission requirements. Finally, it offers high reliability as a triple barrier of three serial valves is implemented, also negating the need for a redundant system. These things together made the AST EPR the clear choice for the pressure regulator.

4.4.4 PROPELLANT TANK DESIGN AND ANALYSIS

The primary design focus for the propulsion subsystem was the propellant budget and tank design. The propellant budget was based on the delta-V requirements outlined in Table 4.3.3. Equation 4.4.1 was used to calculate the propellant mass, as derived from the Tsiolkovsky rocket equation.

$$m_p = m_f(e^{\frac{\Delta V}{I_{sp}g_0}} - 1) \quad \text{Equation 4.4.1 [6]}$$

Here m_p is the necessary propellant mass, m_f is the final mass of the spacecraft after burns, ΔV is the total delta-V, I_{sp} is the specific impulse, and g_0 is standard gravity. The propellant budget was then defined from this minimum propellant mass. The full budget is outlined in section 5.4. The propulsion system is already expected to have a relatively low mass, and there is a large degree of uncertainty surrounding the comet parameters and the amount of propellant that will be needed for constant orbital corrections or evasive maneuvers. Consequently, a high reserve of 50% was selected. Propellant budget must also account for trapped propellant within the regulators and feedline, as well as any loading error. These values were estimated at 3% and 0.5% of the total, respectively. The last piece of the propellant budget is the mass of nitrogen gas left that acts as a pressurant, as discussed in more detail with the tank design below.

The first design decision was the material to be used for the propellant tank. A decision matrix for this selection is provided in Table J2 of Appendix J. Although a high tensile strength is important since the gas is highly pressurized, it was decided that ease of manufacturing was of greater importance due to the very small size of the overall system. Consequently, Aluminum 6061 (Al6061) was selected because it is easy to manufacture and has a relatively low cost. Next, a spherical design was selected as a result of its ability to offer the most pressure resistance structure. It should be noted, however, that this spherical shape is harder to mount and is less volume efficient than alternative geometries. Next, the necessary volume of the tank was calculated using the ideal gas law, which is defined by Equation 4.4.1 below.

$$V = \frac{m_p RT}{P_i - P_f} \quad \text{Equation 4.4.2}$$

V is the total volume of the tank, m_p is the mass usable of propellant, R is the ideal gas constant of nitrogen, T is the temperature in Kelvin, P_i is the initial pressure, and P_f is the desired final pressure. The tank was designed to operate within a maximum and minimum operating pressure for the usable propellant mass. As a result, the pressure used in calculating the volume was the pressure of the usable propellant - which is equal to the difference between the maximum and minimum pressure. The minimum pressure was based on the chamber pressure for the thruster and must remain at or above this value to ensure nominal operation.

The initial tank pressure was another key design decision. A lower initial pressure increases the amount of unusable propellant, and hence, the overall mass of the system. Conversely, increasing the pressure decreases this percentage of unusable propellant but requires a more robust tank design, also driving the mass of the system up after a certain point. As a result, a moderate operating pressure of 100 bars was selected. The required thickness of the tank was calculated using the following equation.

$$t = \frac{Pr}{2\sigma} \quad \text{Equation 4.4.3 [20]}$$

The thickness of the tank is defined by t , P is the maximum pressure, r is the radius of tank, and σ is the yield stress of Al6061. Additionally, a factor of safety of two was introduced, defining the burst pressure of the tank as 200 bars, and a MATLAB script was utilized to calculate the specifications of the propellant tank. This script can be found in Appendix J, and the specifications for the propellant tank can be found below in Table 4.4.2. From these values the total mass of the tank could be calculated using the following equation.

$$m_{tank} = \frac{4}{3}\pi\rho(r_2^3 - r_1^3) \quad \text{Equation 4.4.4 [20]}$$

Here m is the mass of the tank, ρ is the density of Al6061, r_2 is the outer radius of the tank, and r_1 is the inner radius of the tank. Adding the mass of propellant to this value yields the final mass of the full tank.

Table 4.4.2: Propulsion Tank Specifications

Internal Volume	338.9 mm ³
Operating Pressure	100 bars
Burst Pressure	200 bars
Wall Thickness	0.37 mm
Dry Mass	0.256 g
Propellant Mass	36.9 g
Total Mass	37.2 g

4.4.5 RISK ANALYSIS AND MITIGATION

The risk analysis and mitigation for the propulsion subsystem can be found in [Appendix B](#) Table B5.

4.4.6 NON-TECHNICAL CONSIDERATIONS

The non-technical considerations for the propulsion subsystem can be found in [Appendix C](#) Table C5.

4.4.7 PLAN OF PROCESSION

Extensive work is still required before the propulsion system is mission ready. First the feed lines between the tank, pressure regulator, and thruster must be designed. Similarly, pressure sensors must be selected and placed strategically throughout the tank to monitor the operating conditions of the system. Furthermore, an overall system architecture map should be developed for design documentation, and a control system must be created to regulate the thrust. Additionally, the tank will be constructed by welding two hemispheres together to form the spherical design, so areas for the tank welds and structural attachments must be incorporated into the overall tank design (which will increase the overall mass of the system). Also, the extremely thin tank walls and hollow hemispherical shapes required for the proposed tank design will make the manufacturing process exceedingly hard, so further iterations to the design for manufacturability may be necessary. A manufacturer capable of producing such a tank will also need to be identified.

Beyond the general tank design, a propellant loading process must also be developed. This is typically done by loading the tank away from the main structure and measuring the tank mass as it is filled, but a detailed procedure and checks should be developed. In collaboration with the spaceflight mechanics team, analysis will be conducted to identify suitable backup comets for a situation in which 46P/Wirtanen is no longer a viable target. Once this is done, the tank design can be modified such that the propulsion system remains capable of landing without significant design alterations if an alternate target must be selected.

Finally, more detailed analysis and extensive testing should be conducted on all the components comprising the propellant subsystem. For instance, finite element models of the proposed tank design should be developed to assess the tank's robustness, and the effects of depressurization in the tank should be quantified.

4.5 ATTITUDE DETERMINATION AND CONTROL

4.5.1 SUBSYSTEM DEFINITION

The attitude determination and control subsystem details the processes through which the CLP senses its environment and executes proper attitude corrections after departure from the PV. More specifically, this subsystem includes the quantification of torquing requirements, the

selection of components necessary for attitude determination, and the selection of actuators to accomplish the desired attitude adjustments. A system model of the CLP was developed along with its control system. This control system was then tested for varying disturbances to confirm convergence of the system towards the desired attitudes.

4.5.2 PRELIMINARY DESIGN OVERVIEW

In the preliminary design of this subsystem, selections were made regarding the attitude determination methods and the attitude control method. A three-tiered system including sun sensors, star trackers, and a type of inertial measurement unit were chosen for attitude determination. A horizon sensor was not included in the design due to its power requirement, lack of use after landing, and the possible difficulty in determining the border horizon due to uneven terrain of the comet along with the comet's coma. These selections were made to allow for robust attitude determination regardless of the system state. Reaction wheels were also chosen for the control method due to their lower mass requirement than other methods and higher pointing accuracy.

4.5.3 PRODUCT SELECTION

This section serves to summarize the product selections that will be utilized in the design of the ADCS subsystem. Because the general technologies were already chosen in the preliminary design, further down selection was not necessary. The only exception to this was for the inertial measurement unit. A decision matrix for the type of IMU can be seen in Table K1 in Appendix K. Due to the lower cost and mass of the micro-electromechanical system IMU, this technology was chosen. Because the IMU is not the primary method of attitude determination and is only necessary to reduce angular velocity of the spacecraft, the main considerations in this down selection process were the comparative cost and mass requirements to comparable technologies.

Though the system only requires three reaction wheels for control, in order to provide control redundancy, four reaction wheels are used as actuators in the subsystem design. They are mounted in a tetrahedral configuration as shown in Figure 4.5.1 and have rotational axis in the λ_1 , λ_2 , λ_3 , and λ_4 directions denoted by Equations 4.5.1-4.5.4.

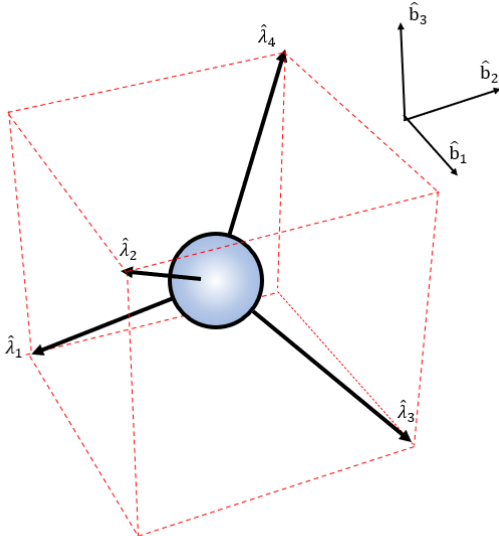


Figure 4.5.1: Tetrahedral Configuration of Reaction Wheels

$$\lambda_1 = \frac{1}{\sqrt{3}}(-\hat{b}_1 - \hat{b}_2 - \hat{b}_3) \quad \text{Equation 4.5.1}$$

$$\lambda_2 = \frac{1}{\sqrt{3}}(\hat{b}_1 - \hat{b}_2 + \hat{b}_3) \quad \text{Equation 4.5.2}$$

$$\lambda_3 = \frac{1}{\sqrt{3}}(\hat{b}_1 + \hat{b}_2 - \hat{b}_3) \quad \text{Equation 4.5.3}$$

$$\lambda_4 = \frac{1}{\sqrt{3}}(-\hat{b}_1 + \hat{b}_2 + \hat{b}_3) \quad \text{Equation 4.5.4}$$

The total angular momentum of the CLP system can then be determined using Equation 4.5.5 (based on equations from [6]).

$$H^S = I^{B/B*} \cdot \omega^{N/B} + \left\{ I^{\omega_1} \cdot \omega^{\omega_1} \cdot \hat{\lambda}_1 + I^{\omega_2} \cdot \omega^{\omega_2} \cdot \hat{\lambda}_2 + I^{\omega_3} \cdot \omega^{\omega_3} \cdot \hat{\lambda}_3 + I^{\omega_4} \cdot \omega^{\omega_4} \cdot \hat{\lambda}_4 \right\} \quad \text{Equation 4.5.5}$$

where H^S is the total angular momentum of the CLP system, $I^{B/B*}$ is the moment of inertia matrix of the CLP, $\omega^{N/B}$ is the angular velocity of the CLP, I^{ω_n} is the moment of inertia for the n^{th} reaction wheel, and ω^{ω_n} is the angular velocity for the n^{th} reaction wheel. By rearranging this equation and setting the total angular velocity to zero, the nominal angular momentum requirement for each of the reaction wheels can be determined. The code for this calculation is shown in Appendix K. This results in a required angular momentum of 1.1584 Nms for each reaction wheel. With this requirement in mind, the RSI 1.6-33/60A reaction wheel was chosen for the orientation actuator.

Specific products chosen to fit the ADCS determination and control requirements are shown in Table 4.5.1. Datasheets of the specific products that were ultimately selected for each major component are shown in Appendix K.

Table 4.5.1: Attitude Determination and Control Product Selection

Component	Manufacturer	Model
IMU	Honeywell	HG4930
Sun Sensor	RedWire	Coarse Sun Sensor Pyramid
Star Tracker	Sinclair Interplanetary	ST-16RT2
Reaction Wheels	Collins Aerospace	RSI 1.6-33/60A

With a three-tiered sensor system based on these product selections, the CLP has been designed to operate in a range of angular velocities from $-400^{\circ}/\text{s}$ to $400^{\circ}/\text{s}$, based on the sensing capabilities of the CLP, and has a pointing accuracy of $\pm 0.0153^{\circ}$ while at angular velocities below $3^{\circ}/\text{s}$ (See Appendix K for information regarding sensor operating ranges). This range is well above expected CLP flight conditions and should provide enough sensing and control to orient the CLP in even the worst of tumbles. In addition, to provide redundancy in case of sensor failure, an extra redundant IMU, sun sensor, and star tracker are included in the final design. A fourth reaction wheel is added to the design to provide redundancy and allow for desaturation of the reaction wheels.

4.5.4 CONTROL LAW DESIGN AND ANALYSIS

The CLP control board will store an ephemeris table detailing the desired orientation of the CLP throughout its mission, which will be used in conducting all of the lander's maneuvers. In order to make proper control commands, though, accurate sensing data is required. The sensing of the CLP is achieved through a three-tier system, which can best be described using a scenario in which the CLP is initially in a tumble with an absolute body angular velocity, $|\omega| \geq 5^{\circ}/\text{s}$. First, the CLP must be taken out of the tumble by lowering its angular velocity. Sensing in this range is done using the inertial measurement unit chosen in Table 4.5.1, with the primary objective of this control system being to lower the angular velocity to be within the operating range of the sun sensor. Once this is accomplished, the sun sensor is used to further reduce the angular velocity to nearly zero while at the same time beginning to reduce the orientation error of the CLP. Finally, the star tracker is used to make precision pointing measurements once $|\omega| \leq 3^{\circ}/\text{s}$. This three-tiered system structure is shown in Figure 4.5.2.

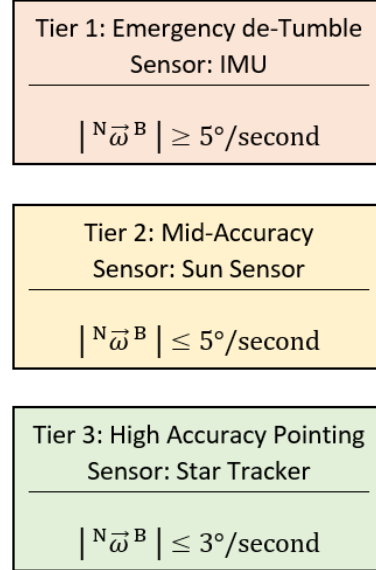


Figure 4.5.2: Three-Tiered Sensor Suite

The control law for the CLP was developed in order to provide methods through which the spacecraft can orient itself to conduct accurate maneuvers. The system block diagram for orientation control can be seen in Figure 4.5.3, though this is also repeated for angular velocity control.

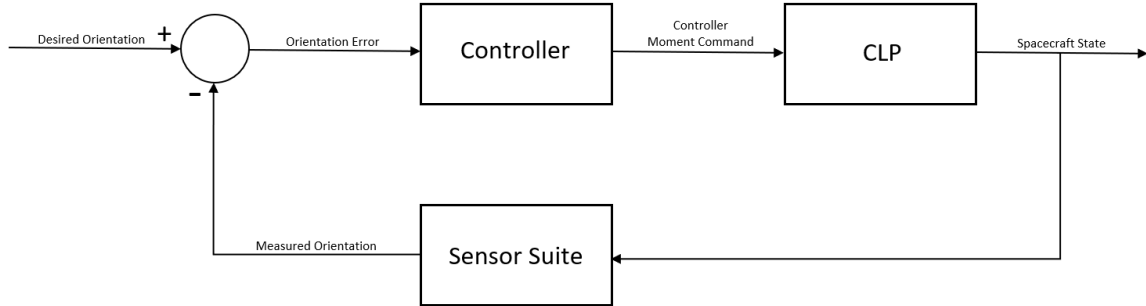


Figure 4.5.3: System Level Orientation Control Block Diagram

With this system level control law in mind, a PID controller for the CLP was developed, as shown below in Figure 4.5.4.

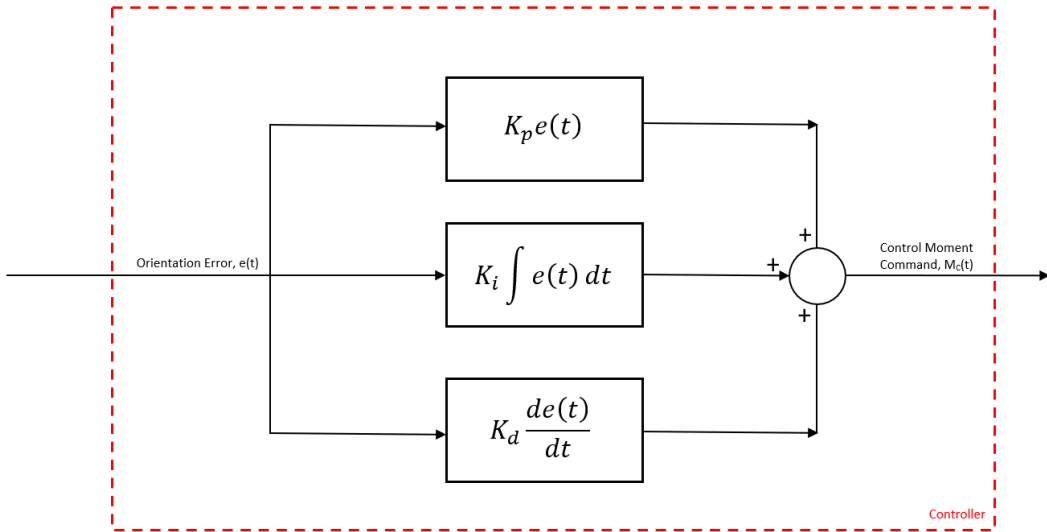


Figure 4.5.4: Orientation PID Controller Block Diagram

In order to test the convergence of the system controller, a simulation environment was developed for the CLP, and the controller was tested at various initial angular velocities to confirm the system converges to the desired angular velocities and orientation angles. For the simulation and the controller, Euler symmetric parameters, or quaternions, were used as the control parameters rather than Euler angles due to the removal of singularities when using quaternions. However, in order to make the desired orientation angle inputs understandable, these desired angles were entered as Euler angles before being converted into quaternions (the code for the simulation and the controller can be found in Appendix K).

Three simulations were conducted for initial angular velocity magnitudes of 6.5 rad/s, 3 rad/s, and 1 rad/s, with pseudo-randomized vector components. The angular velocity, orientation parameters, and control moment histories were then plotted for analysis of the control convergence. These simulations were conducted in idealized environments with no external moments, and assumed no noise in measurement signals from the sensors.

For the first simulation, the initial angular velocity had a magnitude of 6.5 rad/s, a value that is much greater than the maximum angular velocity that is likely to occur on this mission. As shown in Figure 4.5.5, the angular velocity is nearly zero within 10 seconds of the initial condition. Thus, even with a highly oscillatory initial condition, the PID controller is successful in reducing the angular velocity. The controller is also able to converge to the desired orientation as shown in Figure 4.5.6, within approximately 13 seconds. Figure 4.5.7 shows the controller command moments given by the PID controller, which are bounded by the maximum system torque of 3.6 N-m (based on reaction wheel selection).

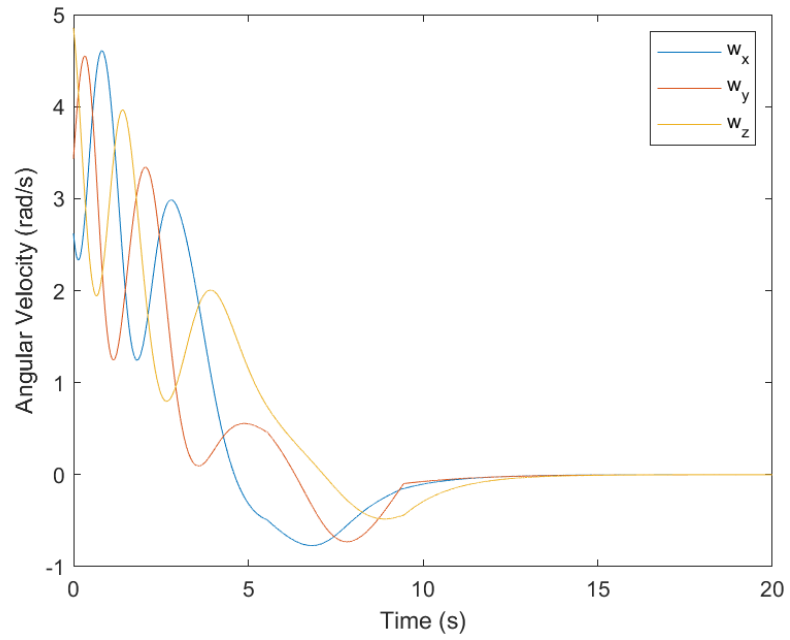


Figure 4.5.5: Angular Velocity vs. Time ($\omega_0 = 6.5 \text{ rad/s}$)

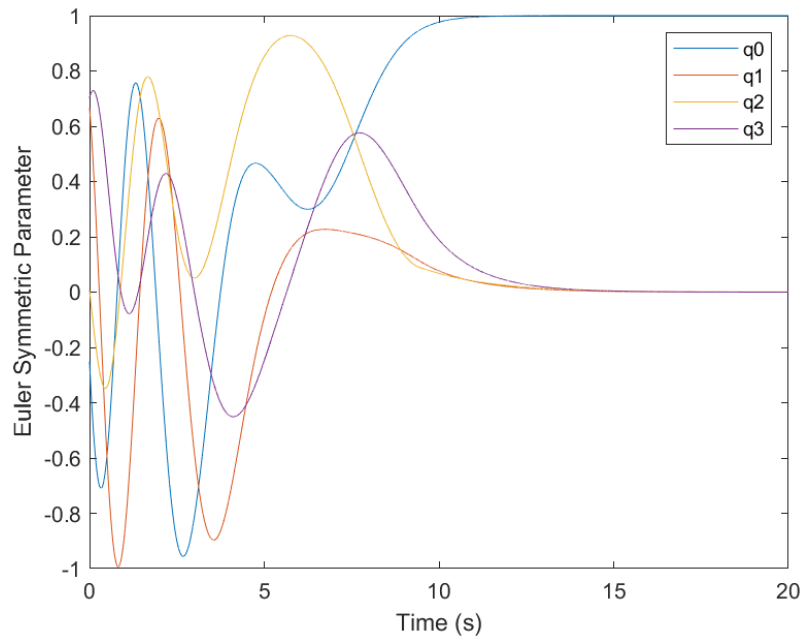


Figure 4.5.6: Orientation vs. Time ($\omega_0 = 6.5 \text{ rad/s}$)

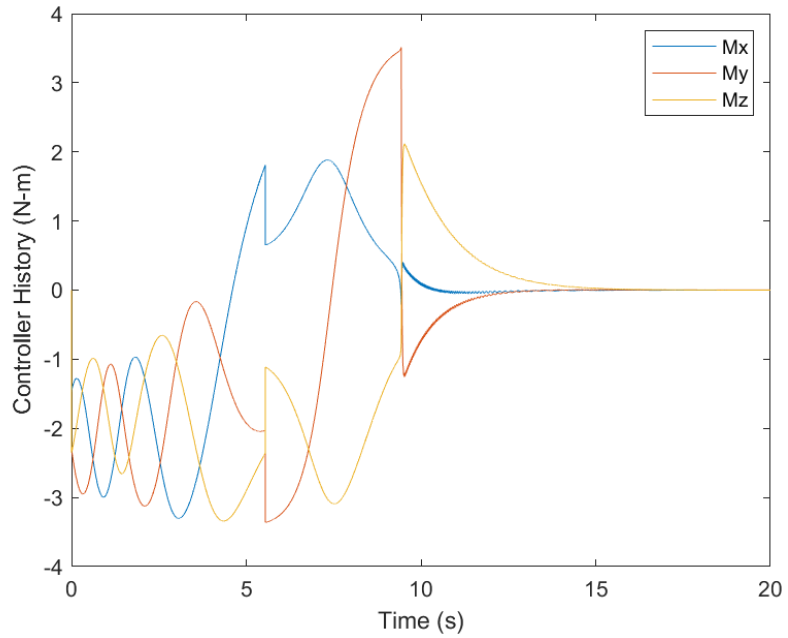


Figure 4.5.7: Control Moments vs. Time ($\omega_0 = 6.5 \text{ rad/s}$)

For the second simulation, the initial angular velocity was set to a magnitude of 3 rad/s, a more reasonable angular velocity to expect during the mission duration. Figure 4.5.8 shows that the controller is able to reduce the angular velocity to nearly zero in approximately 10 seconds, about the same time as the first 6.5 rad/s simulation, however, the controller is able to achieve this with significantly less oscillations. As seen in Figure 4.5.10, the control command moments are significantly less oscillatory than those encountered during the 6.5 rad/s simulation. Furthermore, Figure 4.5.9 shows that the orientation converges to the desired orientation in about 11 seconds.

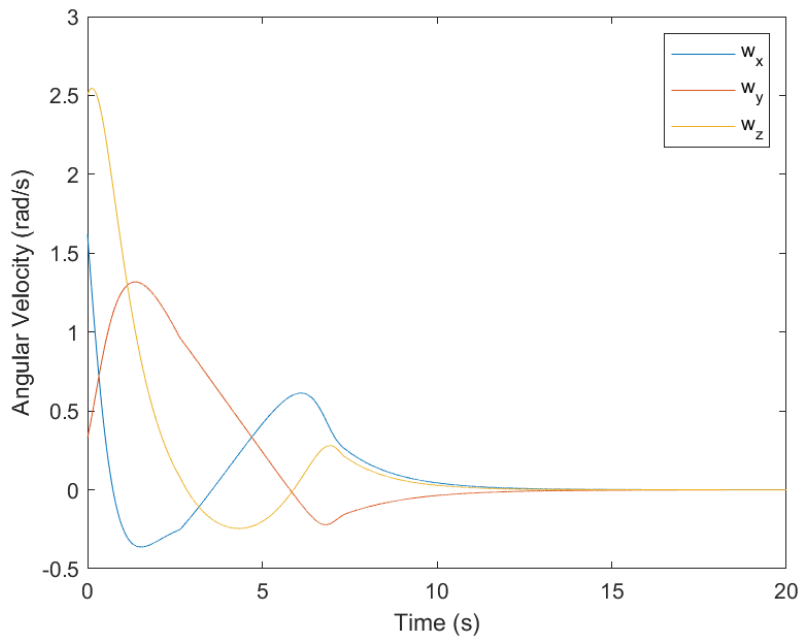


Figure 4.5.8: Angular Velocity vs. Time ($\omega_0 = 3 \text{ rad/s}$)

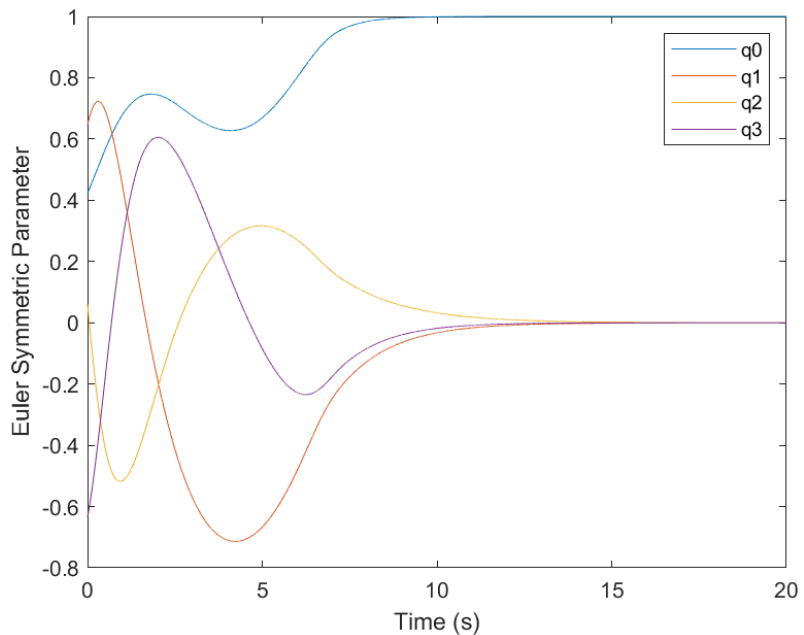


Figure 4.5.9: Orientation vs. Time ($\omega_0 = 3 \text{ rad/s}$)

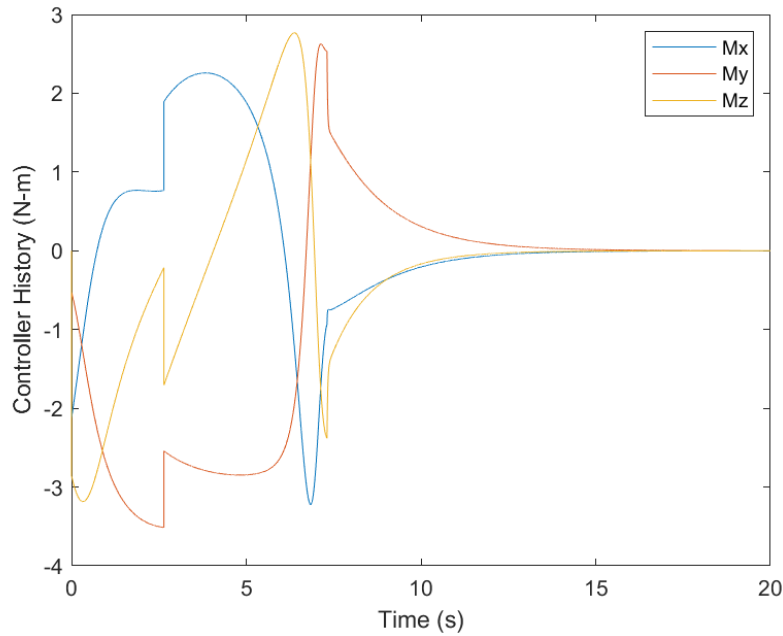


Figure 4.5.10: Control Moments vs. Time ($\omega_0 = 3 \text{ rad/s}$)

A third simulation with an initial angular velocity of 1 rad/s was then conducted to ensure that the desired orientation angles are achieved for low angular velocities. Figure 4.5.11 shows that the angular velocity is reduced to nearly zero within 6 seconds, and Figure 4.5.12 shows that the desired orientation angles are achieved within 7 seconds of the start of the simulation.

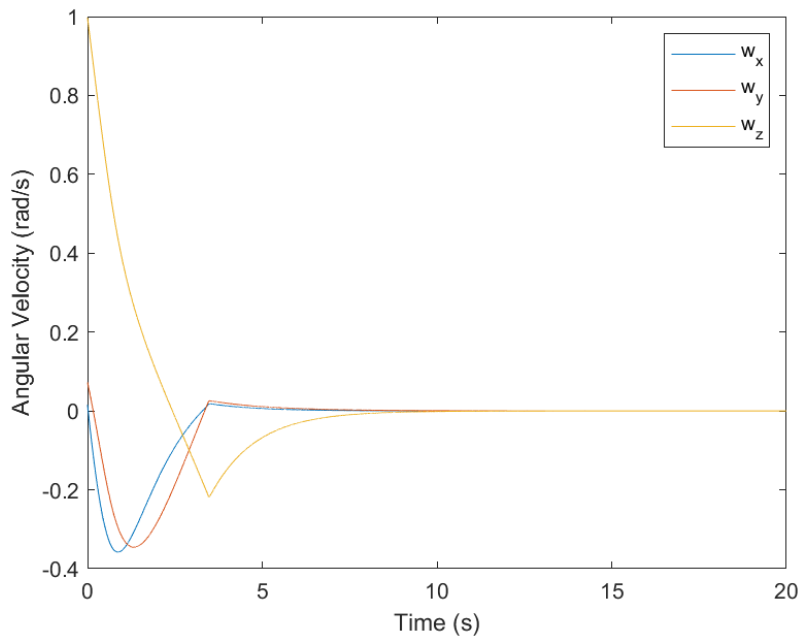


Figure 4.5.11: Angular Velocity vs. Time ($\omega_0 = 1 \text{ rad/s}$)

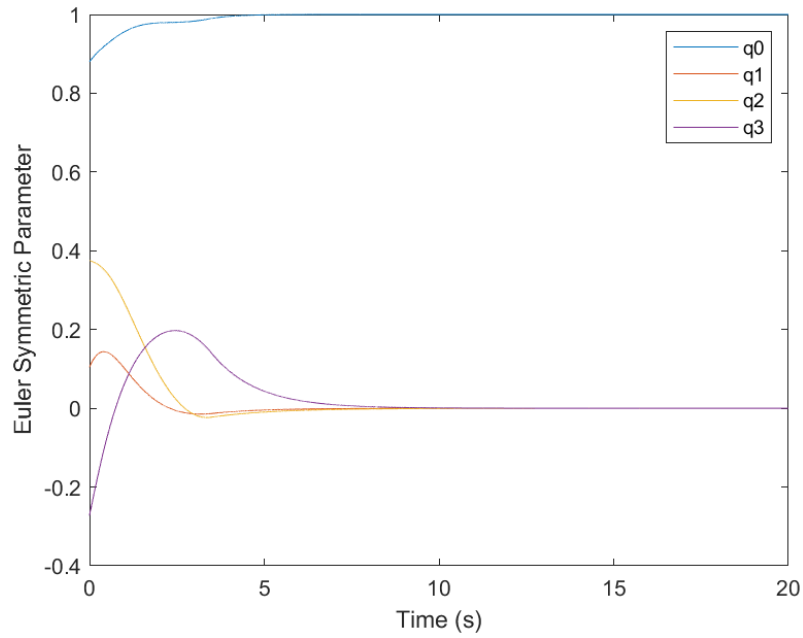


Figure 4.5.12: Orientation vs. Time ($\omega_0 = 1 \text{ rad/s}$)

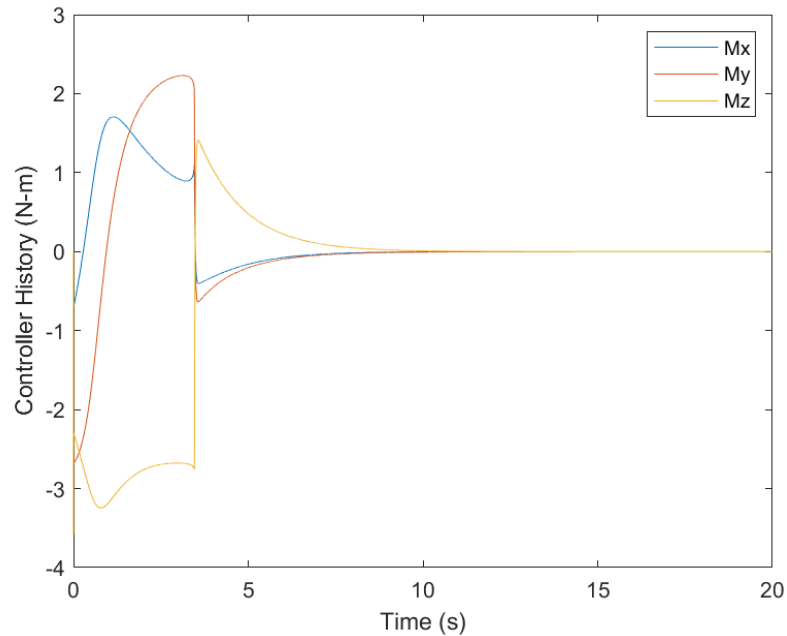


Figure 4.5.13: Control Moments vs. Time ($\omega_0 = 1 \text{ rad/s}$)

4.5.5 RISK ANALYSIS AND MITIGATION

The risk analysis and mitigation for the attitude determination and control subsystem can be found in [Appendix B](#) Table B6.

4.5.6 NON-TECHNICAL CONSIDERATIONS

The non-technical considerations for the attitude determination and control subsystem can be found in [Appendix C](#) Table C6.

4.5.7 PLAN OF PROCESSION

Extensive additional work is required to test and validate both the simulation and control system developed for the CLP. Notably, measurement signal noise and filtering methods were excluded from this analysis, so later models should incorporate these principles. Furthermore, many more simulations should be run in order to validate the control system in the presence of unique external and internal moments. More refined models would also include external disturbances from solar radiation, comet ejecta, or other debris, along with internal disturbances such as those generated from the movement of solar arrays. Additionally, although the PID controller was sufficient in controlling the CLP given this simplistic system model, a more accurate system model may yield differing results. Consequently, it may be beneficial to switch the controller to a model predictive controller (MPC), which may help the CLP converge to desired orientations at a faster rate by utilizing the high specification control board included in the command and data subsystem.

The development of a full ephemeris table detailing the desired orientations and positions of the spacecraft throughout the mission would also have to be developed before launch. This table would also be used in conjunction with a higher fidelity system simulation in order to validate the control system. Furthermore, although it was not considered in the design of this subsystem, a position controller that incorporates thrusting capabilities of the propulsion system would be necessary to develop and test. Finally, additional research into the sensors, such as the star trackers, sun sensors, and inertial measurement units, may be beneficial in order to decide whether lower specification models would be sufficient.

4.6 THERMAL MANAGEMENT

4.6.1 SUBSYSTEM DEFINITION

The thermal management subsystem deals with maintaining appropriate temperatures throughout each respective subsystem to ensure that they function efficiently and safely. In order to accomplish this, the thermal management subsystem will define operating temperature parameters for each subsystem and employ appropriate technologies to ensure that these parameters are met. These technologies can be generally categorized by heat generation, heat transmission, and heat dissipation. This system will also deal with the selection and qualification of boundary layer materials to separate the CLP from the extreme temperatures of space. Finally, this subsystem will be responsible for determining an appropriate arrangement of the selected technologies and quantifying heat transfer rates and power requirements necessary to control critical subsystems.

4.6.2 PRELIMINARY DESIGN OVERVIEW

In the preliminary design of this subsystem, design selections were made for heat generation, heat transmission, heat dissipation, and boundary layer materials. For heat generation, a radioisotope heating unit (RHU) was selected on the basis of its consistent heat output, and its ability to operate passively without electrical energy. For heat transmission, a powered heat pipe (PHP) was selected because it can move heat against a gradient, allowing the CLP to be cooled or heated in specific areas. For heat dissipation, a body mounted radiator (BMR) was chosen to remove heat due to its reliable, minimally complex design. Finally, multi-layer insulation (MLI) was determined to give the most optimal temperature resistance for a boundary layer.

4.6.3 PRODUCT SELECTION

In this section, the specific products that will be used in the thermal management subsystem will be concisely summarized. The RHU chosen will be a 1 Watt model, that weighs about 40 grams, and uses a 1 gram pellet of plutonium-238 [74]. This specific RHU will be used in 15 different places around the CLP to satisfy sufficient temperature margins. Because the RHU uses military grade plutonium, this product is not commercially available, and a specific manufacturer and model are not known. Consequently, these devices will have to be obtained from a governmental agency such as NASA.

The looped heat pipe was not originally chosen in the PDR, but was selected over the original powered heat pipe due to power budget constraints. The looped heat pipe (LHP) uses capillary action to move high energy gas into a liquid state by using ammonia to transfer up to 700 W of energy [25]. Although there were limited options commercially available to choose from, specifications for a LHP produced by Advanced Cooling Technologies are shown in Figure L1 in Appendix L. One advantage of this specific product is that it was utilized on a micro-satellite, indicating that it has flight heritage, a low mass, and a reasonable volume.

The Kenworth T300 radiator will be used twice on this CLP due to its favorable mass and volume. This model radiator has a mass of only 0.29 kg and an effective thermal conductivity of $50 \frac{W}{mK}$ [1]. Although the conductivity is relatively low compared to other radiator models, the limited mass and volume requirements make it an ideal product for this spacecraft.

Finally, for the selection of the MLI, the thickness of each layer will vary depending on its location in the MLI. The outermost layer of the MLI will be ~5 mm thick FEP Teflon, due to its ability to absorb incident radiation. Ten layers of ~6.35 mm thick aluminized kapton will also be used due to its favorable thermal resistance properties. Although a commercially available product with these specifications is not available, these design requests were selected to meet the thermal management requirements of the CLP while limiting the required mass. Although there are many qualified suppliers for a custom MLI with these design specifications, Northrop Grumman will be the planned manufacturer due to their vast experience with spaceflight-grade hardware.

Table 4.6.1: Thermal Management Product Selection

Component	Manufacturer	Model
Radioisotope Heating Unit	N/A	1 Watt, Pu-238, 40 g
Looped Heat Pipe	Advanced Cooling Technologies	TacSat - 4
Body Mounted Radiator	NASA	T-300
Multi-Layer Insulation	Northrop Grumman	Teflon, Aluminized Polyimide -10 layers, Kapton.

4.6.4 THERMAL DESIGN AND ANALYSIS

In order to accurately model the temperature distribution across the CLP, a computational fluid dynamics temperature model was created in Siemens NX. A basic analysis of the exterior of the CLP was performed by first creating a mesh, and then running the model for the heat flux conditions that the CLP will experience at 1.055 au from the Sun (its perihelion point). In order to calculate the approximate heat flux due to solar radiation, Equation 4.6.1 was employed [6]. In this equation, G represents the heat flux in Watts per square meter due to direct solar impingement, and d represents the distance from the Sun in astronomical units [6].

$$G = \frac{1367}{d^2} \quad \text{Equation 4.6.1}$$

After plugging in the perihelion distance into Equation 4.6.1 to solve for the most extreme expected temperature distribution, the heat flux was found to be $1228 \frac{W}{m^2}$. Some other boundary conditions that were necessary in order to constrain the thermal model included specifying an initial temperature of the CLP, which was assumed to be a uniform $-30^\circ C$. Although the temperature of deep space is closer to 3 Kelvin ($-270^\circ C$), the initial temperature was modeled as $-30^\circ C$ because the MLI and RHU's will not allow the spacecraft to reach these extreme temperatures. Additionally, a conduction control was placed on the CLP body and a thermal conductivity of $10 \frac{W}{m \cdot K}$ was specified in order to model the heat transfer by conduction throughout the structure. It should also be noted that a 3D tetrahedron mesh was applied to the CLP body.

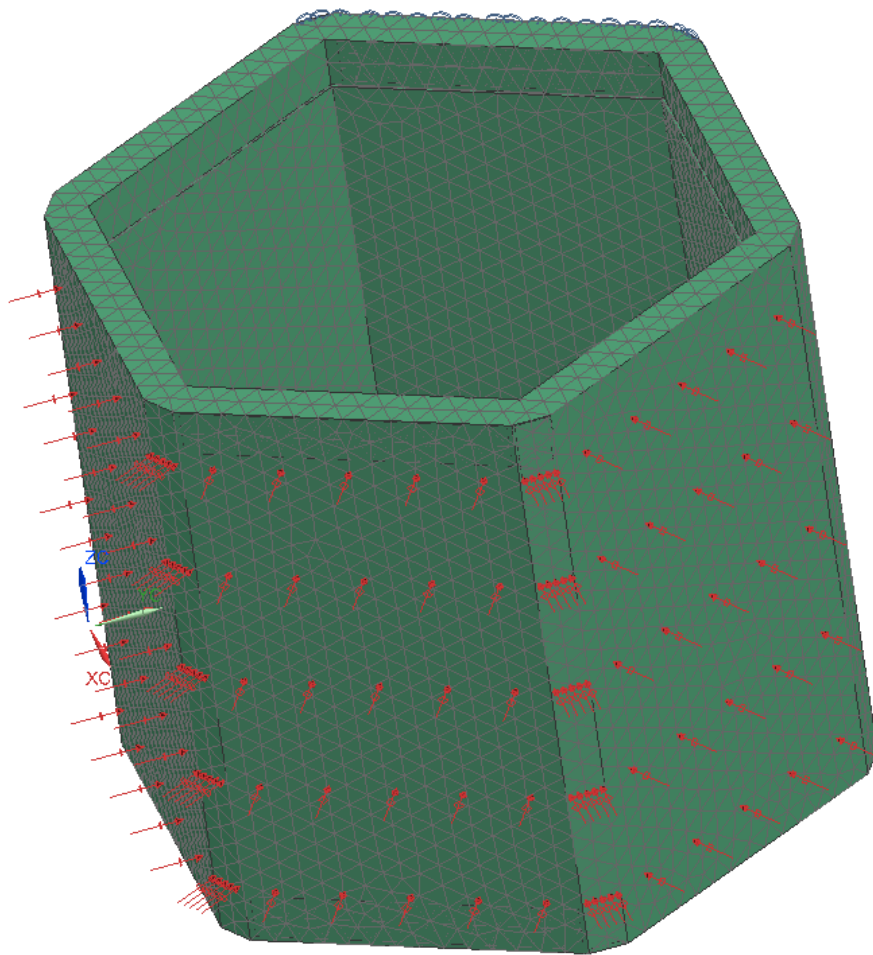


Figure 4.6.1: Structural Mesh with Loads for Thermal Analysis

Figure 4.6.1 pictured above shows the mesh that was used in the thermal analysis. As is shown in this figure, the thermal “loads” act perpendicularly on three out of the six main sides of the hexagonal CLP structure. This is an accurate representation of the thermal conditions that the CLP will experience since half of the lander’s surface area will always be facing towards the Sun. It should also be noted that the thermal “loads” are refined on the edges. After performing the necessary mesh qualifications and checks, and assigning the appropriate boundary conditions, a temperature gradient result was simulated, as shown in Figure 4.6.2 below.

CLP Frame_sim2 : Solution 1 Result
 Subcase - Loads, Constraints 1, Static Step 1, 1
 Temperature - Nodal, Scalar
 Min : -30.001, Max : -24.803, Units = °C

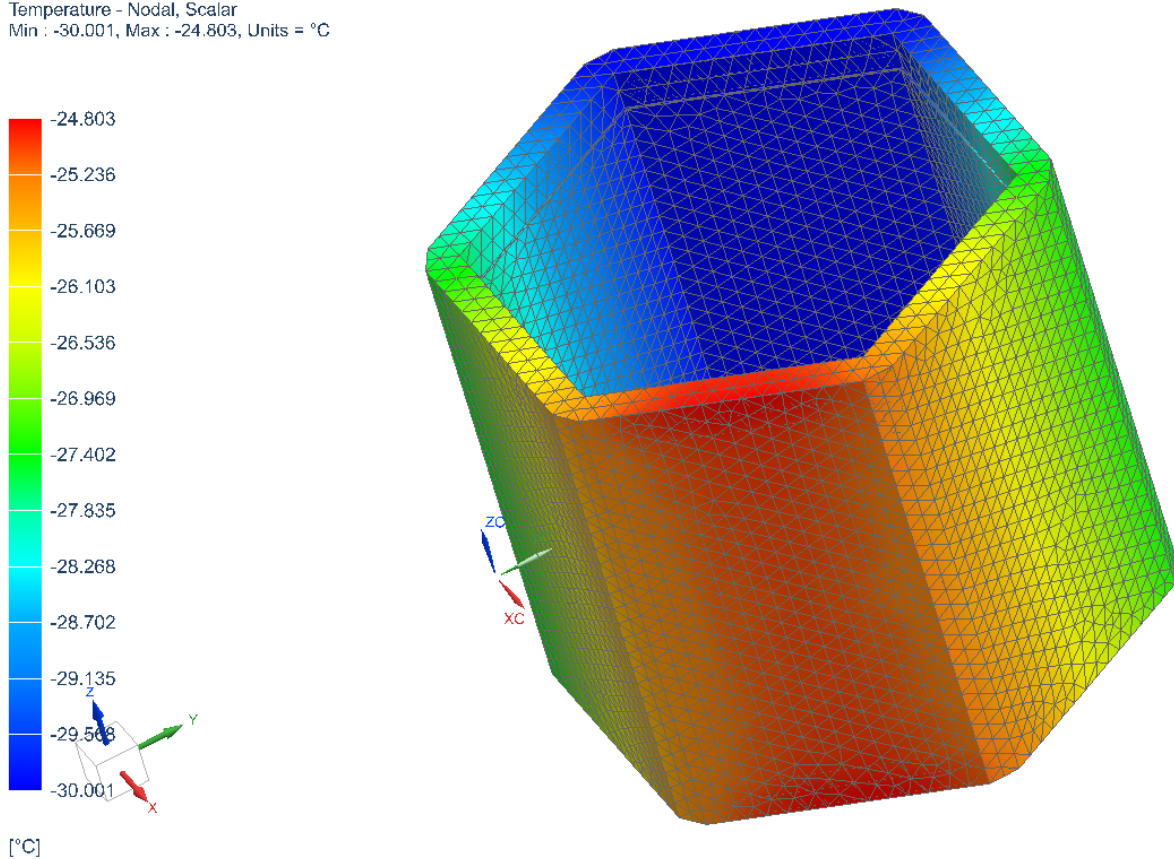


Figure 4.6.2: Temperature Distribution From Thermal Analysis

This finite element analysis shows that the solar radiation from a distance of 1.055 au will cause a notable change in the temperature distribution experienced by the CLP. The temperature ranges from -30° C to -24.8° C , depending on the position of the point with respect to the incident radiation. Another important parameter to consider is the time of this simulation. The results above represent the temperature distribution after 30 minutes over 8 time step intervals, which was selected in order to limit the computations needed to complete this analysis. However, if this analysis were performed for greater lengths of time, the temperature distribution would undoubtedly be even more extreme.

This type of temperature distribution analysis is crucial for the accommodation of the other systems. For instance, this type of analysis would be necessary in order to understand the optimal placement of RHUs. This analysis is also important to ensure that the thermal subsystem is able to maintain the thermal margin as a whole. As detailed in the PDR, the thermal margin is very specific for the range of components that can be found throughout the CLP. The CLP has been designed to have an excess of heat, so that the active body-mounted radiators can dispel heat if needed. This approach will mitigate concerns of the CLP reaching the lower limits of its

thermal margin, but increases the need for effective heat removal in order to avoid the upper limits of the thermal margin.

4.6.5 RISK ANALYSIS AND MITIGATION

The risk analysis and mitigation for the thermal management subsystem can be found in [Appendix B](#) Table B7.

4.6.6 NON-TECHNICAL CONSIDERATIONS

The non-technical considerations for the thermal management subsystem can be found in [Appendix C](#) Table C7.

4.6.7 PLAN OF PROCESSION

Given additional time to continue developing this spacecraft, the design of the thermal system would progress by incorporating more factors into the FEA model, such as the rotational effects of the radiation source, the convective heat transfer associated with the thin atmosphere of the comet, and the placement of RHU's and their effect on the temperature distribution of the lander. Additional simulations would also be run for other points of interest on the CLP, such as the apoapsis or intermediate orbit locations, in order to better assess the temperature distributions that could be expected throughout the mission duration. With greater computational resources, the length of these simulations would also be increased to understand the temperature distributions for longer periods of time. The model would also be refined as additional components and subsystems were added (each with their own specifically designated thermal properties), and more in-depth analysis would be performed on temperature-sensitive components, such as the control board, to ensure a proper thermal margin is maintained.

In addition to work surrounding the refinement of the thermal models, the production of components would occur after the engineering analysis used to select these components was verified by external parties. Thorough testing would then take place in order to test the products for defects and deficiencies that may have not been apparent in the selection process. Finally, there would be a fair amount of work associated with the assembly of the thermal management components and their integration into the overall lander subsystem, all of which would take place closer to the launch window.

4.7 POWER MANAGEMENT

4.7.1 SUBSYSTEM DEFINITION

The power and power management subsystem details the processes through which electrical energy is generated, stored, and distributed throughout the spacecraft. More specifically, this subsystem includes the quantification of power requirements, the model selection of solar arrays and batteries, and the distribution methods employed to power the other

subsystems of the CLP and its payload. An efficient power scheduling system was developed for the CLP for each major phase of the mission. This was done to limit the maximum power draw at any given time.

4.7.2 PRELIMINARY DESIGN OVERVIEW

In the preliminary design of this subsystem, selections were made regarding the method for power generation and power storage within the system. Solar arrays were chosen as the method for power generation due to considerations regarding the length of the mission, mass requirements, and power output. Secondary batteries were also incorporated into the design for storage. Nickel-metal hydride batteries were chosen primarily due to their flight heritage and cycle life, even though other solutions existed with higher specific energies.

4.7.3 PRODUCT SELECTION

Although nickel-metal hydride batteries were the technology selected during the preliminary design, the secondary batteries were changed to lithium-ion batteries due to mass constraints and further analysis that suggested the specific energy of these batteries would be worth the disadvantages posed by safety and flight heritage. Lithium-ion batteries have been shown to be a reliable technology over the last decade, and as such, this change was considered reasonable. Multiple products were compared before arriving at Saft's MP176065 xtd batteries as the final product, primarily due to its extended life and temperature rating and higher amperage output capabilities. Several other models of batteries this product was compared against can also be seen in Figure M1 of Appendix M.

In terms of the type of solar arrays being used, the significant distance from the Sun throughout the mission necessitated high performance solar arrays in order to meet the CLP's proposed mass and volume budgets. Silicon-based solar arrays were not considered due to their relatively low performance as compared to other technologies, leading to a multi-layered solar array being chosen. Ultimately, Spectrolab's Ultra Triple Junction solar array was selected due to the product's high-performance efficiency and the company's experience in producing spaceflight-grade hardware.

Table 4.7.1: Power Management Product Selection

Component	Manufacturer	Model
Secondary Batteries (Li-ion)	Saft	MP176065 xtd
Solar Array	Spectrolab	Ultra Triple Junction (UTJ)

4.7.4 POWER GENERATION DESIGN AND ANALYSIS

In order to determine the size requirements for the solar array and batteries that provide power to the CLP, the power requirements were determined for each phase of the mission, and a

corresponding power schedule was developed. The power requirements for each main phase of the mission, as shown in Figure 4.7.1. Based on these totals, the nominal power requirement for the CLP was approximated as 160W for the purposes of sizing the solar array and batteries.

Stage 1: Disengagement from CLP	Stage 2: Orbit and Descent	Stage 3: Landing
Sep Nuts ----- 5 x 1W (one-time occurrence) RAD 750 ----- 14W RAD 5545 ----- 8W (standby) HC9 ----- 5W (standby)	SMA-R&R ----- 15W (one-time occurrence) AST CGT ----- 3.5W AST EPR ----- 10W RAD 750 ----- 14W RAD 5545 ----- 8W (standby) ISIS-QMS-TPL0045 --- 2W ST-16RT2 ----- 1W HG4930 ----- 2W HC9 ----- 8-112W	removeDEBRIS ----- 7W (one-time occurrence) AST CGT ----- 3.5W AST EPR ----- 10W RAD 750 ----- 14W RAD 5545 ----- 8W (standby) ISIS-QMS-TPL0045 --- 2W ST-16RT2 ----- 1W HG4930 ----- 2W HC9 ----- 8-112W
Total: 27W (+ one-time 5W)	Total: 48.5-152.5W (+ one-time 15W)	Total : 48.5-152.5W (+ one-time 7W)
Stage 4A: Ground Mission – Sample Collection	Stage 4B: Ground Mission – Sample Analysis	Stage 4C: Ground Mission – Hibernate
Perseverance Robotic Arm ----- 73.8W RAD 750 ----- 14W RAD 5545 ----- 8W STC-MS03 S-band Receiver ----- 18W ST-16RT2 ----- 1W	RAD 750 ----- 14W RAD 5545 ----- 35W STC-MS03 S-band Receiver ----- 18W ST-16RT2 ----- 1W + any of the following: CIVA ----- 2.2W APXS ----- 1.5W COSAC ----- 5W CONCERT ----- 3W ROMAP ----- 7W	RAD 750 ----- 3W RAD 5545 ----- 8W STC-MS03 S-band Receiver ----- 4W
Total: 114.8W	Total : 68 + (1.5-7)W (max: 75W)	Total : 15W

Figure 4.7.1: Power Requirements by Mission Phase

In order to determine the proper sizing of the solar array throughout the CLP mission duration, a model for the solar production was required. The magnitude of the solar incident energy (solar intensity) on the solar array was approximated using the determined orbital trajectory of the CLP. The solar intensity, H_I , is given by Equation 4.7.1 [6], the effect of temperature on its production, η_T , is given by Equation 4.7.2 [60], and the effect of pointing errors, η_{plf} , is given by Equation 4.7.3 [6].

$$H_I = \left(\frac{1}{R}\right)^2 \quad \text{Equation 4.7.1}$$

$$\eta_T = 1 - 0.0016(T - 28) \quad \text{Equation 4.7.2}$$

$$\eta_{plf} = \cos(\alpha) \quad \text{Equation 4.7.3}$$

In the equations shown above, R is the distance away from the Sun in astronomical units (au), T is the temperature of the array in °C, and α is the angle between the pointing direction and the normal direction to the solar radiation in radians. It was assumed that the operating temperature of the solar array would be given by a sinusoidal function, which assumed a rotation of the comet that would result in 120-hour “days” with a magnitude of 20°C. The code for this approximation can be seen in Appendix M.

Other factors that affect the power generation of the solar arrays are radiation damage, UV discoloration of the panels, cell mismatch (from manufacturing), interconnection resistance,

and panel contamination. Some of these factors are constant, though others change over the lifetime of the array. The values that were used in the following analysis are shown in Table 4.7.2 (based on values given in [6]).

Table 4.7.2: Solar Generation Inefficiencies

Effect	Factor	Value
Radiation Damage	η_{rad}	[0.8, 0.7]
UV Discoloration	η_{UV}	[1, 0.98]
Cell Mismatch	η_m	0.975
Interconnection Resistance	η_{IR}	0.98
Panel Contamination	η_{con}	0.98

Using these linear inefficiencies and Equations 4.7.1-4.7.3, a model for the solar generation per unit area was developed. The underlying power production model can be illustrated using Equation 4.7.4

$$P = P_{lab} \cdot \eta_{rad} \eta_{UV} \eta_m \eta_{IR} \eta_{con} \eta_T \eta_{plf} H_I \quad \text{Equation 4.7.4}$$

Where P_{lab} is the designed power output of a cell rated at 1[au] from the sun in lab conditions. The code for approximating the solar power generation can be found in Appendix M. The power generation over the mission duration is shown in Figure 4.7.2.

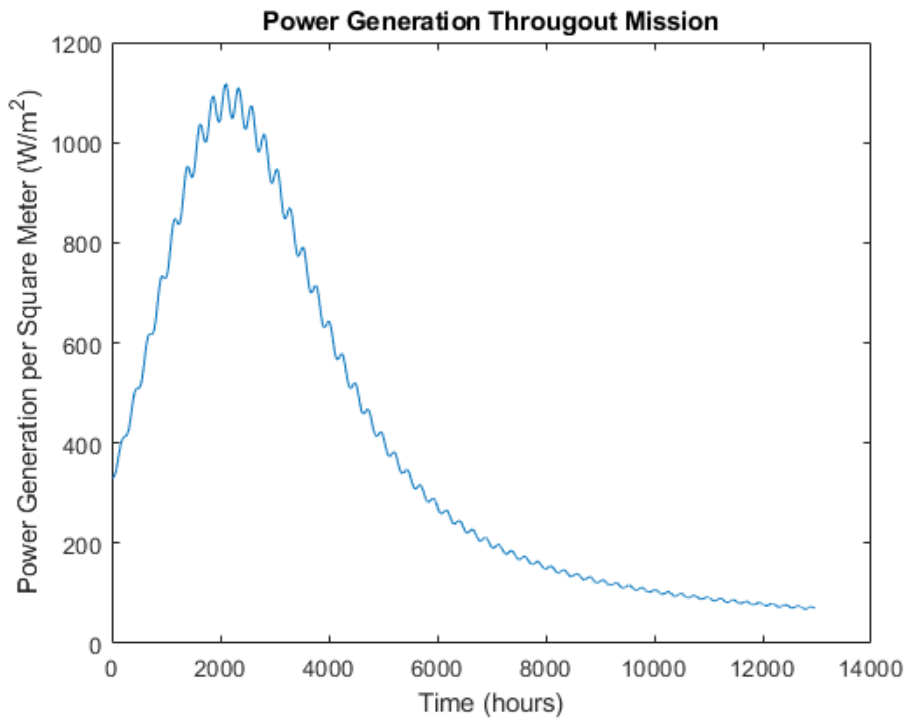


Figure 4.7.2: Power Generation Throughout Mission

Throughout the beginning of the mission, the solar power generation per square meter was above $300 \frac{W}{m^2}$, whereas towards the end of the mission, the power generation was approximately $71.5 \frac{W}{m^2}$. In order to maintain power generation requirements throughout the lifespan of this mission, the solar arrays were sized based on the end-of-mission power generation of approximately $71.5 \frac{W}{m^2}$. Based on the 160 W power requirement defined before, this resulted in a total solar panel area of $2.238 m^2$, which corresponds to 1.88 kg of solar cells. Since the CLP will have six solar arrays (one coming off each side of the hexagonal body) these parameters can be divided by six to obtain the specifications for individual solar arrays.

4.7.5 POWER STORAGE DESIGN AND ANALYSIS

In order to size the batteries for the CLP, a nominal power requirement of 15W (determined by the baseline “hibernation” state of the CLP) for 60 hours (half of the 120 hour rotation cycle as mentioned in the previous analysis) was used as a capacity constraint. This is the minimum capacity required to maintain the baseline power requirements of the CLP for expected periods without power generation. A 20% margin was also included in the design specifications in order to account for the cyclic degradation of the batteries, battery inefficiencies, and other secondary factors. This requirement resulted in a minimum battery capacity of 1080 Whr. Then, Equation 4.7.4 was used to calculate the minimum number of cells required to meet this design constraint.

$$\# \text{ of cells} = (\text{battery capacity [Whr]}) \cdot \left(\frac{1 \text{ cell}}{(\text{cell voltage [V]}) \cdot (\text{nominal capacity [Ahr]})} \right) \quad \text{Equation 4.7.5}$$

Using the Saft MP176065 xtd cell parameters which can be found in Appendix M, the number of cells required can be calculated as $52.84 \approx 54$ cells (rounded up to 54 to evenly divide groups of cells into battery packs). Then, the total mass for the battery pack was calculated to be 7.29 kg from the mass per cell parameter specified in the battery datasheet.

Though the optimal cell configuration would require further analysis of the power distribution system and accurate models or testing, a preliminary cell configuration was developed based on the maximum expected voltage of 36V (from the AST GmbH Cold Gas Thruster). Though any design decision regarding cell configuration is preliminary and has a high likelihood of changing in future designs, several scenarios were considered to meet the maximum voltage and current requirements. The design of the battery pack resulted in nine cells placed in series per battery, with six batteries being placed in the battery pack. This corresponded to a max voltage of 32.85 V per battery and a max current of 66 A.

4.7.6 RISK ANALYSIS AND MITIGATION

The risk analysis and mitigation for the power management subsystem can be found in [Appendix B](#) Table B8.

4.7.7 NON-TECHNICAL CONSIDERATIONS

The non-technical considerations for the power management subsystem can be found in [Appendix C](#) Table C8.

4.7.8 PLAN OF PROCESSION

If more time were allotted to this project after this semester, further testing and analysis of the final design would be conducted. One of the next primary goals of this subsystem would be to develop a proper simulation of the expected solar radiation over the course of the mission, by gathering more detailed information about the rotational rate of 46P/Wirtanen and prospective landing sites.

Additional research on solar array manufacturers may also be valuable as the current selection may be overkill for the mission specifications, and thus an unnecessary burden on the cost budget. Consequently, a cost-benefit analysis should be conducted that incorporates the potential mass reduction and reduced launch costs with the high cost of the solar panels. In a similar fashion, further research on battery manufacturers may be beneficial to further optimize the total cost of the subsystem.

Finally, an analysis of the optimal voltage and current from the batteries should be conducted, with emphasis on modeling the power loss through the conductive wiring and transformers. The inclusion of power dissipation methods should also be incorporated to protect against excessive electrical energy in the system.

4.8 COMMAND AND DATA

4.8.1 SUBSYSTEM DEFINITION

The command and data subsystem includes the command and control computer, the storage of mass digital data, and the communication protocols involved with the transmission of data to and from Earth. More specifically, this subsystem is responsible for autonomously directing the tasks of other subsystems, actively tracking and storing engineering and scientific data, and employing basic data processing schemes to this stored data. In addition to these tasks, the command and data subsystem must also maintain the spacecraft clock to keep the mission on schedule and interpret messages from mission control in order to carry out the necessary actions. Finally, this subsystem plays a critical role in emergencies, as it is responsible for monitoring the status of other subsystems and applying fault protection algorithms and safing routines when appropriate.

4.8.2 PRELIMINARY DESIGN OVERVIEW

In the preliminary design of the command and data subsystem, the general computer architecture was determined, and models for two control boards were selected. As a result of its feasibility and lower mass, power, and volume requirements, a centralized computer architecture will be used instead of distributed or remote computer architectures. The primary control board of the CLP was determined to be a BAE Systems RAD750 6U Extended Single Board computer due to its significant flight heritage and lower power requirements. However, a newer BAE Systems RAD5545 Space VPX computer will also be onboard the lander, as a result of its favorable product features. These features include increased encryption and image processing capabilities, and the ability to run multiple operating systems simultaneously, ultimately providing the CLP with a delicate balance of reliability and value.

Although outside of the command and data subsystem's preliminary analysis conducted in the PDR, it should also be noted that a helix antenna will be used as a result of its high directionality and gain. Due to the critical nature of the telecommunications subsystem, a secondary small patch antenna was selected for emergency situations due to its favorable mass and power requirements. Finally, all data transmissions over these antennas will take place on the S-band frequency, as a result of its high reliability and low power requirements.

4.8.3 PRODUCT SELECTION

This section serves to concisely summarize the specific products that will be under the control of the command and data subsystem. Since the specific products for this subsystem were already selected in the PDR, there is no further down selection process to consider for this subsystem. However, the decision matrices used to arrive at these specific products can be reviewed in Appendix N. Additionally, while the decisions do not warrant product selections (because all connectors and protocols should accomplish the same goal regardless of the supplier) the interface between the two control boards was determined to be a parallel interface

rather than a serial interface, despite its greater complexity, due to the greater transmission speeds and capability to read and write data simultaneously. Furthermore, the communication protocol between the control boards and surrounding subsystems and components was selected to be RS-485 due to its simplicity, greater transmission rates, and robustness to noise.

Table 4.8.1: Command and Data Product Selection

Component	Manufacturer	Model
Master Control Board	BAE Systems	RAD750 6U Extended
Payload Control Board	BAE Systems	RAD5545 Space VPX
Board-Board Interface Wiring	Any	Any
Board-Component Interface Wiring	Any	Any

4.8.4 COMPUTER ARCHITECTURE DESIGN AND ANALYSIS

Due to the critical importance of the control boards in the success of this mission, it is necessary to have redundancy, leading to the selection of two control boards. These control boards must be powerful enough to handle all of the tasks required of this subsystem in case of a system failure in the other control board. However, in normal operating conditions, when both control boards are fully functional, these tasks will be intelligently delegated based on the strengths of the respective control board. For instance, the RAD750 will serve as the “master” control board, as it will be responsible for general operations of the CLP, such as executing the power schedule and propulsive maneuvers. The RAD5545, however, will be used primarily for payload operations, as its newer features and higher processing power will allow more value to be deducted from the scientific experiments being conducted by the sensor suite. These operations will include tasks like analyzing the sensor suite data, processing images taken by the infrared cameras and resonance imaging equipment, and encrypting this data before it is transmitted to the PV.

This delegation of responsibilities will also be advantageous for limiting the processing power and CPU temperatures placed on a single control board, resulting in greater reliability and value to the customer. The control boards will still be located in the same general vicinity, however, to simplify the thermal management architecture and allow for simplified crosslinking for emergency situations.

In order to expand on the aforementioned delegation structure, the following tasks are proposed to be handled by the respective control boards. It should be emphasized that all tasks can be handled by a single control board (with proper power scheduling) but are divided in order to maximize the reliability and efficiency of the equipment that will already be onboard the CLP.

Master Control Board (RAD750):

- Analyze the data from the general CLP sensors to compile the engineering data

- Store and transmit the engineering data via the S-band transceiver
- Monitor general CLP subsystems and apply fault protection algorithms and safing routines when appropriate
- Receive and execute the communication protocols via the S-band transceiver
- Execute the power scheduling routines for the general CLP subsystems
- Maintain the spacecraft clock
- Execute propulsion and ADCS tasks
 - Receive and analyze navigation and ADCS sensor data
 - Execute appropriate thruster and reaction wheel operations to achieve desired position, velocity, and orientation

Payload Control Board (RAD5545):

- Coordinate the sensor suite instrument operation schedule during the scientific data collection phase of the mission (post-landing)
- Analyze the data from the sensor suite to compile the scientific data
 - Apply data processing schemes (such as data compression, encoding, and encryption) to the scientific data
- Store and transmit the scientific data via the S-band transceiver based on the communication protocols executed by the master control board
- Monitor the sensor suite equipment and apply fault protection algorithms and safing routines when appropriate
- Execute the power scheduling routines for the sensor suite

Based on this detailed delegation structure, the command and data subsystem architecture, as it pertains to data collection, analysis, and transmission, can be visualized with Figure 4.8.1 below. The master and payload control boards will communicate via a parallel interface link (PI) in order to allow for greater data transmission rates [84]. The boards will also communicate with their respective subsystems, sensor suites, and the S-band transceiver via an RS-485 standard. This type of transmission protocol has been selected over methods such as USB and ethernet to avoid data packet collision and unnecessary complexity [87]. This method is also preferred over more pervasive communication standards such as RS232 due to its robustness to noise and greater data transmission speeds [122].

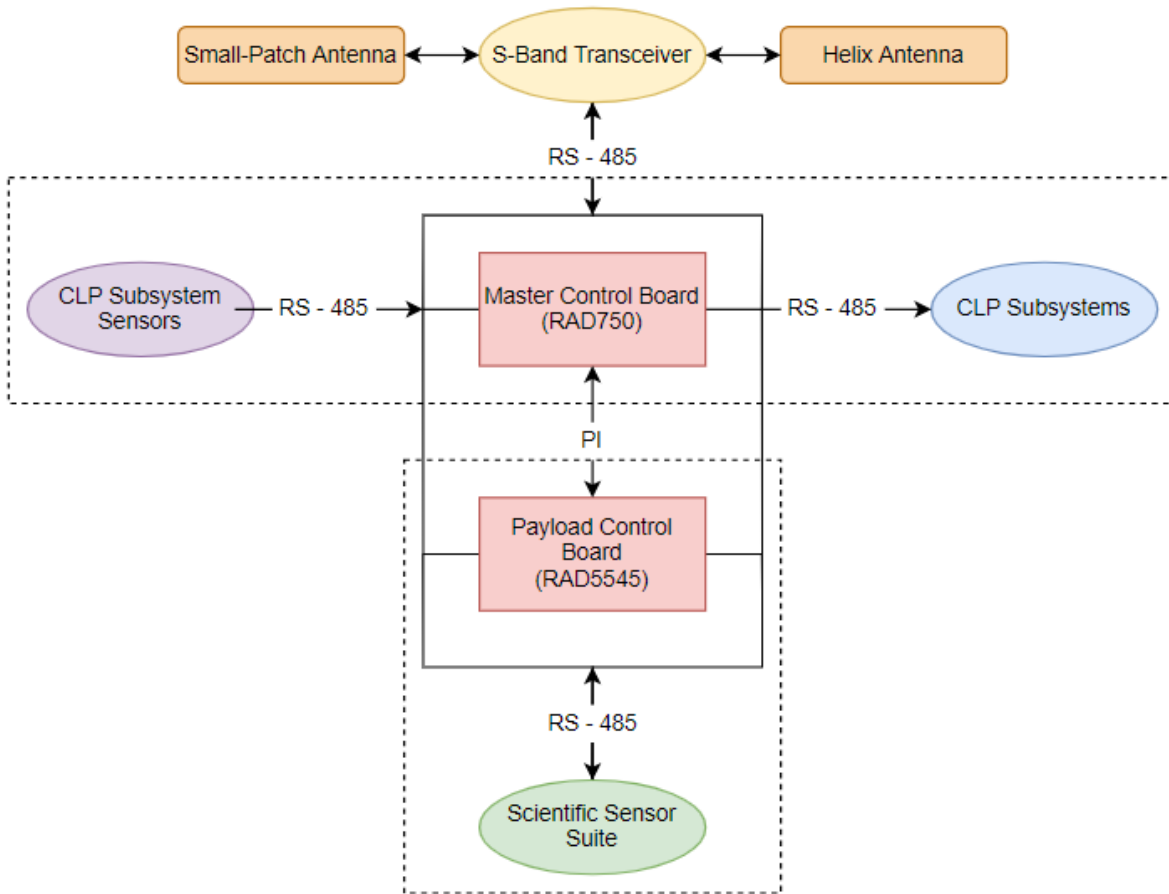


Figure 4.8.1: Command and Data Computer Architecture

4.8.5 OPERATING REGIME PROTOCOL DESIGN AND ANALYSIS

Engineering data collected by the master control board will be uplinked to the PV through the S-band transceiver and helix antenna (or small-patch antenna as a backup). This data will be transmitted regularly to the PV in predictable, recurring transmission windows as dictated by mission control and the transmission schedule proposed below.

Scientific data collected by the payload control board will also be uplinked to the PV through the S-band transceiver and helix antenna, but will occur less frequently than the transmission of engineering data. While engineering data will be collected continuously throughout the CLP mission, the payload control board will remain idle until the CLP has safely landed on the surface of 46P/Wirtanen, when scientific experiments can then be conducted.

During scientific experimentation, both control boards will be running in order to maintain all the necessary subsystems and equipment, but upon completion of these experiments the payload control board will return back to its idle state. Scientific data collected by the PV will be transmitted separately from engineering data and will typically be prioritized over engineering data, except in emergency situations.

The following list serves as a preliminary hierarchy of general transmission protocols based on the urgency and nature of the transmission. This procedure will likely change as additional use cases are developed and further refined.

- 1) Master control board malfunction
 - a) Master control board will initiate the payload control board via a PI command to bring the payload control board out of idle mode
 - b) Payload control board will terminate all scientific operations and attend to master control board responsibilities
- 2) Emergency situation (general CLP hazard)
 - a) Payload control board will terminate all scientific operations to provide additional power for more critical subsystems
 - b) Master control board will initiate fault protection algorithms and safing routines to preserve the mission to the greatest extent possible
 - c) Engineering data will be prioritized in the current or next transmission window to address the hazardous situation with mission control
 - d) If the hazard is deemed unavoidable and end of mission status is inevitable, scientific data will be prioritized in the current or next transmission window
- 3) CLP orbital capture and descent
 - a) Payload control board will remain in the idle state unless deemed necessary for the target landing site selection or atmospheric data collection
 - b) Master control board will autonomously operate to perform the necessary orbital capture and descent maneuvers
 - c) Engineering data will be prioritized in the current or next transmission window to address the critical nature of this mission phase and communicate the situation to mission control
- 4) Payload control board malfunction
 - a) Payload control board will communicate malfunction status to the master control board via a PI command
 - b) Master control board will initiate fault protection algorithms and safing routines to mitigate the consequences of a failure and try to reset the payload control board
 - c) If unsuccessful, the master control board will continue its normal responsibilities until power schedule and external environment allow a viable opportunity to conduct scientific experimentation
- 5) Scientific data collection
 - a) Master control board will initiate the payload control board via a PI command to bring the payload control board out of its idle mode
 - b) Master control board will remain on standby, but the power schedule will allot the majority of power to the sensor suite
 - c) Payload control board will collect and process scientific data from the sensor suite

- d) Scientific data will be prioritized in the current or next transmission window to derive the greatest value from the mission (barring emergency situation)

4.8.6 RISK ANALYSIS AND MITIGATION

The risk analysis and mitigation for the command and data subsystem can be found in [Appendix B](#) Table B9.

4.8.7 NON-TECHNICAL CONSIDERATIONS

The non-technical considerations for the command and data subsystem can be found in [Appendix C](#) Table C9.

4.8.8 PLAN OF PROCESSION

If this design were to be continued past the timeline of this semester, the command and data subsystem development cycle would involve extensive testing of the radiation hardened electronics and thermal management surrounding this critical equipment. Safing routines and fault protection algorithms would also be developed and tested extensively, and the data transmission protocol previously described would have to be developed into code. The control boards would likely also be tested with simulations to ensure that they execute the propulsive and ADCS maneuvers at the proper locations and times. Additionally, a communication protocol would need to be developed or agreed upon, so that extensive procedures could be effectively communicated in short, low-size messages. Finally, after receiving these boards from BAE Systems, there would still be a fair degree of physical labor required to wire the boards to the necessary sensors and subsystems, and crosslink responsibilities between the control boards.

4.9 TELECOMMUNICATION

4.9.1 SUBSYSTEM DEFINITION

The telecommunications subsystem is responsible for communication between the CLP and PV. All communications go through the PV for downlink with Earth. These communications include pertinent scientific and engineering data, which are used to communicate the scientific findings and the status of the spacecraft to the mission operations team. The telecommunications subsystem is also responsible for signal band selection, transceivers, power amplifiers, antenna selection, and tracking of the CLP.

4.9.2 PRELIMINARY DESIGN OVERVIEW

The preliminary design of the CLP focused on four primary design considerations. First it was decided whether or not the lander would have the capacity to directly communicate with Earth. This would prevent a complete mission loss in the event of a PV failure, but it was decided that this increase in reliability was not worth the drastic increases in mass and power.

Additionally, the feasibility of maintaining appropriate pointing accuracy for data transmission on a body with unknown rotational characteristics raised concerns regarding the feasibility and complexity of this design architecture. For these reasons, all communications will go through the PV. It was also decided that the CLP would use landmark based optical navigation for navigation and tracking due to the extremely high precision needed to land on a small body such as 46P/Wirtanen.

While determining the signal band the CLP would communicate on, the S-band frequency was selected over the high frequency band, due to its slightly better performance characteristics. Additionally, this band offered high reliability, and low power requirements. It was also decided that, due to the critical nature of this subsystem, a primary and backup antenna would be included onboard the CLP. For the primary antenna, performance was given slightly higher priority over mass and power considerations. As a result, a helical antenna was ultimately selected. For the secondary antenna, mass and power were more heavily weighted in this consideration due to the redundant nature of the secondary antenna. This down-selection process eventually led to a small patch antenna design being selected as the backup antenna. Finally, it was determined that both of these antennas will transmit in an omnidirectional mode due to the relatively small distances and limited interference expected for transmissions throughout this mission.

4.9.3 PRODUCT SELECTION

Three primary components were selected for the telecommunications system, as summarized below in Table 4.8.1. A more detailed overview of the selection criteria can also be found below. While the use of primary and secondary antenna was decided in the PDR, a more detailed overview of the electronics was decided in the FDR. It was determined that a transceiver alone would be capable of performing all necessary functions as opposed to some combination of transmitters and receivers. Additionally, it was determined that a power amplifier would not be necessary, since the relatively low transmission distances mitigates the risk of substantial signal losses. Furthermore, a power amplifier would dramatically increase the power requirements and complexity of the CLP while providing minimal benefits.

Table 4.9.1: Telecommunications Product Selection

Component	Manufacturer	Model
Primary Antenna	Helical Communication Technologies	Deployable Quadrifilar Helical Antenna
Secondary Antenna	Innovative Solutions In Space	ISIS-QMS-TPL-0045 S-Band Patch Antenna
Transceiver	Honeywell	STC-MS03 S-Band TT&C Transceiver

For the primary antenna, a Deployable Quadrifilar Helical Antenna from Helical Communication Technologies was selected. This antenna was the only commercially available helical antenna found to meet the requirements of the mission, so a down selection process was not necessary. The main advantages of this antenna are its low mass, minimal volume in its stowed configuration, and its high beamwidth. The product specifications can be found in Appendix O Figure O1. It should be noted that the characteristics noted are for a UHF configuration, while for this mission a modified S-Band version of the antenna will be used.

For the secondary antenna, an ISIS-QMS-TPL-0045 S-Band Patch Antenna from Innovative Solutions In Space was selected. A decision matrix summarizing the down selection for the patch antenna can be found in Appendix O. Reliability and bandwidth were given prime importance for this selection in order to select a safe and effective backup to the primary antenna. The ISIS-QMS-TPL-0045 had the highest bandwidth, while also offering relatively low power requirements, moderate reliability, and low mass, making it the most reasonable selection for the secondary antenna.

The transceiver integrates with the antennas to handle radio transmission and reception. It was determined that the primary transceiver that best met the requirements of this mission was the STC-MS03 S-Band TT&C Transceiver from Honeywell. While meeting the frequency requirements, this transceiver is rated for deep space missions with a high data rate and comparatively low mass. In addition it has a large amount of flight heritage, significantly increasing reliability for this critical unit.

4.9.4 TELECOMMUNICATIONS DESIGN AND ANALYSIS

Analysis for the telecommunications system focused on determining the receiver power, maximum reception distance, channel capacity, and bit rate. Before proceeding with this analysis, it is important to note the assumptions that were made and the parameters that were utilized. The most significant assumption was that the specifications for the receiver on the PV, including the transceiver and antennas, were all identical with those selected for the CLP. Although there has been no collaboration with a PV design team, the following analysis was performed in using the MATLAB script `telecomms.m` located in Appendix O. This allows the design parameters to be easily updated once the true specifications of the PV are known. Another important assumption in this analysis was the neglection of the Doppler effect due to the small relative velocity between the CLP and PV. Additionally, only the primary antenna was analyzed for the purpose of this report, but a similar analysis will need to be conducted for the secondary antenna and any conjunction between primary and secondary systems on the CLP and PV. The specifications used in calculations for the antenna and transceiver can be found in Figure O1 of Appendix O. Finally, the transmission frequency selected was 2200 MHz since this S-Band frequency is compatible with both antennas and the transceiver. It should be noted that most systems will separate the telecommand and telemetry link, but for the purposes of this analysis only telecommand was considered.

The transceiver has a minimum input power that it is capable of receiving, so it is important to ensure that the signal received by the PV is strong enough to transmit data from CLP. Equation 4.9.1 was used to calculate the received power. The distance used for this analysis is the nominal apoapsis altitude of 6.4 km of the PV at release, as defined in section 4.3.5.

$$P_r = \frac{P_t G_r G_t c^2}{(4\pi R f)^2} \quad \text{Equation 4.9.1 [44]}$$

P_r is the power received by the PV receiver, P_t is the transmitter power, G_r is the gain of the receiver antenna, G_t is the gain of the transmitter antenna, c is the speed of light, R is the transmission distance, and f is the transmission frequency. The receiver power was calculated to be -69.54 dBm, well above the minimum input power of -135 dBm from the transceiver. From here, it was decided that calculating the maximum transmission range would be beneficial to the outline of the mission. Equation 4.9.1 was rearranged to solve for R and the minimum input power of -135 dBm was inputted. It was determined that, based on the specifications for the primary antenna and transceiver alone, the maximum operating range of the telecommunications system is around 12,000 km, which is well above the expected distance of the PV even in the event of trailing rather than orbiting.

The next metric that was determined was the channel capacity. Equation 4.9.2, defined by Shannon's theorem, governs the maximum theoretical error-free bitrate.

$$C = B * \log_2(1 + SNR) \quad \text{Equation 4.9.2 [44]}$$

Here C is the channel capacity in bits per second (bps), B is the bandwidth in Hz, and SNR is the unitless signal-to-noise ratio. For this a SNR of 15 was selected based on typical values for similar missions [44]. From this, the channel capacity was found to be 32 kbps. It should be noted that this theorem only governs the maximum theoretical errorless transmission rate and does not give any information on how to achieve this value. Consequently, the real value is expected to be lower and depends on the coding scheme that is used. Since the specifications for both antennas and the transceiver exceed this value, this channel capacity will govern the maximum bit rate. As a result, the maximum theoretical bit rate for all telecommunications is 32 kbps.

4.9.5 RISK ANALYSIS AND MITIGATION

The risk analysis and mitigation for the telecommunication subsystem can be found in [Appendix B](#) Table B10.

4.9.6 NON-TECHNICAL CONSIDERATIONS

The non-technical considerations for the telecommunication subsystem can be found in [Appendix C](#) Table C10.

4.9.7 PLAN OF PROCESSION

Moving forward, the design of the telecommunication subsystem will require several important criteria to be fulfilled. The assumptions defined in the previous analysis should all be reevaluated to assess their legitimacy as greater precision and detail are determined by the analysis of other subsystems. In particular, a similar analysis must be conducted for the secondary antenna. The optical tracking hardware must also be selected and software for tracking must be developed. Additionally, while it is known that both antennas will be placed on the top of the CLP, exact placement must be determined with appropriate mounting hardware. These models will also have to be integrated into the structural finite-element model to ensure that the antennas can withstand reasonable loads and vibrations in both the deployed and stowed positions. Extensive testing must occur to ensure that all the components are compatible as a system and can survive the extreme conditions they will be placed under - especially in terms of radiation. Finally, detailed protocols will have to be developed for scientific and telemetry data.

5 DESIGN BUDGETS

5.1 MASS BUDGET

The following table serves to summarize the approximate masses of the individual components comprising each subsystem. These estimates were made by a combination of information provided by the manufacturers and educated guesses. It should be noted, however, that these masses are subject to change, and will be verified upon receiving the actual parts. Furthermore, while the total mass of 230.42 kg comes in slightly under the initially proposed mass budget of 250 kg, there are likely other components that are improperly accounted for in this crude estimate. The additional margin is also favorable as some parts will invariably arrive over the specified manufacturing mass.

Table 5.1.1: Mass Budget

Component	Quantity	Mass (kg)	Mass Sum (kg)	Total Mass (kg)
Structures				44.24
Frame	1	15.13	15.13	
Aluminum Panels	6	4.85	29.11	
Propulsion				0.73
CGT	1	0.04	0.04	
ERP	1	0.65	0.65	
Loaded Fuel Tank	1	0.04	0.04	

Command & Data				3.22
RAD750	1	1.22	1.22	
RAD5545	1	1.00	1.00	
Wiring	N/A	N/A	0.5	
RS-485 Adapters	10	0.05	0.5	
Thermal Management				33.71
RHU	15	0.04	0.6	
MLI	6	5.02	30.11	
LPH	1	2	2	
BMR	1	0.3	1	
Telecommunication				1.23
Primary Antenna	1	0.18	0.18	
Secondary Antenna	1	0.05	0.05	
Transceiver	1	1	1	
ADCSS				8
ST-16RT2	2	0.24	0.47	
HG4930	2	.14	.27	
Coarse Sun Sensor	2	0.13	0.26	
RSI 1.6-33/60A	4	1.75	7	
Power Management				31.29
Solar Panels	6	4	24	
Batteries	54	0.14	7.29	
Sensor Suite				15
CIVA	1	2	2	
APXS	1	2	2	
COSAC	1	5	5	
CONCERT	1	3	3	
ROMAP	1	3	3	

Mechanisms & Deployables				93
Robotic Arm	1	40	40	
Harpoon	1	3	3	
Solar Array Deployer	6	5	30	
Sep-Nuts	4	0.25	1	
Telecom Stem Boom	1	4	4	
Landing Leg Base	1	15	15	
CLP Total				230.42

5.2 VOLUME BUDGET

As described within the PDR, the aim was to limit the size of the lander to a total volume of no more than 1m^3 . With this in mind, the following table illustrates the estimated relative volumes with respect to this target budget. Estimates have been made as exact volumes for everything could not be obtained.

Table 5.2.1: Volume Budget

Subsystem	Volume (m^3)	Percent of Design Budget
Structures	0.04	4%
Propulsion	0.03	3%
Command & Data	0.03	3%
Thermal Management	0.19	19%
Telecommunication	0.02	2%
ADCS	0.08	8%
Power Management	.15	15%
Sensor Suite	.2	20%
Mechanisms	.22	22%
Total	.96	96%

5.3 COST BUDGET

Similar to the mass budget, all of the values shown below were obtained from publicly available resources, but may not accurately reflect the true value at purchase. Because of this,

estimates have been used in an attempt to give an accurate final cost. It should be noted that the costs summarized in this table are for the physical components, and do not account for the labor and facilities associated with the design and development of this mission. Consequently, the overall mission cost will be significantly higher. The estimate for the total mission cost with all of these factors accounted for remains at 300 million USD as per the PDR.

Table 5.3.1: Cost Budget

Component	Quantity	Cost (USD)	Cost Sum (USD)	Total Cost (USD)
Structures				162,000
Frame	1	100,000	100,000	
Aluminum Coating	1	50,000	50,000	
Aluminum Panels	6	2,000	12,000	
Propulsion				30,000
CGT	1	15,000	15,000	
ERP	1	5,000	5,000	
Loaded Fuel Tank	1	10,000	10,000	
Command & Data				660,000
RAD750	1	300,000	300,000	
RAD5545	1	350,000	350,000	
Wiring	N/A	N/A	5000	
RS-485 Adapters	10	500	5000	
Thermal Management				164,810
RHU	15	10,000	150,000	
MLI	6	2,000	12,000	
TacSat - 4	1	1,000	1,000	
Kenworth T300	2	905	1,810	
Telecommunication				64,500
Primary Antenna	1	12,000	12,000	
Secondary Antenna	1	2,500	2,500	
Transceiver	1	50,000	50,000	

ADCS				361,600
ST-16RT2	2	140,000	280,000	
HG4930	2	10,800	21,600	
Coarse Sun Sensor	2	10,000	20,000	
RSI 1.6-33/60A	4	10,000	40,000	
Power Management				9414
Solar Panels	6	1250	7500	
Batteries	54	35.45	1914	
Sensor Suite				360,000
CIVA	1	75,000	75,000	
APXS	1	50,000	50,000	
COSAC	1	50,000	50,000	
CONCERT	1	125,000	125,000	
ROMAP	1	60,000	60,000	
Mechanisms & Deployables				1,415,000
Robotic Arm	1	1,250,000	1,250,000	
Harpoon	1	10,000	10,000	
Solar Array Deployer	6	80,000	80,000	
Sep-Nuts	1	5,000	5,000	
Telecom Stem Boom	1	20,000	20,000	
Landing Leg Base	1	50,000	50,000	
CLP Total				3,227,324

5.4 PROPELLANT BUDGET

In order to provide the necessary delta-V to complete the mission, a propellant budget needed to be established. This goes beyond the absolute minimum required to complete the mission (as defined in the spaceflight mechanics analysis), as it includes additional considerations. A reserve of 50 % is provided in the case of unexpected deviations from the current CLP design, orbital corrections, evasive maneuvers, and potential secondary objectives of the mission (primarily the relocation of the CLP to a nearby target landing site). Additionally,

sources of error such as loading error or trapped propellant in the feedlines and pressure regulator are accounted for as well. Finally, since the cold gas propulsion system uses its own propellant as a pressurant, excess propellant is necessary to ensure the tank remains pressurized and that the thrust of this system does not drop as a result of the dropping pressure. This value is designed so the tank pressure does not fall below a target pressure of 6 bars - as established by the operating characteristics of the cold gas thruster.

Table 5.4.1: Nitrogen Propellant Budget

Propellant Use	Mass
Required Propellant	$2.31 \times 10^{-2} \text{ kg}$
Reserves (50%)	$1.15 \times 10^{-2} \text{ kg}$
Subtotal - Usable Propellant	$3.46 \times 10^{-2} \text{ kg}$
Trapped Propellant (3%)	$1.04 \times 10^{-3} \text{ kg}$
Pressurant	$1.06 \times 10^{-3} \text{ kg}$
Loading Error (0.5%)	$1.84 \times 10^{-4} \text{ kg}$
Total	$3.69 \times 10^{-2} \text{ kg}$

5.5 POWER BUDGET

In order to create an accurate power requirement for differing phases of the mission, a power budget was established. This power budget includes the maximum (and standby) power requirements for all of the included instruments, sensors, actuators, and other electrical devices. These parameters were obtained from the specification sheets provided by parts manufacturers, suggesting a large degree of accuracy can be assumed. However, there are expected to be non-negligible power losses through the wires, in addition to manufacturing errors. Furthermore, this power budget is simply a preliminary design parameter, without power scheduling. A more accurate power budget based on mission phase can be found in the power management subsystem (section 4.7).

Table 5.5.1: Power Budget

Subsystem	Product	Required Power [W]	Totals [W]
Sensor Suite	CIVA	2.2	18.7
	APXS	1.5	
	COSAC	5	
	CONCERT	3	
	ROMAP	7	
Mechanisms and Deployables	Perseverance Robotic Arm	60	91
	RemoveDEBRIS Harpoon	7	
	SMA-R&R Solar Array Deployer	15	
	2-502640 Sep Nuts	5	
	Telecommunications STEM Boom	4	
Propulsion	AST Cold Gas Thruster	0.1-3.5	13.5
	AST Electronic Pressure Regulator	<10	
Command and Data	RAD 750 6U Extended	11-14 (3W standby)	49 (11W standby)
	RAD 5545 Space VPX	35 (8W standby)	
Telecommunications	Deployable Quadrifilar Helical Antenna	13	33
	ISIS-QMS-TPL-0045 S-Band Patch Antenna	2	
	STC-MS03 S-Band TT&C Transceiver	18	
Attitude Determination and Control	ST-16RT2 (Star Tracker)	1	112 (8W standby)
	HG4930 (IMU)	2	
	Redwire Coarse Sun Sensor Pyramid	0	
	RSI 1.6-33/60A (Reaction wheels)	17-28 (2W standby each)	
Spaceflight Mechanics	(None)	0	0
Thermal Management	(None)	0	0
Power and Power Management	(None)	0	0
CLP Total (without power scheduling)			320.2 W

6 CONCLUSION

The Hercules CLP seeks to not only accomplish the objectives set out above, but exceed these objectives and push scientific understanding forward. Traditional spacecraft design practices are very conservative, as there is little chance of mission recovery in the case of most system failures. Consequently, space exploration tends to be confined to very risk-averse designs that rely on flight-proven technologies. The Hercules CLP is superior to competing designs through the combined use of newer products and technologies as primary systems, with more reliable flight-proven technologies providing a safe backup. This design philosophy drove the development of the CLP wherever possible, effectively providing the customer with a comparable reliability to the traditional risk-averse philosophy while simultaneously extracting greater value through the implementation of newer technologies.

The preceding report summarizes the refined design and analysis of the Hercules CLP. This mission seeks to further scientific knowledge through the exploration of the surface, subsurface, and lower atmosphere of the comet through a landing on the comet 46P/Wirtanen in conjunction with a PV. The design of the various subsystems focused on minimizing mass, power usage, and cost, while maximizing safety, reliability, and efficiency in completing the mission objectives. Going forward, the analysis of each subsystem must be further refined with additional engineering analysis, and better models must be developed to determine how the individual subsystems interact with each other. Once individual components have been manufactured and acquired, extensive testing must also be conducted, both on the level of the individual subsystems and integrated as an overall system.

REFERENCES

- [1] 4 State Trucks. (n.d.). *Copper Brass Radiator 36.625 X 26.875 Inch Fits Kenworth T300*. 4 State Trucks. Retrieved December 3, 2021, from <https://www.4statetrucks.com/engine-parts/semi-truck-metal-radiator-fits-kenworth-t300>.
- [2] 46P/Wirtanen. Gary W. Kronk's Cometography. (n.d.). Retrieved October 20, 2021, from <http://cometography.com/pcomets/046p.html>.
- [3] AerospaceFab. (n.d.). *Company profile*. AerospaceFab. Retrieved December 3, 2021, from <https://aerospacefab.com/wp-content/uploads/2021/04/AerospaceFab-File3-2.pdf>.
- [4] Aglietti, G., Bridges, C., & Underwood, C. (n.d.). *RemoveDEBRIS*. Surrey. Retrieved December 3, 2021, from <https://www.surrey.ac.uk/surrey-space-centre/missions/removedebris>.
- [5] Amos, J. (2018, March 15). *Big harpoon is 'solution to space junk'*. BBC News. Retrieved October 20, 2021, from <https://www.bbc.com/news/science-environment-43418047>.
- [6] Anderson, K. S. (n.d.). *SPACECRAFT DESIGN, DYNAMICS & CONTROL PRIMER- Some Useful Information on Space Vehicle Systems Design*. Rensselaer Polytechnic Institute. Retrieved October 19, 2021, from https://lms.rpi.edu/ultra/courses/_10897_1/cl/outline.
- [7] Anis, A. (2012, June 13). *Cold Gas propulsion system an ideal choice for remote sensing small satellites*. InTechOpen. Retrieved December 3, 2021, from <https://cdn.intechopen.com/pdfs>.
- [8] Araujo, K. (n.d.). *Battery Cell Comparison*. Epec Engineered Technologies - Build to Print Electronics. Retrieved October 20, 2021, from <https://www.epectec.com/batteries/cell-comparison.html>.
- [9] ASM. (n.d.). *Aluminum 6061-T6; 6061-T651*. ASM Aerospace Specification Metals Inc. Retrieved October 19, 2021, from <http://asm.matweb.com/search/SpecificMaterial.asp?bassnum=MA6061t6>.
- [10] ASM. (n.d.). *Aluminum 7075-T6; 7075-T651*. ASM Aerospace Specification Metals Inc. Retrieved October 19, 2021, from <http://asm.matweb.com/search/SpecificMaterial.asp?bassnum=MA7075T6>.
- [11] ASM. (n.d.). *Titanium Ti-6Al-4V (Grade 5), Annealed*. ASM Aerospace Specification Metals Inc. Retrieved December 3, 2021, from <http://asm.matweb.com/search>
- [12] AST Advanced Space Technologies GmbH. (2016). *Cold gas thruster (CGT)*. AST Advanced Space Technologies GmbH. Retrieved December 3, 2021, from <https://www.ast-space.com/wp-content/uploads/2021/10/CGT-datasheet.pdf>.
- [13] AST Advanced Space Technologies GmbH. (2016). *Electronic pressure regulator (EPR)*. AST Advanced Space Technologies GmbH. Retrieved December 3, 2021, from <https://www.ast-space.com/wp-content/uploads/2021/10/epr.pdf>.
- [14] AZO Materials. (2013, June 11). *Zirconium - mechanical properties and material applications*. AZoM.com. Retrieved December 3, 2021, from https://www_azom_com/article.aspx?ArticleID=7645.

- [15] BAE. (n.d.). *RAD5545™ SpaceVPX single-board computer*. BAE Systems. Retrieved October 19, 2021, from <https://www.baesystems.com/en-media/uploadFile.pdf>.
- [16] Ball, A. J., Garry, J. R. C., Lorenz, R. D., & Kerzhannovich, V. V. (2007). *This page intentionally left blank - e-reading.life*. e-reading. Retrieved October 20, 2021, from <https://www.e-reading.life/bookreader.php>.
- [17] Barnett, A. (n.d.). *Basics of space flight - solar system exploration*. NASA Science. Retrieved October 19, 2021, from <https://solarsystem.nasa.gov/basics/chapter11-1/#data>.
- [18] Bhaskaran, S., Nandi, S., Broschart, S., Wallace, M. L., Cangahuala, A., & Olson†, C. (n.d.). *SMALL BODY LANDING ACCURACY USING IN-SITU NAVIGATION*. CITESEERX. Retrieved October 19, 2021, from <https://citeseerx.ist.psu.edu/viewdoc/download>.
- [19] Bibring, J. P., Lamy, P., Langevin, Y., & Soufflot, A. (2007, January). *Civa - Researchgate*. ResearchGate. Retrieved December 3, 2021, from https://www.researchgate.net/publication/225004147_CIVA.
- [20] Brown, C. D. (2002). *Elements of spacecraft design*. American Institute of Aeronautics and Astronautics, Inc.
- [21] Buljak, V., & Ranzi, G. (2021). *Shape memory alloy*. ScienceDirect. Retrieved December 3, 2021, from <https://www.sciencedirect.com/topics/engineering/shape-memory-alloy>.
- [22] Cable News Network. (2005, July 4). *Deep Impact Probe Hits comet*. CNN. Retrieved October 20, 2021, from <http://www.cnn.com/2005/TECH/space/07/04/deep.impact>
- [23] Coldewey, D. (2019, February 15). *Deploy the space harpoon*. TechCrunch. Retrieved December 3, 2021, from <https://techcrunch.com/2019/02/15/deploy-the-space-harpoon>
- [24] Curtis, H. D. (2021). *Orbital Mechanics for Engineering Students*. Butterworth-Heinemann, An imprint of Elsevier.
- [25] Dussinger, P. M., Sarraf, D. B., & Anderson, W. G. (1970, January 1). *Loop Heat Pipe for TacSat-4* . 1-Act. Retrieved December 3, 2021, from <https://www.semanticscholar.org/paper/Loop-Heat-Pipe-for-TacSat-4>.
- [26] EaglePicher Technologies. (n.d.). *Bringing Spacecraft Into Our Orbit*. EaglePicher Technologies. Retrieved December 3, 2021, from <https://www.eaglepicher.com/markets/space/satellites/>.
- [27] Engineering ToolBox. (2005). *Thermal Conductivity of Metals, Metallic Elements and Alloys*. Engineering ToolBox. Retrieved October 19, 2021, from https://www.engineeringtoolbox.com/thermal-conductivity-metals-d_858.html.
- [28] ESA. (2014). *LANDER INSTRUMENTS*. ESA. Retrieved December 3, 2021, from <https://sci.esa.int/web/rosetta/-/31445-instruments?section=consert>.
- [29] ESA. (2019, September 1). *Navigation*. ESA Science & Technology. Retrieved October 19, 2021, from <https://sci.esa.int/web/rosetta/-/47366-fact-sheet>.
- [30] ESA. (2019, September 1). *Philae's Instruments*. ESA Science & Technology. Retrieved October 19, 2021, from <https://sci.esa.int/web/rosetta/-/53556-philae-instruments>.

- [31] ESA. (2020, February 13). *Lander Instrument: Introduction*. ESA Science & Technology. Retrieved October 19, 2021, from <https://sci.esa.int/web/rosetta/-/31445-instruments>.
- [32] ESA. (n.d.). *Rosetta's frequently asked questions*. The European Space Agency. Retrieved October 19, 2021, from https://www.esa.int/Science_Exploration/Space_Science/Rosetta
- [33] ESA. (n.d.). *Rosetta Rendezvous Mission with Comet 67P/Churyumov-Gerasimenko*. ESA. Retrieved December 3, 2021, from <https://directory.eoportal.org/web/eoportal/satellite-missions/content/-/article/rosetta>.
- [34] ESCO Technologies. (2004, July 7). *Vacco 2 LBF COLD GAS THRUSTER*. Vacco Space Products. Retrieved December 3, 2021, from https://www.vacco.com/images/uploads/pdfs/cold_gas_thrusters.pdf.
- [35] Espinasse, S., Moura, D., Scheuerle, H., Tilman Spohn, Auster, U., Kletzkine, P., Schulz, R., Komle, N., Szego, K., Rosenbauer, H., Maddock, J., & McKenna-Lawlor, S. (n.d.). *Philae Lander Fact Sheets*. DLR. Retrieved October 20, 2021, from <https://www.dlr.de/rd/Portaldata/28/Resources>.
- [36] Etherington, D. (2017, August 23). *BAE Systems' new radiation-hardened computer is ready to serve in space*. TechCrunch. Retrieved October 19, 2021, from <https://techcrunch.com/2017/08/23/bae-systems-new-radiation-hardened-computer-is-ready-to-serve-in-space/>.
- [37] European Space Agency, ESA. (2014, November 7). *Rosetta: Landing on a comet*. Youtube. Retrieved October 19, 2021, from <https://www.youtube.com/watch?v=mggUVLFpkQg>.
- [38] Fernandez, J. M. (n.d.). *Advanced Deployable Shell-Based Composite Booms For Small Satellite Structural Applications Including Solar Sails*. NASA. Retrieved December 3, 2021, from <https://ntrs.nasa.gov/api/citations/20170001569/downloads/20170001569.pdf>.
- [39] Francis, S. (2020, September 15). *Motiv brings space-grade robotics to industrial sector*. Robotics & Automation News. Retrieved December 3, 2021, from <https://roboticsandautomationnews.com/2020/09/15>.
- [40] Fusaro, R. L., Alley, T. L., Bement, L. J., Brennan, P. C., Carre, D. J., Didziulis, S. V., Glaeser, W. A., Goldstein, S., Gore, B. W., Gurevich, L., Hanna, W. D., Hilton, M. R., Kalogeras, C. G., Kannel, J. W., Lince, J. R., Marten, H. D., Merriman, T. L., Newell, J. M., Paige, S. L., ... Tran, A. N. (1999). *Nasa Space Mechanisms Handbook*. National Aeronautics and Space Administration.
- [41] General Dynamics Mission Systems. (n.d.). *S-band TDRSS / Deep Space Network (DSN) transponder*. General Dynamics Mission Systems. Retrieved December 3, 2021, from <https://gdmissionsystems.com/products/communications/spaceborne-communications>.
- [42] Gilmore, D. G. (2002). *Spacecraft Thermal Control Handbook ; Volume I: Fundamentals Technologies*. The Aerospace Press.
- [43] Goesmann, F., Rosenbauer, H., Roll, R., Szopa, C., Raulin, F., Sternberg, R., Israel, G., Meierhenrich, U. J., Thiemann, W. H., & Munoz-Caro, G. (2007, February). *COSAC, the Cometary Sampling and Composition Experiment on Philae*. ResearchGate. Retrieved December 3, 2021, from https://www.researchgate.net/publication/225710128_COSAC.

- [44] Griffin, M. D., & French, J. R. (2004). *Space vehicle design (2nd edition)*. American Institute of Aeronautics and Astronautics.
- [45] Guzik, A., & Benafan, O. (n.d.). *Design and development of CubeSat Solar Array Deployment Mechanisms Using SHape Memory Alloys*. NASA. Retrieved December 3, 2021, from <https://ntrs.nasa.gov/api/citations/20180003332/downloads/20180003332.pdf>.
- [46] Hartono, N. (2020, July 7). *NASA's insight flexes its arm while its 'mole' hits pause*. NASA. Retrieved December 3, 2021, from <https://www.nasa.gov/feature/jpl/nasas-insight-flexes-its-arm-while-its-mole-hits-pause>.
- [47] Hegler, S., Statz, C., Hahnel, R., Plettemeier, D., Herique, A., & Kofman, W. (2013, October 3). *Operation of CONSERT aboard Rosetta during the descent of Philae*. Planetary and Space Science. Retrieved December 3, 2021, from <https://www.sciencedirect.com/science/article/abs/pii>.
- [48] Hexcel Corporation. (2021, May 25). *Hextow® continuous carbon fiber*. Hexcel. Retrieved December 3, 2021, from <https://www.hexcel.com/Products/Carbon-Fiber/HexTow-Continuous-Carbon-Fiber>.
- [49] Hexcel. (n.d.). *HexTow® HM54 Carbon Fiber*. Hexcel. Retrieved December 3, 2021, from https://www.hexcel.com/user_area/content_media/raw/HM54_HexTow_DataSheet.pdf.
- [50] Honeywell Aerospace. (n.d.). *Compare our inertial measurement units*. Honeywell Aerospace. Retrieved December 3, 2021, from <https://aerospace.honeywell.com/us/en/learn/products/sensors/inertial-measurement-units>
- [51] Honeywell International. (2016, July). *S-Band TT&C Transceiver*. Honeywell. Retrieved December 3, 2021, from <https://aerospace.honeywell.com/content/dam/aerobt/en/documents/learn/products.pdf>.
- [52] HOU. (2017). *THE SHERLOC INVESTIGATION FOR MARS 2020*. HOU. Retrieved December 3, 2021, from <https://www.hou.usra.edu/meetings/lpsc2017/pdf/2839.pdf>.
- [53] Johnson, M. (2019, March 1). *A New Approach to Radiation Hardening Computers*. NASA. Retrieved October 19, 2021, from https://www.nasa.gov/mission_pages/station/research/news/b4h-3rd.
- [54] Johnston, H. (2015, April 14). *Rosetta's bouncing probe finds no magnetic field on Comet 67P*. physicsworld. Retrieved October 20, 2021, from <https://physicsworld.com>.
- [55] Juhasz, A. J. (1998, October). *Design Considerations for Lightweight Space Radiators Based on Fabrication and Test Experience With a Carbon-Carbon Composite Prototype Heat Pipe*. NASA. Retrieved December 3, 2021, from <https://www.google.com/url?q=https://ntrs.nasa.gov/api/citations>.
- [56] Kellas, S. (2002, April). *Design, fabrication and testing of a crushable ... - NASA*. NASA. Retrieved December 3, 2021, from <https://ntrs.nasa.gov/api/citations/20020051120/downloads/20020051120.pdf>.
- [57] Klingelhöfer, A. G., Girones, J. L., Schmanke, D., Markovski, C., Brückner, J., D'Uston, L., Economou, T., Schröder, C., Berhnardt, B., & Gellert, R. (2015, June 11). *The Alpha*

- Particle X-Ray Spectrometer APXS on Rosetta Philae.* DLR. Retrieved December 3, 2021, from <https://www.dlr.de/pf/Portaldatal/6/Resources/lcpm/abstracts.pdf>.
- [58] Kovo, Y. (2020, December 8). *10.0 Communications*. NASA. Retrieved October 19, 2021, from <https://www.nasa.gov/smallsat-institute/sst-soa-2020/communications>.
- [59] L3Harris. (n.d.). *AS-49070 S-band Quadrifilar Helix Antenna*. L3Harris. Retrieved December 3, 2021, from <https://www.l3harris.com/all-capabilities/49070-s-band-quadrifilar-helix-antenna>.
- [60] Landis, G. A. (1994, August 31). *Review of solar cell temperature coefficients for space*. ResearchGate. Retrieved December 3, 2021, from <https://www.researchgate.net/publication>.
- [61] Lawrence, C., Solano, P., & Bartos, K. (2007, August). *Deployable Landing Leg Concept for Crew Exploration Vehicle*. NASA. Retrieved December 3, 2021, from <https://ntrs.nasa.gov/api/citations/20070031904/downloads/20070031904.pdf>.
- [62] Magnes, W. (2001, January). *Comparison of two digital flux-gate magnetometers developed for space application*. ResearchGate. Retrieved December 3, 2021, from <https://www.researchgate.net/publication/>.
- [63] MatWeb. (n.d.). *Aluminum 6061-T6; 6061-T651*. MatWeb. Retrieved December 3, 2021, from <http://www.matweb.com/search/datasheet>.
- [64] MatWeb. (n.d.). *Aluminum, Al*. MatWeb. Retrieved December 3, 2021, from <http://www.matweb.com/search/datasheet.aspx?bassnum=AMEAL00&ckck=1>.
- [65] MatWeb. (n.d.). *Copper, Cu; Annealed*. MatWeb. Retrieved December 3, 2021, from <http://www.matweb.com/search/datasheet>.
- [66] Miller, S. (1995, August). *Thermal System Specification*. TSGC. Retrieved December 3, 2021, from <http://www.tsgc.utexas.edu/tadp/1995/spects/thermal.html>.
- [67] Motiv Space Systems. (2021, March 13). *Space Robotics and motor controllers*. Motiv Space Systems. Retrieved December 3, 2021, from <https://motivss.com/products-capabilities/xlink>.
- [68] Motiv Space Systems. (2021, May 10). *Insight into the robotic arm of the Mars Insight Lander*. Motiv Space Systems. Retrieved December 3, 2021, from <https://motivss.com/insight-into-the-robotic-arm-of-the-mars-insight-lander/>.
- [69] Nakamura, A. (1997). *46P/Wirtanen*. Gary Kronk Cometography. Retrieved December 3, 2021, from <http://cometography.com/pcomets/046p.html>.
- [70] NASA. (1999). *NASA - NSSDCA - spacecraft - details*. NASA. Retrieved December 3, 2021, from <https://nssdc.gsfc.nasa.gov/nmc/spacecraft/display.action?id=1999-003A>.
- [71] NASA. (2004). *Rosetta*. NASA. Retrieved December 3, 2021, from <https://nssdc.gsfc.nasa.gov/nmc/spacecraft/display.action?id=2004-006A>.
- [72] NASA. (2004). *Small-Body Database Lookup*. NASA Jet Propulsion Laboratory. Retrieved October 19, 2021, from https://ssd.jpl.nasa.gov/tools/sbdb_lookup.
- [73] NASA. (2005). *Deep Impact/EPOXI*. NASA. Retrieved December 3, 2021, from <https://nssdc.gsfc.nasa.gov/nmc/spacecraft/display.action?id=2005-001A>.

- [74] NASA. (2017, November 2). *Light-weight radioisotope heater unit*. NASA. Retrieved December 3, 2021, from <https://rps.nasa.gov/power-and-thermal-systems>.
- [75] NASA. (2017, November 2). *Light-weight radioisotope heater unit*. NASA. Retrieved December 3, 2021, from <https://rps.nasa.gov/power-and-thermal-systems>.
- [76] NASA. (2020, May 21). *InSight Lander*. NASA. Retrieved December 3, 2021, from <https://mars.nasa.gov/insight/spacecraft/about-the-lander/#arm>.
- [77] NASA. (2021, September 29). *NASA - NSSDCA - spacecraft - details*. NASA. Retrieved October 20, 2021, from <https://nssdc.gsfc.nasa.gov/nmc/spacecraft>.
- [78] NASA. (2021, June 14). *Hayabusa2*. NASA. Retrieved December 3, 2021, from <https://solarsystem.nasa.gov/missions/hayabusa-2/in-depth/>.
- [79] NASA. (2021, May 1). *Watson takes a closer look – NASA's Mars Exploration Program*. NASA. Retrieved December 3, 2021, from <https://mars.nasa.gov/resources>.
- [80] NASA. (n.d.). *Planetary instrument for X-ray lithochemistry (PIXL)*. NASA. Retrieved December 3, 2021, from <https://mars.nasa.gov/mars2020/spacecraft/instruments/pixl/>.
- [81] NASA. (n.d.). *Robotic arm*. NASA. Retrieved December 3, 2021, from <https://mars.nasa.gov/mars2020/spacecraft/rover/arm/>.
- [82] NASA. (n.d.). *Scanning habitable environments with Raman & Luminescence for Organics & Chemicals (SHERLOC)*. NASA. Retrieved December 3, 2021, from <https://mars.nasa.gov/mars2020/spacecraft/instruments/sherloc/>.
- [83] NASA. (n.d.). *Table 5-5. Star Trackers Suitable for Small Spacecraft*. NASA. Retrieved December 3, 2021, from https://www.nasa.gov/sites/default/files/atoms/files/table_5-5._star_trackers_suitable_for_small_spacecraft.pdf.
- [84] New Haven Display. (n.d.). *Serial vs Parallel Interface - Newhaven Display*. New Haven Display. Retrieved December 3, 2021, from https://www.newhavendisplay.com/app_notes/parallel-serial.pdf.
- [85] Northrop Grumman. (2021, May 24). *Spacecraft Components*. Northrop Grumman. Retrieved December 3, 2021, from <https://www.northropgrumman.com/space/spacecraft-components/>.
- [86] Oerlikon Management. (n.d.). *Metco Aluminum 1100Gr*. oerlikon metco. Retrieved December 3, 2021, from <https://mymetco.oerlikon.com/en-us/product/metcoaluminum1100gr>.
- [87] Ong, D. (2021, July 19). *All about RS485 - how RS485 works and how to implement RS485 into industrial control systems?* Latest Open Tech From Seeed. Retrieved December 3, 2021, from <https://www.seeedstudio.com/blog/2021/03/18>.
- [88] O'Rourke, L., Heinisch, P., Blum, J., Fornasier, S., Filacchione, G., Van Hoang, H., Ciarniello, M., Raponi, A., Gundlach, B., Blasco, R. A., Grieger, B., Glassmeier, K.-H., Küppers, M., Rotundi, A., Groussin, O., Bockelée-Morvan, D., Auster, H.-U., Oklay, N., Paar, G., ... Sierks, H. (2020, October 28). *The philae lander reveals low-strength*

primitive ice inside cometary boulders. Nature News. Retrieved December 3, 2021, from <https://www.nature.com/articles>.

- [89] Pacific Scientific Energetic Materials Company. (2021, October 18). *Separation Nut*. PacSci EMC. Retrieved October 20, 2021, from <https://psemc.com/products/separation-nut/>.
- [90] Pacific Scientific Energetic Materials Company. (2021, September 29). *Pyrotechnic Actuator*. PacSci EMC. Retrieved October 20, 2021, from <https://psemc.com/products/pyrotechnic-actuator/>.
- [91] Pacific Scientific Energetic Materials Company. (2021, September 29). *Pyrotechnic Pin Puller*. PacSci EMC. Retrieved October 20, 2021, from <https://psemc.com/products/pyrotechnic-pin-puller/>.
- [92] Plascore. (2020, April 1). *Plascore CrushLite™*. Plascore. Retrieved December 3, 2021, from <https://www.plascore.com/honeycomb/energy-absorbers/crushlite/>.
- [93] Processors. Artisan Technology Group. (n.d.). Retrieved October 20, 2021, from https://www.artisantg.com/info/BAE_Systems_RAD750_Datasheet_2018222103850.pdf.
- [94] Quest Thermal Group. (n.d.). *Wrapped MLI*. Quest Thermal Group. Retrieved October 19, 2021, from <https://www.questthermal.com/products/wrapped-mli>.
- [95] RedWire. (2021, April). *COARSE SUN SENSOR PYRAMID RAD-HARD Hi-REL*. RedWire. Retrieved December 3, 2021, from <https://brand.redwirespace.com/wp-content/uploads/2021/04.pdf>.
- [96] Rensselaer Polytechnic Institute. (n.d.). *Optical Navigation*. SEAL Sensing, Estimation, and Automation Laboratory. Retrieved October 19, 2021, from <https://seal.rpi.edu/research/optical-navigation>.
- [97] RocketLabUSA. (n.d.). *Star Trackers product sheet*. RocketLabUSA. Retrieved December 3, 2021, from <https://www.rocketlabusa.com/assets/Uploads/Star-trackers-product-sheet.pdf>.
- [98] Rogez, Y., & Puget, P. (2016, August). *The CONCERT operations planning process for the Rosetta mission*. ScienceDirect. Retrieved December 3, 2021, from <https://www.sciencedirect.com/science/article/abs/pii/S0094576516302454>.
- [99] Saft Batteries. (2020, November 2). *LS, LSH, LSP*. Saft Batteries. Retrieved December 3, 2021, from <https://www.saftbatteries.com/products-solutions/products/ls-lsh-lsp>.
- [100] Sakharkar, A. (2020, February 29). *Octopus-inspired Tentacle bot can handle a wide range of objects*. Tech Explorist. Retrieved October 20, 2021, from <https://www.techexplorist.com/octopus-inspired-tentacle-bot-sucker-grasp-objects/30435/>
- [101] SatCatalog. (2007). *RSI 02 Momentum and Reaction Wheels 0.2 – 1.6 Nms with integrated Wheel Drive Electronics*. SatCatalog. Retrieved December 3, 2021, from <https://satcatalog.s3.amazonaws.com/components.pdf>.
- [102] SatCatalog. (n.d.). *Cold Gas Thrusters*. SatCatalog. Retrieved December 3, 2021, from <https://satcatalog.s3.amazonaws.com/components.pdf>.
- [103] SatCatalog. (n.d.). *S-band transceiver*. SatCatalog. Retrieved December 3, 2021, from <https://www.satcatalog.com/component/s-band-transceiver/>.

- [104] satsearch. (n.d.). *CST-S-9882 S-band Patch Antenna*. satsearch. Retrieved December 3, 2021, from <https://satsearch.co/products/celestial-cst-s-9882-s-band-patch-antenna>.
- [105] satsearch. (n.d.). *Deployable quadrifilar helical antenna*. satsearch. Retrieved December 3, 2021, from <https://satsearch.co/products/helical-communication-technologies>.
- [106] satsearch. (n.d.). *Helios deployable antenna*. satsearch. Retrieved December 3, 2021, from <https://satsearch.co/products/helical-communication-technologies>.
- [107] satsearch. (n.d.). *Pulsar-Sant*. satsearch. Retrieved December 3, 2021, from <https://satsearch.co/products/aac-clyde-pulsar-sant>.
- [108] satsearch. (n.d.). *S-band Patch Antenna*. satsearch. Retrieved December 3, 2021, from <https://satsearch.co/products/isis-s-band-patch-antenna>.
- [109] satsearch. (n.d.). *S-band Patch Antenna*. satsearch. Retrieved December 3, 2021, from <https://satsearch.co/products/satrevolution-s-band-patch-antenna>.
- [110] Schmanke, D., Klingelhöfer, G., Lopez, J. G., Brückner, J., & d'Uston, C. (2010). *The Alpha Particle X-Ray Spectrometer APXS on the Rosetta lander Philae to explore the surface of comet 67P/ChuryumovGerasimenko*. EPSC. Retrieved December 3, 2021, from <https://meetingorganizer.copernicus.org/EPSC2010/EPSC2010-898.pdf>.
- [111] SpectroLab. (2018, July 16). *Ultra Triple Junction (UTJ)*. SpectroLab - A Boeing Company. Retrieved December 3, 2021, from https://www.spectrolab.com/photovoltaics/UTJ-CIC_Data_Sheet.pdf.
- [112] Surrey. (2019, February 15). *Harpoon successfully captures Space Debris*. Surrey. Retrieved December 3, 2021, from <https://www.surrey.ac.uk/news/harpoon-successfully-captures-space-debris>.
- [113] University of Maryland. (n.d.). *Comet 46P/Wirtanen*. University of Maryland. Retrieved December 3, 2021, from <https://wirtanen.astro.umd.edu/46P/>.
- [114] University of Maryland. (n.d.). *What is special about comet Wirtanen?* University of Maryland. Retrieved October 20, 2021, from <https://wirtanen.astro.umd.edu/46P/>.
- [115] Vitug, E. (2020, July 15). *High performance spaceflight computing (HPSC)*. NASA. Retrieved October 19, 2021, from <https://www.nasa.gov/directorates/spacetech>.
- [116] Vitug, E. (2020, August 27). *Deployable composite booms (DCB)*. NASA. Retrieved December 3, 2021, from <https://www.nasa.gov/directorates/spacetech>.
- [117] Wikimedia Foundation. (2021, May 25). *Pyrotechnic Fastener*. Wikipedia. Retrieved October 20, 2021, from https://en.wikipedia.org/wiki/Pyrotechnic_fastener.
- [118] Wikimedia Foundation. (2021, October 11). *Cold Gas Thruster*. Wikipedia. Retrieved October 19, 2021, from https://en.wikipedia.org/wiki/Cold_gas_thruster.
- [119] Wikimedia Foundation. (2021, October 11). *Shock mount*. Wikipedia. Retrieved October 20, 2021, from https://en.wikipedia.org/wiki/Shock_mount.
- [120] Wikimedia Foundation. (2021, October 22). *Shape-memory alloy*. Wikipedia. Retrieved December 3, 2021, from https://en.wikipedia.org/wiki/Shape-memory_alloy.
- [121] Yeomans , D. K. (1998, April). *Why study comets?* NASA. Retrieved October 19, 2021, from https://ssd.jpl.nasa.gov/sb/why_comets.html.

- [122] Yida. (2021, May 11). *Serial communications: RS232 vs RS485 - what are their differences?* Latest Open Tech From Seeed. Retrieved December 3, 2021, from <https://www.seeedstudio.com/blog/2019/12/06..>
- [123] Youtube. (2019, January 14). *90 deg. hinge of 4-bar linkage I - youtube*. Youtube. Retrieved October 20, 2021, from <https://www.youtube.com/watch?v=TLROAYXxkvA>.
- [124] Zhao, H., Liu, W., Ding, J., Sun, Y., Li, X., & Liu, Y. (2018, July 24). *Numerical study on separation shock characteristics of pyrotechnic separation nuts*. Acta Astronautica. Retrieved October 20, 2021, from <https://www.sciencedirect.com/science/article/abs/pii>

APPENDICES

APPENDIX A: DEFINITION AND ASSESSMENT OF RISK

Table A1: Severity/Probability Risk Assessment Matrix

Probability	Severity			
	1 Catastrophic	2 Critical	3 Marginal	4 Negligible
A - Frequent	1A	2A	3A	4A
B - Probable	1B	2B	3B	4B
C - Occasional	1C	2C	3C	4C
D - Remote	1D	2D	3D	4D
E - Improbable	1E	2E	3E	4E

Table A2: Risk Acceptance and Approval Level

Risk Acceptance and Management Approval Level	
Severity - Probability	Acceptance Level/Approving Authority
High Risk	Unacceptable: Documented approval from the MSFC EMC or an equivalent level independent management committee.
Medium Risk	Undesirable: Documented approval from the facility/operation owner's Department/Laboratory/office Manager or designee(s) or equivalent level management committee.
Low Risk	Acceptable: Documented approval from the supervisor directly responsible for operating the facility or performing the operation.
Minimal Risk	Acceptable: Documented approval not required, but an informal review by the supervisor directly responsible for the operation of the facility or performing the operation is highly recommended. The use of generic JHA (Job Hazard Analysis) posted on the Safety, Health, Environment (SHE) webpage is recommended, if a generic JHA has been developed.

Table A3: Severity Definitions

Severity Definitions			
Description	Personnel Safety and Health	Facility/Equipment	Environmental
1 - Catastrophic	Loss of life or permanent disabling injury.	Loss of facility, system or associated hardware.	Irreversible severe environmental damage that violates law and regulation
2 - Critical	Severe injury or occupation related illness	Major damage to the facilities, systems, or equipment	Reversible environmental damage causing violation of law or regulation.
3 - Marginal	Minor injury or occupational related illness	Minor damage to the facilities, systems, or equipment	Mitigatable environmental damage without violation of law or regulation where restoration activities can be accomplished.
4 - Negligible	First-aid injury or occupational related	Minimal damage to the facilities, systems, or	Minimal environmental damage not violation of law or regulation.

Table A4: Probability Definitions

Probability Definition		
Description	Qualitative Definition	Quantitative Definition
A - Frequent	High likelihood to occur immediately or expect to continuously experienced	Probability is > 0.1
B - Probable	Likely to occur, or expected to occur frequently within design life	0.1 > Probability > 0.01
C - Occassional	Expected to occur multiple times or occasionally within design life	0.01 > Probability > 0.001
D - Remote	Unlikely to occur, but can reasonably be expected to occur at some time	0.001 > Probability > 10E-6
E - Improbable	Very unlikely to occur and the occurrence is not expected during the design life.	10E-6 > Probability

APPENDIX B: RISK TABLES

Table B1: Mission Risk Analysis and Mitigation

Hazard	Cause	Effect	Pre-RAC	Mitigation	Verification	Post-RAC
Atmospheric reentry	Hardware malfunction, improper spaceflight mechanics procedure	Loss of life, serious destruction	1C	Thorough modeling and testing procedures	Standard space vehicle engineering practices used; reasonable technologies selected; designed checked and approved	3C
Space debris	Hardware malfunction, improper spaceflight mechanics procedure	Destruction of environment, internal and external political tension	2C	Thorough modeling and testing procedures	Standard space vehicle engineering practices used; reasonable technologies selected; designed checked and approved	2D
Harmful manufacturing practices	Hazardous materials and dangerous equipment	Serious injury, destruction of environment	2C	Limited use of hazardous materials and dangerous production processes	Limit contracted work to highly trained and trustworthy professionals	3D
Pollution to Earth and/or 46P/Wirtanen	Harmful propellant byproducts	Loss of scientific objectives, destruction of environment	3B	Relatively safe and limited use of propellant	Controlled testing environments and procedures	4C
Improper use of money	Loss of mission or poorly qualified mission objectives	Loss of value, future funding, and public support	2C	Extensive testing and verification of objectives with customer and scientific community	Survey experts for additional value that can be extracted; thorough qualification processes	3D

Table B2: Structures Risk Analysis and Mitigation

Hazard	Cause	Effect	Pre-RAC	Mitigation	Verification	Post-RAC
Thermal damage to carbon fiber structure	Carbon fiber's poor resistance to thermal cycling and extreme temperature highs and lows that can be experienced in space	Degradation of the carbon fiber structure leading to possible microcracks and eventually total failure	2A	Coating the carbon fiber in a thermally resilient material to protect the primary load bearing structure	Run thermal testing of the structure on the ground to simulate conditions seen in space and test material health with the coating on	3D
Damage to structure during landing	Impact occurs at a faster speed than designed for	Structure could fail or deform in a manner that would lead to some functions of the craft becoming compromised or inoperable	1C	Design the lander to be able to handle 200% of the expected landing speed.	Simulate stresses on the structure equivalent to what would be seen by the CLP in worst case scenario	3C
Cracks forming in the carbon fiber frame	Errors in the fabrication process leading to imperfections in the carbon fiber	Once exposed to the vacuum and thermal cycling of space, cracks could propagate compromising the structure	2C	Have a thorough inspection process and testing of the structure to determine if any such imperfections have occurred	Use various crack sensing technologies such as ultrasonic, X-ray, HF Eddy Current, Radio Wave testing or thermography.	3D
Fogging of sensors and solar panels	Gases escaping the carbon fiber due to outgassing	Could cover up solar sensors and other important sensors on the lander leading to them becoming unusable	2B	Perform outgassing in vacuum chambers on Earth and climate control the lander as much as possible before launch day	Weighting of the structure is taken before and after to determine the total mass lost.	4B

Table B3: Mechanisms and Deployables Risk Analysis and Mitigation

Hazard	Cause	Effect	Pre-RAC	Mitigation	Verification	Post-RAC
Failure of solar panel arrays to maintain spread angle	Mechanical failure due to bending stresses	Inability to generate power. Failure of all systems that require electrical power to operate	2C	Extensive prior testing, taking into account local gravity. Engage central column tether to maintain a solid angle spread	Deploy solar panels prior to launch for extensive testing, simulate maximum stress conditions	2D
Failure of telescoping pole to fully extend	Mechanical failure due to bending stresses, binding/misalignment of motors	Inability to use wireless communications to receive commands and relay information	3C	Extensive prior testing, motor syncing/condensation	Deploy telescoping column prior to launch, accounting for maximum load potential	3D
Inability of robotic arm to grasp desired object	Insufficient grip, range of mobility	Failure of scientific objectives due to inability to obtain debris/ice samples	3D	Utilize higher friction grips, determine maximum enclosure envelope beforehand	Test robotic arm prior to launch, accounting for different object sizes, textures, etc.	3E
Harpoon fails to attach	Failure to penetrate surface, engage anti-release fins	Potential failure to land on surface	1B	Use different levels of launch power to break the surface. Integrate a retraction system to relaunch	Deploy harpoon at maximum range, making penetration occurs even on high-hardness materials	2C
Pyrotechnics fail to deploy successfully	Prematurely triggered pyrotechnics, detonation is excessively strong/weak	CLP fails to enter parking orbit	2D	Ensure backup explosives and proper cushioning for extra detonations	Incorporate backup pyrotechnics. Take extreme care that explosives are controlled perfectly	3B
Space debris is left behind as a result of pyrotechnic detonation	Shock-containing structures fail to remain intact post-detonation	Debris is left behind in the interior of the PV, or in outer space	3C	Strengthen explosion-containing measures	Structures are strengthened enough so that they can handle multiple shocks, instead of a single instance	3D
Landing legs are not stable	Electrical/mechanical failure	CLP fails to balance on surface, or sustains catastrophic damage	2E	Ensure each leg can deploy and rotate asynchronously	Extensive testing prior to deployment	3C

Table B4: Spaceflight Mechanics Risk Analysis and Mitigation

Hazard	Cause	Effect	Pre-RAC	Mitigation	Verification	Post-RAC
CLP cannot maintain parking orbit	Solar radiation pressure, atmospheric drag, and/or gravitational perturbations	Potential loss of mission; destruction to comet environment	1B	Command and control board will frequently course correct using the CLP's telemetry data	Control board will be tested continuously through simulations to ensure proper functionality	2D
CLP's orbital model is not consistent with its actual descent	Other celestial bodies cause non-negligible gravitational perturbations	Potential loss of mission; destruction to comet environment	1B	Develop more advanced 3-body model for the CLP's operating system	Develop models simultaneously on multiple platforms to check results (MATLAB, STK, etc.)	3D
CLP's orbital model is not consistent with its actual descent	Numerical integration errors and floating-point rounding errors	Potential loss of mission; destruction to comet environment	1A	Integration tolerances will be lowered; higher memory/accuracy techniques like double precision variables can be employed	Develop models simultaneously on multiple platforms to check results (MATLAB, STK, etc.)	3D
CLP is damaged by external objects	CLP impacts ice particles or other debris at significant velocity	Potential loss of mission; destruction to comet environment	1C	critical equipment will be protected within the structure of the CLP; sensor suite on the PV and CLP will be used to instruct evasive maneuver protocols	Extensive modeling of impacts, and thorough physical testing of structure	2D

Table B5: Propulsion Risk Analysis and Mitigation

Hazard	Cause	Effect	Pre-RAC	Mitigation	Verification	Post-RAC
Leakage of propellant	Imperfections in tank construction and valves. It is not possible to create a perfectly sealed system with valves.	CLP left without propulsive capabilities; mission loss	2C	Robust tank design. Wax seals over the gas reservoir. Gas selected is larger molecular and less prone to leakage as a result.	Extensive testing including mass and pressure readings.	3E
Rapid loss of propellant	Direct damage to the propellant tanks due to impact.	CLP pushed off-course or otherwise unable to land; loss of mission	1C	Impact-resistant tank design.	Extensive analysis and testing.	1D
Failure to puncture seal or operate valve	Faulty constructions, exposure to solar radiation and extreme temperatures over an extensive time period.	CLP left without propulsive capabilities; mission loss	1D	Thorough testing and research into previous missions.	Extensive analysis and testing.	1E
Contamination of surface or injury to personal	Many propellants are toxic.	Permanent injury, loss of life, invalidity of scientific results.	2B	The ultimate propellant selected is non-toxic and released in small volumes.	Testing of propellant composition prior to fueling.	4D

Table B6: Attitude Determination and Control Risk Analysis and Mitigation

Hazard	Cause	Effect	Pre-RAC	Mitigation	Verification	Post-RAC
Improper landing of the CLP	Insufficient attitude control	Damage to CLP or surrounding comet environment; potential loss of mission	1D	Design control method such that the maximum expected torques can be met or exceeded	Extensive modeling and review of control system that minimizes controller error, overshoot, and delay	1E
Inaccurate pointing of systems such as solar arrays	Inaccurate orientation estimation from sensors	Reduction in efficiency of pointed systems; potential loss of mission	3B	Include redundant orientation sensors, with a three-tiered system for measurements at various CLP angular velocities	Extensive modeling and review of control system to ensure long term accuracy in orientation measurements	4D
Loss of attitude control	Reaction wheel saturation	Loss of attitude control in a given axis; requirement to desaturate reaction wheel or potential loss of mission	1B	Include a redundant reaction wheel in the design	Modeling of expected torques throughout time of departure from PV to landing	3D

Table B7: Thermal Management Risk Analysis and Mitigation

Hazard	Cause	Effect	Pre-RAC	Mitigation	Verification	Post-RAC
Extremely low temperatures on the CLP	Temperatures will decrease drastically as 46P/Wirtanen approaches aphelion	Loss of functionality or reduced performance of mechanical systems	3A	A powered heating pipe can be used to heat a material in an enclosed space.	Thorough testing of powered heating pipe	4A
Extremely high temperatures on the CLP	Temperatures will increase drastically as 46P/Wirtanen approaches perihelion	Loss of functionality or reduced performance of mechanical systems	2B	A body mounted radiator will be used to dissipate heat	Thorough testing of body mounted radiator	4B
Explosion/corruption of components	Increased pressure or temperature of other subsystems	Loss of functionality or reduced performance of mechanical systems	3A	Enclose components to ensure explosion will be limited to the immediate surroundings	Thorough testing and design of enclosure and safeguards	4A

Table B8: Power Management Risk Analysis and Mitigation

Hazard	Cause	Effect	Pre-RAC	Mitigation	Verification	Post-RAC
High excess voltage	Excess solar production	Damage to distribution system; excessive temperature increase; potential loss of efficiency or functionality	2C	Design for power dissipation	Thorough modeling of system power generation throughout mission lifetime and testing of power dissipation methods	2E
Reduction in amperage due to solar cell string failure	Damage to solar cells from external objects	Reduction in solar production; potential loss of CLP functionality	1D	Cross-linked parallel solar cell connections; distributed power generation through multiple solar panels	Extensive simulation and testing of solar array efficiency before and after impact tests	3D
Battery failure	Excessive cycling; manufacturing defects	Amperage drop; reduction in maximum stored energy capacity	1D	Multiple batteries to remove single point failures	Extensive testing of battery solution for mission timeline and battery cycling	3D
Unexpected periods of lower power generation	Improper landing resulting in significant periods with little sunlight	Loss of CLP functionality; potential loss of mission	2B	Implementation of power limitations and strict power scheduling	Thorough simulation of power scheduling methods	3B

Table B9: Command and Data Risk Analysis and Mitigation

Hazard	Cause	Effect	Pre-RAC	Mitigation	Verification	Post-RAC
Failure of main control board	Electrical short, hardware failure, etc.	Potential loss of mission; destruction to comet environment	1C	Extensive testing to ensure this is not a probable outcome; transfer of responsibilities to secondary control board	Thorough quality assurance testing from suppliers	2E
Loss of engineering and/or scientific data	Insufficient memory on primary board	Inability to track status of CLP by mission control	3C	Use secondary board memory as needed; regular transmissions to PV for data downlink	Identify longest windows without communication and design with margin from that	3E
Overheating of control board	Insufficient thermal management; excessive processing on a single control board	Potential loss of mission; decreased ability to complete mission objectives	1C	Extensive thermal management testing and analysis; shared processing responsibilities between control boards	Thorough quality assurance testing from suppliers; models validated by secondary team	2D
Loss of counter on spacecraft clock	Excessive radiation or malfunction	Failure to complete mission objectives	2D	Radiation hardened electronics; safing routines to reset clock; receive time from mission control messages	Testing of clock reset routine prior to launch	3E
Loss of communication with PV	Damage to PV or broken antenna	Failure to complete mission objectives	1D	Safing routines and fault protection algorithms for autonomous operation	Testing of safing routines and fault protection algorithms prior to launch	2D
Corrupted data and operations	Excessive radiation	Failure to complete mission objectives	2C	Extensive radiation hardening and testing; safing routines to reboot systems as needed	Thorough quality assurance testing from suppliers	2E

Table B10: Telecommunication Risk Analysis and Mitigation

Hazard	Cause	Effect	Pre-RAC	Mitigation	Verification	Post-RAC
Damage to antenna, receivers, processors, etc.	Radiation damage, collision damage, thermal damage, etc.	Loss of communication with spacecraft; loss of mission	1B	Backup systems are selected and interlinked where possible to minimize single points of failure.	Extensive analysis and testing, including exposure to potential hazards.	3D
Failure to receive or transmit signal	Improper orientation of antenna	Loss of communication with spacecraft; loss of mission	2B	Omni-directional antennas are used	Product verification and testing.	4C
Failure of antenna, receivers, processors, etc.	Hardware failure, electrical short, etc.	Loss of communication with spacecraft; loss of mission	1C	Flight tested hardware will be selected and extensive analysis testing will be conducted prior to mission launch.	Extensive testing, including within the assembled system.	1E

APPENDIX C: NON-TECHNICAL CONSIDERATION TABLES

Table C1: Mission Non-Technical Considerations

Topic	Consideration
Public Health & Safety	All design choices have been made to mitigate risks to public health and safety, such that regardless of the mission outcome, the general public will not be harmed.
Global	The discovery of new life, materials, or scientific principles has the potential to affect the global community.
Cultural	N/A - There is no foreseeable impact to cultures from this mission, as a result of its dissociations from cultural practices.
Social	The success of this mission is likely to influence the general public's sentiment towards space exploration, thus a high probability of success must be ensured.
Environmental	Appropriate design selections have been made to mitigate the environmental risks associated with the selected technologies; pollution and waste will be limited; the design ensures that 46P/Wirtanen is not excessively polluted or harmed by this mission.
Economic	The mission will benefit suppliers economically by increased business; the mission will also employ an abundance of engineers and scientists, creating additional jobs.
Professional Ethics	All data and analysis conducted in this design will be presented in the most truthful manner possible.

Table C2: Structures Non-Technical Considerations

Topic	Consideration
Public Health & Safety	This design properly ensures that the structure will not fracture around Earth or at impact, mitigating concerns posed to the general public due to reentry.
Global	N/A - The structural subsystem does not have any significant global considerations because this subsystem is unlikely to affect any change on the global level.
Cultural	N/A - The structural subsystem does not have any significant cultural considerations because this subsystem is unlikely to affect any change on the cultural level.
Social	N/A - The structural subsystem does not have any significant social considerations because this subsystem is unlikely to affect any change on the societal level.
Environmental	The structural subsystem will be designed and manufactured with ethically obtained materials that properly consider the environment in their manufacturing processes.
Economic	The materials that will be used in the design of the structure are expensive and difficult to source. With this in mind, the companies selected to obtain the materials and products from will benefit economically from this business.
Professional Ethics	The designer for this subsystem has completed courses in strength of materials and engineering dynamics, and has industry experience as a structural engineer. Furthermore, all services and statements for this subsystem will be truthful to the extent of the CLP team's knowledge.

Table C3: Mechanisms and Deployables Non-Technical Considerations

Topic	Consideration
Public Health & Safety	All manufacturing and testing processes for this subsystem will be conducted under safe conditions in order to mitigate the concern of public safety while developing the necessary mechanisms.
Global	Because many space missions are aimed towards the collection of typical matter, a successful (and ideal), universal design for obtaining such samples can lead to a worldwide adoption of this optimized technology. Therefore, a simple, yet universally effective design will greatly impact the mode of collection of samples in future space expeditions.
Cultural	N/A - The mechanisms and deployables subsystem is unlikely to have any significant cultural considerations because this subsystem does not significantly integrate into the typical aspects of most cultures.
Social	N/A - The mechanisms and deployables subsystem is not likely to have any significant cultural considerations because this subsystem does not significantly integrate into the typical aspects of social situations.
Environmental	The surrounding environment will be minimally impacted by the deployables by limiting physical waste, debris, and byproducts, as well as leaving the terrain minimally undisturbed.
Economic	The mechanisms and deployables require the efficient use of materials and resources. Since this subsystem is often the most intimately acquainted with the end goal of the expedition, it is expected that a large portion of the available capital will be spent on perfecting the stable and reliable deployment and performance of this subsystem.
Professional Ethics	The lead conceptual designer for the mechanisms and deployables has harbored a passion for robotically manipulable and articulable mechanisms, and completed relevant courses in robotics and mechanical design. Therefore, a strong understanding and effort will be invested into the analysis of ideal integration and mechanical design techniques. All services and statements will be reviewed extensively and approved by the secondary lead for this subsystem as well.

Table C4: Spaceflight Mechanics Non-Technical Considerations

Topic	Consideration
Public Health & Safety	The spaceflight mechanics analysis ensures that the CLP travels in a safe and efficient manner that will not directly or indirectly endanger the public (space debris, atmospheric reentry, etc.).
Global	N/A - The spaceflight mechanics subsystem does not have any significant global considerations because this subsystem is unlikely to affect change on the global level.
Cultural	N/A - The spaceflight mechanics subsystem does not have any significant cultural considerations because this subsystem is unlikely to affect change on the cultural level.
Social	N/A - The spaceflight mechanics subsystem does not have any significant social considerations because this subsystem is unlikely to affect change on the societal level.
Environmental	The propellant used in the CLP's maneuvers are harmful to surrounding environments. The use of propellant should be kept to a minimum in order to decrease the harmful effects of its production and use.
Economic	The analysis conducted by the spaceflight mechanics team constrains many other subsystems and necessitates efficient use of capital and resources.
Professional Ethics	The designers for this subsystem have completed MANE 4100: Spaceflight Mechanics, such that only competent students in this subject matter will submit and review work for this subsystem. Furthermore, all services and statements for this subsystem will be truthful to the extent of the CLP team's knowledge.

Table C5: Propulsion Non-Technical Considerations

Topic	Consideration
Public Health & Safety	Certain propellants are extremely toxic. This design ensures that a hazardous material is not used needlessly, and that risks endangering the public during testing, assembly, or launch are limited.
Global	N/A - The propellant subsystem does not have any significant global considerations because this subsystem is unlikely to affect any change on the global level.
Cultural	N/A - The propellant subsystem does not have any significant cultural considerations because this subsystem is unlikely to affect any change on the cultural level.
Social	N/A - The propellant subsystem does not have any significant social considerations because this subsystem is unlikely to affect any change on the societal level.
Environmental	Certain propellants can have extremely adverse effects on the environment. Limited propellants, such as Freon-12, were excluded due to these considerations.
Economic	N/A - The propellant subsystem is subject to the requirements of the spaceflight mechanics team and unlikely to have significant economic impact due to the low impulse of maneuvers and use of proven technologies.
Professional Ethics	All selections and considerations are based on the full knowledge of the engineers on the team and reviewed closely by a secondary lead.

Table C6: Attitude Determination and Control Non-Technical Considerations

Topic	Consideration
Public Health & Safety	Control methods such as reaction wheels contain fast moving parts which could pose a hazard to test engineers. Steps should be taken to limit the possibility of injury during testing and manufacturing.
Global	N/A - The selection of the ADCS design does not have significant global considerations and is unlikely to affect change on the global level.
Cultural	N/A - The selection of the ADCS design does not have significant cultural considerations and is unlikely to affect change on the cultural level.
Social	N/A - The selection of the ADCS design does not have significant social considerations and is unlikely to affect change on the social level.
Environmental	CLP reaction control burns may have an adverse effect on the comet's environment and should be limited to the largest degree possible to minimize contamination.
Economic	Though the ADCS subsystem does not constitute a major expense in terms of the CLP financials, the ADCS design ensures efficient use of capital and resources during design selection.
Professional Ethics	The selection of technologies for this subsystem is purely out of the customer and the general public's best interests. All selections and considerations are based on the full knowledge of the engineers on the team, and are reviewed closely by a secondary lead.

Table C7: Thermal Management Non-Technical Considerations

Topic	Consideration
Public Health & Safety	The manufacturing of thermal equipment will not unreasonably endanger workers or the surrounding community due to hazardous byproducts or processes.
Global	N/A - The use of thermal components has no global considerations because the technology is well understood and is unlikely to cause an incident on the global level.
Cultural	N/A - The use of thermal components has no cultural considerations due to its limited influence on the cultural level.
Social	N/A - The use of thermal components has no meaningful impact on societies as a result of the limited exposure to the public this subsystem will have.
Environmental	The production of some components may be considered harmful to the environment due to the use of non-renewable, hazardous materials. The design of this subsystem ensures that these manufacturing processes will be limited.
Economic	The production of components will provide the manufacturers revenue and business opportunities, generating a small microeconomic impact.
Professional Ethics	The designers for this subsystem have completed Thermodynamics and Physics (which covers basic heat transfer) at the collegiate level.

Table C8: Power Management Non-Technical Considerations

Topic	Consideration
Public Health & Safety	Certain power generation methods are inherently more dangerous as they contain radioactive elements or toxic chemicals. As such, the power systems design ensures that harmful materials are not excessively and needlessly used, and that risks endangering public health and safety during testing, assembly, or launch are limited.
Global	Certain materials are extracted in nations outside of the United States. The power systems design ensures that all materials sourced externally are obtained ethically and legally with respect to the nations in which they reside.
Cultural	N/A - The selection of the power systems design does not have any significant cultural considerations as this subsystem is unlikely to affect any change on the cultural level.
Social	N/A - The selection of the power systems design does not have any significant social considerations as this subsystem is unlikely to affect any change on the societal level.
Environmental	Certain materials such as those contained in batteries and solar cells contain radioactive, toxic, or otherwise environmentally harmful elements, or have processing procedures which produce a significant global emissions footprint. As such, care will be taken in the choices of the system design to minimize environmental harm.
Economic	The power system design is an expensive part of the CLP. The power systems design ensures efficient use of capital and resources during design selections.
Professional Ethics	The selection of technologies for this subsystem is purely out of the customer and the general public's best interests. All selections and considerations are based on the full knowledge of the engineers on the team, and are reviewed closely by a secondary lead.

Table C9: Command and Data Non-Technical Considerations

Topic	Consideration
Public Health & Safety	The command and control design selections ensure that the CLP has sufficient capability to travel in a safe and efficient manner that will not endanger the public either directly or indirectly (space debris, atmospheric reentry, etc.). The manufacturing methods required for the radiation hardening process will also be audited to ensure they are safe.
Global	N/A - The command and data subsystem does not have any significant global considerations because this subsystem is unlikely to affect change on the global level.
Cultural	N/A - The command and data subsystem does not have any significant cultural considerations because this subsystem is unlikely to affect change on the cultural level.
Social	N/A - The command and data subsystem does not have any significant social considerations because this subsystem is unlikely to affect change on the societal level.
Environmental	The radiation hardening process used to manufacture the control boards may be considered an environmentally harmful process. As a result, these operations will be contained and limited. The sourcing of rare metals required for the control boards will also be considered to ensure the process is ethical and safe to the environment.
Economic	The command and control modules are expensive pieces of equipment that will be outsourced to BAE Systems. This selection will be beneficial to this business, so this subsystem has positive economic effects on a small scale.
Professional Ethics	The selections of technologies for this subsystem are purely out of the customer and the general public's best interests. The command and data design team has no conflicting matters to disclose.

Table C10: Telecommunication Non-Technical Considerations

Topic	Consideration
Public Health & Safety	N/A - The telecommunications subsystem does not have any significant global considerations because this subsystem is unlikely to put the public in danger.
Global	N/A - The telecommunications subsystem does not have any significant global considerations because this subsystem is unlikely to affect change on the global level.
Cultural	N/A - The telecommunications subsystem does not have any significant cultural considerations because this subsystem is unlikely to affect change on the cultural level.
Social	N/A - The telecommunications subsystem does not have any significant social considerations because this subsystem is unlikely to affect change on the societal level.
Environmental	N/A - The telecommunications subsystem does not have any significant environmental considerations because this subsystem is unlikely to affect the environment of the Earth or 46P/Wirtanen.
Economic	Failure of the telecommunications system would result in the complete loss of the mission and a major economic waste. As a result, reliability of the subsystem was a major priority.
Professional Ethics	All selections and considerations are based on the full knowledge of the engineers on the team and reviewed closely by a secondary lead.

APPENDIX D: GANTT CHART

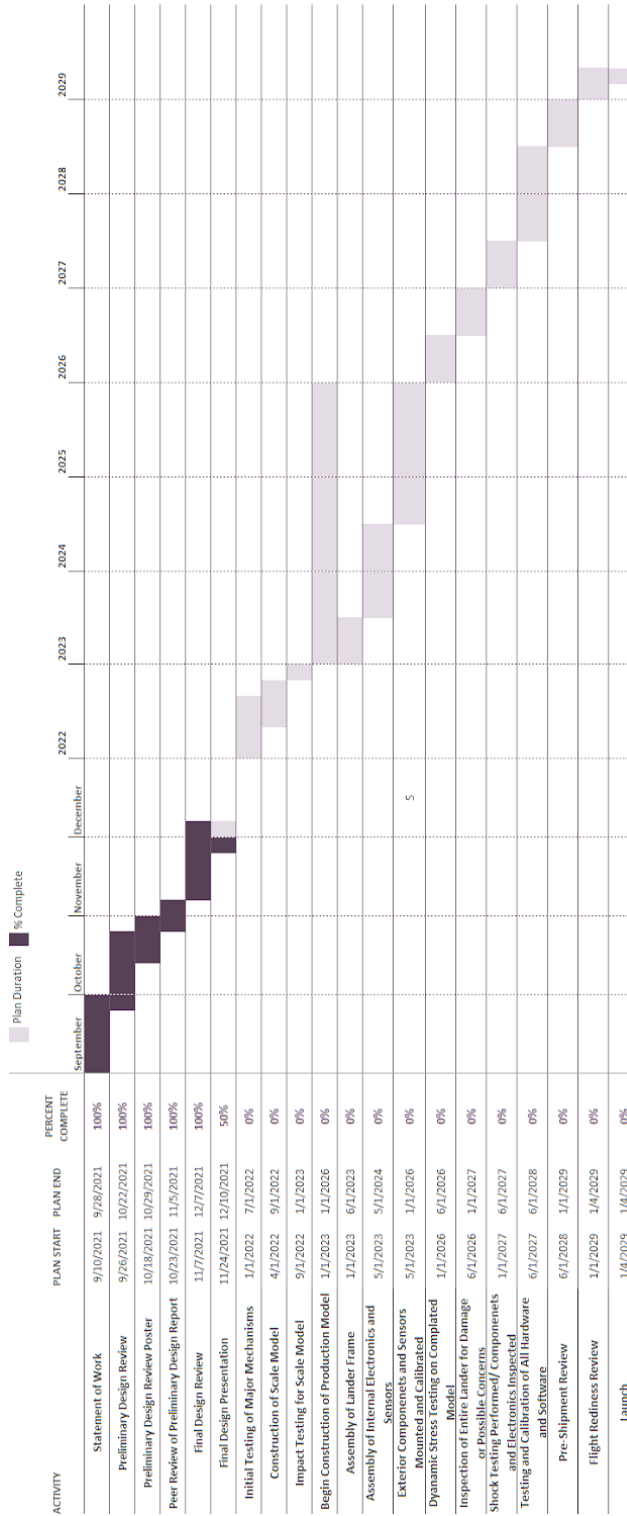


Figure D1: Gantt Chart

APPENDIX E: ORGANIZATIONAL CHART

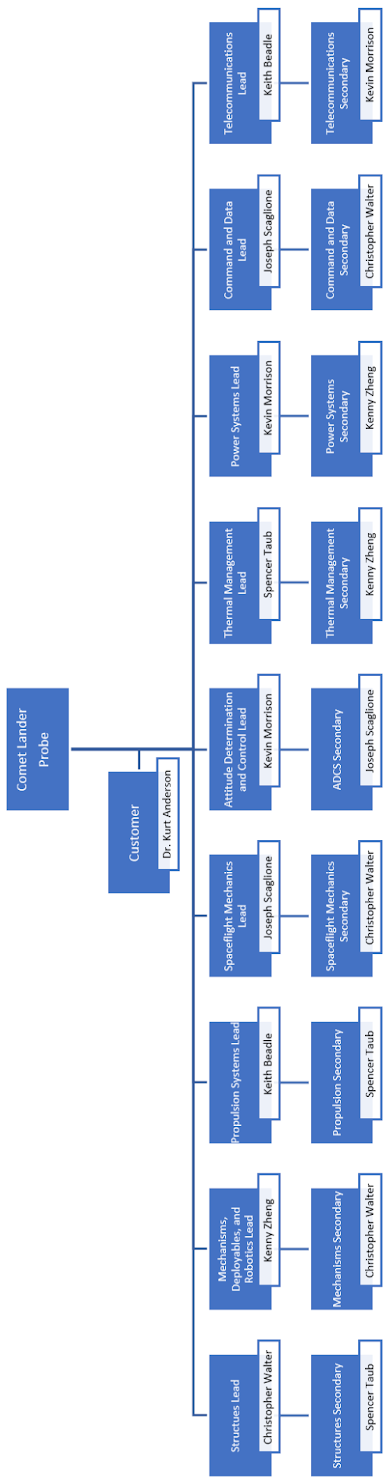


Figure E1: Organizational Chart

APPENDIX F: TEAM MEMBER RESPONSIBILITIES

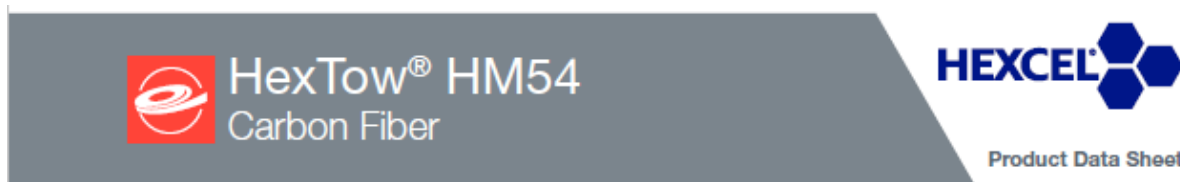
Table F1: Primary and Secondary Leads by Mission Component

Mission Component	Primary Lead	Secondary Lead
Mission Design/Architecture	All	All
Structures	Christopher Walter	Spencer Taub
Mechanisms and Deployables	Kenny Zheng	Christopher Walter
Spaceflight Mechanics	Joseph Scaglione	Christopher Walter
Propulsion	Keith Beadle	Spencer Taub
Attitude Determination and Control	Kevin Morrison	Joseph Scaglione
Thermal Management	Spencer Taub	Kenny Zheng
Power Management	Kevin Morrison	Kenny Zheng
Command and Data	Joseph Scaglione	Christopher Walter
Telecommunication	Keith Beadle	Kevin Morrison

Table F2: Report Sections by Team Member

Team Member	Report Section
Keith Beadle	Executive Summary, 4.4 Propulsion, 4.9 Telecommunication, 5.4 Propellant Budget, 6 Conclusion, Appendix A, Appendix J, Appendix O
Kevin Morrison	1 Introduction, 4.5 Attitude Determination and Control, 4.7 Power Management, 5.5 Power Budget, Appendix E, Appendix K, Appendix M
Joseph Scaglione	General Formatting, 2.3 Constraints, 2.4 Requirements, 2.5 Assumptions, 4.3 Spaceflight Mechanics, 4.8 Command and Data, Appendix F, Appendix I, Appendix N
Spencer Taub	2.1 Customer Needs, 2.2 Objectives, 4.6 Thermal Management, Appendix C, Appendix L
Christopher Walter	4.1 Structures, 5.1 Mass Budget, 5.2 Volume Budget, 5.3 Cost Budget, Appendix D, Appendix G
Kenny Zheng	3 Mission Overview, 4.2 Mechanisms and Deployables, References, Appendix H

APPENDIX G: STRUCTURES



The header of the product datasheet features the HexTow logo (a red circle with a white 'e' shape) and the text "HexTow® HM54 Carbon Fiber". To the right is the Hexcel logo (blue hexagons forming a stylized 'X') and the text "HEXCEL". Below the logos is the text "Product Data Sheet".

HexTow® HM54 carbon fiber is a continuous, high performance, high modulus, PAN based fiber available in 12,000 (12K) filament count tows. This fiber has been surface treated and sized to improve its interlaminar shear properties, handling characteristics, and structural properties. It is suggested for use in premium sporting goods, aerospace, space, and industrial applications.

The unique properties of HexTow® HM54 fiber, such as higher tensile strength and modulus, as well as good shear strength, allow structural designers to achieve both higher safety margins for both stiffness and strength critical applications.

Target Fiber Properties	U.S. Units	SI Units
Tensile Strength	700 ksi	4,826 MPa
Tensile Modulus (Chord 6000-1000)	54 Msi	372 GPa
Ultimate Elongation at Failure	1.3%	1.3%
Density	0.0636 lb/in ³	1.76 g/cm ³
Weight/Length	23.8 x 10 ⁻⁶ lb/in	0.422 g/m
Approximate Yield	3,526 ft/lb	2.37 m/g
Tow Cross-Sectional Area	3.73 x 10 ⁻⁴ in ²	0.24 mm ²
Filament Diameter	0.199 mil	5.1 microns
Carbon Content	99%	99%
Twist	Never Twisted	Never Twisted

Carbon Fiber Certification

This carbon fiber is manufactured to Hexcel industrial grade specification HS-CP-3500. A copy of this specification is available upon request. A certification of analysis will be provided with each shipment.

Available Sizing

Sizing compatible with various resin systems, based on application are available to improve handling characteristics and structural properties. Please see additional information on available sizes on our website or contact our technical team for additional information.

Packaging

Standard packaging of HexTow® HM54 is as follows

Filament Count	Nominal Weight		Nominal Length	
	(lb)	(kg)	(ft)	(m)
12K	1.8	0.82	6,347	1,935

Other package sizes may be available on request.
The fiber is wound on a 3-inch ID by 11-inch long cardboard tube and overwrapped with plastic film..

Safety Information

Obtain, read, and understand the Safety Data Sheet (SDS) before use of this product.

Figure G1: HexTow HM54 Carbon Fiber Product Datasheet [49]

Characteristics	
Product Form	Wire
Achieved Surface Function Primary	Corrosion Resistance
Suitable for Service Environment	Moderate Atmosphere
Melting Temperature (°C)	660
Nominal Chemistry	Al 99.0+
Material "Norm" (Similar Chemistry)	Aluminum
Max. Service Temperature (°C)	538
Achieved Microhardnesss HV	30
Achieved Macrohardness	30 HRB
Recommended Metco Spray Gun	18E 5K LD/Schub 5 LD/U2 LD/U3 PPG

Figure G2: Metco Aluminum 1100Gr Datasheet [86]

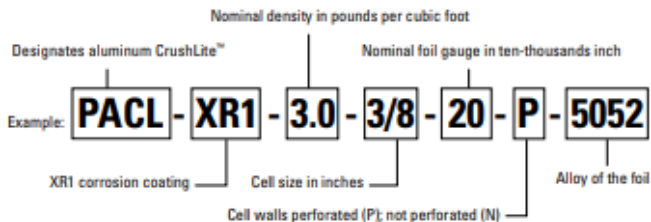
Table G1: Carbon Fiber Coating Decision Matrix [14, 64, 65]

Metric	Weight	Copper	Aluminum	Zirconium
Density	0.3	3	5	3
Thermal Insulation	0.4	2	4	5
Price	0.1	5	5	4
Previous Use	0.2	2	5	1
Total	1	2.6	4.6	3.5

APPENDIX H: MECHANISMS AND DEPLOYABLES

CrushLite™ is specified as follows:

Trade Name - Corrosion Coating - Density - Cell Size - Foil Gauge - Perforation - Alloy



Availability:

CrushLite™ aluminum honeycomb is available in untrimmed sheets, cut to size, machined, or die cut. Pre-crushing, load certification, and other operations are available upon request.

Cell Sizes:	1/8" - 1"
Densities:	0.6 pcf - 8.1 pcf
Sheet "Ribbon" (L):	48" typical maximum
Sheet "Transverse" (W):	96" typical maximum
Sheet "Thickness" (T):	up to 32" maximum

NOTE: Maximum sheet size, thickness, and pre-crush may be limited on certain core types. Contact a Plascore Representative to determine availability.

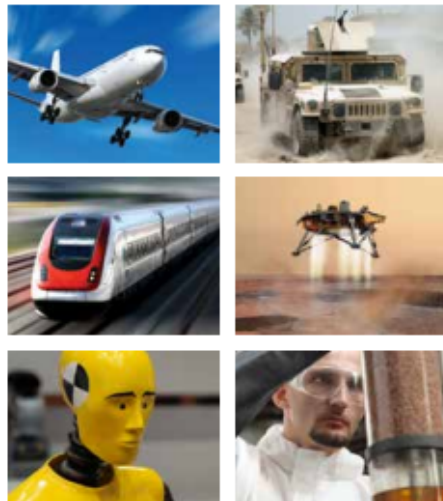
Plascore Honeycomb Designation					Crush Properties		
Nominal Density (lbs/ft ³)	Cell Size (Inch)	Foil Gauge (Inch)	Available in Perforated	Foil Alloy	Crush Strength ¹ (psi)	Standard Crush Tolerance (4/- psi)	Minimum Stroke ² (%)
0.6	3/4	.0007	+	5052	7.5	2.5	70
1.0	1	.002	+	3003	10	2	70
1.2	1	.003	+	3003	25	5	70
1.0	3/8	.0007	+	5052	25	5	70
1.0	3/8	.0007	+	5056	35	5	70
1.8	3/8	.001	+	5052	45	4.5	70
1.8	3/4	.003	+	3003	45	4.5	70
1.6	1/4	.0007	+	5056	50	5	70
2.0	3/16	.0007	+	5052	75	7.5	70
2.3	3/8	.0015	+	5052	80	8	70
2.3	1/4	.001	+	5052	90	9	70
2.3	1/4	.001	+	5056	100	10	70
3.0	3/8	.002	+	5052	120	12	70
3.8	3/8	.003	+	3003	120	12	70
3.1	1/8	.0007	+	5052	130	13	70
3.4	1/4	.0015	+	5052	140	14	70
3.1	1/8	.0007	+	5056	170	17	70
3.7	3/8	.0025	+	5052	180	18	70
4.2	3/8	.003	+	5052	210	21	70
4.3	1/4	.002	+	5052	230	23	70
5.2	1/4	.003	+	3003	245	24.5	70
4.5	1/8	.001	+	5052	275	27.5	70
4.5	1/8	.001	+	5056	320	32	70
5.2	1/4	.0025	+	5052	330	33	70
5.4	3/8	.004	+	5052	350	35	70
5.7	3/16	.002	+	5052	380	38	70
6.0	1/4	.003	+	5052	420	42	70
5.7	3/16	.002	+	5056	440	44	70
6.1	1/8	.0015	+	5052	450	45	70
6.1	1/8	.0015	+	5056	535	53.5	70
8.1	1/8	.002	+	5052	700	70	70
8.1	1/8	FC	+	5052	750	75	70

¹Crush Strength
²Minimum Stroke
Tested per ASTM D7336



Plascore, Inc., employs a quality management system that is Nadcap, AS9100, ISO 9001 and ISO 14001 certified.

IMPORTANT NOTICE: The information contained in these materials regarding Plascore's products, processes, or equipment, is intended to be up to date, accurate, and complete. However, Plascore cannot warrant that this is always the case. Accordingly, it is a purchaser's or user's responsibility to perform sufficient testing and evaluation to determine the suitability of Plascore's products for a particular purpose. Information in these materials and product specifications does not constitute an offer to sell. Your submission of an order to Plascore constitutes an offer to purchase which, if accepted by Plascore, shall be subject to Plascore's terms and conditions of sale. PLASCORE MAKES NO WARRANTIES OF ANY KIND REGARDING THESE MATERIALS OR INFORMATION, EITHER EXPRESS OR IMPLIED, INCLUDING WITHOUT LIMITATION THE IMPLIED WARRANTIES OF MERCHANTABILITY AND FITNESS FOR A PARTICULAR PURPOSE. Plascore owns and shall retain all worldwide rights in its intellectual property, and any other trademarks used in these materials are the property of their respective owners. The information in these materials shall not be construed as an inducement, permission, or recommendation to infringe any patent or other intellectual property rights of any third parties. © 2021 Plascore, Inc. All Rights Reserved. v4.6.2021



Corporate Headquarters

Plascore Incorporated
615 N. Fairview St.
Zeeland, MI 49464-0170
USA
Phone (616) 772-1220
Toll Free (800) 630-9257
Fax (616) 772-1289
Web www.plascore.com
Email sales@plascore.com

Europe

Plascore GmbH&CoKG
Feldborn 6
D-55444 Waldlaubersheim
Germany
Phone +49(0) 6707-9143 0
Fax +49(0) 6707-9143 0
Web www.plascore.de
Email sales.europe@plascore.de



Figure H1: Plascore CrushLite™ Honeycomb Crushable Material Datasheet [92]

SEPARATION NUT

The separation nut is a pyrotechnic device designed as a high strength, fastening hardware with the ability to separate and/or release components or structures on demand. As a pyrotechnical solution for critical release events, the most common uses include satellite deployment along with clamp release applications for weapons launch systems.

Whether in space, on aircraft or in the sea, dependability is required for mission critical systems needing release mechanisms that are designed and developed for low shock, highly reliable separation nuts for applications in submarine, launch vehicle, satellite, and payload systems. An example would be a HDRM for CubeSat and SmallSat launches. Our Mechanisms are custom made to meet your mission requirements, from the separation nut size to the specific materials, the success of your application is at the center point of our design.



SPECIFICATIONS

All-Fire:	5.0/20 millisecond pulse
No-Fire:	1 amp/1 watt for 5 minutes
Operating Temperature:	-65 °F to +225 °F
Axial Load Retention:	Tested with an axial load of $29,500 \pm 500$ pounds
Hermesticity (pre-function):	Leak rate shall not exceed 2.7×10^{-5} cc/sec of Helium at 1 atmosphere differential.

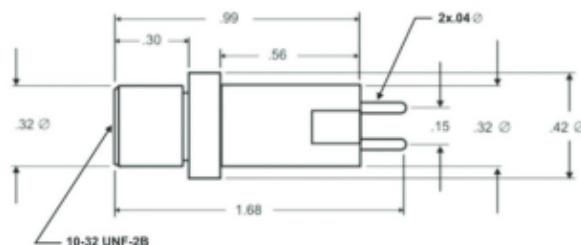
ENVELOPE & DIMENSIONS


Figure H2: Pacific Scientific Energy Materials Company Separation Nut Datasheet [89]

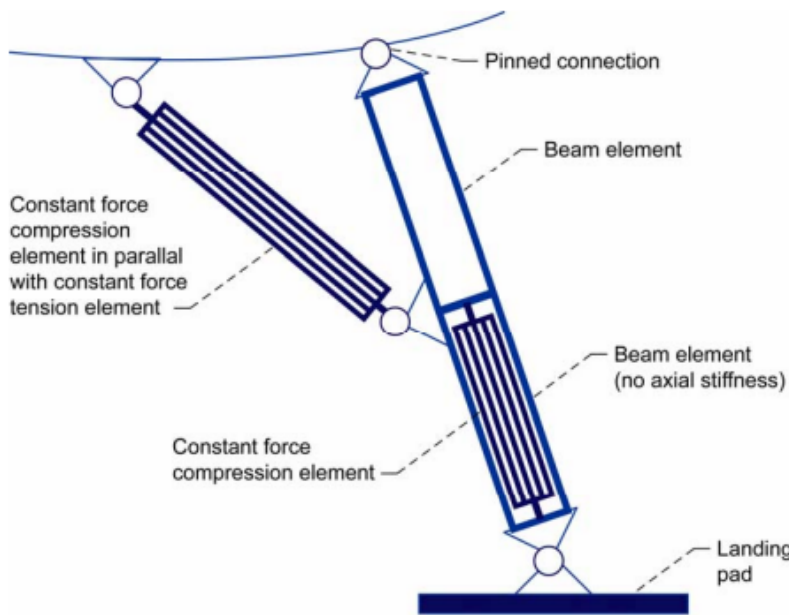


Figure H3: Schematic of Physical Model of a Single Proposed Dampened Landing Leg [61]

Table H1: NASA Dampened Landing Leg Axial Strength Datasheet [61]

Design iteration	Front legs		Rear legs	
	Secondary legs	Primary legs	Secondary legs	Primary legs
1	F _c = 20,000 lb 17-in. stroke	F _c = 20,000 lb 17-in. stroke	F _c = 35,000 lb 17-in. stroke	F _c = 30,000 lb 17-in. stroke
2	F _c = 20,000 lb 17-in. stroke	F _c = 30,000 lb 17-in. stroke	F _c = 50,000 lb 17-in. stroke	F _c = 25,000 lb 17-in. stroke
3	F _c = 20,000 lb 17-in. stroke	F _c = 40,000 lb 30-in. stroke	F _c = 50,000 lb 17-in. stroke	F _c = 20,000 lb 17-in. stroke
4	F _c = 20,000 lb 17-in. stroke	F _c = 30,000 lb 17-in. stroke Add spring—K = 30,000/17	F _c = 50,000 lb 17-in. stroke	F _c = 50,000 lb 17-in. stroke Add spring—K = 50,000/17

Table H2: NASA Dampened Landing Leg Inclination and Velocity Datasheet [61]

[Vertical velocity = 25 fps]

Horizontal velocity, fps	Pitch, degree		
	-15 (nose down)	0	+15 (heel down)
	Maximum acceleration, g		
0	4	9	8
20	8	8	7
40	8	8	9
60	10	8	6

^amaximum of X, Y, or Z body fixed direction.

Table H3: NASA STEM Boom Thin-Ply Material and Form Factor Datasheet [38]

Material (fiber / resin)	Form	Lamina AW (g/m ²)	Measured Cured Ply Thickness (mm)	E ₁₁ (GPa)	$\varepsilon_{11u,c}$ (%)	Vendor (fiber / resin)
MR60H / PMT-F7 (CF)	UD SpT	56	0.040 ± 0.05	174.3	1.10	Oxeon / Patz M&T
IM7 / RS-36 (CF)	UD SpT	44	0.032 ± 0.05	166.0	1.06	Tencate / Tencate
HTA40 / PMT-F7 (CF)	PW SpT	90	0.075 ± 0.01	75.9	1.03	TCS / Patz M&T
T300-1K / PMT-F7 (CF)	BR	125	0.100 ± 0.01	73.8	1.06	A&P / Patz M&T
AstroQuartz II/PMT-F7	PW (525)	93	0.080 ± 0.01	25.6	2.24	JPS Comp /Patz M&T
S2-Glass / PMT-F7	UD SpT	100	0.055 ± 0.05	57.2	2.56	Patz M&T/Patz M&T

Length	7 feet (2.1 meters)
Degrees of Freedom	There are five. They are made possible by tiny motors called "rotary actuators." The five degrees of freedom are known as the shoulder azimuth joint, shoulder elevation joint, elbow joint, wrist joint and turret joint.
"Hand" Turret	At the end of the arm is the "turret." It's like a hand that carries scientific cameras, mineral and chemical analyzers for studying the past habitability of Mars, and choosing the most scientifically valuable sample to cache.
Names of Tools on the Turret	SHERLOC and WATSON, PIXL, GDRT (Gaseous Dust Removal Tool), Ground Contact Sensor, Drill
Drill	The drill is a rotary percussive drill designed to extract rock core samples from the surface of Mars.
Drill Bits	A suite of interchangeable bits: coring bits, regolith bit and an abrader.
Main Function	Assist in Mars surface investigation and sample collection
Diameter of drilled holes	1 inch (27 mm)

Figure H4: Perseverance's Robotic Arm Imaging Equipment Datasheet [39, 81]

Main Job	Fine-scale detection of minerals, organic molecules and potential biosignatures
Location	Mounted on the turret at the end of the robotic arm
Mass	<p>Turret: 6.86 pounds (3.11 kilograms)</p> <p>Body: 3.55 pounds (1.61 kilograms) body</p>
Power	<p>Turret: 32.2 watts</p> <p>Body: 16.6 watts</p>
Volume	10.2 by 7.8 by 2.6 inches (26.0 by 20.0 by 6.7 centimeters)
Data Return	79.7 Mbits (raw)
Spatial Resolution	<p>2 Cameras</p> <p>Autofocus and Context Imager: 10.1 micrometers</p> <p>WATSON Camera: 15.9 micrometers</p> <p>1 Laser: 100 micrometers</p>
Field of View	<p>Imaging: 0.9 to 0.5 inches (2.3 by 1.5 centimeters)</p> <p>Spectroscopy: 7 by 7 millimeters (0.275 inch)</p>

Figure H5: Perseverance's SHERLOC and WATSON Specification Sheet [79]

Main Job	To measure the chemical makeup of rocks at a very fine scale
Location	Mounted on the turret at the end of the robotic arm
Mass	<p>Arm-mounted sensor head: Nearly 10 pounds (4.3 kilograms)</p> <p>Body-mounted electronics: About 6 pounds (2.6 kilograms)</p> <p>Calibration target: About 0.033 pounds (0.015 kilograms)</p>
Power	About 25 watts
Volume	<p>Arm-mounted sensor head: approximately 8.5 by 10.5 by 9 inches (21.5 by 27 by 23 centimeters)</p>
Calibration Targets	<p>Diameter of each of four disks: 0.19 inches (5 millimeters)</p> <p>Pedestal base: 1.53 by 1.18 inches (39 by 30 millimeters)</p>
Data Return	Approximately 16 megabits per experiment, or about 2 megabytes per day

Figure H6: Perseverance's Robotic Arm Collection Equipment Datasheet [81]

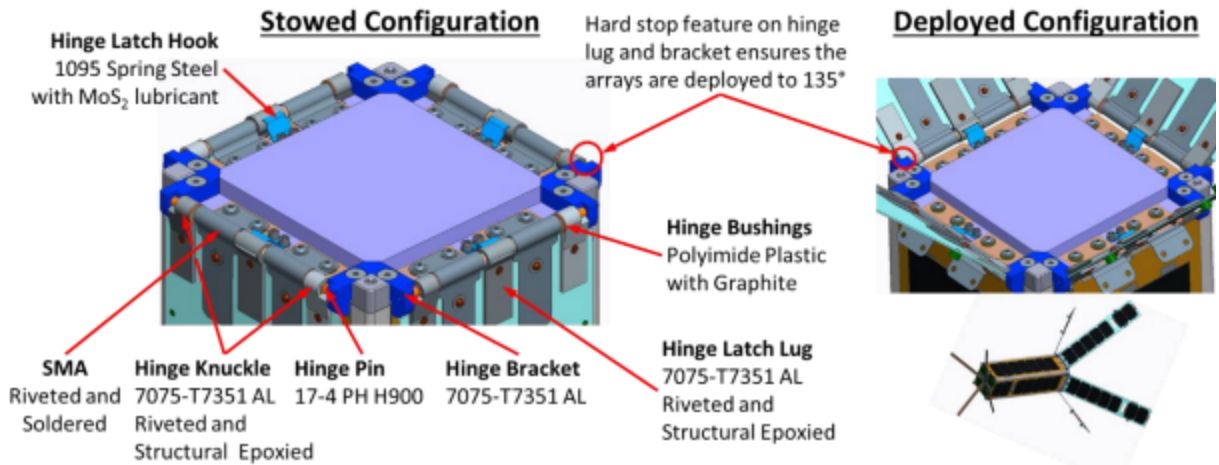


Figure 4. Hinge Component Parts and Design

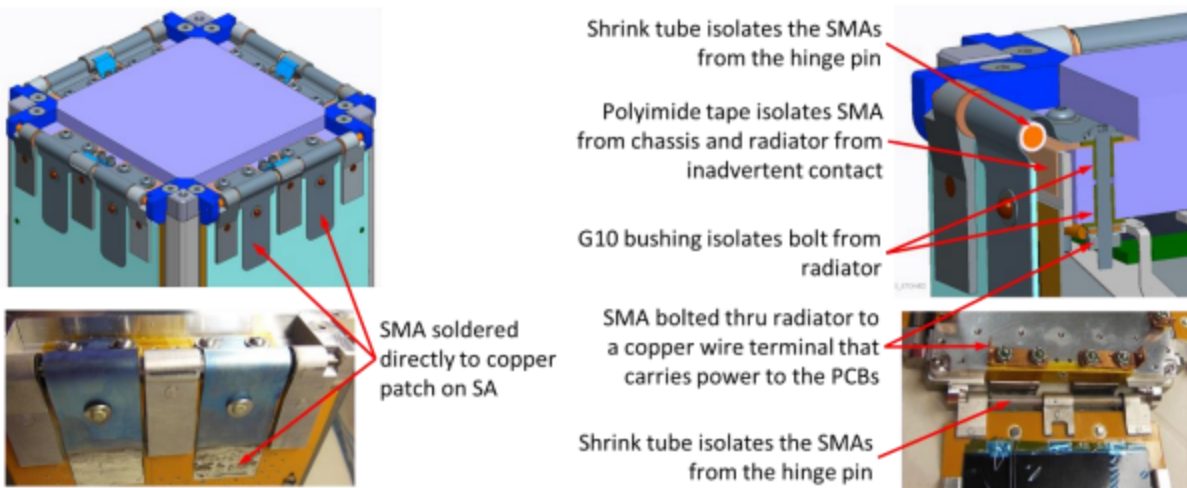


Figure H7: SMA-R&R Conceptual Schematic [45]

Table H4: SMA-R&R Specification Sheet [45]

Specification Description	Value	Requirement (with margin)
R&R Pin-Puller, Pull Force	13.34 N	≥ 12.19 N
R&R Pin-Puller Stroke Length	7.1 mm	≥ 6.14 mm
R&R 2 nd Stage Compression Spring, Spring Rate	0.701 N/mm	0.235 – 0.736 N/mm
R&R 2 nd Stage Compression Spring, Stowed Force	6.05 N	2.03 – 6.35 N
R&R 2 nd Stage Travel Distance	7.62 mm	≥ 5.87 mm
R&R Operating Power Rating	6 volt limited, 3.0 amps	6 volt limited, 3.0 amps max
R&R SMA Transition Temperature	150 to 160°C	> +50°C*
R&R Temperature Operation Range	-51 to +61°C	-40 to +50°C
R&R and Hinge Maximum Random Vibe Exposure**	14.1 gRMS, 3 minutes, 3 axes	10.0 gRMS, 1 minute, 3 axes
Hinge SMA Stowed Spring Torque (1 spring)	0.190 N·m	0.140 – 0.282 N·m
Hinge SMA Transition Temperature***	-20°C	> -40°C
Hinge Temperature Operating Range***	-20 to +61°C	-40 to +50°C
Other R&R Features	High temperature SMA, resettable, one mechanism releases all four SAs	
Other Hinge Features	Utilizes SMAs in a new application to advance the technology and SMAs transmit power from the SAs.	

Table H5: Pyrotechnic Separation Method Decision Matrix

Metric	Weight	Pyrotechnic Actuator (Exploding Bolts)	Separation Nut (Sep-Nuts)	Pyrotechnic Pin Puller
Safety	0.35	3	5	3
Shock Containment	0.25	3	4	4
Accuracy	0.2	3	4	4
Ease of Activation	0.1	2	5	3
Volumetric Constraint	0.05	5	5	5
Reliability	0.05	2	4	3
Total	1	2.95	4.5	3.55

Table H6: Telecommunications Radio System Decision Matrix

Criteria	Weight	STEM Boom	Telescopic Mast
Bending Rigidity	0.35	5	4
Cross-Sectional Properties	0.25	5	4
Material Construction	0.2	4	3
Achievable Height	0.1	4	3
Volumetric Profile	0.05	5	5
Accuracy	0.05	4	4
Total	1	4.65	3.75

Table H7: Robotic Arm Decision Matrix

Criteria	Weight	Perseverance's Robotic Arm	InSight's Robotic Arm	Motiv's xLink Robotic Arm
Sensor Functionality	0.2	5	4	3
Tools Functionality	0.2	4	4	4
Working Envelope	0.15	5	4	5
Degrees of Freedom	0.15	5	3	5
Durability	0.1	4	4	3
Modularity	0.1	3	3	5
Accuracy	0.1	4	3	4
Total	1	4.4	3.65	4.1

APPENDIX I: SPACEFLIGHT MECHANICS

PV Transfer Time Analysis

$$a_{Earth} = 149.6 \times 10^6 \text{ km} [24]$$

$$a_{Mars} = 227.9 \times 10^6 \text{ km} [24]$$

$$\mu_{Sun} = 132.7 \times 10^9 \frac{\text{km}^3}{\text{s}^2} [24]$$

$$a_{Transfer} = \frac{a_{Mars} + a_{Earth}}{2} = \frac{227.9 \times 10^6 + 149.6 \times 10^6}{2} = 188.75 \times 10^6 \text{ km}$$

$$P_{Transfer} = 2\pi \sqrt{\frac{a^3}{\mu_{Sun}}} = 2\pi \sqrt{\frac{(188.75 \times 10^6)^3}{132.7 \times 10^9}} = 44.728 \times 10^6 \text{ sec} \approx 518 \text{ days}$$

$$T_{Transfer} = \frac{P_{Transfer}}{2} = \frac{518}{2} = 259 \text{ days}$$

Engine_Cutoff_Analysis.m Script

```
%% Main Script of CPL Engine Cutoff & Impact Velocity Analysis
```

```
% Written By: Joe Scaglione
```

```
%% Clear Workspace
```

```
clear all
```

```
close all
```

```
clc
```

```
%% Plot Settings
```

```
% Linewidth Setting
```

```

lw = 3;

%% Input Parameters
alt_low = 0;
alt_high = 0.05;

m_clp = 250;

d_46P = 1.2;
d_67P = 4.2;

G = 6.674e-20;

D = 227.9e6;
m_sun = 1.989e30;

%% Gravitational Parameter Approximation
V_46P = (4/3)*(pi)*((d_46P/2)^3);
V_67P = (4/3)*(pi)*((d_67P/2)^3);

m_67P = 9.982e12;
m_46P = ((V_46P)/(V_67P))*m_67P

u_46P = G*m_46P

SOI_46P = ((m_46P/m_sun)^(2/5))*D

%% Analysis
alt = linspace(alt_low,alt_high,100);

Fg = zeros(size(alt),'like',alt);
Ag = zeros(size(alt),'like',alt);

for i=1:length(Fg)
    Fg(i) = (G*m_46P*m_clp)/((d_46P/2)+alt(i))^2;
    Ag(i) = Fg(i)/m_clp;
end

vel_clp = cumtrapz(alt,Ag);

```

```
% Plot Impact Velocity Over Engine Cutoff Altitude
fig1 = figure(1);
plot(alt*1000,vel_clp*1000,'r','LineWidth',lw)
grid on
xlabel('Engine Cutoff Altitude [m]')
ylabel('CLP Impact Velocity [m/s]')
title('CLP Impact Velocity as Function of Engine Cutoff Altitude')
```

CLP_Flight_Mechanics.m Script

```
%% Main Script of Comet Lander Probe Spaceflight Mechanics Analysis
% Written By: Joe Scaglione

%% Clear Workspace
clear all
close all
clc

%% Define Parameters
G = 6.674e-20; %gravitational constant

m_comet = 2.3282e+11; %mass of 46P/Wirtanen from 'Engine Cutoff Analysis' [kg]
m_lander = 250; %mass of Philae lander [kg]

u_comet = G*(m_comet); %comet gravitational parameter [km^3/s^2]
u_sun = 132712440018; %sun gravitational parameter [km^3/s^2]

r_PVp = 5; %desired distance of PV @ periapsis [km]
r_PVa = 7; %desired distance of PV @apoapsis [km]

r_CLP0 = r_PVp; %desired distance of CLP in circular orbit [km]

position_percentage = 85; %percent around circular orbit to start descent (1-100)
velocity_percentage = 30; %percent of circular orbit velocity to start descent (1-100)

%% PV Elliptical Orbit Parameters
a_PV = (r_PVp+r_PVa)/2; %semi-major axis of PV in elliptical orbit [km]
e_PV = (r_PVa-r_PVp)/(r_PVa+r_PVp); %eccentricity of PV in elliptical orbit
p_PV = a_PV*(1-(e_PV^2));
h_PV = sqrt(u_comet*p_PV); %specific angular momentum of PV in elliptical orbit
P_PV = 2*pi*sqrt((a_PV^3)/u_comet); %period of PV elliptical orbit [sec]
```

```

vp_PV = h_PV/r_PVp; %periapsis velocity of PV [km/s]
vesc_PVmin = sqrt((2*u_comet)/r_PVa); %min escape velocity of PV [km/s]

%% CLP Circular Orbit Parameters
vc_CLP = sqrt(u_comet/r_CLP0); %circular velocity of CLP in [km/s]
vesc_CLP = sqrt((2*u_comet)/r_CLP0); %escape velocity of CLP [km/s]

%% ODE45 Settings
% Integration Tolerance
options = odeset('RelTol',1e-13,'AbsTol',1e-13);

%% Define Comet Surface for Plot
comet = nsidedpoly(1000, 'Center', [0 0], 'Radius', 0.6); %representative comet shape in plot

%% Propagate PV Elliptical Orbit Position and Velocity
r0_PV = [r_PVp;0;0]; %initial position matrix of PV [km] [comet-centric frame]
v0_PV = [0;vp_PV;0]; %initial velocity matrix of PV [km] [comet-centric frame]

t_fPV = P_PV;
t_PV = linspace(0,t_fPV,1000);

[t_PV,x1] = ode45(@Two_Body_Comet_Lander,t_PV,[r0_PV;v0_PV],options);

r_PV = x1(:,1:3);
v_PV = x1(:,4:6);

%% Propagate CLP Circular Orbit Position and Velocity
r0_CLPc = [r_CLP0;0;0]; %initial position matrix of CLP [km] [comet-centric frame]
v0_CLPc = [0;vc_CLP;0]; %initial velocity matrix of CLP [km] [comet-centric frame]

P_CLPc = 2*pi*sqrt((r_CLP0^3)/u_comet); %period of CLP circular orbit [sec]

t_fCLPc = P_CLPc;
t_CLPc = linspace(0,t_fCLPc,1000);

[t_CLPc,x2] = ode45(@Two_Body_Comet_Lander,t_CLPc,[r0_CLPc;v0_CLPc],options);

r_CLPc = x2(:,1:3);
v_CLPc = x2(:,4:6);

```

```

%% Propagate CLP Descent Position and Velocity
r0_CLPd = transpose([r_CLPc(((position_percentage/100)*length(r_CLPc)),:)]);
v0_CLPd =
transpose((velocity_percentage/100)*[v_CLPc(((position_percentage/100)*length(v_CLPc)),:)]);

t_fCLPd = t_fCLPc+(0.181*t_fCLPc);
t_CLPd = linspace(t_fCLPc,t_fCLPd,1000);

[t_CLPd,x3] = ode45(@Two_Body_Comet_Lander,t_CLPd,[r0_CLPd;v0_CLPd],options);

r_CLPd = x3(:,1:3);
v_CLPd = x3(:,4:6);

%% Propagate CLP Landing Position and Velocity
r0_CLPl = transpose([r_CLPd(length(r_CLPd),:)]);
v0_CLPl = [v_CLPd(end,1);0;0];

t_fCLPl = t_fCLPd+(0.004*t_fCLPd);
t_CLPl = linspace(t_fCLPd,t_fCLPl,100);

[t_CLPl,x4] = ode45(@Two_Body_Comet_Lander,t_CLPl,[r0_CLPl;v0_CLPl],options);

r_CLPl = x4(:,1:3);
v_CLPl = x4(:,4:6);

%% Plot Settings
% Linewidth Setting
lw = 3;

%% Plot Propagations
fig1 = figure(1);

plot(comet, 'FaceColor', 'b')
hold on
plot(r_PV(:,1),r_PV(:,2),'-k','LineWidth',lw)
hold on
plot(r_CLPc(:,1),r_CLPc(:,2),'-r','LineWidth',lw)
hold on
plot(r_CLPd(:,1),r_CLPd(:,2),'-b','LineWidth',lw)

```

```

hold on
plot(r_CLPl(:,1),r_CLPl(:,2),'-.g','LineWidth',lw)

grid on
axis equal
xlabel('Distance in km')
ylabel('Distance in km')
zlabel('Distance in km')
legend('46P/Wirtanen','PV Elliptical Orbit','CLP Circular Orbit','CLP Descent','CLP Landing')

%% Calculate Approximate Delta-V
%dV for orbit capture
dV1 = vp_PV-vc_CLP;
%dV for descent initiation
dV2 =
norm(v_CLPc(((position_percentage/100)*length(v_CLPc)),:))-norm((velocity_percentage/100)
*[v_CLPc(((position_percentage/100)*length(v_CLPc)),:)]);
%dV for engine cutoff
dV3 = norm(v_CLPd(end,:))-norm(v0_CLPl);

%total dV in km/s
dVT = dV1+dV2+dV3;

%% Calculate Approximate Time
% Approximate time for orbit capture
T1 =(position_percentage/100)*P_CLPc;
T1 = T1*(1/60)*(1/60);
% Approximate time for descent
T2 = t_fCLPd - t_fCLPc;
T2 = T2*(1/60)*(1/60);
% Approximate time for landing
T3 = t_fCLPl - t_fCLPd;
T3 = T3*(1/60)*(1/60);

% Approximate time of orbital trajectory in seconds
Time = T1+T2+T3;

%% Calculate Delta-V from Plane Change
i = linspace(0,90);
dV = zeros(size(i),'like',i);

```

```

for n=1:length(i)
    dVi = 2*norm(v0_CLPc)*sind(i(n)/2);
    dV(n) = (sqrt((dV1^2)+(dVi)^2)+dV2+dV3)*1000;
end

%% Plot Delta-V from Plane Change

fig2 = figure(2);
plot(i,dV,'r','LineWidth',lw)
grid on
xlabel('Inclination Plane Change in degrees')
ylabel('Total Delta-V in m/s')

```

Two_Body_Comet_Lander.m Script

```

function xdot = Two_Body_Comet_Lander(t,x)
%Creates a derivative state matrix to be used in ode45 based on the 2-body
%equation of motion assumption between the comet and the lander probe
% Given a time and state vector, this function assembles and returns a
% 2x3 matrix in which the first row is composed of the 3 velocity
% components and the second row is composed of the 3 acceleration
% components

% Numbers refer to bodies as follows...
% Body 1: Comet
% Body 2: Lander

G = 6.674e-20; %gravitational constant
m_comet = 2.3282e+11; %mass of 46P/Wirtanen from 'Engine Cutoff Analysis' [kg]

% Velocity from input state matrix
v = x(4:6);

% Position from input state matrix
r12 = x(1:3);
r12_mag = norm(r12);

% Gravitational parameters
u_comet = G*m_comet; %km^3/s^2

```

```
% Individual acceleration terms
a = -u_comet*(r12/(r12_mag^3));

% Creates derivative of state matrix
xdot = [v;a];
end
```

APPENDIX J: PROPULSION

propulsion.m Script

```
%%Main script for CLP Propulsion system calculations
%Written by: Keith Beadle

%% Clear Workspace
clear all
close all

%%Mass of propellant

%Final Mass after burn
mf = 230.38725; %kg

%Propellant budget
dV1 = 6.77*10^-2; %m/s
%Propellant Reserves
dV2 = dV1*0.5; %m/s
%Total change in velocity
dV = dV1 + dV2; %m/s
%Specific impulse of propellant
Isp = 69; %s
%Standard gravity acceleration (m/s^2)
g0 = 9.81; %m/s^2

%Total theoretical mass of propellant
np1 = mf*(exp(dV/(Isp*g0))-1); %kg
%Loading error is added
np = np1+(np1*0.03); %kg

X = ['The mass of propellant required is ',num2str(np), 'kg'];
disp(X)
```

```

%%Tank size
%Ideal Gas Constant of Nitrogen
R = 0.2968; %kJ/(kg*k)
%Temperature
T = 300; %K

%Factor of safety
FS = 2;
%Desired Final Pressure
%Based off chamber pressure for thruster
Pf = 600*10^3; %Pa

%Desired Initial Pressure
%Very low Pressures lead to a higher ratio of unusable propellant and
%therefore increased mass. Very high pressures lead to increased tank
%parameters that ultimately overcome the greater usable propellant
%ratio. A moderate value of 200bars burst pressure was selected as a result.
Pi = 1e7; %Pa
%Pressure of needed propellant
P = Pi-Pf; %Pa

%Volume of tank calculated using ideal gas law
V = (np*R*T)/P; %m^3
%Radius of tank
r = ((3*V)/(4*pi))^(1/3); %m

%Initial mass of nitrogen = Unusable mass - usable mass
%Unusable mass is calculated using the ideal gas equation divided by
%the factor of safety. This is done as the actual tank will be filled
%below the theoretical burst pressure.
ni = (((V*Pf)/(R*T))/FS)+np; %kg

%Maximum allowable stress with the factor of safety
sigmax = 124*10^6/FS; %Pa

%Minimum acceptable thickness of membrane
t = (Pi*r)/(2*sigmax); %m
%Thickness of tank membrane with 0.002cm tolerancing
tmax = t+(0.002/100); %m

```

```

%Outside radius of membrane
r2 = r+tmax; %m

%Density of material
p = 2710; %kg/m^3
%Mass of propellant membrane (density times volume of shell)
W = p*((4*pi)/3)*((r2^3)-(r^3)); %kg

%The total mass of the tank when filled
%Mass of filled tank = Mass of tank + mass of propellant + max loading
%error
wetmass = W + ni + (ni*(0.5/100)); %kg

X = ['The mass of the dry tank is ',num2str(W*1000), 'g'];
disp(X)
X = ['The thickness of tank is ',num2str(tmax*1000), 'mm'];
disp(X)
X = ['The total mass of tank is ',num2str(wetmass*1000), 'g'];
disp(X)

```

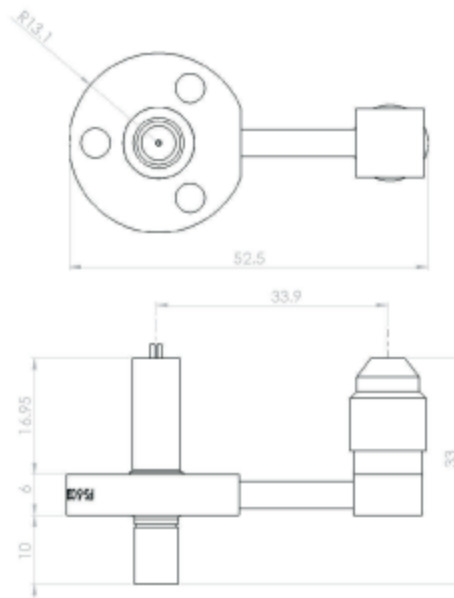
Table J1: Cold Gas Thruster Decision Matrix [12, 34, 102]

Metric	Weight	CGT	Mogg 058E142A	Mogg 58E163A	Mogg 058-118	VACCO
Accuracy	0.5	5	3	1	3	2
Reliability	0.3	4	3	2	3	5
Thrust	0.1	2	3	5	4	3
Mass	0.1	4	5	3	5	2
Total	1	4.3	3.2	1.9	3.3	3

Table J2: Propulsion Tank Material Selection Matrix [11, 63]

Metric	Weight	Al 6061	Ti-6Al-4V
Ease of Manufacturing	0.5	5	3
Tensile Yield Strength	0.4	3	5
Cost	0.1	5	2
Total	1	4.2	3.7

Cold Gas Thruster (CGT)



AST's miniaturized nitrogen cold gas thrusters provide a thrust of 42 mN at more than 69 s specific impulse. The fast switching thruster allows very small impulse bits of 110 μ Ns. Combined with its exceptional lifetime of more than 1 billion (10^9) actuations this opens up new operational modes of small satellite fine control.

The thrust level is linear with the inlet pressure. Together with our electronic pressure regulator it is possible to adjust the thrust level in flight.

The CGT has been fully qualified in the frame of the FORMOSAT 5 mission.

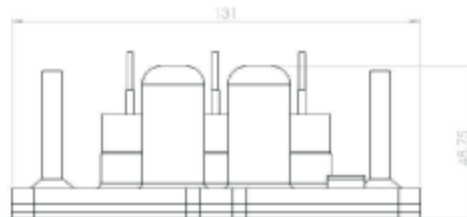
Performance Characteristics

Operating Media	GN ₂
Inlet Pressure (MEOP)	1 ... 6 bar
Proof Pressure	2 x MEOP
Burst Pressure	4 x MEOP
Internal Leakage	< 10 ⁻⁶ sccs GHe
External Leakage	< 10 ⁻⁸ sccs GHe
Thrust	28 mN / bar 42 mN @ 1.5 bar N ₂ nominal
Minimum Impulse Bit	110 μ Ns @ 1 bar
Specific Impulse	> 69 s
Weight	0.042 kg
Operating Voltage	22 ... 36 V pull in 50% hold
Coil Resistance	140 Ohm
Operational Temperature Range	-30° ... +80° C
Vibration	> 20g RMS
Lifetime	1 million actuations qualified 1 billion actuations demonstrated
Other media	GXe

Figure J1: AST GmbH Cold Gas Thruster Datasheet [12]



Electronic Pressure Regulator (EPR)

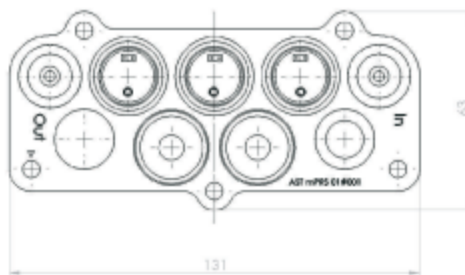


AST's two-stage electronic pressure regulator is used to provide a constant Xenon pressure at the inlet of an electric propulsion system.

The regulator accepts a tank pressure of 300 bar for modern systems with alternative propellants like Krypton.

The fully welded device provides a triple barrier against propellant loss, so no further latch valve is required to build a redundant system. Zero leakage capability eliminates the need of relief valves in the low pressure node. Particle filters in inlet and outlet protect the unit during handling and integration.

An exceptional low mass and size combined with low cost in series production are achieved by the use of AST's fluid SMD technology.



Performance Characteristics	
Operating Media	G Xe (G Kr, G N2)
Inlet Pressure (MEOP)	5 ... 300 bar
Outlet Pressure	1 ... 5 bar
Proof Pressure	1.5 x MEOP
Burst Pressure	2.5 x MEOP
Internal Leakage	< 10^{-6} sccs GHe
External Leakage	< 10^{-8} sccs GHe
Max. Flow Rate (fine mode)	> 50 mg/s GXe
Max. Flow Rate (coarse mode)	> 250 mg/s GXe
Ripple (fine mode)	< 20 mbar
Weight	0.65 kg
Average Power Consumption	< 10 W
Operating Voltage	< 24V
Operational Temperature Range	-20° ... +60° C
Vibration	> 20g RMS each axis
Redundancy	triple barrier against propellant loss (three serial valves)

Figure J2: AST GmbH Electronic Pressure Regulator Datasheet [13]

APPENDIX K: ATTITUDE DETERMINATION AND CONTROL

Table K1: IMU Decision Matrix

	Weight	MEMS	FOG	RLG
Cost	0.20	5	2	1
Mass	0.40	5	3	2
Accuracy	0.15	2	4	5
Noise	0.15	1	4	5
Totals	1	3.45	2.8	2.5

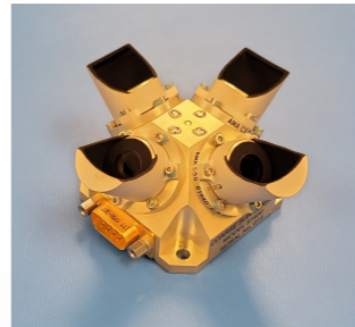


Figure K1: Honeywell IMU Spec Sheet [50]

RAD-HARD Hi-REL

The Redwire Coarse Sun Sensor (CSS) Pyramid is a 2 axis sensor containing four detectors, used for applications including solar array pointing, sun acquisition, and failsafe recovery.

- + The Coarse Sun Sensor Pyramid is a navigational instrument used by spacecraft to detect the position of the sun.
- + Redwire is able to design baffles to accommodate nearly any unique Field of View (FOV) requirements your mission requires.
- + The Coarse Sun Sensor Pyramid is Rad hard to more than 100 krad (Si).



APPLICATIONS

- + Solar-Array Pointing
- + Sun Acquisition
- + Fail-Safe Recovery

PARAMETERS

2π STERADIAN PLUS

Field of View

**±1° AT NULL (TYPICALLY)
±5° THROUGHOUT LINEAR RANGE**

Accuracy

MOUNTING BASE 2.3"×2.3" (58×58) MM WITH BAFFLES 3.5"×3.5"×1.7" (89×89×43 MM)

Dimensions

0.29 LB (0.13 KG) NOMINAL

Mass

NONE

Input Power

500 uA TO 1300 uA, EACH DETECTOR

Peak Output

CONFIGURATION

2

Number of Measurement Axes

4 PER BRACKET

Number of Detectors

2,6,8 DETECTORS PER BRACKET

Other Bracket Configurations

Figure K2: Redwire Coarse Sun Sensor Pyramid [95]

SECOND GENERATION STAR TRACKER (ST-16RT2)



SPECIFICATIONS

Absolute Accuracy	5 arcsecond cross-boresight (RMS) 55 arcsecond around boresight (RMS) (Demonstrated on-orbit, including thermal effects)
Maximum slew rate	3°/second
Lens	Full-custom 16 mm f/1.6 4-element glass, designed for shock and vacuum
Detector	2592 x 1944 CMOS active-pixel sensor, -3 e- system noise
Output Solution	Provides attitude quaternion and angular rates at 2 Hz Zero initial acquisition time
Processing	Full lost-in-space solution each frame Processor and star catalog built into unit Internal corrections for proper motion and stellar aberration
Command / Telemetry	Two half-duplex RS-485, ±70 V fault tolerant Can share data link with Sinclair Interplanetary by Rocket Lab reaction wheels
Supply Voltage	9 V to 34 V, redundant pins, reverse polarity protected
Power Consumption	Average: < 0.5 W Peak: 1.0 W
Environment	Thermal: -40°C to +50°C (operating), -40°C to +95°C (survival), Vibration: > 29.6 gRMS vibration Shock: 2000 G Lifetime: 13 years LEO (800 km) or 9 years GEO
Heritage	13 first generation units on-orbit, first launch November 2013 40 second generation units on-orbit, first launch June 2016



BAFFLE OPTIONS	NO BAFFLE	SHORT BAFFLE	LARGE BAFFLE
Field of View	7.5° x 10° half-angle	8° half-angle	7.5° x 10° half-angle
Sun-Avoidance	N/A	34° sun-to-boresight	22° sun-to-boresight
Moon-Avoidance	Demonstrated orbital operation with full moon in FOV		
Dimensions	62 x 56 x 38 mm	62 x 56 x 68 mm	99 Ø x 120 mm
Total Mass	158 g	185 g	235 g
Heritage	30 units on-orbit	13 units on-orbit	10 units on-orbit
Price	US\$120,000 each	US\$140,000 each	US\$140,000 each

Figure K3: Sinclair Interplanetary ST-16RT2 [97]

Table 5-5. Star Trackers Suitable for Small Spacecraft									
Manufacturer	Model	Mass (kg)	Power (W)	FOV	Cross axis accuracy (3s)	Twist accuracy (3s)	Radiation Tolerance (krad)	T R L	
Adcole Space	MAI-SS Space Sextant	0.282	2	Unk	5.7"	27"	75	9	
Ball Aerospace	CT-2020	3.000	8	Unk	1"	1"	Unk	6	
Berlin Space Technologies	ST200	0.040	0.65	22°	30"	200"	11	9	
Berlin Space Technologies	ST400	0.280	0.65	15°	15"	150"	11	9	
Blue Canyon Technologies	Standard NST	0.350	1.5	10° x 12°	6"	40"	Unk	9	
Blue Canyon Technologies	Extended NST	1.300	1.5	10° x 12°	6"	40"	Unk	9	
Creare	UST	0.840	Unk	Unk	7"	15"	Unk	5	
CubeSpace	CubeStar	0.055	0.264	42° diam eter	55.44"	77.4	Unk	8	
Danish Technical University	MicroASC	0.425	1.9	Unk	Unk	Unk	Unk	9	
Leonardo	Spacestar	1.600	6	20° x 20°	7.7"	10.6"	Unk	9	
NanoAvionics	ST-1	0.108	1.2	21° full-cone	8"	50"	20	9	
Sinclair Interplanetary	ST-16RT2	0.185	1	8° half-cone	5"	55"	Unk	9	
Sodern	Auriga-CP	0.210	1.1	Unk	2"	11"	Unk	9	
Sodern	Hydra-M	1.400	1	Unk	Unk	Unk	Unk	5	
Sodern	Hydra-TC	1.400	1	Unk	Unk	Unk	Unk	5	
Space Micro	MIST	0.520	4	14.5°	15"	105"	30	9	
Space Micro	μSTAR-100M	1.800	5	Unk	15"	105"	100	Unk	
Space Micro	μSTAR-200M	2.100	10	Unk	15"	105"	100	Unk	
Space Micro	μSTAR-200H	2.700	10	Unk	3"	21"	100	Unk	

Space Micro	μSTAR-400M	3.300	18	Unk	15"	105"	100	Unk
Surrey Satellite Technology	Altair HB+	1.000	Unk	Unk	10"	60"	Unk	9
Terma	HE-5AS	2.200	7	22°	3"	15"	100	9
Terma	T1	0.923	0.75	20° circu lar	4.5"	27"	Unk	5
Terma	T2	0.923	0.5	20° circu lar	10.5"	63"	Unk	5
Vectornic Aerospace	VST-41MN	0.900	2.5	14° x 14°	27"	183"	20	Unk
Vectornic Aerospace	VST-68M	0.470	3	14° x 14°	7.5"	45"	20	Unk

Figure K4: Suitable Star Trackers for Small Spacecraft [83]

Main technical data	RSI 02-33/30A	RSI 04-33/60A	RSI 1.6-33/60A
Angular momentum at nominal speed	0.2 Nms	0.4 Nms	1.6 Nms
Operational speed range	± 3,000 rpm	± 6,000 rpm	± 6,000 rpm
Speed limiter (EMF)	< 15,000 rpm	< 15,000 rpm	< 15,000 rpm
Motor torque at nominal speed	± 33 mNm	± 33 mNm	± 33 mNm
Loss torque	< 20 mNm	< 20 mNm	< 20 mNm
Dimensions			
Diameter	135.5 mm	135.5 mm	135.5 mm
Height	110 mm	110 mm	110 mm
Mass	< 1.75 kg	< 1.75 kg	< 2.45 kg
Power consumption			
Steady state at nominal speed	< 10 W	< 17 W	< 17 W
Maximum torque at nominal speed	< 20 W	28 W	< 28 W
Power interface			
Supply voltage	23 to 30 VDC	23 to 30 VDC	23 to 30 VDC
Input current	< 1.0 A	< 1.0 A	< 1.0 A
Galvanic isolation between primary return and secondary return	Yes	Yes	Yes
Preceding stage	Yes	Yes	Yes
On/off relay	Yes	Yes	Yes
Signal interface			
Torque command and direction	Analog/bi-level	Analog/bi-level	Analog/bi-level
Speed measurement and direction	Analog/bi-level	Analog/bi-level	Analog/bi-level
Motor torque (current)	Analog	Analog	Analog
Bearing temperature	Analog (thermistor)	Analog (thermistor)	Analog (thermistor)
On/off status	Bi-level	Bi-level	Bi-level
On/off command	Pulses	Pulses	Pulses
Environmental conditions			
Qualification/protoflight temperature	-20 to +70 °C	-20 to +70 °C	-20 to +70 °C
Operating temperature	-10 to +45 °C	-10 to +45 °C	-10 to +45 °C
Survival/nonoperating temperature	-15 to +60 °C	-15 to +60 °C	-15 to +60 °C
Lifetime	> 15 years (in orbit)	> 15 years (in orbit)	> 15 years (in orbit)

Figure K5: Collins Aerospace Reaction Wheels [101]

QuatDynamics_PIDControl.m Script

```
% This script solves the dynamic behavior of a simple rigid body
% spacecraft. In particular, this script incorporates a simple simulation
% of a rigid body spacecraft described using euler symmetric parameters
% (quaternions). This script also includes a simple control system used to
% apply control moments to the bus in order to produce the desired angular
% velocity and orientation.
```

```
clear;
clc;
```

```

%% Setup

% Simulation Parameters:
global DT
SIM_LENGTH = 20; % length of simulation (in seconds)
DT = 0.001; % timestep length (in seconds)

% Initial Conditions
% though the simulation is done in quaternions, it is simpler for users to
% interface with Euler angles. As such, initial and desired states are
% inputted using Euler Angles and then converted into quaternions for use
% in the simulation.

initial_ang_vel = 10; %change to [1, 3, 6.5]
initial_EulerAngles = (0.5 - rand(3,1))*pi; % radians
initial_AngularVelocity = rand(3,1); % radians/second
initial_AngularVelocity =
initial_ang_vel*(initial_AngularVelocity/norm(initial_AngularVelocity)); % radians/second

desired_EulerAngles = [0; 0; 0];
desired_AngularVelocity = [0; 0; 0];

% Spacecraft Properties
% I = [7.6612  0  0;
%      0  8.7772  0;
%      0  0  8.5277]; % Moment of Inertia (kg*m^2)
I = [7.6612 -2.3588 -2.8751;
     -2.3588  8.7772 -2.8011;
     -2.8751 -2.8011  8.5277]; % Moment of Inertia (kg*m^2)

I_inv = pinv(I);

% Controller Properties
global MC_saturate MC_history
MC_saturate = 1.6*4/sqrt(3); % the saturation value for the control actuator
MC_history = [];

% if PD:
global Kq Kw Kq_int
Kq = 800*[1; 1; 1];

```

```

Kw = 400*[1.5; 1.8; 1.3];
Kq_int = 0.001*[1.5; 1.8; 1.3];

global q_error_prev w_error_prev q_err_int
q_error_prev = 0;
w_error_prev = 0;
q_err_int = [1; 0; 0; 0];
% if MPC:
% variables here

%% Convert to Quaternions
q0 = C_toQuat(EA_toC(initial_EulerAngles)) / norm(C_toQuat(EA_toC(initial_EulerAngles)));
w0 = initial_AngularVelocity;

global q_des w_des
q_des = C_toQuat(EA_toC(desired_EulerAngles)) /
norm(C_toQuat(EA_toC(desired_EulerAngles)));
w_des = desired_AngularVelocity;

%% Simulation

%global q0 w0 q_des w_des I

iters = SIM_LENGTH/DT;
%iters = 60;

q_sim = zeros(4,iters);
w_sim = zeros(3,iters);

q_sim(:,1) = q0;
w_sim(:,1) = w0;

M_ext = [0; 0; 0];
%M_ext = (rand(3,1));

for i = 2:iters
    %M_ext = (rand(3,1));

    M_c = controller(i, q_sim, w_sim);

```

```

q_dot = 0.5*quat_mult(q_sim(:,i-1), [0; w_sim(:,i-1)]);
w_dot = I_inv*((M_ext+M_c)-(wcross(w_sim(:,i-1))*I*w_sim(:,i-1)));
w_sim(:,i) = w_sim(:,i-1) + DT.*w_dot;
q_sim(:,i) = q_sim(:,i-1) + DT.*q_dot;

q_sim(:,i) = q_sim(:,i) / norm(q_sim(:,i));
end

%% Plotting

time = 0:DT:SIM_LENGTH-DT;

fig1 = figure(1);
plot(time, w_sim(1,:))
hold on
plot(time, w_sim(2,:))
plot(time, w_sim(3,:))
xlabel('Time (s)')
ylabel('Angular Velocity (rad/s)')
title('')
legend('w_x','w_y','w_z')
saveas(fig1, sprintf('plots/w_vs_time_%d.png',round(initial_ang_vel)))

fig2 = figure(2);
plot(time, q_sim(1,:))
hold on
plot(time, q_sim(2,:))
plot(time, q_sim(3,:))
plot(time, q_sim(4,:))
xlabel('Time (s)')
ylabel('Euler Symmetric Parameter')
title('')
legend('q0','q1','q2','q3')
saveas(fig2, sprintf('plots/q_vs_time_%d.png',round(initial_ang_vel)))

fig3 = figure(3);
plot(time, MC_history(1,:))
hold on
plot(time, MC_history(2,:))

```

```

plot(time, MC_history(3,:))
xlabel('Time (s)')
ylabel('Controller History (N-m)')
title('')
legend('Mx','My','Mz')
saveas(fig3, sprintf('plots/M_vs_time_%d.png',round(initial_ang_vel)))

%% Useful Functions

function C = EA_toC(EA)
x = EA(1);
y = EA(2);
z = EA(3);

C = [cos(y).*cos(z), -cos(y).*sin(z), sin(y);
      sin(x).*sin(y).*cos(z)+cos(x).*sin(z), -sin(x).*sin(y).*sin(z)+cos(x).*cos(z), -sin(x).*cos(y);
      -cos(x).*sin(y).*cos(z)+sin(x).*sin(z), cos(x).*sin(y).*sin(z)+sin(x).*cos(z), cos(x).*cos(y)];
end

function q = C_toQuat(C)
q4 = 0.5*sqrt(1 + C(1,1) + C(2,2) + C(3,3));
q1 = 0.5*sqrt(1 + C(1,1) - C(2,2) - C(3,3));
q2 = 0.5*sqrt(1 - C(1,1) + C(2,2) - C(3,3));
q3 = 0.5*sqrt(1 - C(1,1) - C(2,2) + C(3,3));

if q4 > q1 && q4 > q2 && q4 > q3
    q4 = 0.5*sqrt(1 + C(1,1) + C(2,2) + C(3,3));
    q1 = (C(3,2) - C(2,3)) / (4*q4);
    q2 = (C(1,3) - C(3,1)) / (4*q4);
    q3 = (C(2,1) - C(1,2)) / (4*q4);
elseif q3 > q1 && q3 > q2 && q3 > q4
    q3 = 0.5*sqrt(1 - C(1,1) - C(2,2) + C(3,3));
    q4 = (C(2,1) - C(1,2)) / (4*q3);
    q1 = (C(1,3) + C(3,1)) / (4*q3);
    q2 = (C(2,3) + C(3,2)) / (4*q3);
elseif q2 > q1 && q2 > q3 && q2 > q4
    q2 = 0.5*sqrt(1 - C(1,1) + C(2,2) - C(3,3));
    q3 = (C(2,3) + C(3,2)) / (4*q2);
    q4 = (C(1,3) - C(3,1)) / (4*q2);
    q1 = (C(1,2) + C(2,1)) / (4*q2);

```

```

else
    q1 = 0.5*sqrt(1 + C(1,1) - C(2,2) - C(3,3));
    q2 = (C(1,2) + C(2,1)) / (4*q1);
    q3 = (C(1,3) + C(3,1)) / (4*q1);
    q4 = (C(3,2) - C(2,3)) / (4*q1);
end
q0 = q4;
q = [q0; q1; q2; q3];

end

function wx = wcross(w)
    wx = [0, -w(3), w(2);
          w(3), 0, -w(1);
          -w(2), w(1), 0];
end

function mult_result = quat_mult(p, q)
    p0 = p(1);
    p1 = p(2);
    p2 = p(3);
    p3 = p(4);

    P = [p0 -p1 -p2 -p3;
          p1 p0 -p3 p2;
          p2 p3 p0 -p1;
          p3 -p2 p1 p0];
    mult_result = P*q;

end

function conjugate = quat_conj(q)
    conjugate = [q(1) -q(2) -q(3) -q(4)].';
end

%% Controller

function M_c = controller(i, q, w)
    global Kq Kw Kq_int q_des w_des MC_saturate q_error_prev w_error_prev q_err_int
    global MC_history

```

```

is_PID = true;
is_MPC = false;

if is_PID == 1
    w_err = w(:,i-1) - w_des;
    q_err = quat_mult(q_des, quat_conj(q(:,i-1)));
    q_err_int = quat_mult(q_err_int, q_err);

    if q_err(1) < 0
        q_err = [-q_err(2) -q_err(3) -q_err(4)].';
    else
        q_err = [q_err(2) q_err(3) q_err(4)].';
    end

    if norm(w(:,i-1)) < 1
        if max(abs(w(:,i-1))) < 1
            % proportional
            M_c_proportional = Kq.*q_err;
        else
            % proportional
            M_c_proportional = [0; 0; 0];
        end
    else
        % proportional
        M_c_proportional = [0; 0; 0];
    end

    %
    % proportional
    M_c_proportional = Kq.*q_err;

    %
    % derivative
    M_c_derivative = -Kw.*w_err;

    %
    % integral (of quaternions)
    M_c_integral = -Kq_int.*q_err_int(1:3,:);

    %
    % totals
    M_c = M_c_proportional + M_c_derivative + M_c_integral;
    if norm(M_c) > MC_saturate

```

```

M_c = MC_saturate*(M_c / norm(M_c));
end

w_error_prev = w_err;
q_error_prev = q_err;

elseif is_MPC == 1
    M_c = [0; 0; 0];
else
    M_c = [0; 0; 0];
end

MC_history(:,i) = M_c;
end

```

APPENDIX L: THERMAL MANAGEMENT

Table L1: MLI Material Decision Matrix

Metric	Weight	Mylar	Kapton
Temperature Resistance	0.6	3	5
Weight	0.1	4	4
Strength	0.3	5	3
Total	1.0	3.7	4.3

Parameter/Description	Quantity/Magnitude
Operating Temperature	-20 to +50 °C
Survival Temperature	-70 to +80 °C
Working Fluid	High Purity Ammonia
Heat Transport Capability	5 to 700 Watts
Effective Thermal Conductance (Pump)	≥120 W/K at 500 Watts
Overall LHP Conductance	≥70 W/K; 200 to 700 Watts
Capillary Pump Length	30.5 cm (12 inches)
Primary Wick Material	Sintered Nickel Powder
Primary Wick Pore Size	≤ 1.5 µm
Primary Wick Permeability	≥ 1.0 x 10 ⁻¹⁴ m ²
Primary Wick Thermal Conductivity	≤ 10 W/m-K
Primary Wick Outer Diameter	2.54 cm (1 inch)
Secondary Wick Static Height Capability	≥ 1.6 cm (0.63 inches)
Secondary Wick Transport Capability	≥ 30.5 W-m (1200 W-in)
Secondary Wick Material	Stainless Steel Screen Composite
Condenser Geometry	Two (2) Parallel Paths
Capillary Flow Balancer Vapor Hold Off	≥ 1000Pa
Capillary Flow Balancer Liquid Delta P	≤ 1000 Pa at 0.7 grams/sec flow
Capillary Pump Material	6063 Aluminum
Compensation Chamber Material	316 Stainless Steel
Transport Line Material	316 Stainless Steel
Condenser Section Material	6063 Aluminum Extrusion

Figure L1: Looped Heat Pipe Specifications [25]

Table L2: Radiator Spec Sheet [55]

Material	T300	P95 WG	K 1100
Thermal conductivity, W/mK	50–80	300–500	750–1000
Heat pipe dimensions, cm			
Length, L	91.4	91.4	91.4
Shell diameter, D	2.5	2.5	2.5
Width, W	2.5	5	7.5
Thickness, T	0.1	0.1	0.1
Heat pipe components mass, g			
C–C shell	169.5	214.0	254.5
Liner with evaporator	41.2	41.2	41.2
End caps	13.1	13.1	13.1
Fill tubes	7.2	7.2	7.2
Braze	22.5	22.5	22.5
Foil wick	24.0	24.0	24.0
Working fluid	13.5	13.5	13.5
Total mass, g	291.0	335.5	376.0
One-sided radiating area, m ²	0.0691	0.116	0.16
Specific mass, kg/m ²	4.21	2.89	2.35
Two-sided radiating area, m ²	0.1382	0.232	0.32
Specific mass, kg/m ²	2.11	1.45	1.18

Estimated Temperature Ranges

Electronics	0 to 40 C
Batteries	0 to 15 C
Solar Arrays	-160 to 60 C (survival) 0 to 20 C (operational)
Propellant	7 to 35 C
Structure	-45 to 65 C
Sensors	-20 to 10 C
IMU	-34 to 71 C
Oxygen Plant	?

Figure L2: Estimated Temperature Operation Ranges [66]

APPENDIX M: POWER MANAGEMENT

Lithium-ion (Li-ion) batteries from Saft						
	ENERGY			EXTENDED LIFE & TEMPERATURE		
Form factor	Cylindrical D	Prismatic	Prismatic	Prismatic	Prismatic	Prismatic
Nominal voltage	3.65 V					
Nominal capacity	5.4 Ah	2.6 Ah	5.3 Ah	6.8 Ah	4.0 Ah	5.6 Ah
Max. continuous discharge current	11.0 A	5.0 A	10.0 A	14.0 A	8.0 A	11.0 A
Max. pulse discharge rate	21.0 A	10.0 A	21.0 A	27.0 A	16.0 A	22.0 A
Max. charge current	5.4 A	2.6 A	5.0 A	6.8 A	4.0 A	5.6 A
Cycle life	>600	1100	950	1800	2700	2700
(Cycled to 70 % of the cells original capacity)	(100 % DoD, C/2-C/2, +20°C)	(100 % DoD, C/2-C/2, +25°C)	(100 % DoD, C/2-C/2, +25°C)			
Typical weight	130 g	66 g	121 g	150 g	97 g	135 g
Discharge temperature range	-35 / + 60°C	-40 / + 85°C	-40 / + 85°C			
Charge temperature range	-30 / + 60°C	-30 / + 85°C	-30 / + 85°C			

Typical values relative to cells stored for one year or less at +30°C max.; Performance may according to charge characteristics (current, duration, frequency, temperature conditions, storage conditions prior to usage and applications acceptable minimum voltage).

Figure M1: Saft Lithium-Ion Battery Selections [99]

Specifications		Specifications	
Part Number	LP 33450	Part Number	LP 33037
Nominal Cell Weight	1.27 kg	Nominal Cell Weight	1.6 kg (3.5 lbs)
Dimensions	See details on back	Dimensions	See details on back
Voltage Range	3.0 to 4.1V	Voltage Range	3.0 to 4.1V
Nominal Voltage	3.6V	Nominal Voltage	3.6V
Nominal Capacity	43Ah at C/5 at 20°C (68°F)	Nominal Capacity	60Ah at C/5 at 20°C (68°F)
Energy Density	378 Wh/L	Energy Density	393 Wh/L
Specific Energy	153 Wh/kg	Specific Energy	160 Wh/kg
Discharge Rates	Max constant current 200A Max pulse current (<1 sec.) 400A	Discharge Rates	Max constant current 250A Max pulse current (<1 sec.) 550A
Nominal Cell Impedance	2mΩ at 20°C (68°F)	Nominal Cell Impedance	1mΩ at 20°C (68°F)
Cycle Life (80% capacity measured at 0.5C discharge current at 20°C (68°F))	>2000 at 100% DOD	Cycle Life (80% capacity measured at 0.5C discharge current at 20°C (68°F))	>2000 at 100% DOD
Standard Charging Method	Constant current 21.5A (0.5C) to 4.1V Constant voltage 4.1V to 0.86A (C/50)	Standard Charging Method	Constant current 12A (0.2C) to 4.1V Constant voltage 4.1V to 1.2A (C/50)
Operating Temperature	-20 to 60°C (-4 to 140°F)	Operating Temperature	-20 to 40°C (-4 to 104°F)
Storage Temperature	-40°C to +60°C (-40 to 140°F)	Storage Temperature	-40 to 40°C (-40 to 104°F)
Specifications		Specifications	
Part Number	SAR-10199	Part Number	LP 33081
Weight Not to Exceed	35.0 kg (77.2 lbs)	Nominal Cell Weight	950 g (2.1 lbs)
Maximum Dimensions	Width: 27.3 cm (10.8 in.) Length: 50.8 cm (20.0 in.) Height: 27.3 cm (10.8 in.)	Dimensions	See details on back
Nominal Voltage	33.3 V	Voltage Range	3.0 to 4.1V
Operating Voltage	27.0 to 36.9 V	Nominal Voltage	3.6V
Beginning of Life Capacity/Energy	100 Ah/3663 Wh at 20°C (68°F)	Nominal Capacity	30Ah at C/5 at 20°C (68°F)
Specific Energy	104.6 Wh/kg	Energy Density	335 Wh/L
Maximum Current Charge	55 A	Specific Energy	141 Wh/kg
Maximum Continuous Discharge	100 A	Discharge Rates	Max constant current 150A Max pulse current (<1 sec.) 300A
Maximum Discharge Pulse	330 A for 5 sec	Nominal Cell Impedance	2mΩ at 20°C (68°F)
Operating Temperature	-5 to 35°C (23 to 95°F)	Cycle Life (80% capacity measured at 0.5C discharge current at 20°C (68°F))	>2000 at 100% DOD
Survival Temperature (non-operating)	-15°C to 40°C (5 to 104°F)	Standard Charging Method	Constant current at 6A (C/5) to 4.1V Constant voltage at 4.1V to 0.6A (C/50)
Random Vibe Levels	14 g	Operating Temperature	-20 to 60°C (-4 to 140°F)
Surge Vibe Levels	15 g	Storage Temperature	-40°C to 20°C (-40 to 68°F)
Shock Levels	1135 g		

Figure M2: Eagle Picher Lithium-Ion Batteries [26]

Ultra Triple Junction (UTJ)



2 Per (26.6 cm²)



LEONE (59.6 cm²)

High Efficiency Space Photovoltaics

Product Features

- Small and large cell sizes offered for optimum packing factor and cost competitiveness
- All sizes qualified for LEO and GEO missions
- Discrete Si bypass diode protection
- Performance for cells <32 cm² is 28.4% efficiency (minimum average @ max power, 28°C, AM0)
- Performance for cells >32 cm² is 27.9% efficiency (minimum average @ max power, 28°C, AM0)
- Available as CIC assembly (Cell-Interconnect-Coverglass with diode) for ease of integration or delivered on completed solar panels (please refer to Panel Data Sheet)

Space Heritage

- Sustained quality without a single anomaly throughout six decades of space flight heritage
- Highest competitive EOL dollar per Watt solutions
- More than 4 million multi-junction cells **delivered**
- More than 2 MW of multi-junction arrays **on orbit**
- Large area LEONE cell (59.6 cm²) delivered on solar panels for over 37 satellites (LEO constellation)
- 1 MW annual capacity - cells and panels
- On orbit performance for multi-junction solar cells validated to +1% of ground test results on average



ENVIRONMENTAL MANAGEMENT SYSTEM
CERTIFIED BY DNV

ISO 14001

ISO 9001:2000
REGISTERED

Qualification

Key Qualification Results

Low Earth Orbit (LEO)	> 75,000 cycles
Geostationary Orbit (GEO)	> 15,550 cycles
Interplanetary Missions	Mars, Jupiter, Asteroid
Testing	ESD Survivability Tested to ISO Standards
Qualification	Fully Qualified for all Mission Types

Product Description

Substrate	Germanium
Solar Cell Structure	GaInP ₂ /InGaAs/Ge
Method	Metal Organic Vapor Phase Epitaxy
Device Design	Monolithic, two terminal triple junction. n/p GaInP ₂ , InGaAs, and Ge solar cells interconnected with two tunnel junctions
Standard Sizes	26.6 cm ² and 59.6 cm ² are most cost effective and common standard sizes; other sizes available
Assembly Method	Welded
CIC Assembly	Coverglass thickness range from 3 mils to 30 mils with various coatings. Interconnects available with either out-of-plane or in-plane stress relief

Figure M3: Spectrolab UTJ Description [111]

Ultra Triple Junction (UTJ)

Typical Electrical Parameters
(AM0 (135.3 mW/cm²) 28°C, Bare Cell)

Parameters	< 32 cm ²	> 50 cm ²
Jsc	17.14 mA/cm ²	17.22 mA/cm ²
Jmp	16.38 mA/cm ²	16.46 mA/cm ²
Jload _{min avg}	16.48 mA/cm ²	16.56 mA/cm ²
Voc	2.660 V	2.660 V
Vmp	2.350 V	2.300 V
Vload	2.310 V	2.270 V
Cff	0.85	0.83
Effload	28.1%	27.8%
Effmp	28.4%	27.9%

Radiation Degradation
(Fluence 1MeV Electrons/cm²)

Parameters	1x10 ¹⁴	5x10 ¹⁴	1x10 ¹⁵
I _{mp} /I _{mp0}	0.99	0.98	0.96
V _{mp} /V _{mp0}	0.94	0.91	0.89
P _{mp} /P _{mp0}	0.93	0.89	0.86

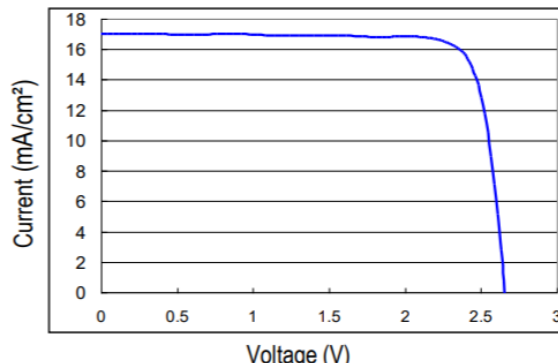
Thermal Properties

Solar Absorptance	0.92 (5 mil CMG-AR, 0.90 for bare cells)
Emittance (Normal)	0.85 (Ceria Doped Microsheet)

Temperature Coefficients (15°C - 80°C)
(Fluence 1MeV Electrons/cm²)

Parameters	BOL	5x10 ¹⁴	1x10 ¹⁵
Jmp (μA/cm ² /°C)	1.2	5.3	6.9
Jsc (μA/cm ² /°C)	5.3	6.5	6.9
Vmp (mV/°C)	-6.5	-6.7	-6.8
Voc (mV/°C)	-5.9	-6.3	-6.5

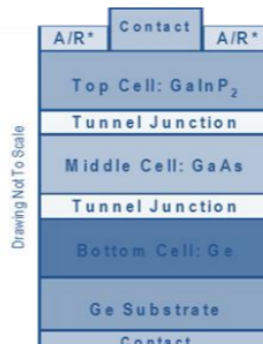
Typical IV Characteristic
AM0 (135.3 mW/cm²) 28°C, Bare Cell



Weight

84 mg/ cm² (Bare) @ 140 μm (5.5 mil) Ge wafer thickness

Solar Cell Structure



*A/R : Anti-Reflective Coating

Intellectual Property

This product is protected by Spectrolab's portfolio of patents including the following:

- 6,150,603
- 6,255,580
- 6,380,601
- 7,119,271
- 7,126,052

Regulatory

Spectrolab's products are fully qualified and are ISO9001 and AS9100 certified

7/16/18

Figure M4: Spectrolab UTJ Characteristics [111]

Power.m Script

```
clc;
clear;

%% Orbit Parameters

% the distance from the sun every month (in au)
sun_dist = [4.087 3.964 3.818 3.667 3.499 3.326 3.136 2.932 2.723 ...
             2.493 2.258 2.003 1.740 1.495 1.258 1.098 1.069 1.186 1.403];

x = 1:19;
P = polyfit(x, sun_dist, 5);
yfit = P(1).*x.^5 + P(2).*x.^4 + P(3).*x.^3 + P(4).*x.^2 + P(5).*x + P(6);

figure(101)
scatter(x, sun_dist)
hold on
plot(x, yfit)

sun_dist_func = @(x) P(1).*x.^5 + P(2).*x.^4 + P(3).*x.^3 + P(4).*x.^2 + P(5).*x + P(6);

timesteps = 12960;

figure(1)
plot(sun_dist)
xlabel('Time (months)')
ylabel('Distance from Sun (au)')
title('Solar Distance')

%% Solar Power
T0 = 28; % degrees C
P_rated = 1353; % W/m^2

H_I = @(R) (1./R).^2;
N_T = @(T) 1 - (1.6e-3).*(T - T0);
N_plf = @(alpha) cos(alpha);

N_rad = linspace(0.99, 0.9, timesteps);
N_uv = linspace(1, 0.98, timesteps);
N_cy = linspace(0.99, 0.97, timesteps);
```

```

N_m = 0.975;
N_i = 0.98;
N_con = 0.98;
N_s = 1; % assume negligible shadowing

P_array = @(ts, T, R, alpha)
P_rated.*N_rad(ts).*N_uv(ts).*N_cy(ts).*N_m.*N_i.*N_con.*N_T(T).*H_I(R).*N_plf(alpha);

T_arr = @(i) 20 + 20.*sin((i).*pi/120);
alpha_arr = @(i) 0*(pi/180);

Power_per_square_meter = [];
Temperature_hist = [];

for i = 1:timesteps
    Power_per_square_meter(i) = P_array(i, T_arr(i), sun_dist_func(i/720), alpha_arr(i));
    Temperature_hist(i) = T_arr(i);
end

figure(2)
plot(Power_per_square_meter)
xlabel('Time (hours)')
ylabel('Power Generation per Square Meter')
title('Power Generation Throughout Mission')

figure(3)
plot(Temperature_hist)
xlabel('Time (hours)')
ylabel('Temperature')
title('Temperature History')
ylim([-20, 60])

%%

x = 1:19;
sun_dist = [4.087 3.964 3.818 3.667 3.499 3.326 3.136 2.932 2.723 ...
            2.493 2.258 2.003 1.740 1.495 1.258 1.098 1.069 1.186 1.403];

P = polyfit(x, sun_dist, 5);
yfit = P(1).*x.^5 + P(2).*x.^4 + P(3).*x.^3 + P(4).*x.^2 + P(5).*x + P(6);

```

```

figure(101)
scatter(x, sun_dist)
hold on
plot(x, yfit)

sun_dist_func = @(x) P(1).*x.^5 + P(2).*x.^4 + P(3).*x.^3 + P(4).*x.^2 + P(5).*x + P(6);

```

APPENDIX N: COMMAND AND DATA

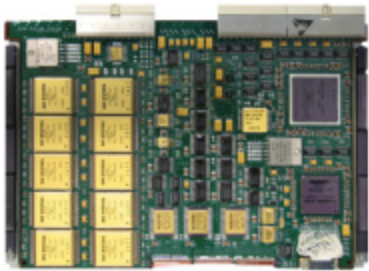
Table N1: Command and Control Decision Matrix [15, 36, 53, 93, 115]

Metric	Weight	BAE RAD750	BAE RAD5545	HPE Spaceborne Computer	Boeing HPSC
Flight Heritage	0.4	5	4	1	0
Performance	0.25	3	4	4	5
Power Requirements	0.2	4	3	3	4
Mass	0.15	3	4	3	3
Total	1	4	3.8	2.45	2.5

Table N2: BAE Systems RAD750 Model Decision Matrix [93]

Metric	Weight	6U Single Board	6U Extended Single Board	3U Single Board
Performance	0.5	4	5	2
Power Requirements	0.2	3	3	4
Mass	0.1	3	2	5
Volume	0.1	3	2	5
Cost	0.1	3	3	4
Total	1	3.5	3.8	3.2

RAD750® 6U CompactPCI single-board computer



The 6U CompactPCI singleboard computer, available in seven configurations, employs the PowerPC RAD750® microprocessor, the radiationhardened version of the IBM PowerPC750 microprocessor. The companion Power PCI Bridge ASIC provides access to the memory and the PCI version 2.2 backplane bus.

Key features

- Example startup ROM and VxWorks boardsupport package provided for all hardware configurations
- Green Hills Software's INTEGRITY real-time operating system can serve as an alternate board support package
- Hardware reference manuals and software user guide provided
- Software developed for the RAD6000® processor is easily ported to RAD750® computers
- All compilers currently available for the commercial PowerPC 750 microprocessor are fully compatible with the RAD750®
- Operating systems for PowerPC 750-based computers are easily ported to RAD750® computers- VXWorks and INTEGRITY operating systems available
- Virtutech offers a RAD750® simulator

Supports variable memory configurations:

- SRAM:
 - 16-MB standard
 - Options from 4 MB to 48 MB and ECC
 - Device-sparing
- SUROM:
 - 64 kB and ECC
 - EEPROM for engineering units (256 kB to 1 MB)
 - PROM for flight units (64 kB to 256 kB)
- EEPROM:
 - 4 MB and ECC

baesystems.com

Figure N1: BAE Systems RAD750 6U Extended Datasheet [93]

Specifications

Form factor	CompactPCI 6U (233 mm x 160 mm) CompactPCI 6U-220 (233mm x 220mm) Weight: 1000 to 1220 grams, varies with memory
Memory	SRAM: 4 to 48 MB EEPROM: 4 MB
Radiation-hardness	Total dose: >100 Krad (Si) SEU: 1.9 E-4 errors/card-day (90 percent W. C. GEO) varies with orbit Latchup-immune
Performance	>260 Dhrystone 2.1 MIPS at 132 MHz 4.3 SPECint95 4.6 SPECfp95 at 132 MHz
Power supply	- 5 volts ± 10 percent and 3.3 volts ± 5 percent (2.5 volts generated via onboard regulator)
Power dissipation	11 to 14 watts
Rail temperature range	-28 degrees celsius to +70 degrees celsius

RAD750 6U flexible architecture

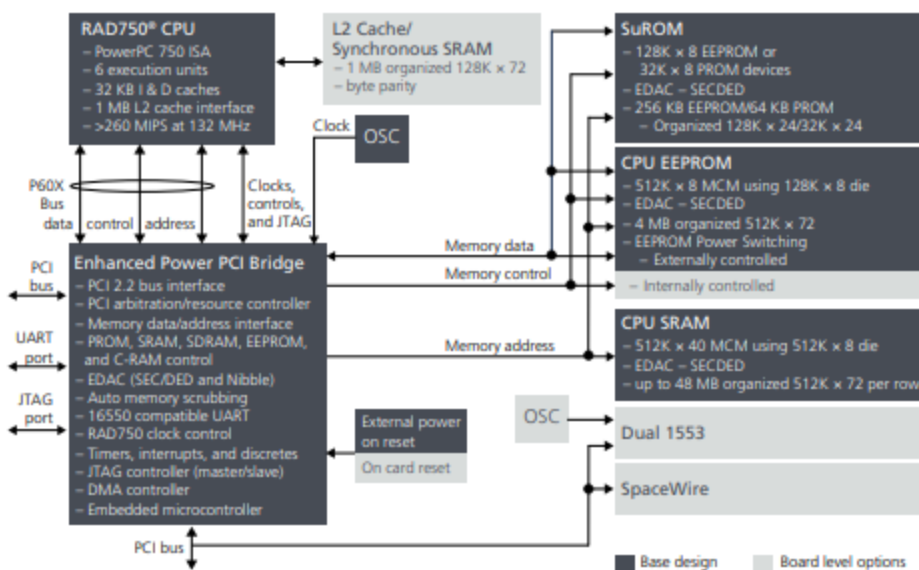


Figure N1: BAE Systems RAD750 Datasheet [93]

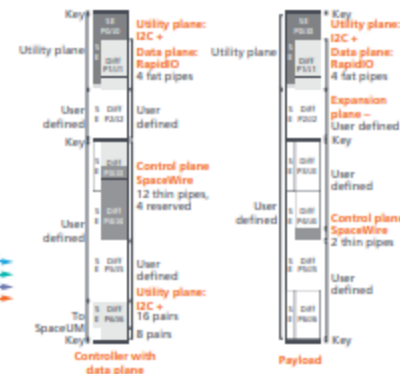
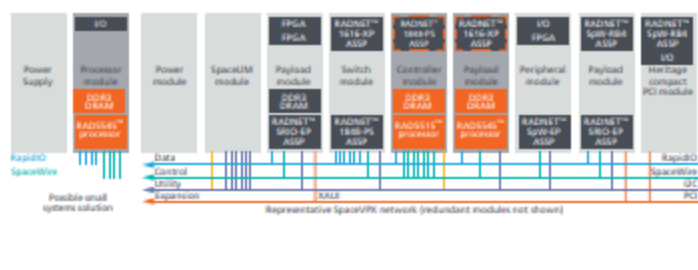
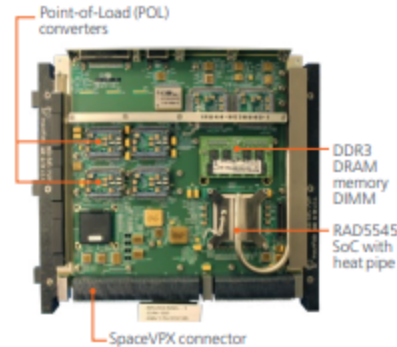
RAD5545™ SpaceVPX single-board computer

Multi-core single-board computer

The RAD5545™ SpaceVPX singleboard computer (SBC) integrates the version 1.2 RAD5545 system-on-chip (SoC) processor with volatile and non-volatile memory on a 6U-220 format module compliant to the ANSI/VITA 78.00 SpaceVPX standard.

The SBC is designed to support operation as either a payload or system controller in a SpaceVPX backplane. Based on BAE Systems' RAD5545 or RAD5515 QorIQ® Power Architecture® radiation-hardened SoC processor, the SBC offers both high performance and high I/O throughput.

It includes 4 GBytes of DDR3 SDRAM with error correction at 800 MTransfers/second and 1 GBytes of triple modular redundant non-volatile flash memory and optional 4MB MRAM. Up to four RapidIO ports at 10 Gbits/second each and 12 SpaceWire links at 320 Mbits/second each are provided to the SpaceVPX backplane. An optional daughter card with PCI, RapidIO, and/or SpaceWire interfaces can be used to personalize the SBC for unique needs.



boesystems.com

Figure N2: BAE Systems RAD5545 Space VPX Datasheet [15]

Key features and benefits

- Processor throughput of up to 5.6 giga-operations per second/3.7 giga-floating-point operations per second offers more than 10 times the performance of the fastest RAD750® processor
- Memory bandwidth of up to 51 Gb/s and I/O throughput of up to 40 Gb/s provide balance to prevent bottlenecks to or from the processor cores
- Dual in-line memory module mounting supports ease of memory replacement or upgrade
- Optional user-personalized daughter card with parallel peripheral component interconnect, RapidIO, and/or SpaceWire interfaces supports mission-specific SBC personalization
- Designed for insertion into the SpaceVPX backplane, supporting the RapidIO data plane, SpaceWire control plane, and system management inter-integrated circuit utility plane for interoperability with other SpaceVPX-compliant boards
- Multiple levels of on-die cache and high-performance DDR3 main memory all with error correction provide maximum effective throughput and reliability
- Triple modular redundant (TMR) flash memory and optional MRAM enables high-density, non-volatile storage with high reliability
- Trust architecture security infrastructure provides secure boot, integrity code testing, data encryption, and partitioning of the system to minimize the likelihood of corruption due to intentional or environmental-based intrusion
- Up to four RapidIO ports with integrated message managers support high-performance data streaming and messaging and support system architectures based on either mesh or switch-based backplanes

Specifications

SpaceVPX	Slot profiles: payload, system controller with data plane Module profiles: Payload: MOD6-PAY-4F1Q2T-12.2.1-5-22 Controller: MOD6-CON-4F12T12U-12.6.1-2-22 Mechanical size: 6U-220 Card pitch: 1.2 inches Cooling: Conduction Power profile (no daughter card) 5.0 V (+/- 10 percent): 6.7 Amps 3.3 V AUX: <1.0 Amps User-defined I/O: Differential
Temperature	Operating at -55 to 125 degrees Celsius
Radiation-hardness	Total ionizing dose: 100 Krad (Si) Single event upset: 1e-3 upsets/card-day Latchup immune
Power dissipation	35 Watts at 95 degrees Celsius and +5 percent voltage with all dissipation interfaces operational (no daughter card)
Interfaces	Up to four 4-lane RapidIO ports up to 3.125 Gbaud/lane (also supports 2.5, and 1.25 Gbaud/lane) Up to 12 SpaceWire serial links to the backplane up to 320 Mb/s each I2C and related utility plane control signals JTAG test and debug Aurora high speed trace debug
Daughter card interfaces	Up to 4 SpaceWire links One RapidIO port (the RapidIO port is mutually exclusive with the 4th RapidIO port to the backplane) 32-bit parallel PCI

Hardware block diagram

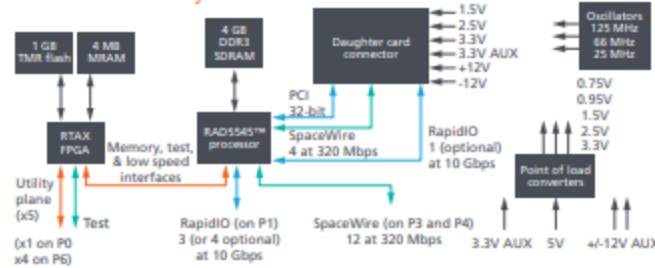


Figure N2: BAE Systems RAD5545 Space VPX Datasheet [15]

APPENDIX O: TELECOMMUNICATION

telecomms.m Script

```
%%Main script for CLP Propulsion system calculations
%Written by: Keith Beadle

%% Clear Workspace
clear all
close all

%Max transmission power
Pt = 3.16; %W
%Gain of helical antenna
Gr = 37.27*10^-5.5; %dBic
%Gain of helical antenna
Gt = 3.5; %dBic
%Transmission frequency
f = 2200*10^6; %Hz

%Distance between transmitter and receiver
%150km is assumed as an absolute maximum as the PV should remain close
%to the comet for the duration of the mission
R = 6.4*10^3; % m

%Speed of light
c = 299792458; % m/s

%Power received by PV
Pr = (Pt*Gr*Gt*(c^2)) / ((4*pi*R*f)^2); %W
%Convert power to dBm
PdBm = 10*log10(1000*Pr); %dBm

%Minimum input power for receiver
Prmin = -135; %dBm
%Convert power to Watts
Prmin = (10^(Prmin/10))/1000; %W
%Maximum transmission distance
Rmax = (((Pt*Gr*Gt*(c^2))/Prmin)^(1/2))/(4*pi*f); %m

%%
%Bozeman's constant
```

```

k = 1.38*10^-23; %J/K
%Temperature
T = 315; %K
%From transceiver datasheet
B = 8*10^3; %Hz

%Signal to noise ratio from textbook
SNR = 15;

%Channel capacity
C = B*log2(1+SNR); %bit/s

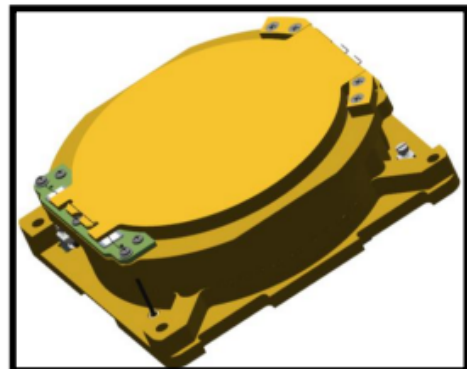
```

1. Heritage QHA

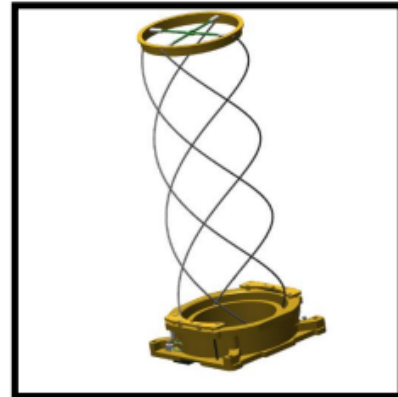
A QHA is a type of antenna consisting of 4 radiating wires wound in a helix. The filars that form the antenna are constructed from super-elastic Shape Memory Alloy materials. HCT Heritage QHA has been part of numerous projects, displaying flight heritage since December 2018.

1.1 Module Mechanical Dimensions

Mechanical Parameter	Nominal Value
Depth	~100mm
Width	~100mm
Height (400MHz Deployed)	<=270mm
Height (437MHz Deployed)	<=260mm
Height (Stowed)	<=40mm
Mass	<=180g
Thermal Knife Cord Material	50lb. test line
Housing Construction	Ultem 1000 with 18-8 stainless steel fasteners
Filar Construction	Super elastic Shape Memory Wire
Deployment Mechanism	Thermal Knife/Spring Loaded/Super-Elastic Filars
DC Connector	10-Pin Harwin Connector



STOWED



DEPLOYED

1.2 Electrical Specifications

Prior to QHA deployment, the filars are held in stowed configuration by a thermal knife retention system. During deployment, electrical power is applied to the thermal knife, heating up the resistors until severing the retention line. The deployment sensor provides an indication to an external interface that the filars have been released for deployment.

DC Electrical Parameter	Nominal Value
Voltage Input	+5VDC or +12VDC or +24VDC or +28VDC
Thermal Knife Power Dissipation	13W
TK Current (at +5VDC)	2.6A
TK Current (at +12VDC)	1.1A
TK Current (at +24VDC)	542mA
TK Current (at +28VDC)	464mA
Displacement Sensor Voltage	3VDC or 3.3VDC or 5VDC or 12VDC
Deployment Sensor Output (stowed in pull-up configuration)	< 0.8VDC
Deployment Sensor Output (stowed in pull-down configuration)	Vcc
Deployment Sensor Output (deployed in pull-up configuration)	Vcc
Deployment Sensor Output (deployed in pull-down configuration)	~0 VDC
Deployment Sensor Output (stowed in open-collector configuration)	< 100µA
Deployment Sensor Output deployed in open-collector configuration)	> 1mA
Optical Sensor Collector Input	3VDC or 3.3VDC or 5VDC or 12VDC
Thermal Knife deployment time	< 20 seconds (typical)
Deployment Sensor Current	<= 20mA (typical)

1.3 RF Specifications

RF Parameter	Nominal Value
Frequency	400 MHz or 437MHz
Gain	3.5dBi
-3dB Beamwidth	120° *Other beamwidths available
Axial Ratio	<2dB
VSWR	<1.5:1
Polarization	RHCP, LHCP
Transmit Power	10W
RF Connector	SMA (Straight/Right Angle) or SMP (Straight/Right Angle)

*If QHA desired frequency is not listed, customized QHA are available from 350 MHz to 3000 MHz. Module mechanical dimensions and RF specs may vary upon desired frequency.

Figure O1: HCT 400 or 437 MHz Heritage QHA Datasheet [105]

Table O1: Secondary Patch Antenna Decision Matrix [104, 107, 108, 109]

Metric	Weight	CST	Pulsar	ISIS	SATREV
Reliability	0.3	5	5	3	3
Bandwidth	0.3	3	2	5	3
Mass	0.2	2	2	3	5
Power	0.2	3	5	4	3
Total	1	3.4	3.5	3.8	3.4

Specification

Table 1 SSPA Specification

Parameter	Typical Value	Units
Environmental Characteristics		
Operational temperature	-20 ... +50	°C
RF Characteristics		
Frequency Range	2200-2290	MHz
Gain in boresight (centre frequency)	6.5	dBi
Half Power Beam Width	100	° (degrees)
Return Loss (across frequency range)	> 13	dB
Bandwidth:	> 100	MHz
Axial Ratio	< 3 (for +/-100 degrees)	dB
Polarization	RHCP	-
Power handling	2	W
Physical Characteristics		
Mass	< 50	g
Diameter	80	mm
Height (without connector)	5.0	mm
Connector height (straight)	8.8	mm
Interfaces		
Mechanical interfaces	4 x M2.5	-
RF connector	50Ω SMA female Orientation: straight (default), right angle (optional)	-

RF Description

Radiation Pattern

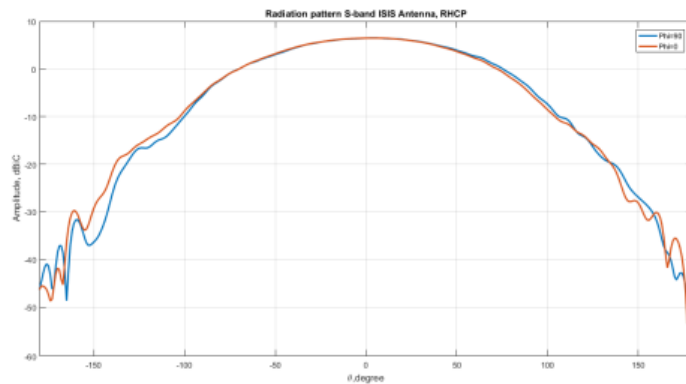


Figure 1 Typical co-polar radiation pattern at 2245 MHz

Figure O2: ISIS-QMS-TPL-0045 S-Band Patch Antenna Datasheet [108]

STC-MS03 S-Band TT&C Transceiver Technical Specifications

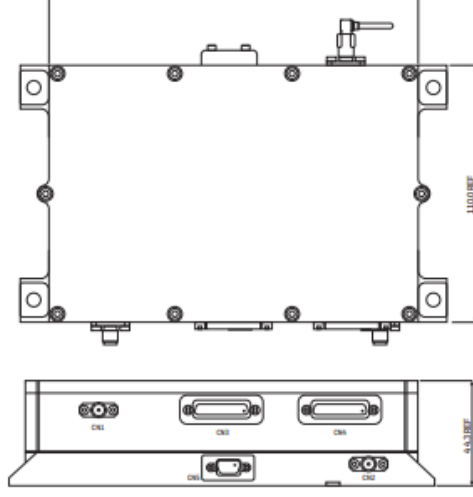
GENERAL		S-BAND TRANSMITTER			
EXPECTED LIFE	7 years	Tx FREQUENCY RANGE	2200 to 2290 MHz		
MASS	1kg (without diplexer or 1.25Kg with diplexer)	Tx POWER CONSUMPTION	Less than 14W at 34.4 dBm RF-out		
VOLUME	160 x 110 x 44mm	OUTPUT POWER RANGE	0.2 to 3.16W (23 to 35 dBm)		
DC POWER CONSUMPTION	18 W typical (Total at 34.4 dBm output power)	TM MODULATION FORMATS	QPSK, OQPSK, BPSK		
SUPPLY VOLTAGE	28V ±6 V	DATA MODULATION FORMATS	BPSK, (O)QPSK SRRC filter, NRZ/BPSK/PCM, SP-L		
DATA INTERFACES	Dual RS-422	DATA RATE	32 to 1024 kbps BPSK 1024 to 6250 kbps QPSK/OQPSK		
OPERATING TEMPERATURE RANGE	-20°C to +60°C	ENCODING	Convolutional 1/2, NRZ-M, NRZ-L, PCM		
RADIATION TOLERANCE	10 kRad				
S-BAND RECEIVER		DIMENSIONS			
Rx FREQUENCY RANGE	2025 to 2120 MHz	LENGTH	6.29" (160 mm)		
MODULATION FORMAT / DATA RATES	PCM (NRZ-L)/PSK/PM 8kHz (0.5,1,2 Kbps) & 16kHz SC (1,2,4 Kbps), PCM (NRZ-L)/BPSK (8 to 1024 kbps)	WIDTH	4.33" (110 mm)		
MODULATION INDEX TC	0.2 to 1.5 rad	HEIGHT	1.74" (44.3 mm)		
RECEIVER NOISE AND IMPLEMENTATION LOSS	2 dB typical				
RECEIVER POWER CONSUMPTION	< 4 W				
INPUT POWER RANGE	-135 to -40 dBm				
CARRIER ACQUISITION THRESHOLD	-120 dBm				
CARRIER ACQUISITION SWEEP RATE	±32 kHz/s				
CARRIER TRACKING RANGE	±150 kHz				
<p>Optional peripherals that can be supplied include:</p> <ul style="list-style-type: none"> ▪ Rx and Tx filters for separate Rx and Tx antennas ▪ Diplexer for sharing Rx/Tx Antenna ▪ Hybrids ▪ Switch ▪ RF Harness 					
Dimensions in mm					
					
					

Figure O3: STC-MS03 S-Band TT&C Transceiver Datasheet [51]

APPENDIX P: SENSOR SUITE

Channel	Microscope (M/V)	IR spectrometer (M/I)
Number of heads	1	1
IFOV	$7 \mu\text{m} \times 7 \mu\text{m}$	$40 \mu\text{m} \times 40 \mu\text{m}$
FOV	3 mm diameter	3 mm diameter
Wavelength range	525 nm, 640 nm, 880 nm	$1-4 \mu\text{m}$
Spectral sampling	3 LEDs, 20 nm each	10 nm at $4 \mu\text{m}$
Spatial sampling	$7 \mu\text{m}/\text{pix}$	$40 \mu\text{m}/\text{pix}$
Stereo imaging	No	No
Artificial illumination	LEDs	Monochromator
Illumination optics	n/a	Same as foreoptics
Focal ratio	f/20	f/3.5
Detector	1024 \times 1024 CCD	128 \times 128 HgCdTe
Operating temperature		
Detector	$\geq 170 \text{ K}$	120–140 K
Optics		150–200 K
Integration time (typ.)	0.01–1 s	$< 1 \text{ s}/\Delta\lambda$
Duration of measurement cycle (typ.)	60 s	$< 1000 \text{ s}$
No. of cycles (one per sample)	10	10
S/N	>100	>100
Dynamic range	10 bits	12 bits
Data volume (compressed)	5 Mbit/sample	$\sim 24 \text{ Mbits}/\text{spectrum.sample}$
Mass (g)	276	455
Box envelope (footpads and radiator not included)	$70 \times 50 \times 94 \text{ mm}^3$	$80 \times 50 \times 120 \text{ mm}^3$
Radiator size		$90 \times 160 \text{ mm}^2$
Power consumption (W)	~ 2.2 (heater included)	~ 8.4
Mounting position	Philae baseplate (balcony)	
Measurement period	Favoured at night	

Figure P1: Rosetta's CIVA Sensor Unit Datasheet [19]

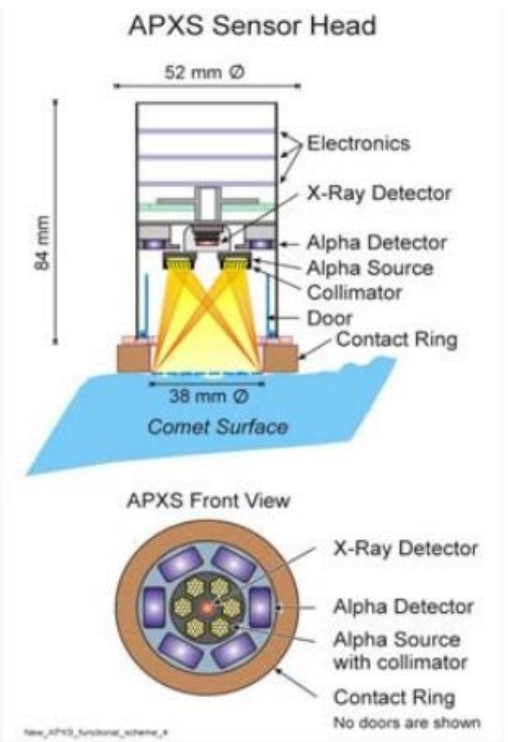


Figure P2: Rosetta's APXS Sensor Unit Datasheet [57, 110]

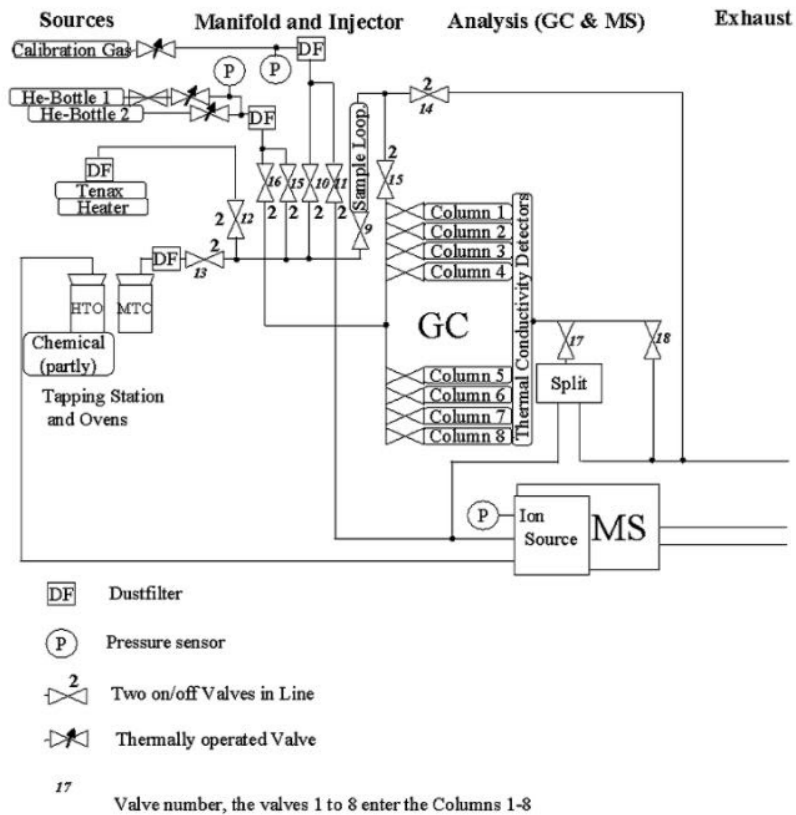


Figure P3: Rosetta's COSAC Sensor Unit Datasheet [43]

SPECIFICATION	VALUES
Mass	3 kg on Orbiter, 2.3 kg on Philae
Average power	3 W on Orbiter and on Philae
Peak power	11 W on Orbiter and on Philae
Clocks	10 MHz Sorep micro-OCXO (Oven Controlled Crystal Oscillator)
Nominal operation	$\Delta f \leq 2 \cdot 10^{-7}$
Degraded mode if offset	$2 \cdot 10^{-7} < \Delta f < 4 \cdot 10^{-7}$
Transmission	90 MHz carrier, BPSK modulation
Pseudo noise code	$255 \times 100 \text{ ns} = 25.5 \mu\text{s}$
Code repetition	Up to 200 ms
RF power	2 W/Orbiter, 0.2 W/Lander
Receiver	Band 86–94 MHz (-3 dB), linear phase
Gain range	30–90 dB with AGC
Demodulation	I and Q “synchronous” detection
ADC	8 bits 10 MHz ADC on each channel
Processing	
Real time coherent integrations	1024 code periods (26 ms, +30 dB on SNR) 256 periods (+24 dB on SNR), in degraded mode.
On-board the Lander	Code compression (+24 dB on SNR) and peak detection
Telemetry (data rate)	Orbiter: 8 kbytes/measurement point $\sim 65 \text{ Mbytes}/\text{Orbit}$ Lander: $\sim 20 \text{ Mbytes}/\text{Orbit}$ (depending on how often the complete set of data will be transmitted)

Figure P4: Rosetta’s CONCERT Sensor Unit Datasheet [47, 98]

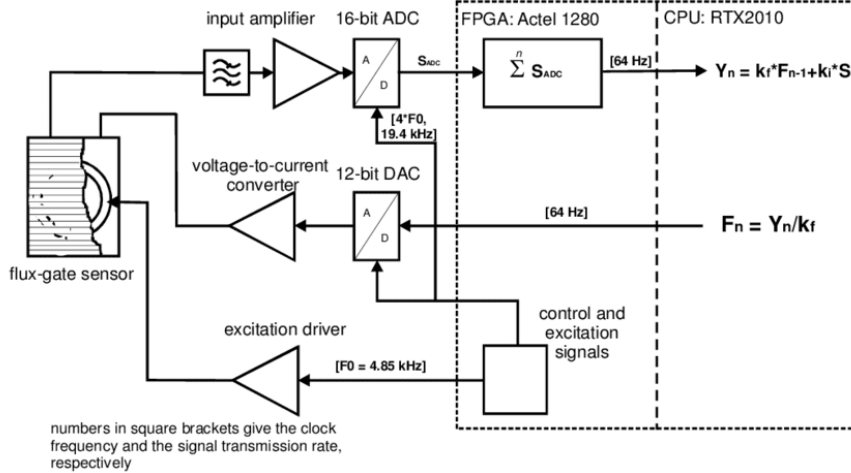


Figure P5: Rosetta’s ROMAP Sensor Unit Datasheet [62, 88]

APPENDIX Q: PRELIMINARY DESIGN REPORT

Please see the following pages for the attachment of the preliminary design review (PDR).

Hercules Lander Probe Mission

Preliminary Design Report

MANE 4250 - Space Vehicle Design
Section 2
Design Team #7

Report Submission Date: October 22nd, 2021

Prepared By:
Keith Beadle
Kevin Morrison
Joseph Scaglione
Spencer Taub
Christopher Walter
Kenny Zheng

TABLE OF CONTENTS

1 EXECUTIVE SUMMARY	1
2 INTRODUCTION	2
3 PROJECT SCOPE	2
3.1 MISSION OBJECTIVES	2
3.2 MISSION CONSTRAINTS	3
3.3 MISSION ASSUMPTIONS	3
3.4 NON-TECHNICAL CONSIDERATIONS	4
4 MISSION ARCHITECTURE	4
4.1 COMET SELECTION	4
4.2 LANDING SITE SELECTION	6
4.3 PAYLOAD OVERVIEW	6
4.4 SENSOR SUITE OVERVIEW	7
5 DESIGN APPROACH	8
5.1 STRUCTURES	8
5.1.1 SUBSYSTEM DEFINITION AND REQUIREMENTS	8
5.1.2 BENCHMARKING SELECTION	9
5.1.3 NON-TECHNICAL CONSIDERATIONS	11
5.1.4 RISK ASSESSMENT AND MITIGATION	11
5.1.5 PLAN OF PROCESSION	12
5.2 MECHANISMS, DEPLOYABLES, AND ROBOTICS	13
5.2.1 SUBSYSTEM DEFINITION AND REQUIREMENTS	13
5.2.2 BENCHMARKING SELECTION	14
5.2.3 NON-TECHNICAL CONSIDERATIONS	24
5.2.4 RISK ASSESSMENT AND MITIGATION	26
5.2.5 PLAN OF PROCESSION	26
5.3 PROPULSION	27
5.3.1 SUBSYSTEM DEFINITION AND REQUIREMENTS	27
5.3.2 BENCHMARKING SELECTION	27
5.3.3 NON-TECHNICAL CONSIDERATIONS	29
5.3.4 RISK ASSESSMENT AND MITIGATION	30
5.3.5 PLAN OF PROCESSION	30
5.4 SPACEFLIGHT MECHANICS	30
5.4.1 SUBSYSTEM DEFINITION AND REQUIREMENTS	30
5.4.2 DEPARTURE FROM PRIMARY VEHICLE	31
5.4.3 INCLINATION CHANGE AND ORBIT CAPTURE	33

5.4.4 DESCENT PATH TOWARDS COMET	34
5.4.5 LANDING	35
5.4.6 NON-TECHNICAL CONSIDERATIONS	35
5.4.7 RISK ASSESSMENT AND MITIGATION	36
5.4.8 PLAN OF PROCESSION	37
5.5 ATTITUDE DETERMINATION AND CONTROL	38
5.5.1 SUBSYSTEM DEFINITION AND REQUIREMENTS	38
5.5.2 ATTITUDE DETERMINATION METHOD	38
5.5.3 ATTITUDE CONTROL	39
5.5.4 NON-TECHNICAL CONSIDERATIONS	40
5.5.5 RISK ASSESSMENT AND MITIGATION	41
5.5.6 PLAN OF PROCESSION	41
5.6 THERMAL MANAGEMENT	41
5.6.1 SUBSYSTEM DEFINITION AND REQUIREMENTS	41
5.6.2 BACKGROUND	42
5.6.3 THERMAL ARCHITECTURE	43
5.6.4 HEAT GENERATION	44
5.6.5 HEAT TRANSMISSION	45
5.6.6 HEAT DISSIPATION	45
5.6.7 BOUNDARY LAYER	46
5.6.8 NON-TECHNICAL CONSIDERATIONS	47
5.6.10 PLAN OF PROCESSION	48
5.7 POWER AND POWER MANAGEMENT	48
5.7.1 SUBSYSTEM DEFINITION AND REQUIREMENTS	48
5.7.2 POWER GENERATION	49
5.7.3 POWER STORAGE	50
5.7.4 NON-TECHNICAL CONSIDERATIONS	51
5.7.5 RISK ASSESSMENT AND MITIGATION	52
5.7.6 PLAN OF PROCESSION	53
5.8 COMMAND AND DATA	53
5.8.1 SUBSYSTEM DEFINITION AND REQUIREMENTS	53
5.8.2 COMPUTER ARCHITECTURE	54
5.8.3 BENCHMARKING SELECTION	55
5.8.4 NON-TECHNICAL CONSIDERATIONS	57
5.8.5 RISK ASSESSMENT AND MITIGATION	57
5.8.6 PLAN OF PROCESSION	58
5.9 TELECOMMUNICATION	59
5.9.1 SUBSYSTEM DEFINITION AND REQUIREMENTS	59

5.9.2 BENCHMARKING SELECTION	59
5.9.3 NAVIGATION AND TRACKING	61
5.9.4 NON-TECHNICAL CONSIDERATIONS	62
5.9.5 RISK ASSESSMENT AND MITIGATION	62
5.9.6 PLAN OF PROCESSION	63
6 DESIGN BUDGETS	63
6.1 MASS BUDGET	63
6.2 VOLUME BUDGET	64
6.3 COST BUDGET	64
7 SALES PITCH	65
8 CONCLUSION	66
REFERENCES	67
APPENDICES	70
APPENDIX A: DEFINITION AND ASSESSMENT OF RISK	70
APPENDIX B: SUMMARY OF NON-TECHNICAL CONSIDERATIONS	71
APPENDIX C: GANTT CHART	72
APPENDIX D: ORGANIZATIONAL CHART	73
APPENDIX E: TEAM MEMBER RESPONSIBILITIES	74
APPENDIX F: TECHNICAL DOCUMENTATION	77

LIST OF FIGURES

- Figure 5.2.1: Mechanically Actuated and Foldable Solar Panel Array
- Figure 5.2.2: Radially Folding Solar Panel Array
- Figure 5.2.3: Four-Bar Telecommunications Deployment Linkage
- Figure 5.2.4: Telescoping Tower Column Mechanism
- Figure 5.2.5: Two-Claw Grabber Arm for Sample Retrieval
- Figure 5.2.6: Three-Way Rotating “Suction” Claw
- Figure 5.2.7: Soft-Body Tentacle Claw
- Figure 5.2.8: Quad-Legged Touchdown Mechanism
- Figure 5.2.9: Skates-Style Landing Platforms
- Figure 5.2.10: Spearhead Harpoon with Deployable Subsurface Anti-Release Tethers
- Figure 5.4.1: CLP Primary Descent Path
- Figure 5.5.1: Reaction Wheel and Control Moment Gyro
- Figure 5.6.1: Thermal Margin General Requirements
- Figure 5.7.1: Electrical Power Generation Technologies
- Figure F1: BAE Systems RAD750 6U Product Specifications
- Figure F2: BAE Systems RAD5545 6U Product Specifications

Figure F3: Common Specifications by Battery Chemistry

Figure F4: Specific Energy and Cycle Life for Common Battery Types

Figure C1: Gantt Chart

Figure D1: Organizational Chart

LIST OF TABLES

Table 3.4.1 Mission Non-Technical Considerations

Table 4.1.1: Team Decision Matrix for the Down-Selection of Each Proposed Comet

Table 4.2.1: Decision Matrix for Selection of Potential Landing Sites

Table 4.3.1: Overview of CLP's Functional Requirements and Associated Subsystems

Table 4.4.1: Overview of Sensor Suite with Comparable Example Sensors

Table 5.1.1: CLP Structural Shape Decision Matrix

Table 5.1.2: Material Properties for Materials of Interest

Table 5.1.3: Structures Material Selection Decision Matrix

Table 5.1.4: Structures Non-Technical Considerations

Table 5.1.5: Structures Risk Analysis and Mitigation

Table 5.2.1: Solar Panel Deployment Mechanism Decision Matrix

Table 5.2.2: Telecommunications Deployment Mechanism Decision Matrix

Table 5.2.3: Robotic Sample Retrieval Arm Decision Matrix

Table 5.2.4: CLP Landing Deployable Landing Mechanism Decision Matrix

Table 5.2.5: Physical Internal Detachment Type from PV Decision Matrix

Table 5.2.6: Pyrotechnically-Induced Separation Techniques Decision Matrix

Table 5.2.7: Pyroshock-Dampening Measures Decision Matrix

Table 5.2.8: Mechanisms & Deployables Non-Technical Considerations

Table 5.2.9: Mechanisms & Deployables Risk Analysis and Mitigation

Table 5.3.1: Propulsion System Type Decision Matrix

Table 5.3.2: Propellant Decision Matrix

Table 5.3.3: Propulsion Non-Technical Considerations

Table 5.3.4: Propulsion Risk Analysis and Mitigation

Table 5.4.1: CLP Departure Location Decision Matrix

Table 5.4.2: CLP Departure Type Decision Matrix

Table 5.4.3: CLP Orbit Capture Decision Matrix

Table 5.4.4: Spaceflight Mechanics Non-Technical Considerations

Table 5.4.5: Spaceflight Mechanics Risk Analysis and Mitigation

Table 5.5.1: Attitude Determination Sensor Decision Matrix

Table 5.5.2: Attitude Control Method Decision Matrix

Table 5.5.3: ADCS Non-Technical Considerations

Table 5.5.4: ADCS Risk Analysis and Mitigation

Table 5.6.1: Thermal Management Architecture Decision Matrix

Table 5.6.2: Heat Generation Technologies Decision Matrix

- Table 5.6.3: Heat Transmission Technologies Decision Matrix
- Table 5.6.4: Heat Dissipation Technologies Decision Matrix
- Table 5.6.5: Boundary Layer Options Decision Matrix
- Table 5.6.6: Thermal Management Non-Technical Considerations
- Table 5.6.7: Thermal Management Risk Analysis and Mitigation
- Table 5.7.1: Power Generation Decision Matrix
- Table 5.7.2: Battery Type Decision Matrix
- Table 5.7.3: Power Management Non-Technical Considerations
- Table 5.7.4: Power Management Risk Analysis and Mitigation
- Table 5.8.1: Computer Architecture Decision Matrix
- Table 5.8.2: Command and Control Board Decision Matrix
- Table 5.8.3: BAE Systems Rad750 Model Decision Matrix
- Table 5.8.4: Command and Data Non-Technical Considerations
- Table 5.8.5: Command and Data Risk Analysis and Mitigation
- Table 5.9.1: Backup Telecommunications System Decision Matrix
- Table 5.9.2: Frequency Band Decision Matrix
- Table 5.9.3: Primary Antenna Decision Matrix
- Table 5.9.4: Secondary Antenna Decision Matrix
- Table 5.9.5: Telecommunications Non-Technical Considerations
- Table 5.9.6: Telecommunications Risk Analysis and Mitigation
- Table 6.1.1: Subsystem Mass Distribution
- Table 6.3.1: Mission Cost
- Table A1: Severity/Probability Risk Assessment Matrix
- Table A2: Severity/Probability Risk Acceptance Level and Procedure
- Table B1: Non-Technical Consideration Legend
- Table B2: Non-Technical Factor Matrix for All Subsystems
- Table E1: Primary and Secondary Leads by Mission Components
- Table E2: Report Sections by Team Member
- Table E3: PDR Component Authors

LIST OF ACRONYMS

- ADCS - Attitude Determination & Control System
- BMR - Body Mounted Radiator
- CH - Cartridge Heater
- CLP - Comet Lander Probe
- CMG - Control Moment Gyros
- CPL - Capillary Pumped Loop
- DSN - Deep Space Network
- DR - Deployable Radiator
- EPH - Electric Path Heater

- ESA - European Space Agency
- FDR - Final Design Review
- FEA - Finite Element Analysis
- HF - High Frequency
- IMU - Inertial Measurement Unit
- LHP - Looped Heat Pipe
- MLI - Multi Layer Insulation
- PHP - Powered Heat Pipe
- PV - Primary Vehicle
- RHU - Radioisotope Heating Unit
- RJT - Reaction Jet Thrusters
- RTG - Radioisotope Thermal-Electric Generator
- SOI - Sphere of Influence

1 EXECUTIVE SUMMARY

The primary objective of the Hercules Lander Probe is to land on the surface of the comet 46P/Wirtanen and carry out sustained scientific experiments. These experiments seek to investigate 46P/Wirtanen's surface, subsurface, and lower atmosphere through a variety of sensors aboard the comet lander probe (CLP). This comet was chosen primarily for its short orbital period, favorable approach timeline, and notable scientific opportunities.

Design of the various subsystems is based on a number of considerations, including mass, power usage, cost, safety, and reliability. The CLP will be delivered to 46P/Wirtanen's sphere of influence (SOI) by a primary vehicle (PV), upon which it will separate using separation nuts. After detaching from the PV, the probe will perform a propulsive maneuver to enter a circular parking orbit and change its inclination plane (if necessary). A cold-gas nitrogen thruster will be used to perform all burns and any evasive maneuvers. A star tracker, sun sensor, and inertial measurement unit will be used for attitude determination and attitude will be controlled using reaction wheels. After the PV and CLP have determined an ideal landing site, the CLP will perform a retro-burn to begin the desired descent path. The CLP will then perform a final retro-burn to reduce its velocity to near zero slightly above the target landing site. A quad-legged mechanism equipped with crushable material will then be used to land on the surface of 46P/Wirtanen. Upon touching the surface, the CLP will also fire a harpoon that will tether it to the surface of the comet to prevent bouncing or relocation.

The structure of the CLP will be a hexagonal, carbon-fiber body, and the CLP will use solar arrays (deployed using a radially-folding mechanism) and Ni-MH batteries for power generation and storage. The thermal management architecture will use a radioisotope heating unit for heat generation, a powered heat pipe for heat transmission, and a body mounted radiator for heat dissipation. Multi-layer insulation will be used on the outermost layer of the spacecraft to act as a thermal boundary layer against the conditions of space. The telecommunications system will communicate with the PV using the S-band frequency on a helix antenna, with a small patch secondary antenna available as a backup as well. A vertically telescoping mechanism will also be used to raise the antenna to optimal height and range coverage conditions. The command and control subsystem of the spacecraft will use a centralized computer architecture that uses a BAE Systems RAD750 6U CompactPCI extended single-board as the primary control board with a RAD5545 Space VPX 6U single-board as the secondary control board. Upon reaching the surface of 46P/Wirtanen, a rotation suction claw will also be used to retrieve samples for scientific analysis of the surface and subsurface.

For each subsystem, special non-technical considerations were made. These included public health and safety, global, cultural, social, environmental, economic, and professional ethics considerations. Additionally, risk management was an important focus of this analysis, so special attention was paid to the root causes of system failures and the mitigation of such possibilities.

2 INTRODUCTION

Comets are the remains of the processes that formed the solar system billions of years ago. Scientifically, their compositions provide information regarding the formation of the solar system and insight as to how carbon-based molecules were first brought to Earth [43]. Though there have been multiple spacecraft missions to investigate comets, the majority of these missions have not landed on the surface of a comet. Landing on the surface of a comet will provide superior scientific data than previous orbiters as a result of the proximity and tangibility of scientific studies that can be conducted. Consequently, analyzing the physical properties and composition of both the surface and subsurface of a comet are the primary objectives of the CLP.

The short-period comet 46P/Wirtanen was discovered in 1948 by Carl A. Wirtanen [1]. With its short orbital period and close approach to the Earth, it has been a notable scientific target for multiple space missions, but it has yet to be investigated with a lander or other form of spacecraft. The next close approach to Earth that allows for sufficient time to develop, launch, and reach this comet with the CLP occurs in October, 2029 [1]. Another notable characteristic of 46P/Wirtanen is the fact that it is a “hyperactive” comet - a comet that emits more water than it should given the size of its nucleus [38].

The CLP intends to study the surface and composition of 46P/Wirtanen during its approach, landing, and subsequent ground studies while anchored to the comet. Though scientific instruments are the payload of the lander, these will be significantly limited by mass and volume limits imposed by the CLP and the PV. These scientific instruments and their use cases will be discussed in greater detail in subsequent sections.

3 PROJECT SCOPE

3.1 MISSION OBJECTIVES

Mission objectives are considered to be either scientific goals, or technical achievements that the mission hopes to accomplish. For scientific goals, this mission hopes to achieve:

- Categorization of the type of comet based on physical properties such as size and mass
- Measure the elemental, molecular, and mineralogical composition of 46P/Wirtanen’s surface and subsurface
- Drill into the subsurface and collect samples for microscopic inspection
- Analyze the lower atmosphere of the selected comet
- Determine the age of the comet and its origin

In order to achieve these scientific goals, the following technical goals will also need to be accomplished:

- Safely land the CLP on the surface of 46P/Wirtanen in a desirable target location

- Deploy solar panels to create power needed for the scientific instruments and subsystems
- Keep all systems within operational limits of temperature, stress, and pressure
- Communicate regularly with the PV to relay both telemetry data and scientific data for eventual downlink to the DSN

Secondary objectives are not necessary for the success of the mission but can increase the yield of the mission once the primary objectives are met. These objectives are as follows:

- Relocate the CLP through a series of maneuvers to sample another area on the comet.
- Dislodge a portion of 46P/Wirtanen's surface for detailed imaging and analysis by the orbiting PV
- Follow 46P/Wirtanen's path through perihelion to obtain information on how the comet's composition and properties change as it is warmed by the Sun

3.2 MISSION CONSTRAINTS

While each subsystem has defined unique constraints based on design practices, mission objectives, and non-technical considerations, the following constraints are general and apply to the mission as a whole.

- All CLP subsystems must be designed to operate in the presence of large temperature fluctuations caused by the CLP's operation in space (discussed further in section 5.6)
- The CLP will have limited power generation and power storage capacity which affect the ability to operate all CLP systems (discussed further in section 5.7)
- The CLP has a constrained mass due to types of propulsion used, the amount of fuel on board the CLP, and the magnitude of velocity changes needed to safely land on 46P/Wirtanen (discussed further in section 6.1)
- The CLP has a constrained volume budget that is dictated by the volume and propulsion capabilities of the PV (discussed further in section 6.2)
- The CLP has a constrained cost budget due to the finite value this mission will provide and the financial constraints of the customer (discussed further in section 6.3)

3.3 MISSION ASSUMPTIONS

The preliminary design outlined in this report is reliant upon several key assumptions that influence nearly every aspect of this mission. These general mission assumptions are summarized below. Some individual subsystems have been designed with additional assumptions in the absence of more detailed information.

- All preliminary analysis and design selections for this subsystem were conducted in the metric system and follow standard engineering practices followed in the United States

- This mission is set to take place in the latter half of 2029 and assumes that this time window will be sufficient to complete all steps required to design and build a mission of this nature and complexity
- This preliminary design assumes that all design selections are compatible with the PV, of which little information is currently known
- The previously mentioned PV is assumed to drop off the CLP within the SOI of 46P/Wirtanen and enter an elliptical parking orbit with a periapsis of 6 km

3.4 NON-TECHNICAL CONSIDERATIONS

While designing the overall mission architecture, the following non-technical considerations were made to ensure that the design properly considered factors that are often overlooked by technical personnel.

Table 3.4.1 Mission Non-Technical Considerations

Topic	Consideration
Public Health & Safety	All design choices have been made to mitigate risks to public health and safety, so that regardless of the mission outcome, the general public will not be harmed
Global	The discovery of new life, materials, or scientific principles has the potential to affect the global community
Cultural	N/A - There is no foreseeable impact to cultures as a result of this mission, as a result of its dissociations from cultural practices
Social	N/A - This mission is aimed at scientific discovery, and therefore has negligible impact on social aspects of communities
Environmental	Appropriate design selections have been made to mitigate the environmental risks associated with the technologies used; pollution and hazardous waste will be extremely limited; the design ensures that 46P/Wirtanen is not excessively polluted or harmed by this mission
Economic	The mission will benefit all suppliers economically by increased business; the mission will also employ and abundance of engineers and scientist creating more jobs in the economy
Professional Ethics	This mission will only be designed by engineers and scientists that are qualified to work on a project of this nature; all data and analysis conducted in this design will be presented in the most truthful manner possible

4 MISSION ARCHITECTURE

4.1 COMET SELECTION

Prior to the design of the CLP, a comet upon which scientific study would be conducted was proposed by each member of the CLP team. Many mission-critical criteria were considered, such as the feasibility of the mission, the scientific significance of the research, how well the foreseeable approaches matched up with the timeline of the CLP design, the location of the

comet at the time of desired landing, and known physical properties like gravitational attraction and terrain. The following table details the subjective analysis of each team member's findings for a comet of their choice. The following down-selection process also details the consensus the CLP team came to when assigning values to each comet.

Table 4.1.1: Team Decision Matrix for the Down-Selection of Each Proposed Comet

Metric	Weight	7P/ Pons-Winnecke	81P/ Wild	C/ 2020 K1	88P/ Howell	46P/ Wirtanen	289P/ Blanpain
Scientific Significance	0.3	3	2	5	5	5	3
Orbital Period	0.2	4	4	0	5	5	5
Time Feasibility	0.1	3	2	1	4	5	4
Terrain	0.1	2	1	2	2	4	2
Rotational Qualities	0.1	2	2	2	2	4	2
Orbital Proximity to Earth	0.1	4	2	1	3	4	4
Gravitational Attraction	0.1	4	3	2	4	2	2
Total	1	3.2	2.4	2.3	4	4.4	3.3

The comet that was ultimately decided upon from the CLP team's analysis was 46P/Wirtanen. This comet lined up favorably with the time window of this design, with a close Earth flyby in 2029 (and another in 2034 if this one was missed) [29]. It should also be noted that 46P/Wirtanen was the original target of the comet exploration mission, *Rosetta* [19]. This provided the team with confidence that the scientific research would be valuable and that the mission would be feasible, since the European Space Agency (ESA) had already planned a mission there. As is shown in the table above, though, this selection was also based on thorough research by the CLP team and was not blindly selected to poach the research and hard work of the ESA.

Now that a comet has been selected, there exists a greater understanding of the mission objectives, challenges, and constraints. With this selection in mind, the known information about this comet will be used in the following sections to design more intelligent subsystems and applications that take into account the actual conditions the CLP is likely to experience on a mission to 46P/Wirtanen.

4.2 LANDING SITE SELECTION

The next step after choosing the comet around which the mission will be centered was to select an ideal location on the surface of the comet to land at. To a large extent, the geography, terrain, and scientific interest of particular locations on the comet are unknown, so it is difficult to compare specific locations. The following decision matrix, however, is used to compare three types of general landing sites: the poles of the comet, near the equator of the comet, or making an impromptu landing decision upon reaching a parking orbit that relies on actual data taken from the PV and CLP.

Table 4.2.1: Decision Matrix for Selection of Potential Landing Sites

Metric	Weight	Poles	Equator	Impromptu Selection
Sunlight Line-of-Sight	0.25	5	3	4
Communication Windows	0.25	5	2	4
Feasibility	0.2	3	4	4
Weather/Temperature	0.2	2	3	4
Balance	0.1	3	5	5
Total	1	3.8	3.15	4.1

Several high-importance criteria are considered in this down selection process. The criterion of greatest importance is the ability of the CLP to gain effective line-of-sight to incident incoming solar rays for solar power generation. The ability of the CLP to communicate regularly with the PV is also of high importance, since this will be the only way to relay data to Earth. Additionally, physical factors such as the surface quality for balancing on the comet, and weather, temperature, and safety at each potential site are considered. Ultimately, the impromptu selection will be the most ideal approach to landing, as it will account for the most accurate and relevant data to the mission. Since the CLP will be immobile, the landing site is of tremendous importance to the success of this mission. Therefore, it is better to spend more time in a parking orbit and select an ideal landing location, than to make a mission critical decision based on the limited information that is currently available.

4.3 PAYLOAD OVERVIEW

The following section is used to provide a high-level overview of the CLP's functional requirements and the associated subsystems that achieve these objectives. These criteria detail the mission that is to be completed upon reaching 46P/Wirtanen, and the acceptable workable

conditions and ranges that the CLP will operate in. The technologies and approaches used to meet these requirements will be discussed in detail in the subsequent subsystem sections.

Table 4.3.1: Overview of CLP's Functional Requirements and Associated Subsystems [3, 23]

Functional Requirement	Associated Subsystem
An overall comet lander structure must be constructed to house the internal instruments and deployables. It must withstand predictable stresses, chemical radiation, temperature conditions, and potential debris.	Structures
The instruments, internal machinery, structure, and mechanisms must be able to function even when subjected to the extreme temperature conditions in deep space.	Thermal Management
The overall mass envelope of the comet lander must fall within the nominally proposed mass budget. This will allow the CLP to maneuver predictably on its descent to 46P/Wirtanen and limit the design complexity and cost of the PV and launch vehicle.	Mass Budget
The CLP must be deployed successfully from the PV to reach a parking orbit and land at the chosen target location. Additional maneuvers must be considered as well.	Attitude Determination & Control Systems, Spaceflight Mechanics, Propulsion Systems
The CLP must have adequate communications channels and range to communicate with the PV for adequate command, information, and radio communication.	Command & Data, Telecommunications
Deployable mechanisms and instruments must successfully deploy at the desired time after surface touchdown in order to complete the space mission.	Mechanisms, Deployables, and Robotics, Power Management

4.4 SENSOR SUITE OVERVIEW

The CLP will also feature a large array of sensors and instruments within its sensor suite. These will be integral in the scientific portion of the mission upon landing. The following table analyzes the target mission objective, as well as the type of instrument or sensor proposed to complete the desired task. In addition, an example sensor from the *Rosetta* mission aboard the *Philae* lander is used for comparison and analysis of the implemented sensors.

Table 4.4.1: Overview of Sensor Suite with Comparable Example Sensors [17]

Mission Objective	Associated Instrument/Sensor Type	Example Sensor Used on the <i>Philae Lander of the Rosetta Mission</i>
Analyze elemental, molecular and mineralogical composition of 46P/Wirtanen's surface	Microscope, spectrometer, crystal microscopy	Alpha Proton X-Ray Spectrometer (APXS)
Return information, high-resolution images, and imaging results to command station	Infrared Cameras, Resonance Imaging, Visibility Analyzer	Comet Nucleus Infrared and Visible Analyzer (CIVA), Comet Nucleus Sounding Experiment by Radio-wave Transmission (CONSERT)
Sampling surface and subsurface layers by means of drilling for soil and mineral sample collection and analysis	Motorized Drill	Sampling, Drilling, and Distribution System (SD2)

5 DESIGN APPROACH

5.1 STRUCTURES

5.1.1 SUBSYSTEM DEFINITION AND REQUIREMENTS

The structures subsystem consists of selecting a structure capable of safely carrying all major components, on either its interior or exterior, required for the mission. In addition to this requirement, an ideal structural design also accomplishes this task in an efficient manner that minimizes mass. These requirements lead to the consideration of several major design parameters, including the mass of the structure, its strength under the stresses expected during the mission, and its efficiency with regards to the volume it takes up. As the backbone for the spacecraft, these considerations can be taken for granted, as each plays a major role in the overall success of the mission.

To ensure a sufficient structural design, there are three major requirements that must be met. These requirements are as follows:

- The structure must be able to withstand all stresses that CLP will endure from launch to touchdown on 46P/Wirtanen's surface, and do so with reasonable factors of safety (proposed to be 1.2-1.5)
- The structure must be robust enough to handle the extreme environmental conditions that exist within space

- The structure must be designed to properly carry all mounted subsystems and scientific equipment

5.1.2 BENCHMARKING SELECTION

As previously discussed, some of the major points of interest when designing the structure are the total mass required for the designed structure, the ability of that structure to endure stresses that may be placed on it during the mission, and the volume that the structure will take up in proportion to the rest of the vehicle. Along with these considerations, the external space available for mounting equipment, such as solar arrays, is an important design aspect for this subsystem. The ranking and selection of these design considerations are shown below in Table 5.1.1.

These metrics, although salient, are not all equally important. Since a more massive structure does not inherently add more value to the mission, minimizing the mass is the highest priority. Furthermore, it is imperative that the structure be able to properly protect all components for the mission from failure under the highest stresses that can reasonably be expected during the mission. This structure must also be intelligently designed to fit well within the fairing that will house it, yet leave ample room for other subsystems and the scientific equipment needed to carry out the main objectives of this mission. Exterior mounting points for other subsystems is another pertinent design parameter, as it provides flexibility for the design team to add on components more freely. Finally, the cost of the structure is the last main consideration that will be evaluated in the decision matrix below. The cost of the structure can quickly become a leading expense in the design of the spacecraft due to the high costs of space-grade materials.

Table 5.1.1: CLP Structural Shape Decision Matrix

Metric	Weight	Truss	Hexagonal	Octagonal
Mass	0.4	2	5	4
Strength	0.2	5	4	4
Use of Volume	0.1	1	4	5
Mounting Points	0.1	4	4	5
Cost	0.1	2	4	3
Total	1	2.5	4	3.7

Based on this decision matrix, a hexagonal structural design will be used. As can be seen from Table 5.1.1, this selection is primarily due to its superior use of mass compared to its overall volume, as well as its strong ability to distribute stress around the structure evenly to its

edges between faces. Additionally, this design selection, although slightly worse than the octagonal shape, still maximizes the fairing volume advantageously, leaving significant room for internal subsystems and scientific equipment. Furthermore, the six faces allow for several orientations to mount exterior systems such as landing legs and solar panels. Finally, it has a favorable use of material, which allows for a reasonable cost.

Another equally pertinent design selection is the material the structure will be made with. In order to select an ideal material, a decision matrix was used, following a similar approach as the one used to decide the shape. The material properties for possible selections are shown below in Table 5.1.2 with the decision matrix for them shown in Table 5.1.3.

Table 5.1.2: Material Properties for Materials of Interest [5, 6, 7]

Metric	Aluminum 6061	Aluminum 7075	Carbon Fiber	Titanium
Tensile Yield Strength (MPa)	276	503	1230	880
Density (g/cm ³)	2.7	2.81	1.41	4.43
Cost Per Kilogram (\$/kg)	1.2	8.69	15-140	21.2
Temperature Rating	Average	Good	Poor	Great

Table 5.1.3: Structures Material Selection Decision Matrix

Metric	Weight	Aluminum 6061	Aluminum 7075	Carbon Fiber	Titanium
Tensile Yield Strength	0.3	2	3	5	4
Density	0.3	3	3	5	2
Cost Per Kilogram	0.1	5	4	2	3
Temperature Rating	0.2	3	4	2	5
Feasibility to Work With	0.1	5	5	3	3
Total	1	3.1	3.5	3.9	3.4

This matrix prioritized material strength and density properties, as these two parameters play the most major role in the success of the mission and the design of the lander. Temperature rating was the next greatest consideration, with a high level of importance due to the extreme temperature ranges the structure will experience. Finally, cost and feasibility to manufacture were also considered. Although worth examining, these two metrics carry less weight because if all other properties of the material fit the mission well, these parameters can be managed.

As is shown in the decision matrix above, a carbon fiber structure was selected as the most ideal material. This was primarily the result of its great yield strength and lightweight properties. While favorable for these properties, it should be noted that carbon fiber possesses less ideal thermal properties. However, additional materials can be used as a cover or coating to provide the carbon fiber with improved thermal properties, while maintaining its superior strength and weight for the structural design.

5.1.3 NON-TECHNICAL CONSIDERATIONS

In addition to the above technical factors, the CLP team has also considered a variety of non-technical factors for this subsystem. These non-technical considerations are outlined below and summarized in Appendix B.

Table 5.1.4: Structures Non-Technical Considerations

Topic	Consideration
Public Health & Safety	This design properly ensures that the structure will not fracture around Earth or at impact, mitigating concerns posed to the general public due to reentry.
Global	N/A - The structural subsystem does not have any significant global considerations because this subsystem is unlikely to affect any change on the global level.
Cultural	N/A - The structural subsystem does not have any significant cultural considerations because this subsystem is unlikely to affect any change on the cultural level.
Social	N/A - The structural subsystem does not have any significant social considerations because this subsystem is unlikely to affect any change on the societal level.
Environmental	Due to the possibility of the use of rare earth metals such as titanium and other materials, the sourcing of these materials must be done from companies that do their best to obtain them in the most environmentally considerable manner possible.
Economic	The materials that may be used in the design of the structure may be expensive and more difficult to source depending on the final design. With this in mind, the companies selected to obtain the materials and products from will benefit economically from this business.
Professional Ethics	The designer for this subsystem has completed courses in strength of materials and engineering dynamics, and has industry experience as a structural engineer. Furthermore, all services and statements for this subsystem will be truthful to the extent of the CLP team's knowledge.

5.1.4 RISK ASSESSMENT AND MITIGATION

With all other subsystems on the lander reliant on the structure, any failures in the structure would likely lead to the loss of the overall mission. With this in mind, the risks of such a failure have been seriously considered and plans for mitigation have been put in place. Due to the high level of understanding and modeling capabilities that are currently possessed, as well as

the ease of testing, many of the risks can be mitigated by thorough modeling, analysis, and testing. The list of risks summarized below is not intended to be exhaustive, but rather, will summarize preliminary high level risks and the mitigation plans that can be taken.

Table 5.1.5: Structures Risk Analysis and Mitigation

Risk	Cause	Mitigation
Thermal damage to carbon fiber structure	Carbon fiber's poor resistance to thermal cycling and extreme temperature highs and lows that can be experienced in space	Coat the carbon fiber material in another material better suited to handle the thermal factors experienced in space
Damage to structure during landing	Impact occurs at a faster speed than designed for	Design the structure with a higher factor of safety to allow for high stresses than predicted stresses
Cracks forming in the carbon fiber frame	Errors in the fabrication process leading to imperfections in the carbon fiber	Rigorous testing process meant to determine the location of any microcracks or other possible concerns
Fogging of sensors and solar panels	Gases escaping the carbon fiber due to outgassing	Attempt to outgas as much as possible on ground to limit the effect on mission

5.1.5 PLAN OF PROCESSION

Moving forward, there are several points of interest that must be addressed in this design. The first of these is the selection of the material that will coat the carbon fiber so that it is thermally protected from the environment. Following this, a design must be made in a modeling software that adequately provides space for internal components within the CLP, while allowing sufficient mounting points for external hardware. Once this is completed, an FEA model must be created to model the system of forces and stress the structure will experience to verify that it is able to withstand them. Following the model verification, the total volume and weight will be noted to make sure it is within an acceptable range. All of these tasks will be completed by the end of the semester and presented in the final design review (FDR).

With the limitations of time and funding, not all the work that is necessary to develop this subsystem will be able to be performed. One such example of this future work would be the construction of a scale model to verify the structural models simulated on the computer. With this model, scaled down masses for all major subsystems will be simulated on the structure to see how the entire system would perform under stresses as a whole. Once the scaled down model is sufficient, the final structure will be constructed and tested to scale and run through expected stresses on the mission. All of this is done to make sure the final structure and design will not fail in any mission critical way.

5.2 MECHANISMS, DEPLOYABLES, AND ROBOTICS

5.2.1 SUBSYSTEM DEFINITION AND REQUIREMENTS

The mechanisms, deployables, and robotics subsystem details the mechanical processes that must occur post-landing. This section will describe the dynamics, decision making, mechanical interactions, and material selection that determines the optimal setup for each deployable mechanism. The probe must have the ability to perform several key functions after completing a successful landing on 46P/Wirtanen [23].

The first deployable mechanism aims to deploy solar panel arrays that will be integral in the power generation required by the probe. This mechanism focuses on providing rigidity and orientability to the solar panel array, as maximum power generation will be necessary to achieve peak efficiency. To achieve this, the solar panel array will need to be oriented such that the panel faces are normal to the sun's incident rays as often as possible. As such, a mechanism must be devised to effectively fold out the panels and orient them such that the normal position is achieved, while properly considering the mechanical stresses that the arrays are likely to experience on a mission of this nature.

The second deployable mechanism aims to successfully deploy a selected, high frequency, long-range communication system to maintain wireless communication with the PV. The communication mechanism will focus primarily on a mechanism that will allow the chosen omni-directional radio device to reach a height that will allow it to successfully communicate with the PV. Its secondary, lower priority aim will be to rotate the radio about its primary axis in cases where the telecommunications device needs to be rotated when its omnidirectional capabilities are orientated too far off of its effective range. The communication device orientation mechanism will be compared for its dimensional demands (weight and volume), motorization accuracy, and resistance to physical and chemical wear.

The third necessary CLP deployable will be a robotic apparatus that will perform the payload's primary scientific objectives upon reaching 46P/Wirtanen. This apparatus will handle the effective detection, maneuvering, collection, analysis, and storage of desired samples, collected from the surface of the comet. This apparatus, likely similar in function to a robotic arm with interchangeable and/or rotatable end-effectors, will need to be versatile, lightweight, and resistant to bending stresses, corrosion, weather damage, and radiation. The sampling apparatus will also need to be driven by a reliable motor setup that is nimble, responsive, and extremely precise.

An additional necessary deployable mechanism will be the method by which the probe lands on the surface of 46P/Wirtanen. The probe must be able to deploy its landing mechanism in order to facilitate a safe and concise landing on the chosen surface, without fear of toppling, slipping, or collapse. A system must be devised that will accommodate different landing modes and methods, as well as the expected terrain. While it is assumed that the probe will land in a "safe" area, defined as a relatively flat or low-slope surface, with minimal changes in elevation in its immediate area of landing, it should be able to continue to use this deployed mechanism to

stay safely anchored to the surface. It should be noted that due to 46P/Wirtanen's extremely small mass and gravitational attraction, the CLP will not maneuver about the surface, but instead focus on a single ideal landing site where it will conduct all of its scientific experiments.

In addition to these mechanisms, the lander must also consider the following two processes: the method by which the CLP detaches from the PV, as well as the deployable mechanism that will allow for the CLP to secure initial physical attachment with the surface of 46P/Wirtanen [23].

5.2.2 BENCHMARKING SELECTION

The following section details the analysis used in the selection of different mechanism designs, taking into account high-priority and high-importance criteria in order to make a sound and educated selection [3].

The first mechanism examines the deployment method of the solar panel arrays. The first design, shown in Figure 5.2.1, depicts a mechanically dependent, folding mechanism that allows for the panel to be stowed parallel to the body of the CLP. When use of the panel is required, the actuating arms will motorize outwards from the body, and rotate the panel out of its stowed position, mechanically aligning it with incoming incident solar rays.

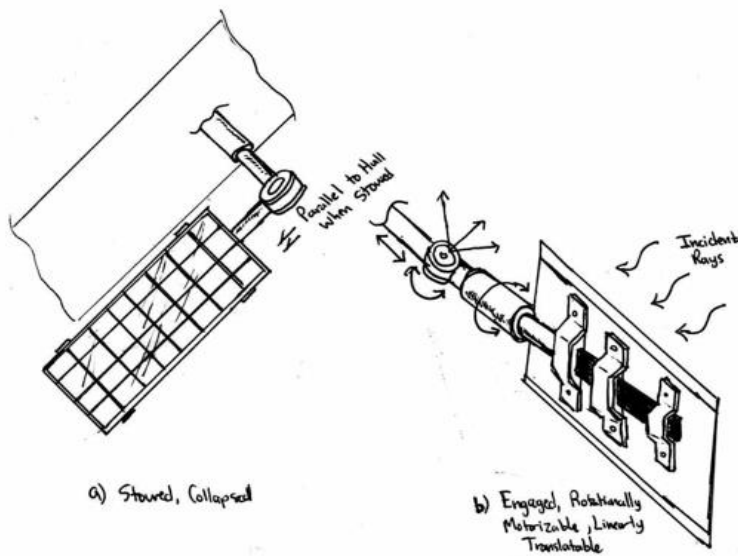


Figure 5.2.1: Mechanically Actuated and Foldable Solar Panel Array [3]

The second proposed mechanism for engaging the solar panel array, as shown in Figure 5.2.2, is a folded, radially-extending, flower pattern mechanism. In the folded state, all of the panels are aligned linearly with each other, taking only a cylindrical volume profile. Once engagement is required, the entire base will rotate towards incoming incident rays, and radially fold out. The angle at which the panels fold out can also be used to control the tightness of the cone shape to focus sunlight as needed. Optionally, another ring of interfolded, layered panels,

similar to the layers of petals on bulbous flowers, can be incorporated to increase sunlight draw, while still maintaining the cylindrical volume profile originally proposed.

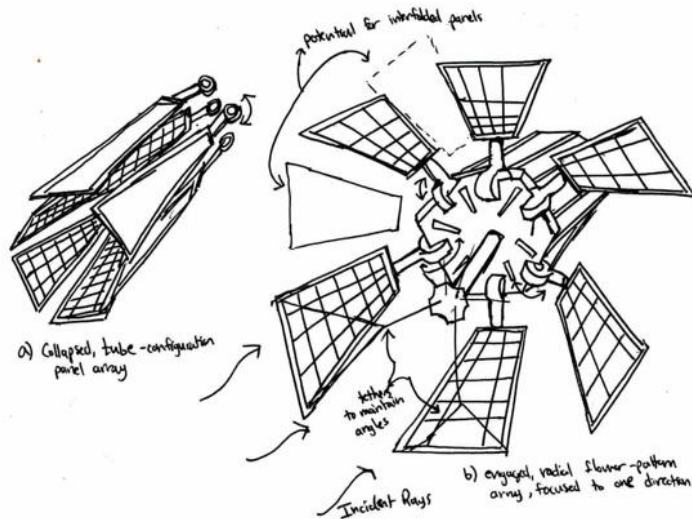


Figure 5.2.2: Radially Folding Solar Panel Array

The following table summarizes the down selection of the mechanism proposed in the use of deploying the solar panels. High-relevance and important criteria are chosen, with relative weights assigned to them.

Table 5.2.1: Solar Panel Deployment Mechanism Decision Matrix

Metric	Weight	Mechanical Actuator	Radial Fold
Rotational Orientability	0.4	4	5
Bending Rigidity	0.25	4	4
Volumetric Requirement	0.2	4	3
Ease of Use	0.1	3	4
Mass	0.05	4	3
Total	1	3.9	4.15

The second deployable mechanism aims to successfully set up the proposed radio telecommunications device. The telecommunications device should be set up such that it reaches an optimal height to effectively transmit data and information without fear of physical sources of interruption.

The first design (Figure 5.2.3) proposes a simple levered assembly that will use rotational actuation to gain elevation. A four-bar linkage is proposed in order to maintain rigid stability during the adjustment, as well as provide a stable, parallel, and level base upon which the communications device is situated.

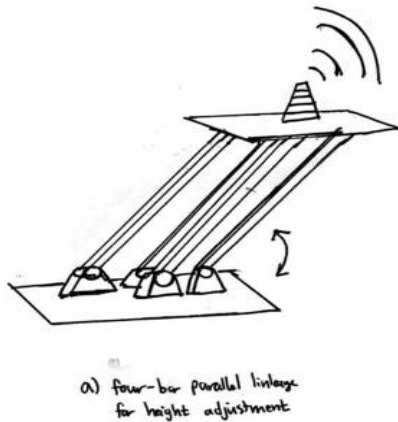


Figure 5.2.3: Four-Bar Telecommunications Deployment Linkage [23, 44]

A secondary design (Figure 5.2.4) proposed for the deployment of the telecommunications device is a simple, vertically driven telescoping beam method for the heightening of the communications device. The main focus of this mechanism discusses the overall performance of the system, but the method by which the telescoping technique is driven should also be considered, such as hydraulically driven or lead screw driven. Chemical and physical interactions of a fluid used in hydraulics with the atmosphere of 46P/Wirtanen will be considered.



Figure 5.2.4: Telescoping Tower Column Mechanism

The following table describes the down selection process for the deployment mechanism of the telecommunications system. Once again, relative weights are assigned to each high-importance criteria in order to make an informed decision. Because height adjustment has been

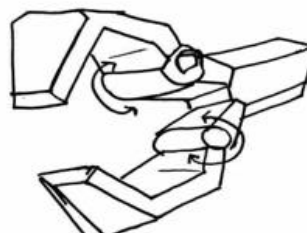
deemed of greater importance for effective ranged communication over rotational adjustability, the telescoping column is the more effective selection in this proposed deployable.

Table 5.2.2: Telecommunications Deployment Mechanism Decision Matrix

Metric	Weight	4-Bar Linkage	Telescoping Column
Bending Rigidity	0.4	4	3
Volumetric Requirement	0.25	2	5
Ease of Use	0.15	3	5
Height Adjustability	0.1	3	5
Rotational Adjustability	0.05	3	4
Chemical Interaction	0.05	2	4
Total	1	3.1	4.1

The third deployable mechanism is a manipulable robotic appendage that will interact with the surface of 46P/Wirtanen to carry out the payload objectives for scientific study. Three potential mechanisms are proposed for this task. These mechanisms focus on the end effector method for picking up a desired object, but further analysis will be conducted for the mechanical manipulation and rotation of the arm to achieve the desired position.

The first proposed design is similar to many older robotic end effector designs for picking up desired objects. This consists of two claws hinged and motorized to close around the desired object. This design is relatively simple, relying on clamping and squeezing force to maintain stability around the object, for retrieval to the CLP.



a) simple 2-grip ^{claw} grabber

Figure 5.2.5: Two-Claw Grabber Arm for Sample Retrieval

The second proposed design consists of a three-prong assembly. Similar to the previous two-claw design, this mechanism relies on a trapping, clamping force to maintain stability on the

object. However, rather than using simple hinged motor actuation, this method uses a technique similar to multiple conveyor belts aligned in a circular pattern, all rotating towards a central point to draw an object in. Therefore, using rotational actuation only, each of the three arched prongs will simultaneously rotate inwards, using three gripping methods on each. The first gripper is a soft, malleable block that will initiate contact with the object, exerting frictional force for first alignment, and then engaging the second set of small hooks to draw the midbody of the object in. Finally, the large claw on the outer edges of the arches will close around the remainder of the object, securing it in place. Rather than estimating the angle of approach and site of closure from the previous design in Figure 5.2.5, this design only needs to be approximately close to the desired object, allowing a mechanical “suction” technique to self-align the object, and draw it in.

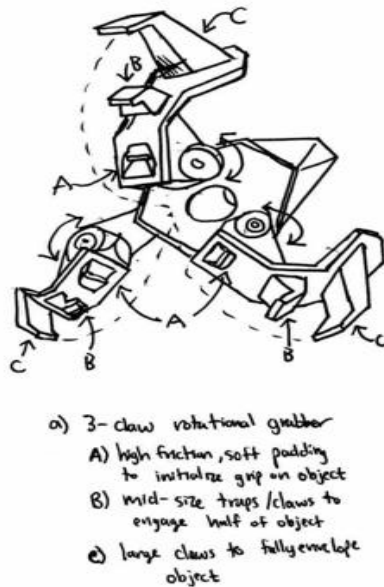


Figure 5.2.6: Three-Way Rotating “Suction” Claw

The final proposed mechanism for a mechanical appendage is inspired by a biologically based mechanism. This mechanism, often considered a “soft-body robot”, is based on the biological mechanism of an octopus tentacle, retracting and extending as necessary, actuated by a muscle contraction analogy: induced pressurization. Pressurizing the inside of the soft body will cause the arm to curl in a predetermined method, latching onto an object within its circular range of motion. In the following design, this manipulator used three of these arms to more successfully capture the desired object. Rather than conforming perfectly to the geometry of the desired object, these arms take advantage of their soft-body design to conform around the other geometry of the object, allowing for much more lenient approximation of the object’s location.

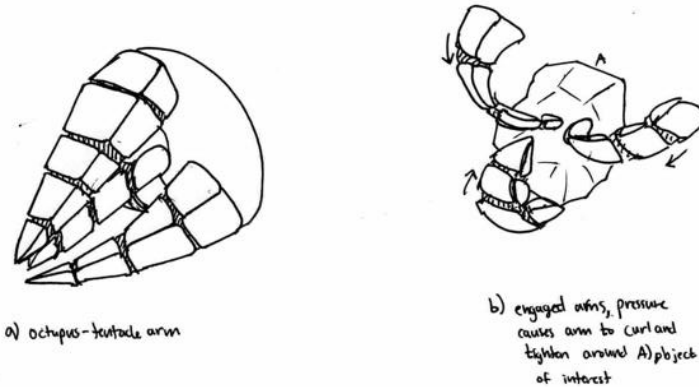


Figure 5.2.7: Soft-Body Tentacle Claw [37]

The following table details the down selection of the three proposed robotic manipulator designs. Precision and holding strength are the most heavily weighted considered metrics, due to their relevance in the functionality of this mechanism.

Table 5.2.3: Robotic Sample Retrieval Arm Decision Matrix

Metric	Weight	Two-Claw Grabber	Rotational Suction Claws	Soft-Body Tentacle
Required Precision	0.3	2	4	4
Holding Strength	0.2	2	4	3
Ease of Use	0.15	3	5	5
Durability	0.15	3	4	3
Complexity of Design	0.15	4	3	2
Versatility of Use	0.05	2	3	3
Total	1	2.6	3.95	3.45

The fourth deployable mechanism involves the touchdown and landing of the CLP on the 46P/Wirtanen's surface. The first of two mechanisms proposed is an independently extendable quad-leg touchdown. Each of its four legs can independently fold out from under the CLP, supported by secondary arches. Each leg can independently extend, allowing it to conform to terrains with high roughness and elevation changes. This type of landing mechanism is utilized in many space expedition probes.

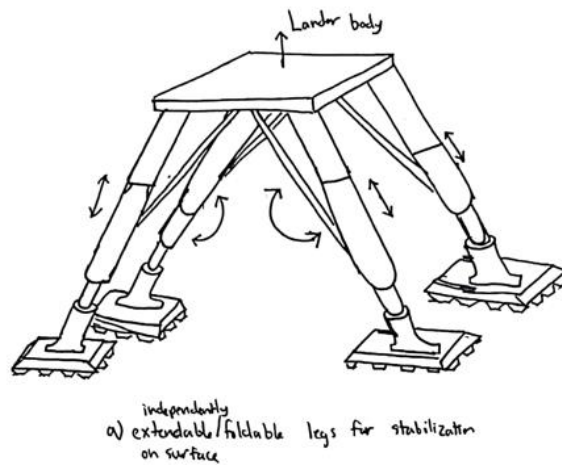


Figure 5.2.8: Quad-Legged Touchdown Mechanism

The second proposed method by which the CLP lands and maintains stability on the surface of 46P/Wirtanen is by a skates-style platform, which ensures high contact-area with the ground and greater stability than the quad-legged mechanism if the terrain is relatively flat.

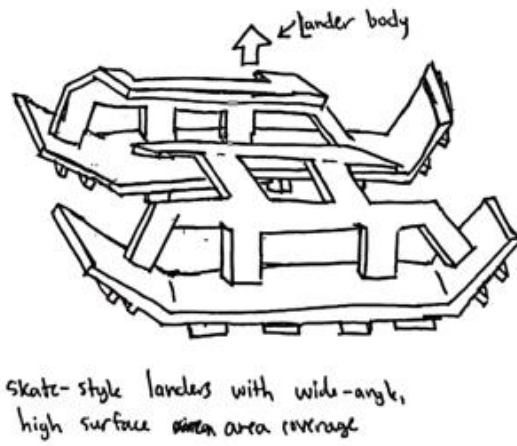


Figure 5.2.9: Skates-Style Landing Platforms

Each of these two mechanisms is analyzed for predicted performance and quantified for higher-level importance in the following decision matrix. In addition to the overall structure of the landing mechanism, it is proposed that a crushable material, in an aluminum honeycomb style, is incorporated as an end-of-flight cushioning material. This single-use, light, compact material will effectively cushion the initial impact with the comet surface and subsequent bounces, allowing for the safe deployment of the landing mechanism.

Table 5.2.4: CLP Landing Deployable Landing Mechanism Decision Matrix

Metric	Weight	Quad-Leg Touchdown	Skates-Style Lander
Stability	0.3	4	3
Ease of Deployment	0.3	3	3
Volumetric Constraint	0.15	4	3
Traction	0.1	4	4
Terrain Conformability	0.1	5	2
Independency	0.05	5	3
Total	1	3.85	3

In addition to these primary mechanisms and deployables, a single-use, end-of-flight method of attaching to the surface of the comet upon first approach is required. This will allow for the probe to remain tethered to the surface of 46P/Wirtanen despite its small gravitational attraction. Proposed is a harpoon design that is meant to be aimed and fired at the surface of 46P/Wirtanen. These harpoons will penetrate the surface with a sharpened point and deploying anti-release fins underneath the surface to mitigate untethering.

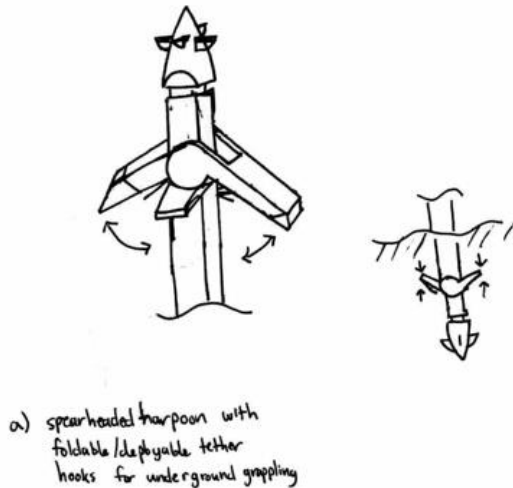


Figure 5.2.10: Spearhead Harpoon with Deployable Subsurface Anti-Release Tethers [2]

Lastly, a proposal is set forth for the PV team regarding the successful containment of the CLP within the body of the PV. Upon reaching 46P/Wirtanen, the probe will need to dynamically separate from the PV to initiate its parking orbit maneuvers. As such, several stages

must be analyzed. Firstly, the attachment method by which the CLP remains secured to the inside of the PV while the PV is traveling through deep space is proposed.

Using a down selection design matrix, the type of attachment and detachment method is determined, choosing between a mechanical, non-destructive type of attachment and release, or a pyrotechnically induced, high-energy type of attachment and release.

Table 5.2.5: Physical Internal Detachment Type from PV Decision Matrix [40, 45]

Metric	Weight	Mechanical Actuation	Pyrotechnical Release
Safety	0.35	4	3
Shock	0.25	4	3
Accuracy	0.2	3	5
Ease of Actuation	0.1	2	5
Speed of Detachment	0.05	2	5
Reliability	0.05	3	4
Total	1	3.45	3.75

This decision focuses on the relative safety of each detachment type, assuming proper handling. However, the speed and accuracy of detachment is also of great importance. A mechanical means of detachment is overall very safe, but loses out in terms of speed, which is integral in detaching at exactly when desired. Pyrotechnically induced detachments are decidedly more accurate and quicker in a controlled environment, where the detonation is highly controlled and damped as necessary. Having chosen a pyrotechnic technique for the detachment of the CLP from within PV, the following attachment and detachment mechanisms are proposed.

The first of three potential internal attachment methods is a series of pyrotechnic actuators, or exploding bolts. The external chassis will be bolted to the inside of the PV at many different locations, ensuring stability and stillness while traveling through space [32]. The bolts will have typical external threading, while also threading onto a standard internal-thread lug or nut at each location a bolt is deemed necessary. However, each bolt will have an internal charge, composed by a mix of combustible powders, that will be detonated on command.

The second internal attachment method is by use of separation nuts, or “sep-nuts”. While all methods proposed are pyrotechnically driven processes, the separation nuts excel at keeping a load rigid and locked in place while in transit [31]. When the detachment event occurs, the separation nuts are activated via electrical impulse, and provide a highly controlled pyrotechnical charge within its chambers to separate.

The final internal attachment method proposed is known as a pyrotechnic pin-puller. A pin within the cylindrical volume profile of the pyrotechnic device is actuated, releasing an explosive charge. However, this technique excels in the speedy deployment of rods, cables, booms, and mechanisms, by means of quick, pyrotechnically enhanced lateral movement [33].

Evaluating each of the three pyrotechnic attach-and-release options, a final choice is made that considers the primary functions, speed, and ability to contain the explosion in the following decision matrix.

Table 5.2.6: Pyrotechnically-Induced Separation Techniques Decision Matrix [31, 32, 33]

Metric	Weight	Pyrotechnic Actuator (Exploding Bolts)	Separation Nut (Sep-Nuts)	Pyrotechnic Pin Puller
Safety	0.35	3	5	3
Shock Containment	0.25	3	4	4
Accuracy	0.2	3	4	4
Ease of Activation	0.1	2	5	3
Volumetric Constraint	0.05	5	5	5
Reliability	0.05	2	4	3
Total	1	2.95	4.5	3.55

In addition to the detachment mechanisms proposed, a dampening structure is also needed to soften, absorb, and control the shock of the pyrotechnic devices. The following down selection of three potential methods will be proposed to the PV team.

The first shock-dampening technique proposes the use of sacrificial material, called structural shims. These shims, composed of sheets of metal fastened between the interface of structural members, allow for extreme dampening of pyroshocks, protecting from internal damage to the PV, as well as the external chassis of the CLP [3]. These standalone shims will be fastened to each connection occurring between internals of the PV and the external chassis of the CLP, allowing for modularity and simple changes in required shims per connection location.

The second dampening method proposed is the use of mechanically actuated shock mounts, in which long cylindrical structures, similar to the spring damped shocks used in the suspensions of motor vehicles, are fastened in tandem with the pyrotechnic device, allowing for

physical obstruction of shaking and vibration upon initial detonation. This technique will allow for stability of the CLP within the PV, but requires external mechanical bonds to secure [42].

A final technique for absorbing pyroshocks is to use a system identical to the previously discussed crushable material used in the cushioning of the initial landing of the CLP. This sacrificial material, used in close proximity of the pyrotechnic devices, will be greatly damaged in place of other important components, accepting and diverting high energy outputs along its proposed large surface area [23]. This simple-to-integrate, single-use, and end-of-flight means of absorbing pyroshock is ideal when considering ease of access, and cost.

The following decision matrix down-selects the proposed shock-dampening measures described, prioritizing safety and shock containment above all else.

Table 5.2.7: Pyroshock-Dampening Measures Decision Matrix [42]

Metric	Weight	Structural Shims	Shock Mounts	Crushable Material
Shock Containment	0.4	3	4	4
Reliability	0.25	4	3	5
Volumetric Constraint	0.2	3	2	5
Autonomy	0.05	3	2	2
End-of-Life Use	0.05	3	3	4
Waste Produced	0.05	4	3	4
Total	1	3.3	3.15	4.35

These pyrotechnical attachment and detachment mechanisms are set forth by the CLP team for the PV team to consider. Because this is a system influenced primarily by the PV team, the proposals set forth are primarily informative and aim to propose a potential method of effective attachment, detachment, and containment, but is subject to change based on the decisions determined by the PV team.

5.2.3 NON-TECHNICAL CONSIDERATIONS

In addition to the technical designs and considerations performed within the down selection processes, the following non-technical considerations were put forth for the general acknowledgment of the public.

Table 5.2.8: Mechanisms & Deployables Non-Technical Considerations [3]

Topic	Consideration
Public Health & Safety	The deployable mechanisms subsystem is unlikely to directly impact public health and safety in any physical way, especially as the mechanics used will be maintained on a separate celestial body that is completely isolated from Earth. Nonetheless, the deployables and mechanisms used in deep space will be considered for their effectiveness and robustness and can potentially be integrated to mechanisms on Earth for the future safe handling and analysis of foreign matter.
Global	Because many space missions are aimed towards the collection of typical matter, such as gases, soils, rocks, and surface debris, a successful (and ideally) universal design for obtaining such samples can lead to a worldwide adoption of this optimized technology. Therefore, a simple, yet universally effective design will greatly impact the mode of collection of samples in future space expeditions.
Cultural	N/A - The mechanisms and deployables subsystems are unlikely to have any significant cultural considerations because this work does not significantly affect the typical aspects of cultural life.
Social	N/A - The mechanisms and deployables subsystem is not likely to have any significant cultural considerations because its focus does not significantly integrate into the typical aspects of social situations.
Environmental	The electrical energy required to drive and operate the sensors and motors needed for effective articulation on a deployable is often cleanly harvested and used. Therefore, there is little impact on the environment from mechanisms and deployables. It is important, however, to note that the surrounding environment should be minimally impacted by the deployables by leaving minimal physical waste, debris, and byproducts behind, as well as leaving the terrain minimally disturbed. This is best practice and sets a standard and expectation that future expeditions should respect this etiquette.
Economics	The mechanisms and deployables subsystem requires the efficient use of materials and energy. As the mechanisms deployed are often the most intimately acquainted with the end goal of the expedition (such as the interfacing of a mechanical arm with the surrounding soil), a large portion of the available capital will likely be spent on perfecting the stable and reliable deployment and performance of the desired mechanisms.
Professional Ethics	The lead conceptual designer for the mechanisms and deployables has harbored a passion for robotically manipulable and articulable mechanisms, and completed relevant courses and studies in the area of robotics and elements of mechanical design. Therefore, a strong understanding and effort will be invested in the analysis of ideal integration and mechanical design techniques. All services and statements will be reviewed extensively and approved by the secondary lead for this subsystem as well.

5.2.4 RISK ASSESSMENT AND MITIGATION

Assuming a successful deployment and landing of the CLP, the next step would be the deployment of the mechanisms described in the previous section. If mechanisms were to fail, the entire success of the mission would be in jeopardy. Therefore, potential failure scenarios and risks are considered in the following table, which analyzes the type of failure, the reason for the failure, and potential mitigation and backup methods for correcting the failure.

Table 5.2.9: Mechanisms & Deployables Risk Analysis and Mitigation

Risk	Cause	Mitigation
Failure of solar panel arrays to maintain spread angle	Mechanical failure due to bending stresses	Extensive prior testing, taking into account local gravity; engage central column tether to maintain a solid angle spread
Failure of telescoping pole to fully extend	Mechanical failure due to bending stresses, or motor binding/misalignment	Extensive prior testing; motor syncing/condensation
Inability of robotic arm to grasp desired object	Insufficient grip, range of mobility	Utilize higher friction grips; determine maximum enclosure envelope beforehand
Harpoon fails to attach	Failure to penetrate surface, engage anti-release fins	Use different levels of launch power to break the surface; integrate a retraction system
Crushable materials fail to fully cushion pyroshock	Not enough material, material is not dense enough	Store excess material due to end-of-travel expectation; extensive testing beforehand for the case of maximum impact energy
Pyrotechnics fail to deploy successfully	Pyrotechnics are prematurely triggered; detonation is too strong/weak	Ensure backup explosives and proper cushioning for extra detonations
Landing legs are not stable	Unsynchronized deployment, electrical/mechanical failure	Extensive testing prior to deployment; each of four legs are deployed independently to different lengths to conform to surface

5.2.5 PLAN OF PROCESSION

Future work for the mechanisms, deployables, and robotics subsystem includes determining appropriate locations to place the mechanisms and creating detailed depictions of the articulation movements. Several materials will also be compared on the basis of performance, strength, cost, manufacturability, thermal properties, and other factors to select appropriate materials for each mechanism. For mission critical mechanisms, such as the solar array arms, a finite element model, CAD models, and engineering dynamics analysis will be detailed in order to validate the current design.

Although enough time cannot be allotted within the duration of a single semester, it is noted that in an ideal situation, all mechanisms proposed would be prototyped, iteratively

improved, and would be tested vigorously with hardware and simulated physical conditions as well, to validate the previously proposed analyses.

5.3 PROPULSION

5.3.1 SUBSYSTEM DEFINITION AND REQUIREMENTS

The propulsion subsystem encompasses all system functions that require the application of an external force to the spacecraft. This includes thrusters and ignition sources. The primary focus of the propulsion system for the CLP is orbital adjustments, guided descent, and landing.

The propulsion system must execute four primary maneuvers for a successful landing. Injection into a parking orbit, entrance onto a desired descent path, execution of evasive maneuvers, and a final burn immediately before landing. The requirements for the propulsion system are outlined below.

- Burn to enter a desirable parking orbit for landing, including any inclination changes
- Perform a retroburn to place the CLP on a favorable descent path
- Execute evasive maneuvers in the event of unforeseen hazards
- Perform a retroburn immediately prior to landing to bring the CLP to a near zero-velocity in order to prevent bouncing and damage to the spacecraft

5.3.2 BENCHMARKING SELECTION

The different types of propulsion systems were considered in Table 5.3.1. As the CLP is delivered to the comet by the PV, the primary concern of the propulsion system is minimizing mass while still being capable of landing. In this same vein, it was desirable to minimize the amount of infrastructure to reduce mass, volume, and complexity. Propellant stability was also of importance, as the CLP will likely be in orbital transit for several years. The spacecraft also needs the ability to throttle in order to provide controlled descent and execute precise maneuvers in a low gravity environment. Specific impulse and thrust are primary concerns in many missions, however due to the small impulse of maneuvers and extremely low gravity of the comet, these were not of large concern for the CLP. Novel technologies such as solar sails and nuclear propulsion were not considered in order to minimize risk.

Table 5.3.1: Propulsion System Type Decision Matrix [3, 12]

Metric	Weight	Electrical	Cold-Gas	Mono-Propellant	Bi-Propellant	Dual-Mode	Solid
Mass	0.3	2	5	4	2	2	3
Infrastructure	0.2	2	5	3	2	1	4
Stability	0.2	3	4	4	2	3	5
Throttling	0.2	5	3	5	4	4	1
Specific Impulse	0.1	5	1	3	4	4	3
Total	1	3.1	4	3.9	2.6	2.6	3.2

Based on the weighted parameters, the cold-gas propulsion system was selected. While cold-gas systems have very low specific impulse, the primary advantages of cold-gas propulsion are its low mass and infrastructure requirements. These align closely with the mission requirements outlined above. Cold-gas also offered high stability and a moderate throttling capability.

The various propellant types were considered in Table 5.3.2. Mass was again of important consideration due to the nature of the CLP as an attachment to the primary vehicle. It should be noted that mass encompasses general tank design and volume. Specifically, hydrogen scored lower in this category due to these considerations. Furthermore, additional infrastructure is required for butane and carbon dioxide, as a heater is required in order to expel the propellant in a gaseous phase. Propellant stability was also of prime importance due to the potential for a long mission duration. Hydrogen again scored low due to the likelihood of propellant leaks. Handling considerations were made to minimize hazards and environmental impact. The liquid nature of the butane and carbon dioxide is an advantage in terms of mass, but can cause complications due to sloshing. Specific impulse was again of little importance due to the low delta-V requirements of maneuvers.

Table 5.3.2: Propellant Decision Matrix [3, 41]

Metric	Weight	Butane	Nitrogen	Carbon Dioxide	Hydrogen
Mass	0.3	4	4	4	3
Stability	0.2	4	5	4	3
Handling	0.2	3	5	4	3
Phase	0.2	3	5	3	5
Specific Impulse	0.1	2	3	3	5
Total	1	3.4	4.5	3.7	3.6

Nitrogen was selected as the propellant type. Nitrogen offers a high storage density without the need for additional infrastructure. Additionally, it has contamination free characteristics, high reliability, and is stored in a gaseous phase. Specific impulse is moderate, but is again not of high importance. As a result of these advantages, nitrogen was selected as the most favorable propellant type.

5.3.3 NON-TECHNICAL CONSIDERATIONS

A variety of non-technical considerations were made for the propulsion subsystem. These considerations are outlined below in Table 5.3.3 and summarized in Appendix B.

Table 5.3.3: Propulsion Non-Technical Considerations

Topic	Consideration
Public Health & Safety	Certain propellants are extremely toxic. Propellant selection ensures that a hazardous material is not used needlessly and risks endangering the public during testing, assembly, or launch are limited.
Global	N/A - The propellant subsystem does not have any significant global considerations because this subsystem is unlikely to affect any change on the global level.
Cultural	N/A - The propellant subsystem does not have any significant cultural considerations because this subsystem is unlikely to affect any change on the cultural level.
Social	N/A - The propellant subsystem does not have any significant social considerations because this subsystem is unlikely to affect any change on the societal level.
Environmental	Certain propellants can have extremely adverse effects on the environment. Limited propellants, such as Freon-12, were excluded due to these considerations.
Economic	N/A - The propellant subsystem is subject to the requirements of the spaceflight mechanics team and unlikely to have significant economic impact due to the low impulse of maneuvers and use of proven technologies.
Professional Ethics	All selections and considerations are based on the full knowledge of the engineers on the team and reviewed closely by a secondary lead.

5.3.4 RISK ASSESSMENT AND MITIGATION

The propulsion subsystem is of utmost importance for the success of the mission. The primary thruster for the CLP is used to execute maneuvers and guide the descent. Any significant failure would be catastrophic and result in the loss of the mission. As a result, risk consideration and mitigation is of prime importance. These considerations are non-exhaustive and require deeper assessment once more parameters are defined, such as the feed system and tank design.

Table 5.3.4: Propulsion Risk Analysis and Mitigation

Risk	Cause	Mitigation
Leakage of propellant	Imperfections in tank construction and valves. It is not possible to create a perfectly sealed system with valves.	Robust tank design. Wax seals over the gas reservoir. Gas selected is larger molecular and less prone to leakage as a result.
Rapid loss of propellant	Direct damage to the propellant tanks due to impact.	Impact-resistant tank design.
Failure to puncture seal or operate valve	Faulty constructions, exposure to solar radiation and extreme temperatures over an extensive time period.	Extensive testing and research into previous missions.
Contamination of surface	Many propellants are toxic.	The ultimate propellant selected is non-toxic and released in small volumes.

5.3.5 PLAN OF PROCESSION

Several other parameters must be defined in the near future. The propellant feed system for a cold-gas system is simple, but will be outlined in detail in the FDR. Material selection and sizing for the propellant tanks will also be defined. Furthermore, several aspects of this design will be driven by the mass budget and delta-V requirements defined by the spaceflight mechanics subsystem. At the moment, it has not been determined if a proper nozzle design for the mission requirements is available, or if a higher-level preliminary analysis will need to be performed.

Later evaluations must include extensive testing and a high-level analysis of all components within this system. Propulsion is a critical subsystem with extensive complexities, so ground testing and verification would be essential.

5.4 SPACEFLIGHT MECHANICS

5.4.1 SUBSYSTEM DEFINITION AND REQUIREMENTS

The spaceflight mechanics subsystem involves the planning and modeling of maneuvers to ensure the CLP lands at the desired target location on the surface of 46P/Wirtanen in a safe and efficient manner. This subsystem will entail a highly designed ideal descent path, but also must account for inefficiencies or deviations to ensure the CLP has enough propellant and resources to land safely on the surface through a variety of descent paths. The requirements of this subsystem are stringent because they dictate the difference between a probable mission

success and a catastrophic mission failure. Furthermore, these requirements influence many aspects of the other subsystems, in particular the type and amount of propellant used by the propulsion subsystem, and the overall mass budget available to all physical subsystems.

The spaceflight mechanics portion of the CLP mission can be divided into four main components: departure from the primary vehicle, inclination change & orbit capture, descent towards the surface, and landing. The nature of these four phases will vary widely based on the chosen orbital capture, the initial location, and the type of departure from the PV. The same fundamental requirements, however, will govern these four phases regardless of the scenarios that are chosen. These requirements are listed concisely below.

- Identify several viable descent paths that will allow the CLP to safely soft-land on the surface of 46P/Wirtanen at the target location
- Determine the necessary inclination plane and parking orbit needed to reach the target landing sight and the propulsive maneuver(s) associated with this orbit
- Perform a maneuver that places the CLP on a favorable descent path
- Model appropriate evasive maneuvers in the presence of unforeseen debris, micrometeorites, ice plumes, or other objects
- Quantify a retroburn above the surface of 46P/Wirtanen to reduce the velocity to nearly zero, so that the CLP can impact the surface at a safe velocity
- Soft land on the surface of the comet in a defined target region while minimizing the required delta-V
- Ensure that the total time of descent is acceptable for all other mission objectives

5.4.2 DEPARTURE FROM PRIMARY VEHICLE

Until this point in the mission, the CLP has been completely at the will of the PV. The nature of this departure is still largely in the hands of the PV team, but it will have dramatic effects on the complexity of the orbital capture and descent of the CLP, so several different viable options have been benchmarked for the purpose of communicating ideal conditions to the PV design team.

The first major decision that governs the departure of the CLP from the PV is the relative distance between 46P/Wirtanen and the CLP when it departs from the PV. If the CLP departs while within the SOI, the descent is primarily governed by two-body mechanics between the CLP and 46P/Wirtanen. This will greatly reduce the propellant needed, general complexity, and time of the descent. However, if the departure takes place when the comet is approximately 230×10^6 km (semimajor axis of Mars orbit) from the Sun, 46P/Wirtanen's SOI is only about 5.5 km above its surface, which may be uncomfortably close for the PV's orbital capture [14]. Although the mass of 46P/Wirtanen is unknown, it was estimated by assuming a spherical geometry with a diameter of 1.2 km and the same density as the comet 67P/Churyumov-Gerasimenko [1, 29]. This analysis yielded an approximate mass of 2.328×10^{11} kg, which was

used to estimate the SOI. Ultimately, this will be a decision that is left to the discretion of the PV spaceflight mechanics team.

A departure of the CLP outside of 46P/Wirtanen's SOI will result in the CLP's descent first being governed primarily by two-body mechanics between the CLP and the Sun (or nearest major body), and then two-body mechanics between the CLP and 46P/Wirtanen (once it enters its SOI). This type of departure will also require a much larger delta-V because the CLP will need additional propellant to get into 46P/Wirtanen's SOI. These two types of descents have been compared in the decision matrix below.

Table 5.4.1: CLP Departure Location Decision Matrix

Metric	Weight	Within SOI	Outside SOI
Required Delta-V	0.3	5	1
Required Mass	0.3	5	1
Feasibility for CLP	0.2	4	2
Feasibility for PV	0.2	2	5
Total	1	4.2	2

It should be noted that these metrics and their assigned weights are likely biased from the viewpoint of the CLP design team. To have a greater perspective of the meaningful metrics and challenges faced by the PV team for the location of the CLP departure, input from the PV design team would be needed.

In addition to the location, the type of departure is also a critical parameter that needs to be considered. The type of departure involves the motion of the PV around 46P/Wirtanen when the CLP disconnects from it. Popular departure types for a mission of this nature include the PV orbiting the comet in a hyperbolic, elliptical, or circular orbit. A hyperbolic orbit would be useful if the PV was dropping off the CLP and then leaving for another celestial body. However, this type of orbit requires a great deal of energy and will not allow the CLP to be in contact with the PV after the departure, which would greatly increase the complexity and mass of the telecommunications subsystem.

An elliptical parking orbit would involve the PV ranging in altitude and speed about 46P/Wirtanen. This type of orbit would have several advantages, including the ability for the PV to conduct experiments at varying ranges in the atmosphere and take images from several different vantage points. However, this varying range and speed may result in fluctuating line of site communication windows between the CLP and PV.

The final departure type that will be considered is a circular orbit. In this type of orbit, the PV would remain at a constant altitude and speed about 46P/Wirtanen, allowing for consistent line of sight communication windows between the PV and CLP. However, the PV will be limited

to analysis from the same altitude and vantage point without transferring to a different altitude orbit. Other notable advantages of closed orbits (elliptical and circular) include the ability to test certain CLP hardware and to closely analyze viable landing sites prior to the departure. These three major departure types have been compared in the decision matrix below.

Please note that metrics like required delta-V and required mass have not been considered because these factors would be considerations for the PV team.

Table 5.4.2: CLP Departure Type Decision Matrix

Metric	Weight	Hyperbolic	Elliptical	Circular
Scientific Analysis	0.35	1	5	3
Communication w/ CLP	0.2	0	4	5
Feasibility	0.2	2	4	4
Hardware Check Ability	0.2	0	4	5
Energy of Orbit	0.05	1	3	4
Total	1	0.8	4.3	4.05

Similar to the departure location down selection process, this decision matrix is likely biased from the perspective of the CLP team. The ideal orbit for the PV is highly dependent on the analysis needed from the PV and the design of its subsystems, which are not currently part of the CLP team's focus. As a result, the following analysis will move forward with the assumption that the PV will be in an elliptical parking orbit, but collaboration with the PV team would be needed to determine the ideal departure type for the mission as a whole.

5.4.3 INCLINATION CHANGE AND ORBIT CAPTURE

Once the CLP is detached from the PV, it will either enter a parking orbit or drop straight to the surface of 46P/Wirtanen. While straight drops will require less propellant and time, they do not allow the CLP any buffer window to test hardware or target landing site conditions before the descent to the surface. This type of descent was used in the *Rosetta* mission with the *Philae* lander, and it resulted in a fair share of complications, including *Philae* bouncing off the surface of the comet twice and landing in a crevice due to the failed deployment of harpoons [22]. As a result of these disadvantages, a parking orbit is likely more favorable for this type of mission. Although a parking orbit would drastically increase the time of the descent due to the small gravitational parameter of 46P/Wirtanen, time is not extremely critical as long as the landing is successful. Thus, it is better to focus on a landing approach that maximizes the probability of success, rather than one that minimizes the time of descent.

As previously mentioned, the amount of work that needs to be done by the CLP will be highly dependent on the location of the departure from the PV. Another aspect of this departure that was not considered, however, is the inclination plane. In order to capture an orbit that passes over the desired target landing site, the inclination plane of the orbit will likely need to be changed unless the PV drops off the CLP in a desirable inclination plane. Changes in the inclination plane are relatively expensive maneuvers, so the magnitude of its change should be kept to a minimum. The same burn that will place the CLP into another plane of inclination will also place the CLP into a desirable parking orbit. Below, a decision matrix has been used to determine the most advantageous type of parking orbit. Please note that the straight descent has also been compared to rule out this descent type.

Table 5.4.3: CLP Orbit Capture Decision Matrix

Metric	Weight	Straight Descent	Elliptical	Circular
Required Delta-V	0.25	4	2	3
Required Mass	0.25	4	2	3
Hardware Check Ability	0.2	0	4	4
Feasibility	0.2	2	4	4
Vantage Point	0.1	0	3	4
Total	1	2.4	2.9	3.5

It should be noted that the time spent in the parking orbit is completely dependent on the target landing site conditions and the status of hardware checks. If everything is going according to plan, the CLP can begin its descent before completing a full orbit, but more importantly, it has the availability to stay in the parking orbit as needed without expelling any significant propellant.

5.4.4 DESCENT PATH TOWARDS COMET

Once the mission control team and CLP deem it safe to begin the descent, the CLP will perform a retroburn shortly before the periapsis point with the landing site. While a Hohmann-type transfer (retro-burn 180 degrees away from the target landing site) would be the most energy efficient descent path, it will also take significantly longer than a burn that is closer to periapsis. This burn will decrease the energy of the orbit and drop the CLP's altitude to a point of intersection with 46P/Wirtanen's surface at the target landing site. The magnitude of this retroburn will be dependent on the altitude of the circular parking orbit and the location of the burn prior to periapsis. The altitude of the circular parking orbit and the location of the retro burn will be determined from analysis conducted for the FDR report.

5.4.5 LANDING

The final stage of the CLP's descent will be the landing. Based on the proposed descent path, the CLP will be on course to marginally clear the target landing site and will have a non-negligible velocity. In order to prevent the CLP from deflecting off the surface of 46P/Wirtanen, or being damaged by the impact, an additional final retroburn will be used to decelerate the CLP's velocity to nearly zero prior to impact. While this burn will take place shortly prior to impact, it would be undesirable to contaminate the target landing site with emissions, so the burn will occur roughly 15-30 meters above the surface and the CLP will "free fall" the rest of the way. While a drop of this height would certainly damage the CLP on Earth, it will fall towards the surface of 46P/Wirtanen with a very small velocity as a result of the microgravity. Finally, once the CLP impacts the surface, harpoons will be used to tether the lander to the surface of the comet to prevent bouncing or relocation.

Based on the selections made in previous sections, the CLP's primary descent path will look similar to the following figure. Note that the figure is not to scale since the exact parameters of the parking orbits have not been determined. The figure below also assumes coplanar orbits to illustrate the two vehicle's parking orbits more clearly.

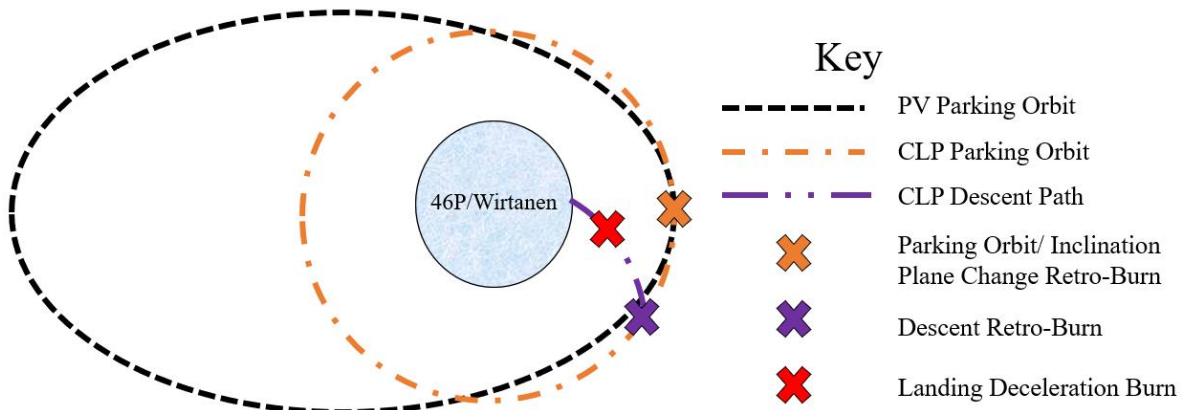


Figure 5.4.1: CLP Primary Descent Path

It should be noted that the figure above does not account for evasive maneuvers due to unexpected objects or course corrections due to forces like solar radiation pressure or atmospheric drag. These types of maneuvers will not occur on a predictable basis and will thus not be modeled in the spaceflight mechanics analysis in the FDR. A sufficient buffer of propellant, however, will be included so that these maneuvers are possible.

5.4.6 NON-TECHNICAL CONSIDERATIONS

In addition to the above technical factors, the CLP team has also considered a variety of non-technical factors for this subsystem. These non-technical considerations are outlined below and summarized in Appendix B.

Table 5.4.4: Spaceflight Mechanics Non-Technical Considerations

Topic	Consideration
Public Health & Safety	The spaceflight mechanics analysis ensures that the CLP travels in a safe and efficient manner that will not directly or indirectly endanger the public (space debris, atmospheric reentry, etc.).
Global	N/A - The spaceflight mechanics subsystem does not have any significant global considerations because this subsystem is unlikely to affect any change on the global level.
Cultural	N/A - The spaceflight mechanics subsystem does not have any significant cultural considerations because this subsystem is unlikely to affect any change on the cultural level.
Social	N/A - The spaceflight mechanics subsystem does not have any significant social considerations because this subsystem is unlikely to affect any change on the societal level.
Environmental	The propellant used in the CLP's maneuvers are harmful to surrounding environments. The use of propellant should be kept to a minimum to decrease the harmful effects of its production and use.
Economic	The analysis conducted by the spaceflight mechanics team constrains many other subsystems and necessitates efficient use of capital and resources.
Professional Ethics	The designers for this subsystem have completed MANE 4100: Spaceflight Mechanics, such that only competent students in this subject matter will submit and review work for this subsystem. Furthermore, all services and statements for this subsystem will be truthful to the extent of the CLP team's knowledge.

5.4.7 RISK ASSESSMENT AND MITIGATION

The spaceflight mechanics subsystem is a critical component of success for the mission, so a thorough assessment of risk and a proper plan for mitigation is of the utmost importance. The following analysis highlights major risks that have been considered for the spaceflight mechanics subsystem and an appropriate plan to mitigate such risks. It should be noted that this list is non-exhaustive and will certainly be expanded as the design of the descent path becomes more refined.

Table 5.4.5: Spaceflight Mechanics Risk Analysis and Mitigation

Risk	Cause	Mitigation
CLP cannot maintain parking orbit	Solar radiation pressure, atmospheric drag, and/or micrometeorite collisions are inconsistent with two-body model	Command and control board will be intelligent enough to course correct using the CLP's current position and velocity data
CLP's orbital model is not consistent with its actual descent	Other celestial bodies cause non-negligible gravitational perturbations	A more advanced 3-body model can be developed for the CLP's orbital mechanics operating system (beyond timeline of this class); these perturbations can also be corrected by the command and control board
CLP's orbital model is not consistent with its actual descent	Numerical integration errors and/or floating-point rounding errors	Integration tolerances will be lowered to sufficiently accurate levels; higher memory/accuracy techniques like double precision variables can be employed; powerful supercomputers will be used for final modeling
CLP fails to depart properly from PV	Departure mechanism failure	Thorough testing of departure mechanism to ensure reliable results; secondary pyrotechnic release option
CLP is damaged by external objects	CLP impacts ice particles or other debris at significant velocity while in orbit or during descent	To a reasonable degree, critical equipment will be protected within the structure of the CLP; cameras and sensor suite on the PV and CLP will identify potential hazards prior to departure stage and during orbit/descent to instruct evasive maneuver protocols

5.4.8 PLAN OF PROCESSION

A key focus in the coming weeks will be to model the aforementioned descent path using the patched conics method. This analysis will be used to determine an approximate delta-V required for the CLP in order to validate the propulsion subsystem design and set a general mass budget. Additionally, this analysis will be used to determine ideal parking orbit parameters and locations for the retroburns that properly consider time and propellant consumption. This analysis will be conducted using MATLAB and be presented in the FDR.

The following tasks would also need to be completed by the spaceflight mechanics subsystem team but will not be completed this semester due to time limitations. Backup descent paths would also be analyzed so that mission control can be aware of alternative options allowed by the amount of propellant on board the CLP. The spaceflight mechanics models would likely also be expanded to a higher order model with 3 or 4-body assumptions and tighter integration tolerances for increased accuracy. This analysis would likely take place on more robust platforms like STK or other industry-level software packages. Finally, course correction and evasive

maneuver algorithms would be modeled, developed, and tested before uploading them onto the command and control board.

5.5 ATTITUDE DETERMINATION AND CONTROL

5.5.1 SUBSYSTEM DEFINITION AND REQUIREMENTS

The ADCS subsystem includes the quantification of mission pointing requirements and accuracy, along with the translational and rotational maneuvering requirements for the CLP. The ADCS also plays a significant role in the maneuvering of the CLP throughout its descent and is responsible for the location and orientation control of the system. This requires the accurate sensing of the vehicle's attitude and relative position to mission targets, and corresponding actuators to minimize the error between the vehicle's actual and target locations and orientations for each point in the mission. Additionally, a control law for the system must be developed that accounts for internal and external disturbances, such as gravitational variations and appendage motion. The requirements for the ADCS subsystem are listed below:

- Design or selection of attitude sensors fulfill pointing accuracy requirements of all components of the CLP
- Selection of attitude control method fulfills precision requirements based on pointing accuracies of the CLP
- System must maintain orientation and stability of CLP throughout landing procedure

5.5.2 ATTITUDE DETERMINATION METHOD

In order to accurately determine a spacecraft's attitude, it is necessary to have multiple determination methods and sensors, as the current state of the system may significantly impact the accuracy of an individual sensor. For example, star trackers cannot provide accurate attitude measurements at angular velocities above 0.0025rad/s [3], so another method, such as an inertial measurement unit (IMU), would be necessary. Determination methods based on magnetometers were eliminated due to the absence of reliable measurements confirming significant magnetic fields around comets [27]. Methods based on GPS were eliminated due to the distance away from the earth and its GPS infrastructure. A multi-tier attitude determination method was chosen, with selections shown in Table 5.5.1. The star tracker will be the primary method for accurate attitude determination. A sun sensor was selected as compared to the horizon sensor due to its use in determining sun direction after landing for the purposes of solar panel angling. An IMU is also included in the system to mitigate the risk of complete loss of attitude determination in a case where the CLP experiences high angular velocities.

Table 5.5.1: Attitude Determination Sensor Decision Matrix

Metric	Weight	Sun Sensor	Horizon Sensor	Star Tracker	IMU
Mass	0.3	3	3	2	4
Power	0.2	3	3	2	5
Accuracy	0.4	3	3	4	1
Cost	0.1	4	4	2	5
Total	1	3.1	3.1	2.8	3.1

5.5.3 ATTITUDE CONTROL

Two of the most common methods for attitude control of a spacecraft are reaction wheels and control moment gyros (CMGs), which are both shown in Figure 5.5.1 [3]. A reaction wheel control method works by rotating a large disk, creating a counter-rotating moment about the system as a whole. A CMG works by rotating either an inner or outer gimbal, which in turn can control the orientation of a rotating disk connected to the inner gimbal. By rotating the inner or outer gimbal, an angular velocity, which is perpendicular to this rotation, is generated on the spacecraft.

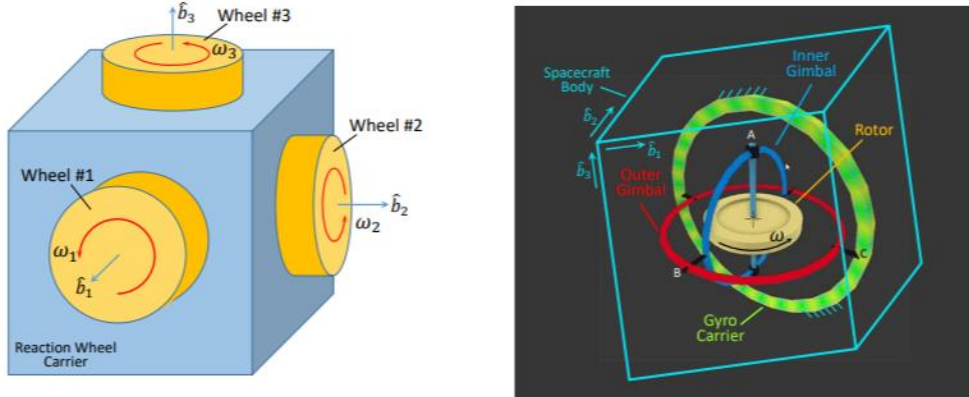


Figure 5.5.1: Reaction Wheel and Control Moment Gyro

These methods of three-axis stabilization control were compared, along with reaction jet thrusters (RJT), in Table 5.5.2 in order to determine the primary attitude control method. Reaction wheels were ultimately chosen for attitude control. Though reaction wheel saturation would typically be a concern in long missions, because the total flight time for the CLP is relatively short, saturation of the system is not a significant concern.

Table 5.5.2: Attitude Control Method Decision Matrix

Metric	Weight	Reaction Wheels	CMG	RJT
Mass	0.25	4	3	5
Power	0.15	2	2	3
Volume	0.05	3	2	4
Response Speed	0.1	3	4	4
Accuracy	0.25	5	4	2
Infrastructure	0.2	2	3	1
Total	1	3.4	3.15	3

5.5.4 NON-TECHNICAL CONSIDERATIONS

In addition to the aforementioned technical considerations, the following non-technical considerations were made for the ADCS.

Table 5.5.3: ADCS Non-Technical Considerations

Topic	Consideration
Public Health & Safety	Control methods such as reaction wheels and CMGs may contain fast moving parts which could pose a hazard to test engineers. Steps should be taken to limit the possibility of injury during testing and manufacturing.
Global	N/A - The selection of the ADCS design does not have significant global considerations and is unlikely to affect change on the global level.
Cultural	N/A - The selection of the ADCS design does not have significant cultural considerations and is unlikely to affect change on the cultural level.
Social	N/A - The selection of the ADCS design does not have significant social considerations and is unlikely to affect change on the social level.
Environmental	CLP reaction control burns may have an adverse effect on the comet's environment and should be limited to the largest degree possible to minimize surface contamination.
Economic	Though the ADCS subsystem does not constitute a major expense in terms of the CLP financials, the ADCS design ensures efficient use of capital and resources during design selection.
Professional Ethics	The selection of technologies for this subsystem is purely out of the customer and the general public's best interests. All selections and considerations are based on the full knowledge of the engineers on the team and are reviewed closely by a secondary lead.

5.5.5 RISK ASSESSMENT AND MITIGATION

Mission objectives will rely on accurate orientation and position of the spacecraft and its components, such as solar arrays and antennae, for power production and telecommunication. As such, risk mitigation in the system is important to ensure these roles can be conducted throughout the entire mission. The major risks to the ADCS are shown below in Table 5.5.4, along with their cause and possible mitigation strategies.

Table 5.5.4: ADCS Risk Analysis and Mitigation

Risk	Cause	Mitigation
Loss of attitude control	Gimbal Lock	Incorporate gimbal stops into design
Loss of sensing from start tracker	High angular velocity of CLP during maneuvers	Add IMU as another attitude measurement unit
Loss of attitude control	Saturation of reaction wheel	Incorporate reaction jet thrusters to provide desaturation torque

5.5.6 PLAN OF PROCESSION

The max torque requirements for the system should be quantified, along with expected internal and external disturbance levels and their frequencies (due to gravity variations, solar pressure, appendage movements, etc.). The design for the reaction wheels, along with the selection of specific sensor hardware to be used in the final design will be determined. After this, the control algorithm for the system can be developed.

Though there may be insufficient time in the semester, the control system should be sufficiently modeled and tested, and worst-case-scenarios should be simulated with proper procedures developed to reduce the possibility of mission failure. Sensors should also be adequately tested prior to system implementation.

5.6 THERMAL MANAGEMENT

5.6.1 SUBSYSTEM DEFINITION AND REQUIREMENTS

The thermal management subsystem deals with maintaining appropriate temperatures throughout each respective subsystem to ensure that they function efficiently and safely. Temperatures throughout different subsystems of the CLP can range from 3 to 353 Kelvin, which necessitates an intentional focus on thermal management. As a result of this design challenge, the thermal management subsystem will define operating temperature parameters for each subsystem and employ appropriate technologies to ensure that these parameters are met. The general requirements of the thermal management subsystem are presented concisely below.

- Identify operational and non-operational temperature ranges for each subsystem
- Select appropriate heat generation, heat transmission, and heat dissipation technologies and techniques to properly maintain all CLP subsystems in their operational temperature ranges
- Select a boundary layer material that can handle all the environmental temperatures the CLP may experience throughout the course of the mission
- Quantify the heat transfer rates and power requirements needed to keep critical systems in their operational ranges
- Determine a general arrangement scheme for thermal management systems depending on location of other subsystems

5.6.2 BACKGROUND

A thermal margin is the technical definition of the operating temperature range for a component or subsystem. In many cases, a component outside of an ideal thermal margin will not deteriorate, but may not be able to operate efficiently, or at all. Furthermore, components need to maintain their margin or there may be consequences such as:

- Rupture (a failure mode caused by overheating)
- Expansion of components
- Increased system pressure

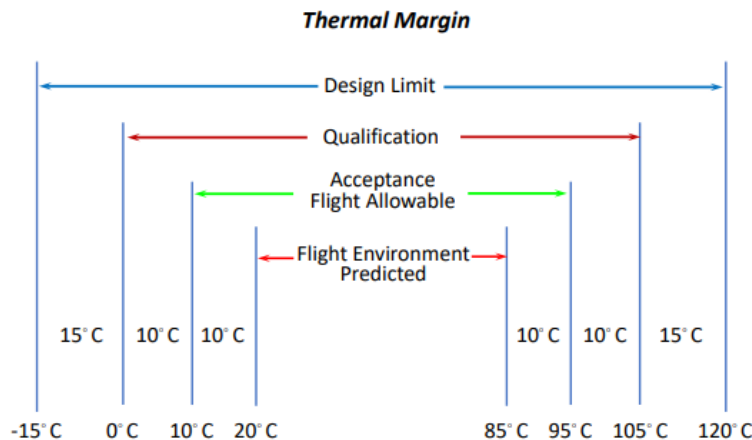


Figure 5.6.1: Thermal Margin General Requirements [3]

The thermal margin can be narrowed down or expanded depending on the condition of the components. For the most stringent environments, the predicted flight environment represents the optimal design range of components. This gives a margin of +/- 10 degrees Celsius to allow temperatures to fluctuate within the acceptable flight temperature range. When the temperature fluctuates another +/- 10 degrees Celsius from the acceptable flight temperature, the component is said to be operating in the qualification thermal margin, which indicates that

components will survive that temperature based on testing requirements done in research and development but should not stay at the current operating temperatures. Finally, the design limit is the limit of allowable thermal margin. Components that exist up to this point can only remain in this range for a short period of time before they become corrupted in some form. Temperatures outside of the design limit are likely to result in a complete failure of the component or system in a short amount of time.

5.6.3 THERMAL ARCHITECTURE

The environment the CLP is in will change drastically throughout the course of the mission as it follows 46P/Wirtanen's path through perihelion. As a result of these large environmental changes, the requirements of the thermal management system will vary greatly. Before choosing specific thermal management technologies, though, a proper consideration of the overall system should be made.

There are three main types of thermal management system architectures that will be considered. An active system is only used at critical times when necessary, while passive systems continuously maintain the thermal energy requirements at all times. Finally, a hybrid system would be a combination of these two architectures, with both active and passive methods to control the thermal requirements. These three architecture types are compared to one another on a variety of design metrics in the decision matrix below.

Reliability is the most important factor to check for, as the mission is extremely sensitive to failure. Individual components need to be able to reliably perform their functions so that the system as a whole can be functional. Speed is also a considered metric because faster thermal management systems will mitigate the risk of hazardous situations by responding quickly to discrepancies between desired and measured results. Additionally, endurance is used to assess the technology's ability to withstand a mission of this length and complexity. The endurance of thermal management systems is measured based on the number of cycles, or length of time, to expected failure. The consequences of a system failing were also considered in the volatility metric, and the flexibility metric was used to account for a system's ability to adapt to unforeseen situations or applications due to the complex nature of this mission. Finally, cost and weight were also considered to ensure that the mass and cost budgets were maintained.

Table 5.6.1: Thermal Management Architecture Decision Matrix

Metric	Weight	Active	Passive	Hybrid
Reliability	0.3	2	4	4
Speed	0.1	5	3	4
Endurance	0.1	2	5	4
Volatility	0.1	2	4	1
Weight	0.1	3	4	2
Cost	0.1	3	5	5
Flexibility	0.2	4	2	5
Total	1	2.9	3.7	3.8

As is shown in the decision matrix, the hybrid system will be the most robust method to keep the vehicle's subsystems within their respective thermal margins. The technologies used to achieve this system architecture will be discussed in the benchmarking section.

5.6.4 HEAT GENERATION

There are several methods of generating heat. While an Electric Path Heater (EHP) or a Cartridge Heater (CH) actively uses power, a Radioisotope Heating Unit (RHU) can be considered a passive technology, as it emits heat constantly throughout its lifespan.

Table 5.6.2: Heat Generation Technologies Decision Matrix

Metric	Weight	EHP	CH	RHU
Reliability	0.3	3	3	5
Speed	0.1	4	5	3
Endurance	0.1	3	2	5
Volatility	0.1	3	3	4
Weight	0.1	3	2	4
Cost	0.1	3	4	5
Flexibility	0.2	4	5	1
Total	1	3.3	3.5	3.8

5.6.5 HEAT TRANSMISSION

Heat transmission is important for distributing heat from one area on the CLP to another. There are passive and active methods of transmitting heat. The passive methods rely on either capillary action or a heat imbalance, while the active methods use a pump and heat pipe. One advantage of active systems is that they can fight against a heat gradient, unlike the passive alternatives.

A Capillary Pumped Loop (CPL) is a transmission system that uses the adhesion and surface tension properties of a liquid to move heat throughout a system, whereas a Looped Heat Pipe (LHP) uses the natural diffusion of heat in a fluid to homogenize the heat throughout a system. Finally, a Powered Heat Pipe (PHP) works similarly, but can use electric power to force heat against diffusion.

Table 5.6.3: Heat Transmission Technologies Decision Matrix

Metric	Weight	CPL	LHP	PHP
Reliability	0.3	3	4	5
Speed	0.1	2	3	4
Endurance	0.1	5	5	3
Volatility	0.1	5	4	3
Weight	0.1	5	3	3
Cost	0.1	3	3	3
Flexibility	0.2	3	3	5
Total	1	3.5	3.6	4.1

5.6.6 HEAT DISSIPATION

Heat dissipation is necessary for maintaining the CLP against the buildup of excess heat generated from powered functions. Heat dissipation is the process of letting heat out of a structure and can be accomplished by using a Body Mounted Radiator (BMR) or a Deployable Radiator (DR). Radiators serve the function of releasing heat into an exterior environment (in this case, space).

A BMR is a radiator that does not move, and is always in a deployed position, providing a reliable, minimally-complex design. The DR, however, is a mechanical system that is more effective, but is also more complex as a result of increased chances of mechanical failure and large power requirements.

Table 5.6.4: Heat Dissipation Technologies Decision Matrix

Metric	Weight	BMR	DR
Reliability	0.3	5	4
Speed	0.1	3	3
Endurance	0.1	4	2
Volatility	0.1	3	3
Weight	0.1	3	3
Cost	0.1	4	2
Flexibility	0.2	3	5
Total	1	3.8	3.5

5.6.7 BOUNDARY LAYER

The boundary layer refers to the outermost layer of the CLP, which makes contact with the external environment. Due to the harsh environmental conditions of space, measures need to be taken to create an effective thermal boundary between space and the temperature-sensitive equipment inside the CLP.

Paint layers can be a low-weight solution to maintaining the internal environment. Louvers can also be used to change the radiators into an active heat dissipation system. They function as a cap on the radiator that can be changed to release a certain amount of heat. Multi-layer insulation (MLI) uses different layers of material to halt the flow of heat by adding more resistance to the CLP. A Thermal shield is an external layer that is typically used to dissipate and absorb heat but is also heavier and thicker than the normal exterior would be.

Table 5.6.5: Boundary Layer Options Decision Matrix

Metric	Weight	Paint Layers	Louvers	MLI	Thermal Shield
Reliability	0.3	4	4	5	5
Speed	0.1	3	4	4	4
Endurance	0.1	5	4	5	3
Volatility	0.1	5	4	3	3
Weight	0.1	5	2	3	2
Cost	0.1	5	3	4	2
Flexibility	0.2	3	5	4	5
Total	1	4.1	3.9	4.2	3.9

5.6.8 NON-TECHNICAL CONSIDERATIONS

In addition to the aforementioned technical factors, several non-technical considerations were made for the thermal subsystem. These considerations account for less tangible reflections in the design of this subsystem and are summarized concisely in the table below.

Table 5.6.6: Thermal Management Non-Technical Considerations

Topic	Consideration
Public Health & Safety	The manufacturing of thermal equipment will not unreasonably endanger workers or the surrounding community due to hazardous byproducts or processes.
Global	N/A - The use of thermal components has no global considerations because the technology is well understood and is highly unlikely to cause an incident on the global level.
Cultural	N/A - The use of thermal components has no effects on cultures due to its limited nature of influence on the cultural level.
Social	N/A - The use of thermal components has no meaningful impact on societies as a result of the limited exposure to the public this subsystem will have.
Environmental	The production of some thermal components may be considered harmful to the environment due to the use of non-renewable, hazardous materials. The design of this subsystem ensures that such manufacturing processes will be limited to the largest degree possible.
Economic	The production of thermal components will provide the manufacturers revenue and business opportunities, and thus can be considered to have a small microeconomic impact.
Professional Ethics	The designers for this subsystem have completed Thermodynamics and Physics (which covers basic heat transfer) at the collegiate level.

5.6.9 RISK ASSESSMENT AND MITIGATION

In order to address potential risks to this subsystem, the following risks and root causes were considered. Plans to mitigate such risks were also devised and are summarized in the table below.

Table 5.6.7: Thermal Management Risk Analysis and Mitigation

Risk	Cause	Mitigation
Extremely low temperatures on the CLP	Temperatures will decrease drastically as 46P/Wirtanen moves away from the Sun (past perihelion) as a result of decreased radiation	A Peltier or other heating system can be used to heat a material in an enclosed space.
Extremely high temperatures on the CLP	Temperatures will increase drastically as 46P/Wirtanen approaches perihelion due to increased radiation and/or refraction; a component could also malfunction and leak heat.	To release a buildup of heat, a Peltier system could operate in such a way that the inside of the CLP would be cooled.
Explosion or corruption of components	In the case of system failure, an explosion or leak can occur and drastically change the temperature of components.	Enclose components such that the risk of an explosion will be limited to the immediate surroundings and implement safeguards like extinguishers or fans.

5.6.10 PLAN OF PROCESSION

As the CLP design becomes more refined, the thermal margins of specific subsystems will also be more constrained. In the remaining portion of the semester, some thermal analysis studies will be conducted to ensure critical subsystems that are prone to heating effects (such as solar panels or the control board CPU) remain at appropriate temperatures. General specifications for the technologies selected in the benchmarking section will also be made.

Although there is insufficient time and resources in the remaining semester, the design of the thermal management subsystem would also involve thorough testing routines of critical components. Additionally, more hardware and design scenarios would be modeled using industry-level CFD software packages.

5.7 POWER AND POWER MANAGEMENT

5.7.1 SUBSYSTEM DEFINITION AND REQUIREMENTS

The power and power management subsystem involves the design and planning of the generation, storage, and distribution systems of electrical energy throughout the spacecraft. The primary goal of this system is to provide and distribute the necessary operating power for each of the spacecraft subsystems. Because the final design for the spacecraft has not yet been determined, estimates for power usage and mission duration were devised based on previous spacecraft landers such as the *Philae* [20] and preliminary estimates based on the current CLP design. Given these considerations, the power and power management subsystem will include the following requirements:

- Fulfill power generation requirements (nominally estimated to be 150W)
- Operate throughout the full duration of the mission (expected 18 months)
- Minimize excess power generation or dissipate as excess heat

- Distribute appropriate power to all subsystems and payload

5.7.2 POWER GENERATION

The methods for the generation of electrical power were filtered based on approximate power requirements and the mission duration for the CLP. This down selection was conducted based on Figure 5.7.1 shown below.

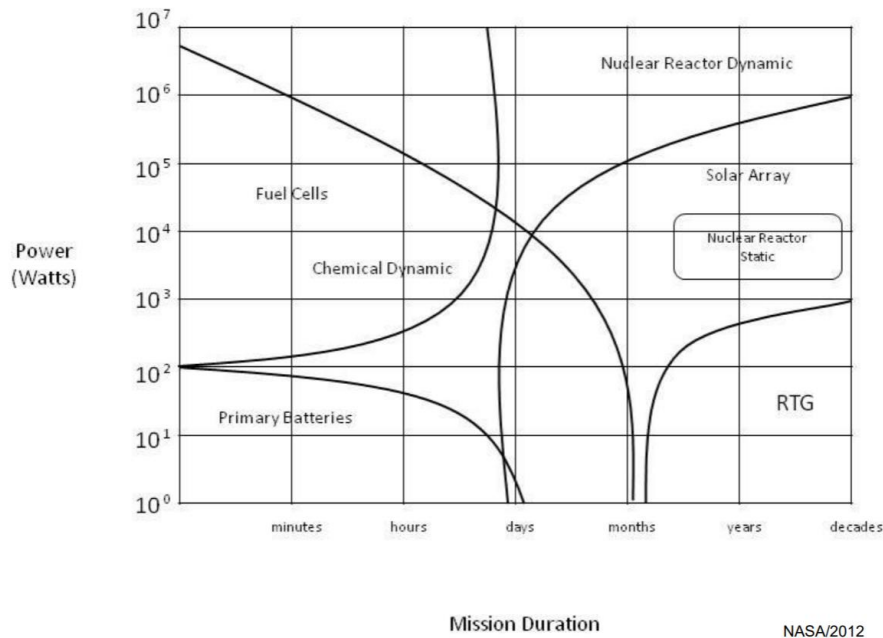


Figure 5.7.1: Electrical Power Generation Technologies [3]

Based on preliminary analysis, providing electricity from primary batteries, chemical reactions, or fuel cells was eliminated based on the total mission time, which is planned to exceed the scale of months. The dynamic nuclear reactor was also eliminated due to the fact that it would produce significant excess power and has never been tested in space.

The selection of the primary electrical power generation was then selected from the remaining technologies: solar arrays, radioisotope thermal-electric generators (RTG), and static nuclear reactors, using the design matrix shown in Table 5.7.1. It was determined that the primary generation method for CLP would be based on solar arrays under a regulated power architecture.

Table 5.7.1: Power Generation Decision Matrix

Metric	Weight	Solar Arrays	RTG	Nuclear Reactor (Static)
Mass	0.35	4	2	1
Lifespan	0.1	3	5	4
Flight Heritage	0.2	5	4	1
Power Output	0.1	4	5	3
Safety	0.15	5	3	1
Economic Cost	0.05	4	2	2
Environmental Concerns	0.05	4	2	1
Total	1	4.25	3.15	1.55

5.7.3 POWER STORAGE

In order to power the CLP in instances of low light exposure or higher power needs, power storage is required. Thus, secondary batteries are incorporated into the power management design. These batteries will be designed such that the battery energy storage capacity meets or exceeds 140% of baseline power requirements (as recommended by NASA) [3]. This margin is included to account for a larger operational power need than originally planned for, and to account for degradation of the batteries over time due to cycling and environmental effects.

A preliminary selection for the secondary battery type was then conducted, with the nickel-metal hydride battery ultimately being chosen as the secondary power source. The design matrix for this decision can be seen in Table 5.7.2, with battery properties shown in Appendix F.

Table 5.7.2: Battery Type Decision Matrix

Metric	Weight	Ni-MH	Li-Ion	Ni-Cd
Specific Energy	0.35	3	4	2
Cycle Life	0.3	5	4	4
Temperature Range	0.1	4	4	4
Flight Heritage	0.15	4	3	4
Safety	0.1	4	3	2
Total	1	3.95	3.75	3.1

5.7.4 NON-TECHNICAL CONSIDERATIONS

In addition to the technical design factors previously mentioned, several non-technical considerations were made with regard to the power management design. These considerations are summarized in Table 5.7.3.

Table 5.7.3: Power Management Non-Technical Considerations

Topic	Consideration
Public Health & Safety	Certain power generation methods are inherently more dangerous as they contain radioactive elements or toxic chemicals. As such, the power systems design ensures that harmful materials are not excessively and needlessly used and that risks endangering public health and safety during testing, assembly, or launch are limited.
Global	Certain materials are extracted in nations outside of the United States. The power systems design ensures that all materials sourced externally are obtained ethically and legally with respect to the nations in which they reside.
Cultural	N/A - The selection of the power systems design does not have any significant cultural considerations as this subsystem is unlikely to affect any change on the cultural level.
Social	N/A - The selection of the power systems design does not have any significant social considerations as this subsystem is unlikely to affect any change on the societal level.
Environmental	Certain materials such as those contained in batteries and solar cells contain radioactive, toxic, or otherwise environmentally harmful elements, or have processing procedures which produce a significant global emissions footprint. As such, care will be taken in the choices of the system design so as to minimize the environmental harm.
Economic	The power system design is an expensive part of the CLP. The power systems design ensures efficient use of capital and resources during design selection.
Professional Ethics	The selection of technologies for this subsystem is purely out of the customer and the general public's best interests. All selections and considerations are based on the full knowledge of the engineers on the team and are reviewed closely by a secondary lead.

5.7.5 RISK ASSESSMENT AND MITIGATION

Due to the vital role that the power systems play in the operation of the CLP, risk assessment and mitigation is of the utmost importance. A subsystem failure has the strong possibility of causing a complete mission failure. Major risks for this subsystem are mentioned in Table 5.7.4, and although these considerations are not comprehensive, they provide insight into how the design of the system will mitigate risk.

Table 5.7.4: Power Management Risk Analysis and Mitigation

Risk	Cause	Mitigation
High excess voltage	Excess solar power production	Design for power dissipation (shunts)
Reduction in amperage due to solar cell string failure	Cell crack or electrical interconnection failure in cells	Cross-linked parallel solar cell connections
Amperage drop	Battery failure	Multiple batteries in parallel
Significant reduction in expected power generation	Excessive periods without sunlight due to Improper landing	Implementation of power limitations and strict power scheduling
Significant reduction in expected power generation	Excessive periods without sunlight due to improper landing	Implementation of power limitations and strict power scheduling

5.7.6 PLAN OF PROCESSION

After the total power requirements for each of the subsystems has been determined and confirmed, the power system and power schedule can be modeled and developed. The type of solar panels will then be determined, along with proper sizing. Theoretical battery and photovoltaic cell life will be analyzed and compared to experimental data and similar past missions, which will ultimately be used to properly schedule mission objectives. The supplied voltage and current to individual systems will then be determined to minimize power loss throughout the CLP.

Although there is insufficient time and resources for this semester, sufficient hardware tests for critical components such as the solar panels should be conducted, and electrical components should be cycled to confirm functionality. In addition, the mission should be simulated such that power scheduling methods are adequately tested. Procedures for worst-case-scenarios, such as battery or solar panel failure, should also be developed to reduce the risk of a mission failure.

5.8 COMMAND AND DATA

5.8.1 SUBSYSTEM DEFINITION AND REQUIREMENTS

The command and data subsystem includes the command and control computer, the storage of mass digital data, and the communication protocols involved with transmission to and from Earth. Additionally, the command and control subsystem plays a key role in emergency situations, as it is responsible for identifying issues both internal and external to the space vehicle, classifying their nature, and isolating the problem if possible. The command and control subsystem also must be intelligent enough to identify and carry out the most favorable course of action for a given problem, or at a minimum, reduce the severity of the situation until a decision

can be made by the mission control team. As a result of its wide-ranging responsibilities, the command and control subsystem ranges in states of operation from standby to baseline-nominal to emergency operation status [3].

The command and control subsystem will play an extremely integral role in the success of the CLP mission. The primary requirements of the command and control subsystem have been included in a list below. These requirements will guide the down selection process in the following sections [3, 10].

- Autonomously direct the individual subsystems to carry out the primary descent path identified in the spaceflight mechanics section, and course-correct or change the descent path if necessary
- Actively track and store engineering data (such as position, velocity, pressure, and temperature) and scientific data (such as sample retrieval readings, magnetometer data, and images taken) produced by the sensor suite on board the CLP, and transmit this data to the PV to be downlinked to the DSN
- Employ basic data processing schemes (data compression, encoding to reduce data loss, or encryption) as necessary
- Maintain the spacecraft clock to regulate routine tasks and ensure that the mission stays on schedule
- Interpret messages from the mission control team and carry out the necessary actions requested in the message
- Autonomously monitor the status of all other subsystems and apply fault protection algorithms when appropriate to handle internal or external issues to the CLP
- Enact safing routines (shutting down or reconfiguring components or subsystems) as appropriate for the preservation of the CLP mission

5.8.2 COMPUTER ARCHITECTURE

The three main common computer architecture schemes for space missions of this nature are distributed systems, centralized systems, and remote systems [10]. Distributed systems require each subsystem to have its own processor and memory hardware. This approach increases the mass and volume demands, as there is more hardware on board the space vehicle, but allows each subsystem to have hardware specially tailored for its needs (ex. strong processors for ADCS and additional memory for command and data).

Centralized systems contain one main hub for processing and memory which is shared by all subsystems appropriately. This approach is more advantageous for mass and volume budgets, but places more strain on the finite processing power and memory of a single computer.

Finally, remote systems require a powerful antenna and a large bandwidth capacity to send large amounts of data back to Earth (in the CLP mission it would be to the PV then Earth). This approach outsources most of the processing power to computers back on Earth, allowing for systems with much less mass and volume requirements, but involves significant delays in

transmissions that make it unreasonable for this mission. The decision matrix below demonstrates a down selection of the general computer architecture scheme that will be used for this mission.

Table 5.8.1: Computer Architecture Decision Matrix

Metric	Weight	Distributed	Centralized	Remote
Feasibility	0.25	4	5	0
Mass	0.2	1	3	5
Performance	0.2	5	4	0
Volume	0.15	1	4	5
Cost	0.1	2	4	4
Power Requirements	0.1	1	4	4
Total	1	2.65	4.05	2.55

Based on this decision matrix, the CLP team will move forward with a centralized computer architecture for the command and control subsystem.

5.8.3 BENCHMARKING SELECTION

The two main components of the command and control subsystem are an onboard flight processor and a solid state memory drive [3]. As a result of this tremendous responsibility and single point of failure, the command and control subsystem will also contain a backup control board that is intelligently cross-linked to the primary board for redundancy. The decision matrix below serves to compare four viable control boards that were considered for this mission.

Table 5.8.2: Command and Control Board Decision Matrix [8, 21, 26, 34, 39]

Metric	Weight	BAE RAD750	BAE RAD5545	HPE Spaceborne Computer	Boeing HPSC
Flight Heritage	0.4	5	4	1	0
Performance	0.25	3	4	4	5
Power Requirements	0.2	4	3	3	4
Mass	0.15	3	4	3	3
Total	1	4	3.8	2.45	2.5

As shown in the decision matrix above, the BAE Systems RAD 750 is a clear favorite, primarily due to its unmatched flight heritage and superior power requirements. Within the RAD 750 product family however, there are a range of products to consider. An additional decision matrix is included below to illustrate the down-selection process for the exact control board model.

Table 5.8.3: BAE Systems RAD750 Model Decision Matrix [34]

Metric	Weight	6U Single Board	6U Extended Single Board	3U Single Board
Performance	0.5	4	5	2
Power Requirements	0.2	3	3	4
Mass	0.1	3	2	5
Volume	0.1	3	2	5
Cost	0.1	3	3	4
Total	1	3.5	3.8	3.2

The previous two decision matrices illustrate the reasoning for the selection of the BAE Systems RAD750 6U CompactPCI extended single-board computer as the primary control board for the CLP mission. Despite its many favorable attributes, the BAE Systems RAD750 is extremely inferior to the RAD5545 Space VPX single board computer in several product features. These features include the ability to run multiple operating systems at once, process extremely high-resolution images, and autonomously operate the spacecraft [21]. While the favorable flight heritage and power requirements associated with the RAD750 warrant its selection as the primary control board, the RAD5545 Space VPX single board computer will make it an ideal “backup” control board. Furthermore, since the manufacturer of both of these boards is BAE Systems, the control boards will be able to intelligently interface with one another and cross-link responsibilities more suited for the strengths of the respective control board. Thus, the RAD750 will serve as the workhorse of the mission, performing the majority of traditional control board responsibilities, but will delegate actions like image processing and encryption to the RAD5545, which will also serve as a complete backup if the RAD750 becomes dysfunctional.

5.8.4 NON-TECHNICAL CONSIDERATIONS

In addition to the above technical factors, the CLP team has also considered a variety of non-technical factors for this subsystem. These non-technical considerations are outlined below and summarized in Appendix B.

Table 5.8.4: Command and Data Non-Technical Considerations

Topic	Consideration
Public Health & Safety	The command and control design selections ensure that the CLP has sufficient capability to travel in a safe and efficient manner that will not endanger the public either directly or indirectly (space debris, atmospheric reentry, etc.).
Global	N/A - The selection of the command and control board does not have any significant global considerations because this subsystem is unlikely to affect any change on the global level.
Cultural	N/A - The selection of the command and control board does not have any significant cultural considerations because this subsystem is unlikely to affect any change on the cultural level.
Social	N/A - The selection of the command and control board does not have any significant social considerations because this subsystem is unlikely to affect any change on the societal level.
Environmental	The radiation hardening process used to prepare the processors for the command and control module may be considered an environmentally harmful manufacturing process. However, this operation is highly contained and unlikely to harm the environment on a notable scale.
Economic	The command and control modules are expensive pieces of equipment that will be outsourced to BAE Systems. This selection will be beneficial to this business, so this subsystem has positive economic effects on a small scale.
Professional Ethics	The selections of technologies for this subsystem are purely out of the customer and the general public's best interests. The command and control design team has no conflicting matters to disclose.

5.8.5 RISK ASSESSMENT AND MITIGATION

A proper assessment of risk, and a plan to mitigate such risks are necessary steps in all designs of a space vehicle, especially for a subsystem as critical as command and control. The table below illustrates these critical design considerations for the command and control module. This assessment only includes major risks and is a non-exhaustive list. It will be further developed as the design of the command and control subsystem becomes more refined.

Table 5.8.5: Command and Data Risk Analysis and Mitigation

Risk	Cause	Mitigation
Failure of main control board	Electrical short, hardware failure, etc.	Extensive testing to ensure this is not a probable outcome; transfer of responsibilities to secondary control board
Loss of engineering and/or scientific data	Insufficient memory on primary board	Use secondary board memory as needed; regular transmissions to PV for data downlink
Overheating of control board	Insufficient thermal management and/or excessive processing on a single control board	Extensive thermal management testing and analysis; shared processing responsibilities between primary and secondary control boards
Loss of counter on spacecraft clock	Excessive radiation or malfunction	Radiation hardened electronics; safing routines to reset clock; receive time from mission control messages
Loss of communication with PV	Damage to PV or broken antenna	Safing routines and fault protection algorithms for autonomous operation
Corrupted data and operations	Excessive radiation	Extensive radiation hardening and testing; safing routines to reboot systems as needed

5.8.6 PLAN OF PROCESSION

As the design of the CLP becomes more refined, specific technical parameters and needs for the command and control system will be explored and researched. The final design of the telecommunications subsystem will determine the communication protocols that will be used in this subsystem, and the necessary memory capacity will primarily be driven by the engineering and scientific data that is deemed necessary from the tool suite and the communication windows available with the PV. In the FDR, specific values for power requirements, memory capacity, processor power, volume, and mass for the selected control boards will also be defined. These quantitative parameters will allow for a more thorough and accurate design of various budgets such as mass, power, and volume.

Additional steps in this design process that will not be conducted this semester due to time constraints would include thorough radiation and electronic testing of the control boards, and intelligently cross-linking and delegating responsibilities between the primary and secondary control boards. Fault protection and safing algorithms would also be developed and tested.

5.9 TELECOMMUNICATION

5.9.1 SUBSYSTEM DEFINITION AND REQUIREMENTS

The telecommunications subsystem is responsible for communications with the PV and Earth. This includes data uplink for analysis on Earth, an essential operation as the transmission of the payload data is the primary objective of the mission. Additionally, telemetry data must be sent to keep the mission operations team regularly updated on how the spacecraft is functioning. The telecommunications subsystem is responsible for the selection of signal bands, antennas, and methods of tracking. It must also be decided if the CLP will only attempt communications with PV or also provide a backup system for direct communications with Earth.

In order to ensure successful communications with the primary lander and Earth, the following requirements must be met.

- The telecommunications system must handle navigation and tracking of the CLP
- The telecommunications system must facilitate two-way communication between the CLP and PV, transmitting scientific and telemetry data
- The telecommunications system must uplink with Earth and downlink with the CLP, either directly or through the PV

5.9.2 BENCHMARKING SELECTION

First, it must be decided if the CLP will have the capability to communicate with Earth directly. The system requirements specify that the CLP must be capable of two-way communication with the PV. However, in the event of an orbiter failure, the CLP would also be lost, as it would be rendered incapable of communication with Earth. One way of reducing this risk is including a backup system capable of direct communication with Earth. The merits of this solution were considered below in Table 5.9.1.

Table 5.9.1: Backup Telecommunications System Decision Matrix

Metric	Weight	CLP to PV	CLP to Earth
Risk	0.5	3	5
Mass	0.3	5	3
Power	0.2	5	2
Total	1	4	3.8

Although the capability to communicate with Earth would drastically reduce risk, this type of system would necessitate large mass and power requirements that would be unfavorable

to the design of other CLP subsystems. Because the CLP is such a low mass system, inclusion of an antenna capable of reaching Earth would take a significant portion of the overall mass budget when compared to the much smaller antenna needed for communication with the PV. The power needs would also significantly increase, as a higher bandwidth and greater data storage capabilities would be required. As a result of these considerations, the backup telecommunications system will also direct communication through the PV.

To facilitate effective communication between the PV and CLP, a proper frequency band must be selected. Generally, higher frequency bands (HF) offer more range and higher transmissions rates, but require larger antennas and higher power consumption. Reliability was considered to be of the utmost importance as a result of the critical nature of this subsystem. Power was also rated to be of high importance in order to minimize energy consumption and mass. Range and speed were considered to be of little importance as the CLP only needs to directly communicate with the PV, which is always within a few kilometers distance.

Table 5.9.2: Frequency Band Decision Matrix [12, 28]

Metric	Weight	HF	S	X	K
Reliability	0.4	5	5	3	2
Power	0.3	5	4	2	2
Speed	0.2	2	3	5	5
Range	0.1	2	3	5	5
Total	1	4.1	4.1	3.3	2.9

The S-band was selected as the frequency band. The S-band offers slightly higher performance at the cost of higher power consumption when compared to the high frequency (HF) band. X and K bands were deemed impractical in terms of power requirements for the nature of this mission. As a result, the S-band will be used to transmit data and receive commands.

The CLP will have two antennas, one primary and one backup. This was deemed essential due to the critical nature of the telecommunications system. A range of different antennas were considered. These were selected based on prior flight heritage for their respective bands. Small patch, dipole, turnstile, and helix antennas were all considered viable candidates. For the primary antenna, performance was prioritized above power and mass. Directional capabilities were considered of low importance due to the relatively low transmission distances. On many spacecraft high directionality is required as signal strength drops over distance. In order to have a reasonable signal strength, the signal must be focused. However, the CLP is communicating with the PV over a very small distance, thus negating the requirement for high directionality. Power and mass were considered of equal value in this case. The helix was selected, despite its higher mass and power consumption, as it has the highest gain.

Table 5.9.3: Primary Antenna Decision Matrix [12, 28]

Metric	Weight	Small Patch	Dipole	Turnstile	Helix
Gain	0.4	2	3	3	5
Power	0.3	5	4	3	3
Mass	0.2	5	5	3	3
Directionality	0.1	3	4	5	5
Total	1	3.6	3.8	3.2	4

For the secondary antenna, mass and power consumption were prioritized over performance. This is necessary due to the low mass nature of the system, which can afford to be cut due to the higher performance of the primary system. The small patch antenna was chosen due to its low mass and power consumption. The dipole also performed well in this analysis, but the small patch was ultimately chosen for its lower power needs.

Table 5.9.4: Secondary Antenna Decision Matrix [12, 28]

Metric	Weight	Small Patch	Dipole	Turnstile	Helix
Mass	0.4	5	5	3	3
Power	0.3	5	4	3	3
Gain	0.2	2	3	3	4
Directionality	0.1	3	4	5	5
Total	1	4.2	4.2	3.2	3.4

5.9.3 NAVIGATION AND TRACKING

The CLP will use autonomous optical navigation with the comet surface and known star field [25, 36]. This is necessary due to the constraints of the mission. Landing on a small body requires extreme precision as the bodies themselves are small and the target areas landing sites are even smaller [11]. Additionally, the CLP does not directly communicate with Earth, so cannot take advantage of ground-based tracking methods. Autonomous optical navigation uses onboard imaging to provide navigation for the spacecraft. The CLP will use landmark based optical navigation during its descent and landing. Known landmarks observations of the comet's surface are used to determine the orbital characteristics and position of the spacecraft [11, 36].

5.9.4 NON-TECHNICAL CONSIDERATIONS

In addition to the aforementioned technical factors, several non-technical considerations were also made for the telecommunications subsystem. The considerations are collected below in Table 5.9.5 and outlined in Appendix B.

Table 5.9.5: Telecommunications Non-Technical Considerations

Topic	Consideration
Public Health & Safety	N/A - The telecommunications subsystem does not have any significant global considerations because this subsystem is unlikely to put any members of the public in danger.
Global	N/A - The telecommunications subsystem does not have any significant global considerations because this subsystem is unlikely to affect any change on the global level.
Cultural	N/A - The telecommunications subsystem does not have any significant cultural considerations because this subsystem is unlikely to affect any change on the cultural level.
Social	N/A - The telecommunications subsystem does not have any significant social considerations because this subsystem is unlikely to affect any change on the societal level.
Environmental	N/A - The telecommunications subsystem does not have any significant environmental considerations because this subsystem is unlikely to affect the environment of the Earth or the comet.
Economic	Failure of the telecommunications system would result in the complete loss of the mission and hence a major economic waste. As a result, reliability of the subsystem was a major priority.
Professional Ethics	All selections and considerations are based on the full knowledge of the engineers on the team and reviewed closely by a secondary lead.

5.9.5 RISK ASSESSMENT AND MITIGATION

Risk mitigation is of utmost importance for the telecommunications system. Failure of the telecommunications system would leave the CLP dead in the water - unable to transmit data or receive commands. As a mission critical system, risks and mitigations are defined below in Table 5.9.6. These risks are non-exhaustive and will require deeper assessment once the telecommunications system has been further defined.

Table 5.9.6: Telecommunications Risk Analysis and Mitigation

Risk	Cause	Mitigation
Damage to antenna, receivers, processors, etc.	Radiation damage, collision damage, thermal damage, etc.	Backup systems are selected and interlinked where possible to minimize single points of failure
Failure to receive or transmit.	Improper orientation of antenna	Omni-directional antennas are used as the PV is close enough to not warrant focused signals
Failure of antenna, receivers, processors, etc.	Hardware failure, electrical short, etc.	Flight tested hardware will be selected and extensive analysis testing will be conducted prior to mission launch
Signal interference	Atmospheric absorption, weather, etc.	Lower bands are used and the spacecraft is only communicating with the PV in deep space

5.9.6 PLAN OF PROCESSION

It should be noted that once a PV has been selected, the telecommunications subsystem may require adjustment to ensure compatibility. Going forward, specific antennas will be selected, and their performance and specifications will be gathered and defined. Additionally, receivers, processors, transceivers, and power amplifiers will be selected.

Beyond the scope of this semester, higher level analysis of the different components and how they interact must be performed. Electrical and radiation testing on the antenna and electrical components should be performed. Additionally, transmission times should be evaluated and routines for data upload and reception should be defined.

6 DESIGN BUDGETS

Budgets for mass, volume and cost all must be laid out as a framework for all subsystems to be defined by. These budgets are devised to allow the spacecraft to meet the constraints that are associated with sending a vehicle into deep space in an efficient and effective manner. Currently, this is a preliminary analysis for the needs of each system which will be adjusted and optimized further as the designs become more refined.

6.1 MASS BUDGET

The lander that is being designed for should not exceed a mass of 250 kg in total in order to meet the limitations of the PV. This metric was determined by approximating subsystem mass allocations as shown in Table 6.1.1. As previously described, these are subject to change as the

subsystems are finalized. The current mass budget also leaves ~8% clearance for unforeseen design modifications or general discrepancies in manufacturing processes and designs.

Table 6.1.1: Subsystem Mass Distribution

Subsystem	Mass (kg)	Percent of Maximum
Structures	50	20.00%
Mechanisms & Deployables	18	7.20%
Propulsion	75	30.00%
ADCS	16	6.40%
Thermal Management	5	2.00%
Power Management	30	12.00%
Command & Data	8	3.20%
Telecommunications	8	3.20%
Sensor Suite	20	8.00%
Total	230	92.00%

6.2 VOLUME BUDGET

As a result of the finite volume on the launch vehicle and PV, the design volume of the CLP will also be limited. Although the volume of many subsystems is still unknown, previous missions, and assumptions based on the selected technologies, were used to determine an approximate volume budget. Similar to the previously mentioned mass budget, this number is subject to change as the final design takes form. While this analysis relies on many assumptions, the CLP was designed with an intended volume budget of 1 cubic meter [19].

6.3 COST BUDGET

A primary goal of any mission is to keep the overall capital allocation to accomplish all mission objectives to a minimum. By designing with cost in mind, the spacecraft vendor can also be more competitive in the market against other similar spacecraft options. While this report will only seek to quantify a budget for the lander portion of this mission, the total cost of this project

will come from combining the cost of the CLP, the PV and the launch vehicle. Table 6.3.1 shown below outlines comparable missions in scale and magnitude with their associated mission costs. The costs of these missions is the total cost of the development and production of the final product that ended up in space. *Philae* was the only mission out of those listed to actually land on a comet, but the other missions had similar overall objectives. The expected cost of each individual subsystem will be outlined more in depth in the FDR. Based on these previous missions, the previously outlined CLP design is expected to cost roughly \$300,000,000 USD.

Table 6.3.1: Mission Cost [13,19,30]

Vehicle	Cost (USD)
Philae (Lander Only)	~\$260,000,000
Deep Impact	~\$330,000,000
Stardust	~\$213,000,000

7 SALES PITCH

The previously described CLP design stands to meet and exceed all of the preexisting objectives for this mission. It goes without saying that the successful completion of these mission objectives would guarantee a tremendous realization of value to both the customer and the general science community. But great reward does not come without great risk. Most competing space vehicle suppliers, however, are unable to balance the fine line between such risk and reward. Space exploration over the previous few decades has been inundated with both risk-averse designs that use 20+ year old technology, doing little to advance science in any meaningful way, and radically unconventional approaches that promise true advancement if successful, but have little chance of consummation (or require massive investments and time).

This CLP design, however, stands as a true exception to these two schools of thought in space vehicle design. It intelligently combines conservative architectures and traditional hardware selections with modern technology and approaches to maximize value proposition, while ensuring high probabilities of success. Traditional design selections with extensive flight heritage provide the customer with confidence that their efforts and capital are well spent, because the subsystems comprising this design are well-understood and have been thoroughly documented and tested. However, the customer is still able to benefit from increased value added by the latest technological developments and products.

A perfect example of this is the two command and control boards that will be used on the CLP. The primary board is the BAE Systems RAD750 that has flown in hundreds of space expeditions and has been tasked with nearly every objective that can be expected for a mission of this nature. The secondary board, however, is the newer BAE Systems RAD5545 which has

increased capabilities, like high resolution image processing, stronger encryption capabilities, and the ability to run multiple operating systems at once. Rather than traditional designs that use similar control boards and rely heavily on the primary board until issues arise, this design intelligently delegates responsibilities to unique control boards that are more well-suited for a particular task, allowing the customer to derive more value from the same reliable hardware.

As a result of this design philosophy, customers can expect success rates on par with risk averse approaches, all while deriving the value of an inherently riskier design philosophy. Furthermore, as a result of many traditional design selections, competitive prices can be offered that undercut the massive investments needed for unconventional approaches, while promising many of the same benefits these pioneering approaches would offer. By balancing the salient motives of risk and reward, this CLP design poses a value proposition that is unmatched by its competitors.

8 CONCLUSION

The ultimate goal of the CLP is to investigate the surface of the comet 46P/Wirtanen in conjunction with the PV. Analysis of the surface, subsurface, and lower atmosphere will provide significant scientific discoveries, as comets are a record of the conditions of the early solar system. Going forward, the CLP will require more detailed analysis for all the subsystems, which will be delivered to the customer in the FDR. Additionally, a PV must be selected, and some of the previously designed components of the mission may have to be adapted to perform in conjunction with the PV. Individual subsystems may require specific part selection, scheduling, detailed modeling, and/or numerical analysis. For each subsystem, budget estimations for mass, power, and volume will be required in order to define a more thorough analysis of the spacecraft as a whole. Outside the scope of the FDR, extensive modeling and testing on individual components and subsystems would also be required in order to more fully understand how these subsystems will interact.

REFERENCES

- [1] 46P/Wirtanen. Gary W. Kronk's Cometography. (n.d.). Retrieved October 20, 2021, from <http://cometography.com/pcomets/046p.html>.
- [2] Amos, J. (2018, March 15). *Big harpoon is 'solution to space junk'*. BBC News. Retrieved October 20, 2021, from <https://www.bbc.com/news/science-environment-43418047>.
- [3] Anderson, K. S. (n.d.). *SPACECRAFT DESIGN, DYNAMICS & CONTROL PRIMER-Some Useful Information on Space Vehicle Systems Design*. Rensselaer Polytechnic Institute. Retrieved October 19, 2021, from https://lms.rpi.edu/ultra/courses/_10897_1/cl/outline.
- [4] Araujo, K. (n.d.). *Battery Cell Comparison*. Epec Engineered Technologies - Build to Print Electronics. Retrieved October 20, 2021, from <https://www.epectec.com/batteries/cell-comparison.html>.
- [5] ASM. (n.d.). *Aluminum 6061-T6; 6061-T651*. ASM Aerospace Specification Metals Inc. Retrieved October 19, 2021, from <http://asm.matweb.com/search/SpecificMaterial.asp?bassnum=MA6061t6>.
- [6] ASM. (n.d.). *Aluminum 7075-T6; 7075-T651*. ASM Aerospace Specification Metals Inc. Retrieved October 19, 2021, from <http://asm.matweb.com/search/SpecificMaterial.asp?bassnum=MA7075T6>.
- [7] ASM. (n.d.). *Titanium Ti-6Al-4V (Grade 5), Annealed*. ASM Aerospace Specification Metals Inc. Retrieved October 19, 2021, from <http://asm.matweb.com/search/SpecificMaterial.asp?bassnum=MTP641>.
- [8] BAE. (n.d.). *RAD5545™ SpaceVPX single-board computer*. BAE Systems. Retrieved October 19, 2021, from <https://www.baesystems.com/media/uploadFile/20210404061759/1434594567983.pdf>
- [9] Ball, A. J., Garry, J. R. C., Lorenz, R. D., & Kerzhannovich, V. V. (2007). Retrieved October 20, 2021, from https://www.e-reading.life/bookreader.php/138786/Ball_-_Planetary_Landers_and_Entry_Probes.pdf.
- [10] Barnett, A. (n.d.). *Basics of space flight - solar system exploration*. NASA Science. Retrieved October 19, 2021, from <https://solarsystem.nasa.gov/basics/chapter11-1/#data>.
- [11] Bhaskaran, S., Nandi, S., Broschart, S., Wallace, M. L., Cangahuala, A., & Olson†, C. (n.d.). *SMALL BODY LANDING ACCURACY USING IN-SITU NAVIGATION*. CITESEERX. Retrieved October 19, 2021, from <https://citeseerx.ist.psu.edu/viewdoc/download?doi=10.1.1.452.1311&rep=rep1&type=pdf>.
- [12] Brown, C. D. (2002). *Elements of spacecraft design*. American Institute of Aeronautics and Astronautics, Inc.
- [13] Cable News Network. (2005, July 4). *Deep Impact Probe Hits comet*. CNN. Retrieved October 20, 2021, from <http://www.cnn.com/2005/TECH/space/07/04/deep.impact/#:~:text=At%20a%20cost%20of%2024330,supports%20low%2Dbudget%20science%20missions>.
- [14] Curtis, H. D. (2021). *Orbital Mechanics for Engineering Students*. Butterworth-Heinemann, An imprint of Elsevier.
- [15] Engineering ToolBox. (2005). *Thermal Conductivity of Metals, Metallic Elements and Alloys*. Engineering ToolBox. Retrieved October 19, 2021, from https://www.engineeringtoolbox.com/thermal-conductivity-metals-d_858.html.

- [16] ESA. (2019, September 1). *Navigation*. ESA Science & Technology. Retrieved October 19, 2021, from <https://sci.esa.int/web/rosetta/-/47366-fact-sheet>.
- [17] ESA. (2019, September 1). *Philae's Instruments*. ESA Science & Technology. Retrieved October 19, 2021, from <https://sci.esa.int/web/rosetta/-/53556-philae-instruments>.
- [18] ESA. (2020, February 13). *Lander Instrument: Introduction*. ESA Science & Technology. Retrieved October 19, 2021, from <https://sci.esa.int/web/rosetta/-/31445-instruments>.
- [19] ESA. (n.d.). *Rosetta's frequently asked questions*. The European Space Agency. Retrieved October 19, 2021, from https://www.esa.int/Science_Exploration/Space_Science/Rosetta/Frequently_asked_questions.
- [20] Espinasse, S., Moura, D., Scheuerle, H., Tilman Spohn, Auster, U., Kletzkine, P., Schulz, R., Komle, N., Szego, K., Rosenbauer, H., Maddock, J., & McKenna-Lawlor, S. (n.d.). *Philae Lander Fact Sheets*. DLR. Retrieved October 20, 2021, from https://www.dlr.de/rd/Portadata/28/Resources/dokumente/rx/Philae_Lander_FactSheets.pdf.
- [21] Etherington, D. (2017, August 23). *BAE Systems' new radiation-hardened computer is ready to serve in space*. TechCrunch. Retrieved October 19, 2021, from <https://techcrunch.com/2017/08/23/bae-systems-new-radiation-hardened-computer-is-ready-to-serve-in-space/>.
- [22] European Space Agency, ESA. (2014, November 7). *Rosetta: Landing on a comet*. Youtube. Retrieved October 19, 2021, from <https://www.youtube.com/watch?v=mggUVLFPkQg>.
- [23] Fusaro, R. L., Alley, T. L., Bement, L. J., Brennan, P. C., Carre, D. J., Didziulis, S. V., Glaeser, W. A., Goldstein, S., Gore, B. W., Gurevich, L., Hanna, W. D., Hilton, M. R., Kalogeras, C. G., Kannel, J. W., Lince, J. R., Marten, H. D., Merriman, T. L., Newell, J. M., Paige, S. L., ... Tran, A. N. (1999). *Nasa Space Mechanisms Handbook*. National Aeronautics and Space Administration.
- [24] Gilmore, D. G. (2002). *Spacecraft Thermal Control Handbook ; Volumei: Fundamentals Technologies*. The Aerospace Press.
- [25] Griffin, M. D., & French, J. R. (2004). *Space vehicle design (2nd edition)*. American Institute of Aeronautics and Astronautics.
- [26] Johnson, M. (2019, March 1). *A New Approach to Radiation Hardening Computers*. NASA. Retrieved October 19, 2021, from https://www.nasa.gov/mission_pages/station/research/news/b4h-3rd/eds-new-approach-radiation-hardening.
- [27] Johnston, H. (2015, April 14). *Rosetta's bouncing probe finds no magnetic field on Comet 67P*. physicsworld. Retrieved October 20, 2021, from <https://physicsworld.com/a/rosettas-bouncing-probe-finds-no-magnetic-field-on-comet-67p/>.
- [28] Kovo, Y. (2020, December 8). *10.0 Communications*. NASA. Retrieved October 19, 2021, from <https://www.nasa.gov/smallsat-institute/sst-soa-2020/communications>.
- [29] NASA. (2004). *Small-Body Database Lookup*. NASA Jet Propulsion Laboratory. Retrieved October 19, 2021, from https://ssd.jpl.nasa.gov/tools/sbdb_lookup.html#/?des=46P&view=VOP.

- [30] NASA. (2021, September 29). *NASA - NSSDCA - spacecraft - details*. NASA. Retrieved October 20, 2021, from <https://nssdc.gsfc.nasa.gov/nmc/spacecraft/display.action?id=1999-003A>.
- [31] Pacific Scientific Energetic Materials Company. (2021, October 18). *Separation Nut*. PacSci EMC. Retrieved October 20, 2021, from <https://psemc.com/products/separation-nut/>.
- [32] Pacific Scientific Energetic Materials Company. (2021, September 29). *Pyrotechnic Actuator*. PacSci EMC. Retrieved October 20, 2021, from <https://psemc.com/products/pyrotechnic-actuator/>.
- [33] Pacific Scientific Energetic Materials Company. (2021, September 29). *Pyrotechnic Pin Puller*. PacSci EMC. Retrieved October 20, 2021, from <https://psemc.com/products/pyrotechnic-pin-puller/>.
- [34] Processors. Artisan Technology Group. (n.d.). Retrieved October 20, 2021, from <https://www.artisantg.com/info/BAE%20Systems%20RAD750%20Datasheet%202018222103850.pdf>.
- [35] Quest Thermal Group. (n.d.). *Wrapped MLI*. Quest Thermal Group. Retrieved October 19, 2021, from <https://www.questthermal.com/products/wrapped-mli>.
- [36] Rensselaer Polytechnic Institute. (n.d.). *Optical Navigation*. SEAL Sensing, Estimation, and Automation Laboratory. Retrieved October 19, 2021, from <https://seal.rpi.edu/research/optical-navigation>.
- [37] Sakharkar, A. (2020, February 29). *Octopus-inspired Tentacle bot can handle a wide range of objects*. Tech Explorist. Retrieved October 20, 2021, from <https://www.techexplorist.com/octopus-inspired-tentacle-bot-sucker-grasp-objects/30435/>
- [38] University of Maryland. (n.d.). *What is special about comet Wirtanen?* University of Maryland. Retrieved October 20, 2021, from <https://wirtanen.astro.umd.edu/46P/>.
- [39] Vitug, E. (2020, July 15). *High performance spaceflight computing (HPSC)*. NASA. Retrieved October 19, 2021, from https://www.nasa.gov/directorates/spacetech/game_changing_development/projects/HPS_C.
- [40] Wikimedia Foundation. (2021, May 25). *Pyrotechnic Fastener*. Wikipedia. Retrieved October 20, 2021, from https://en.wikipedia.org/wiki/Pyrotechnic_fastener.
- [41] Wikimedia Foundation. (2021, October 11). *Cold Gas Thruster*. Wikipedia. Retrieved October 19, 2021, from https://en.wikipedia.org/wiki/Cold_gas_thruster.
- [42] Wikimedia Foundation. (2021, October 11). *Shock mount*. Wikipedia. Retrieved October 20, 2021, from https://en.wikipedia.org/wiki/Shock_mount.
- [43] Yeomans , D. K. (1998, April). *Why study comets?* NASA. Retrieved October 19, 2021, from https://ssd.jpl.nasa.gov/sb/why_comets.html.
- [44] Youtube. (2019, January 14). *90 deg. hinge of 4-bar linkage 1 - youtube*. Youtube. Retrieved October 20, 2021, from <https://www.youtube.com/watch?v=TLROAYXxkvA>.
- [45] Zhao, H., Liu, W., Ding, J., Sun, Y., Li, X., & Liu, Y. (2018, July 24). *Numerical study on separation shock characteristics of pyrotechnic separation nuts*. Acta Astronautica. Retrieved October 20, 2021, from <https://www.sciencedirect.com/science/article/abs/pii/S0094576518304648#:~:text=In%20aerospace%20engineering%2C%20pyrotechnic%20separation,spacecraft%20and%20launched%20when%5B1%5D.&text=When%20the%20separation%20signal%20is,when%20the%20spacecraft%20is%20released>.

APPENDICES

APPENDIX A: DEFINITION AND ASSESSMENT OF RISK

Risk is the assessment of an adverse event that may occur and interrupt the mission. This can be before or after launch, and can range in damage anywhere from a single day setback to a complete mission loss.

The major risks for each subsystem were evaluated individually, but operate under the same scale. Table A.1 compares the probability an event is to occur and the severity of such an occurrence. The probability is evaluated from A-E - where A is ‘Improbable’ and E is ‘Chronic.’ Severity is evaluated on a scale of 1-4 - where the consequence of a 1 is ‘Negligible’ and the consequence of 4 is ‘Catastrophic.’ These combined values are then evaluated based on the acceptance level in Table A.2 and given a respective color. Here an event of ‘Minimal Risk’ is highlighted in green where a ‘High Risk’ event is highlighted in red. Table A.3 outlines the collected risks of each subsystem.

Table A1: Severity/Probability Risk Assessment Matrix

		Severity			
Probability		1 Negligible	2 Moderate	3 Crucial	4 Catastrophic
A - Improbable	1A	2A	3A	4A	
B - Unlikely	1B	2B	3B	4B	
C - Moderate	1C	2C	3C	4C	
D - Likely	1D	2D	3D	4D	
E - Chronic	1E	2E	3E	4E	

Table A2: Severity/Probability Risk Acceptance Level and Procedure

Severity - Probability	Acceptance Level
Minimal Risk	Acceptable - No formal review required
Low Risk	Acceptable - Formal verification and approval must be provided
Moderate Risk	Undesirable - Documented approval from higher level management
High Risk	Unacceptable - Documented approval from top independent management committee

APPENDIX B: SUMMARY OF NON-TECHNICAL CONSIDERATIONS

This appendix is useful for showing the applications of non-technical considerations for each subsystem. For specific details regarding the non-technical consideration, please refer back to the respective report section.

Table B1: Non-Technical Consideration Legend

Application of Non-Technical Considerations
Subsystem Has This Consideration (O)
Subsystem Does Not Have This Consideration (X)

Table B2: Non-Technical Factor Matrix for All Subsystems

Section	Mission	5.1	5.2	5.3	5.4	5.5	5.6	5.7	5.8	5.9
Public Health & Safety	O	O	O	O	O	X	O	O	O	X
Global	O	X	O	X	X	X	X	O	X	X
Cultural	X	X	X	X	X	X	X	X	X	X
Social	X	X	X	X	X	X	X	X	X	X
Environmental	O	O	O	O	O	X	O	O	O	X
Economic	O	O	O	X	O	O	O	O	O	O
Professional Ethics	O	O	O	O	O	O	O	O	O	O

As is evident from Table B2, cultural and social considerations were negligible for subsystems and the mission as a whole. This is a result of the nature of the space mission and its minimal impact on cultures and societies it would have as a result of being largely removed from the public eye. The same is also true for global considerations in many cases.

APPENDIX C: GANTT CHART

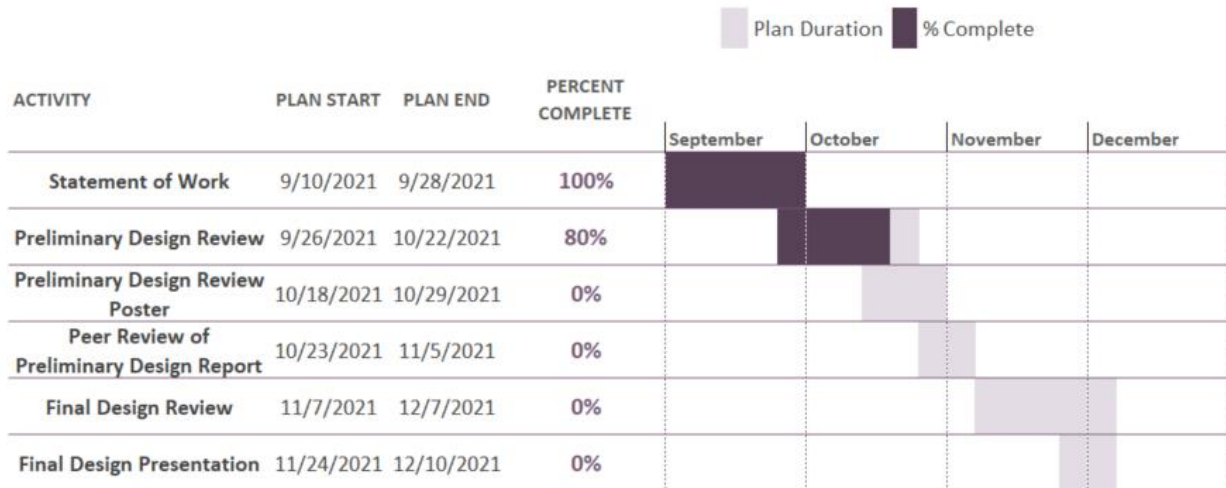


Figure C1: Gantt Chart

APPENDIX D: ORGANIZATIONAL CHART

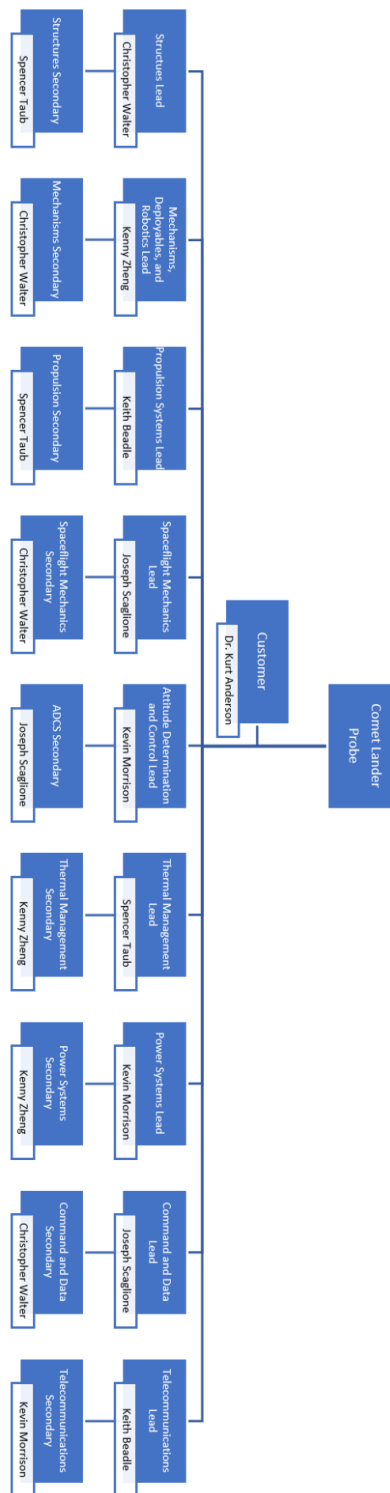


Figure D1: Organizational Chart

APPENDIX E: TEAM MEMBER RESPONSIBILITIES

Table E1: Primary and Secondary Leads by Mission Components

Mission Component	Primary Lead	Secondary Lead
Mission Design/Architecture	All	All
Structures	Christopher Walter	Spencer Taub
Mechanisms and Deployables	Kenny Zheng	Christopher Walter
Propulsion	Keith Beadle	Spencer Taub
Flight Mechanics	Joseph Scaglione	Christopher Walter
Attitude Determination and Control	Kevin Morrison	Joseph Scaglione
Thermal Management	Spencer Taub	Kenny Zheng
Power and Power Management	Kevin Morrison	Kenny Zheng
Command and Data	Joseph Scaglione	Christopher Walter
Telecommunication	Keith Beadle	Kevin Morrison

Table E2: Report Sections by Team Member

Team Member	Report Section
Keith Beadle	1 Executive Summary
	5.3 Propulsion
	5.9 Telecommunication
	8 Conclusions
	Appendix A
Kevin Morrison	2 Introduction
	5.5 Attitude Determination & Control
	5.7 Power and Power Management
	Appendix D
Joseph Scaglione	5.4 Spaceflight Mechanics
	5.8 Command and Data
	7 Sales Pitch
	Appendix E
Spencer Taub	3 Project Scope
	5.6 Thermal Management
	Appendix B
Christopher Walter	5.1 Structures
	6 Design budgets
	Appendix C
Kenny Zheng	4 Mission Architecture
	5.2 Mechanisms, Deployables, & Robotics
	References

Table E3: PDR Component Authors

PDR Component	Author
1 Executive Summary	Keith Beadle
2 Introduction	Kevin Morrison
3 Project Scope	
3.1 Mission Objectives	Spencer Taub
3.2 Mission Constraints	Spencer Taub
3.3 Mission Assumptions	Spencer Taub
3.4 Non-Technical Considerations	Spencer Taub
4 Mission Architecture	
4.1 Comet Selection	Kenny Zheng
4.2 Landing Site Selection	Kenny Zheng
4.3 Payload Overview	Kenny Zheng
4.4 Sensor Suite Overview	Kenny Zheng
5 Design Approach	
5.1 Structure	Christopher Walter
5.2 Mechanisms, Deployables, & Robotics	Kenny Zheng
5.3 Propulsion	Keith Beadle
5.4 Spaceflight Mechanics	Joseph Scaglione
5.5 Attitude Determination & Control	Kevin Morrison
5.6 Thermal Management	Spencer Taub
5.7 Power and Power Management	Kevin Morrison
5.8 Command and Data	Joseph Scaglione
5.9 Telecommunication	Keith Beadle
6 Design Budgets	
6.1 Mass Budget	Christopher Walter
6.2 Volume Budget	Christopher Walter
6.3 Cost Budget	Christopher Walter
7 Sales Pitch	Joseph Scaglione
8 Conclusions	Keith Beadle
References	Kenny Zheng
Appendices	
Appendix A: Definition and Assessment of Risk	Keith Beadle
Appendix B: Summary of Non-Technical Considerations	Spencer Taub
Appendix C: Gantt Chart	Christopher Walter
Appendix D: Organizational Chart	Kevin Morrison
Appendix E: Team Member Responsibilities	Joseph Scaglione
Appendix F: Technical Documentation	All

APPENDIX F: TECHNICAL DOCUMENTATION

Form factor	CompactPCI 6U (233 mm x 160 mm) CompactPCI 6U-220 (233mm x 220mm) Weight: 1000 to 1220 grams, varies with memory
Memory	SRAM: 4 to 48 MB EEPROM: 4 MB
Radiation-hardness	Total dose: >100 Krad (Si) SEU: 1.9 E-4 errors/card-day (90 percent W. C. GEO) varies with orbit Latchup-immune
Performance	>260 Dhystone 2.1 MIPS at 132 MHz 4.3 SPECint95 4.6 SPECfp95 at 132 MHz
Power supply	-5 volts ± 10 percent and 3.3 volts ± 5 percent (2.5 volts generated via onboard regulator)
Power dissipation	11 to 14 watts
Rail temperature range	-28 degrees celsius to +70 degrees celsius

Figure F1: BAE Systems RAD750 6U Product Specifications [34]

SpaceVPX	Slot profiles: payload, system controller with data plane Module profiles: Payload: MOD6-PAY-4F1Q2T-12.2.1-5-22 Controller:MOD6-CON-4F12T12U-12.6.1-2-22 Mechanical size: 6U-220 Card pitch: 1.2 inches Cooling: Conduction Power profile (no daughter card) 5.0 V (+/- 10 percent): 6.7 Amps 3.3 V AUX: <1.0 Amps User-defined I/O: Differential
Temperature	Operating at -55 to 125 degrees Celsius
Radiation-hardness	Total ionizing dose: 100 Krad (Si) Single event upset: 1e-3 upsets/card-day Latchup immune
Power dissipation	35 Watts at 95 degrees Celsius and +5 percent voltage with all dissipation interfaces operational (no daughter card)
Interfaces	Up to four 4-lane RapidIO ports up to 3.125 Gbaud/lane (also supports 2.5, and 1.25 Gbaud/lane) Up to 12 SpaceWire serial links to the backplane up to 320 Mb/s each I2C and related utility plane control signals JTAG test and debug Aurora high speed trace debug
Daughter card interfaces	Up to 4 SpaceWire links One RapidIO port (the RapidIO port is mutually exclusive with the 4th RapidIO port to the backplane) 32-bit parallel PCI

Figure F2: BAE Systems RAD5545 Space VPX 6U Product Specifications [8]

Specifications by Battery Chemistry

Specifications	Lead Acid	NiCd	NiMH	Li-ion				
				Cobalt	Manganese	Phosphate		
Specific Energy Density (Wh/kg)	30-50	45-80	60-120	150-190	100-135	90-120		
Internal Resistance (mΩ) 12V pack	<100	100-200 6V pack	200-300 6V pack	150-300 7.2V	25-75 per cell	25-50 per cell		
Life Cycle (80% discharge)	200-300	1000	300-500	500- 1,000	500-1,000	1,000- 2,000		
Fast-Charge Time	8-16h	1h typical	2-4h	2-4h	1h or less	1h or less		
Overcharge Tolerance	High	Moderate	Low	Low. Cannot tolerate trickle charge				
Self-Discharge/month (room temp)	5%	20%	30%	<10%				
Cell Voltage (nominal)	2V	1.2V	1.2V	3.6V	3.8V	3.3V		
Charge Cutoff Voltage (V/cell)	2.40 Float 2.25	Full charge detection by voltage signature		4.20	3.60			
Discharge Cutoff Voltage (V/cell, 1C)	1.75	1.00		2.50-3.00	2.80			
Peak Load Current Best Result	5C 0.2C	20C 1C	5C 0.5C	>3C <1C	>30C <10C	>30C <10C		
Charge Temperature	-20 to 50°C -4 to 122°F	0 to 45°C 32 to 113°F	0 to 45°C 32 to 113°F					
Discharge Temperature	-20 to 50°C -4 to 122°F	-20 to 65°C -4 to 149°F	-20 to 60°C -4 to 140°F					
Maintenance Requirement	3-6 Months (topping charge)	30-60 days (discharge)	60-90 days (discharge)	Not required				
Safety Requirements	Thermally stable	Thermally stable, fuse protection common		Protection circuit mandatory				
In Use Since	Late 1800s	1950	1990	1991	1996	1999		
Toxicity	Very High	Very High	Low	Low				

Figure F3: Common Specifications by Battery Chemistry [4]

Battery type	Chemical formula	Specific energy Wh kg ⁻¹	Cycle life 75%-25% DoD
Silver-zinc	AgZn	100	75–2000
Nickel-cadmium	NiCd	30	800–30 000
Nickel-hydrogen	NiH	60	4000–30 000
Lithium-sulphur dioxide	LiSO ₂	200	
Lithium-thionyl chloride	LiSOCl ₂	200	

Figure F4: Specific Energy and Cycle Life for Common Battery Types [9]